Endoscopy in Early Gastrointestinal Cancers, Volume 1

Diagnosis

Philip W. Y. Chiu
Yasushi Sano
Noriya Uedo
Rajvinder Singh
Editors

Springer

Endoscopy in Early Gastrointestinal Cancers, Volume 1

Philip W. Y. Chiu • Yasushi Sano
Noriya Uedo • Rajvinder Singh
Editors

Endoscopy in Early Gastrointestinal Cancers, Volume 1

Diagnosis

Springer

Editors
Philip W. Y. Chiu
Department of Surgery
Faculty of Medicine
The Chinese University of Hong Kong
Hong Kong
Hong Kong

Noriya Uedo
Department of Gastrointestinal
Oncology, Endoscopy Training
and Learning Center
Osaka Medical Center for Cancer
& Cardiovascular Diseases
Higashinari-ku
Osaka
Japan

Yasushi Sano
Gastrointestinal Center & Institute
of minimally-invasive endoscopic care
(iMEC)
Sano Hospital
Kobe
Hyogo
Japan

Rajvinder Singh
Gastroenterology Department
Lyell McEwin Hospital
Gastroenterology Department
Adelaide
SA
Australia

ISBN 978-981-10-6768-6 ISBN 978-981-10-6769-3 (eBook)
https://doi.org/10.1007/978-981-10-6769-3

This Springer imprint is published by the registered company Springer Nature Singapore Pte Ltd.
The registered company address is: 152 Beach Road, #21-01/04 Gateway East, Singapore 189721, Singapore

Foreword

I am very much pleased to introduce this book entitled *Endoscopy in Early Gastrointestinal Cancers* from Springer. This book consists of two parts, that is, Volume I focuses on "Diagnosis" and Volume II focuses on "Treatment." All of the contributors of this book are the members of ANBIIG (Asian Novel Bio-Imaging and Intervention Group). I would like to provide introductory remarks for Volume 2—Treatment in the preface here.

The history of endoscopy over the past three decades has been marked by steady and rapid progress in endoscopic treatment, starting from the development of the video endoscope in 1983, which led to more progress in the subsequent years. The period during the 1980s was characterized by improvements in endoscopic treatment of early gastrointestinal cancers using endoscopic mucosal resection (EMR). In the 2000s, the rapid dissemination of endoscopic submucosal dissection (ESD) has led to further advances in endoscopic treatment, while the introduction of the HDTV endoscope to the market in 2002, together with more recent innovations such as image-enhanced endoscopy (IEE) and magnifying endoscopy, has provided the basis for a new diagnostic study.

Historically, ANBIIG was founded as a nongovernmental organization (NGO) in 2013. At first, in the first four years, more than 45 workshops have been conducted, and more than 2000 young doctors received comprehensive trainings. Throughout all those trainings, we came to realize the necessity to establish an actual consensus on how much Asian practitioners have common knowledge of endoscopic diagnosis related to IEE.

"ANBIIG Consensus Meeting" was started in January 2016, aiming to figure out consensus on the present situation of Asia in the field of endoscopic diagnosis of early gastrointestinal cancers. The policies of ANBIIG activities comprise the aim, the means, and also the performers taking part in healthcare practices. These policies were "**ORIGINATED IN ASIA**," "**DEVELOPED BY ASIA**," and "**OPTIMIZED FOR ASIA**." We set our destination to be most suitably optimized and implemented in Asia. In reality, there is a big difference between Asian and Western countries in many ways, such as frequency of disease and ways of thinking and practices.

We, in charge of clinical practices in Asia, are striving to provide meaningful results from our research by Asian endoscopists, widely. Back in the day, we used to learn most of medicine from Western countries. However, I believe that we have now reached "**Asian Endoscopic Revolution**."

I would like to emphasize the importance and benefits of ANBIIG Consensus in Asia, which is being realized now. For example, IEE diagnosis was unified as Asian Guideline, which is to deliver consistent diagnostic procedures as daily practices with the same contexts, to prevent any deviations at teaching and learning procedures, skills, and knowledge on IEE, and also to optimize IEE practices in Asia. It is important to lift up the level of standard in the field of Asian endoscopic diagnosis, which will lead to early diagnosis and treatment. Also it is expected that Asian endoscopic medicine will develop and expand globally from now.

I regard this Consensus as the best compass for the journey on "**ASIAN IEE OCEAN**," which certainly guides young and ambitious Asian practitioners to master IEE diagnosis. And it will increase the number of IEE practitioners in Asia for sure.

In this book, based on the above background, indications for endoscopic resection of early GI cancers, real procedure of EMR, real procedure of ESD, management of noncurative resection and local recurrence after endoscopic resection, complications of endoscopic resection, and management for each organ are stated by experts as easy to understand and in detail. In the last chapter, special ESD cases illustrations are mentioned for every country as in Japan, China, Korea, and Hong Kong SAR, which makes it educational and fascinating.

I hope that doctors who are about to start ESD, those who are confronted with difficulties during conducting ESD in real, and also those who are at the side to direct ESD would read this book of practices widely in Asia. And then, all those doctors can enter the matured world of endoscopic resection of early GI cancers and perform their value at an advanced level. It would be grateful for me if those who read this book could heal as many patients as they could as one of skillful practitioners of Asia-Pacific Society for Digestive Endoscopy.

I believe that the contents covered by this book will give our readers the confidence to take on the unity of clinical medicine in the field of endoscopic diagnosis, which has surmounted the problems associated with conventional manners and advanced new functional studies.

Finally, I would like to express my deepest gratitude to the many doctors and compiling staffs who contributed to this book even though they were very busy.

Hisao Tajiri
Senior Advisor of Japan Gastroenterological Endoscopy Society (JGES)
Vice President of Asia-Pacific Society for Digestive Endoscopy (A-PSDE)
Professor, Dept. of Innovative Interventional Endoscopy Research
The Jikei Univ. School of Medicine
Tokyo, Japan

Foreword

I wish to congratulate the success of experts from the Asian Novel Bio-Imaging and Intervention Group (ANBIIG) to publish these important books on diagnostic and therapeutic for early gastrointestinal cancers. Gastrointestinal cancers are among the commonest cancers worldwide with significant risks in cancer-related mortality. Gastric and esophageal cancers had been an important cause of cancer mortality in Asia, with 70% of patients with gastric cancers coming from Asia. Recently, there is an increase in the number of patients diagnosed to have colorectal cancers worldwide which incurs concerns from gastroenterologists, surgeons, oncologists as well as the government in diagnosis and treatment of these cancers. To impact on the prognosis, it is essential to diagnose these gastrointestinal cancers at an early stage.

Image-enhanced endoscopy had been tremendously advanced over the past decade, with the clinical application of technologies including narrow band imaging and magnifying endoscopy demonstrating the effect of improving recognition and characterization of early gastrointestinal cancers. The mission of ANBIIG is to provide a learning platform for education and training of novel endoscopic imaging and therapeutic technologies for Asian endoscopists. I must congratulate the success of ANBIIG in achieving this goal, as more than 110 workshops in Asia, providing training for more than 7,000 healthcare professionals. Moreover, two consensus papers were published on standards and quality of endoscopy for diagnosis of early gastrointestinal cancers.

One of the important initiatives for education and training of ANBIIG is to publish two books focusing on the diagnosis and endoscopic treatments. These books served as important educational material to propagate exchange of knowledge in these areas. Serving as an advisor for ANBIIG, I am delighted to see these books published with high quality in the content.

With the current advances in artificial intelligence and robotics, I look forward to future technological advances in diagnosis and treatment of early gastrointestinal cancers as well as additional chapters on these topics in the second edition of these books.

Joseph Sung
Department of Medicine and Therapeutics, Faculty of Medicine
The Chinese University of Hong Kong
Hong Kong, Hong Kong

Contents

1 Esophago-Gastrointestinal Pathology on Early Carcinoma for Endoscopists

Takahiro Fujimori

1.1 Introduction

General rules for treatment of early carcinoma have been determined in cooperation by clinicians, pathologists, and radiologists belonging to the Japan Esophageal Society (JES) [1], the Japanese Research Society for Gastric Cancer (JRSGC) [2], and the Japanese Society for Cancer of the Colon and Rectum (JSCCR) [3, 4], with repeated revision from the 1960s to the 1990s in Japan. One of the purposes of this chapter is to introduce the latest information on them.

We describe the items regarding histopathological diagnosis to introduce topics in Japan by extracting these rules in this chapter.

1.2 Developments and Normal Structure

Gastrointestinal tract, which is originally a simple tube, forms different organs with the development. Formation of the gastrointestinal tract starts with tubulation of endoderm by folding of early embryo. As a result of craniocaudal folding, saclike foregut and hindgut are formed in the head and tail of the embryo. The midgut in between is widely in contact with the yolk sac at first, and subsequently becomes tubular being in contact with yolk sac only through yolk duct.

For gastrointestinal tract, the part from pharynx to around opening of duodenal common bile duct originates in foregut, and the part from the remaining of duodenum to right two-third of transverse colon and the part from light one-third of transverse colon to the upper anus originates in in midgut and hindgut, respectively. In addition, generally, while endoderm lining of intestinal tract differentiates into epithelium controlling digestive and absorptive function, splanchnic mesoderm around endoderm differentiates into lamina propria, submucosal tissue, muscularis mucosae, and muscle layer. Neural crest cells entering into the bowel wall by cell migration differentiates into ganglion cell to form plexuses beneath the mucous membrane or in between muscle layers

1.2.1 Esophagus

The length of esophagus is approximately 25 cm with tube from the pharynx with height at the level of Sixth cervical vertebra to the esophagogastric junction with height at the level of 11th thoracic vertebra. There are sphincters in pharyngoesophageal junction and gastroesophageal junction to prevent inhalation of air from phar-

T. Fujimori (✉)
Fukushima Medical University, Fukushima, Japan

Department of Pathology, Shinko Hospital, Kobe, Hyogo, Japan
e-mail: t-fuji@kind.ocn.ne.jp

P. W. Y. Chiu et al. (eds.), *Endoscopy in Early Gastrointestinal Cancers, Volume 1*,
https://doi.org/10.1007/978-981-10-6769-3_1

ynx and reflux from stomach to esophagus by closing lumen at any other time but swallowing movement. In adults, the depth from the incisors to the upper esophageal sphincter is 15–18 cm, and to lower esophageal sphincter is 37–40 cm. The diameter of esophagus is 1.5–2.5 cm with a tendency of the lower half of lumen being larger and the largest part being above the diaphragm (esophageal hiatus). The lumen of esophagus is covered by stratified squamous epithelium having a sufficient protective function. The lymphocyte population exists in the lamina propria underneath the epithelium. There are small mucous glands in submucosal tissue under the muscularis mucosae. The inner circular layer is clearly distinguished from the outer longitudinal layer in the muscle layer. It is said that the first stage of swallowing movement is voluntarily adjustable with striated muscle in muscle layer of the upper one-third part of esophagus.

At the outside of muscle layer, blood vessel rich adventitia extends to the surrounding connective tissues. The upper esophageal sphincter includes the cricopharyngeal muscle constituting the lowest part of hypopharyngeal sphincter. The lower esophageal sphincter is called LES with specific function and response for various stimulus. This lower esophageal sphincter causes the formation of high-pressure zone by tonic contraction even during non-active stage to separate esophageal lumen from gastric lumen. Normal pressure of lower esophageal sphincter is 15–35 mm Hg.

1.2.2 Stomach

Stomach can be anatomically divided into cardia, fundus, corpus, pyloric antrum, and pylorus. It is histologically divided into three areas containing cardiac gland, fundic gland, and pyloric gland. There are boundaries between each area, which is readily modified by age and inflammation. The gastric glands consisting of units of secretory part and the opening part as gastric pits (foveola, crypt, pit) are recognized as groove or depression from the mucosal surface gathering to form atypical mucosal elevation, which is called gastric area.

The surfaces of gastric mucosa and gastric pits (foveola, crypt, pit) are covered by columnar epithelium. This cell is called surface mucus cell because of the secretory ability of special mucus with the secretion fluid which is insoluble in hydrochloric acid to protect mucous membrane from hydrochloric acid. Surface mucus cells accompanied by goblet cells or cilia represents metaplasia.

The lamina propria of corpus is occupied by fundic glands including a few fundic glands producing opening into gastric pits (foveola, crypt, pit). Fundic glands consist of three types of cells as principal cell, parietal cell, and mucous neck cell. Principal cells exist in the deepest part to produce pepsinogen, a precursor of pepsin. Parietal cells are disseminated throughout the intermediate layer to secrete hydrochloric acid. Mucous neck cells exist at the side of gastric pit (foveola, crypt, pit) to secrete mucus. Cardiac glands and pyloric glands are both mucous glands.

Fundic gland and pyloric gland include cells having endocrine factor other than the above exocrine cells. Especially in pyloric gland, endocrine cells are substantially observed including 50% of G cells (gastrin-secreting), 30% of enterochromaffin cells (EC cell, serotonin-secreting), 15% of D cells (somatostatin-secreting). The main endocrine cells in fundic glands are EC-like (ECL) cells to secrete histamine and also include EC cells and a small amount of X cells (secretion is unspecified). The layer of gastric wall consists of surface epithelium, lamina propria, muscularis mucosae, submucosa, and muscle layer.

1.2.3 Colon and Rectum

Large intestine is an organ with the total length of approximately 1.5 m consisting of vermiform appendix, caecum, ascending colon, transverse colon, descending colon, sigmoid colon, and rectum. Unlike small intestine, large intestine has no plicae circulares or villi with formation of lam-

ina propria by crypts formed by simple tubular glands. Large intestine wall underneath consists of submucosa, muscle layer, and serosa. The surface of crypt is covered by absorptive epithelial cells with a number of goblet cells. Although absorptive epithelial cells are similar to absorptive epithelial cells of the villi in the small intestine, the microvilli of the brush border have a length of a half of that in the small intestine. The function of this cells is to absorb large volumes of water and electrolytes.

Observation by electron microscope demonstrates existence of secretory granule with very small diameter around the upper end of absorptive epithelium, indicating an opening into the upper surface of cells. Acid mucopolysaccharide detected in this granule is considered to secrete sugar coating components on the surface of microvilli. In addition, presence of IgA in the upper part of nucleus has been confirmed, indicating that secretory IgA are aggregated in this granule to be released.

Goblet cells are observed in crypt more than surface epithelium, especially in the lateral wall. Mucus of goblet cells show positive for alcian blue staining, suggesting intestinal type mucus and also, intestinal type mucus shows positive for high iron diamine (HID) staining.

Many basal granulated cells appear on the crypt epithelium with several types of cells other than enterochromaffin cell (EC cells, serotonin secreting), although hormonal secretion is unknown.

Table 1.1 Mucin staining requiring diagnosis and the location

Core protein	Secretion Membrane binding	Region
MUC 1	Membrane	Pancreatic acinus, mammary gland
MUC 2	Secretion	Small intestine, large intestine goblet cell respiratory tract
MUC 3	Membrane	Small intestine, large intestine, gallbladder
MUC 4	Membrane	Large intestine, respiratory tract
MUC5AC	Secretion	Gastric surface epithelium
MUC5B	Secretion	Esophageal glands, respiratory tract, salivary glands
MUC 6	Secretion	Pyloric gland, cardiac glands, mucous neck cell of stomach, duodenal Brunner's glands, esophageal cardiac gland
MUC 7	Secretion	Salivary glands

Table 1.2 Macroscopic classification

Type 0: Superficial type
Type 1: Protruding type
Type 2: Ulcerative and localized type
Type 3: Ulcerative and infiltrative type
Type 4: Diffusely infiltrative type
Type 5: Unclassifiable type
Type 5a: Unclassifiable type without treatment
Type 5b: Unclassifiable type after treatment

1.3 Definitions of Early Carcinoma in Japan and Macroscopic Type Classification in Esophago-Gastrointestinal Tracts (EGI) [1] (Tables 1.1, 1.2, 1.3, 1.4, 1.5, and 1.6)

Principles of Tumor Type Classification

The tumor type classification is based on the macroscopic findings. Radiological and endo-

Table 1.3 Subclassification of superficial type (type 0)

Type 0-Ip: Superficial and protruding type
Type 0-Ip: Pedunculated type
Type 0-Is: Sessile (broad based) type
Type 0-II: Superficial and flat type
Type 0-IIa: Slightly elevated type
Type 0-IIb: Flat type
Type 0-IIc: Slightly depressed type
Type 0-III: Superficial and excavated type

Combined type: When multiple macroscopic tumor types are mixed in one lesion, it is called a combined type. The wider type is described first and types are connected with +

Table 1.4 Esophagus: depth of tumor invasion (T)

TX: Depth of tumor invasion cannot be assessed
T0: No evidence of primary tumor
T1a: Tumor invaded mucosa *Note 1*
T1a-EP: Carcinoma in situ (Tis: M1)
T1a-LPM: Tumor invades lamina propria mucosa (LPM: M2)
T1a-MM: Tumor invades muscularis mucosa (MM: M3)
T1b: Tumor invades submucosa (SM)
SM1: Tumor invades the upper third of the submucosal layer
SM2: Tumor invades the middle third of the submucosal layer
SM3: Tumor invades the lower third of the submucosal layer
T2: Tumor invades muscularis propria (MP)
T3: Tumor invades adventitia (AD)
T4: Tumor invades adjacent structures (AI)

In endoscopically resected specimens, a tumor invading the submucosa to a depth of 200 μm or less from the lamina muscularis mucosa is classified as SM1, while a tumor extending more than 200 μm is classified as SM2

Table 1.6 Depth of submucosal invasion in T1 (SM) colon carcinomas [3, 5]

1. When it is possible to identify the muscularis mucosae, the depth of submucosal invasion is the distance between the deeper edge of the muscularis mucosae and the deepest invasion
2. When it is not possible to identify the muscularis mucosae, the depth of submucosal invasion is the distance between the surface of the tumor and the deepest invasion
3. In polypoid tumor (Ip) with **disrupted muscularis mucosae**, the depth of submucosal invasion is the distance between the deepest invasion and the **Haggitt level 2 line** being defined as the boundary between the tumor head and the pedicle
When cancer does not invade beyond the level 2 line, it is defined as **head invasion** Migration of adenomatous glands (pseudocarcinomatous invasion or submucosal misplacement) should be differentiated from true submucosal invasion

Table 1.5 Comparison of Japanese classification in early carcinoma of EGI tracts with UICC

	Esophagus		Stomach		Colon	
	UICC	JES	UICC	JRSGC	UICC	JSCCR
Tis	Carcinoma in situ (CIS)/ high grade dysplasia	CIS(Tis)	Carcinoma in situ (CIS)		CIS and invasion of lamina propria	Tis M
T1	M/SM	M/SM	M/SM	M/SM	SM	SM
T1a	Tumor invades mucosa and muscularis mucosa	T1a-LPM(M2) or T1a-MM(M3)	Tumor invades mucosa and muscularis mucosa	M		T1a (SM_1) < 1 mm
T1b	Tumor invades submucosa	T1b SM1 SM2 SM3 (SM1 ≦ 0.2 mm)	Tumor invades submucosa	SM T1b1 < 0.5 mm T1b2 ≧ 0.5 mm		T1b (SM_2) ≧ 1 mm
		Japan Esophageal Society (JES)		Japanese research Society for Gastric Cancer (JRSGC)		Japanese Society for Cancer of the colon and Rectum (JSCCR)

Regardless of the presence of lymph node or distant organ metastasis, T1a can be designated as early esophageal carcinoma and T1 can be designated as early carcinoma of stomach and colorectum in Japan

scopic classifications are based on the macroscopic classification.

Tumors in which invasion is macroscopically diagnosed to be limited to within the submucosa are classified as superficial type (early carcinoma: Tis/T1), while tumors in which invasion is diagnosed to extend to the muscularis propria (MP) or beyond are classified as T2–4.

The superficial type has the prefix "0" and is classified into 0-I, 0-II, or 0-III. The carcinomas of EGI with more than invasion to MP is divided into four categories: 1, 2, 3, or 4. When a tumor cannot be classified into any of the 5 (0–4) categories or their combinations, it is classified as 5.

1.4 Handling of Endoscopic Resected Specimen [1]

Macroscopic Examination and Handling of Endoscopically Resected Specimens

Specimens obtained by complete endoscopic excision (en bloc excision) are handled as follows. Whenever possible, specimens obtained by partial excision should be handled as those obtained by complete endoscopic excision.

1. Stretching and fixation

   When the lesion is sessile type or superficial type, the specimen is stretched lightly, pinned with the mucosal side up to a flat board with stainless steel pins, and then completely immersed with the mucosal side down in a container of formalin solution. Polyps are immersed in formalin solution immediately.
2. Macroscopic examination

   The side of the resected specimen and the following features of the tumor are recorded; side, macroscopic type, length of the stalk, surface appearance, color, and distances from horizontal/lateral and vertical/deep margins.

   It is recommended that the resection margins are marked with ink immediately after endoscopic excision.
3. Sectioning

   Pedunculated polyps with a thick stalk (2 mm or more in diameter): The first cut is made 1 mm from the center of the stalk and the polyp is sectioned at 2 mm intervals. The entire polyp is sectioned and examined histologically.

   Pedunculated polyps with a thin stalk (less than 2 mm in diameter): The stalk is totally embedded in paraffin and thin sections of the paraffin block are cut for examination.

   Sessile lesion and superficial type lesion:

   The specimen if cut at 2 mm intervals to determine the margin of clearance.

   Stereomicroscopic examination can be useful for identifying the extent of the lesion and for proper sectioning.

   In principle, all section lines are made in the same direction. However, sectioning in different directions is permissible when necessary.

   If submucosal invasion is suspected, then the first cut should be made in longitudinal axis 1 mm from site of suspected deepest invasion.
4. Photography

   Photography is performed before and after sectioning.

   To make a histological map of the tumor, it is essential to photograph the tumor with section lines.

   Shallow section lines in the mucosal surface are recommended for photography.

1.5 Topics of Esophago-Gastrointestinal Pathology in Japan

1.5.1 Esophagus: Barrett Adenocarcinoma [1] (Table 1.7)

Barrett adenocarcinoma is an adenocarcinoma arising from Barrett mucosa. Barrett mucosa is

Table 1.7 Barrett esophagus

The esophageal having Barrett mucosa is designated Barrett esophagus
At least one of the following conditions must be satisfied:
1. Esophageal glands in the area of columnar epithelium
2. Squamous islands in the columnar epithelium
3. Double layer structure of muscularis mucosa

defined as columnar epithelium extending from stomach to esophagus in succession. While it must be associated with intestinal metaplasia as the definition in Europe and the United States, presence/absence of intestinal metaplasia is not considered in Japan. Recently, some researchers in Europe and the United States reported that presence/absence of intestinal metaplasia is not taken into account. Circumferential Barrett mucosa with the length of 3 cm or more is defined as long segment Barrett esophagus (LSBE), and Barrett mucosa which is not circumferential with the length of less than 3 cm in some part is defined as short segment Barrett esophagus (SSBE).

Intestinal metaplasia (involvement of CDX2, etc.) is considered to arise from metaplasia of the gastric metaplasia due to abnormality in differentiation of esophageal squamous stem cells or circulating bone marrow stem cells associated with chronic inflammation.

Adenocarcinoma of esophagus may include invasion to esophagus of gastric cardia adenocarcinoma and Barrett adenocarcinoma, those which are difficult to distinguish for progressed cancer. Although there is concern for increase in adenocarcinoma of the esophagogastric junction including Barrett adenocarcinoma with decreasing *H. pylori* infection rate in Japan, the frequency of Barrett adenocarcinoma among esophageal carcinoma in Japan is currently lower compared with that in the EU or the United States (small percent of esophageal carcinoma).

For stage of adenocarcinoma arising in Barrett mucosa, the rule is same as the previously mentioned rules for esophageal carcinoma. For this disease, however, sometimes there is new muscularis mucosa just under the columnar epithelium. In the Japanese classification, the primary muscularis mucosa is called deep muscularis mucosa (DMM), and the new muscularis mucosa is called superficial muscularis mucosa (SMM). The identification of SMM and DMM is occasionally difficult due to fusion of both of the layers, thickness, and irregularity.

When the location of muscularis mucosae and cancer invasion are evaluated, careful evaluation may be required for endoscopic therapy, including evaluation of vessels invasion. This is the issue that does not exist in other EGI together with muscularis mucosae-tangled case of Ip cancer of large intestine.

1.5.2 Stomach: Fundic Gland Type Tumor [6]

Recently, fundic gland type tumor has been a focus of attention as neoplastic change associated with non-Hp, with lesion which is difficult to be diagnosed by biopsy. It is sometimes difficult to distinguish benign tumor from malignant tumor. This disease caught the public's attention in 2010 as low-grade differentiated gastric cancer indicating differentiation to fundic glands with predominantly principal cell. MUC6 (mucous neck cell) or pepsinogen I becomes positive immunohistologically. Parietal cells stained by ATPase are often observed in tumor and this is considered to support the diagnosis. The appearance may be endoscopically similar to carcinoid. It is called oxyntic gland polyp/adenoma in Europe and the United States. This tumor is considered to be *H. pylori* negative; however, it also develops in *H. pylori* positive mucosa of the fundic gland. Therefore, it would catch the public's attention as a target of endoscopic therapy in the future.

1.5.3 Colon and Rectum

1.5.3.1 SSA/P with Cytological Dysplasia

Colorectal serrated lesions are pathologically classified as hyperplastic polyps (HPs), sessile serrated adenoma/polyps (SSA/Ps), or traditional serrated adenomas (TSAs). Of these, SSA/Ps and TSAs are regarded as premalignant lesions in the serrated neoplastic pathway to colorectal carcinoma (CRC). Thus, these serrated polyps have attracted much attention in the study of carcinogenesis [7].

SSA/Ps have molecular feature of activating point mutations in the *braf* and hypermethylation of CpG islands in the promotor of tumor suppressor (i.e., the CpG island methylation phenotype (CIMP)) [8]. Both these features are detected in

colorectal carcinomas with microsatellite instability (MSI), suggesting SSA/Ps are the most potent processor lesions of colorectal carcinomas.

Interval colorectal cancers (post-colonoscopy colorectal cancer: PCCRC) have been demonstrated to be more likely to exhibit CIMP and MSI than non-interval colorectal cancers, indicating SSA/Ps may also be precursor lesions of interval cancers [9]. Some SSA/Ps may be overlooked or incompletely removed because of their subtle, flat morphology, or indistinct borders, which can result in the development of interval cancers.

However, from the general statement of tumor, the problem of SSA/P is whether it is tumor or remains tumor-like lesion. It is currently considered to be tumor-like lesion; however, some consider as tumor because it is genetically monoclonal. Considering the diagnosis for tumor by both of cellular atypia and structural atypia, it may be difficult to make morphological diagnosis. On the other hand, no one would deny that SSA/P with cytological dysplasia is regarded as tumor based on morphological diagnosis [10].

Cytological dysplasia (CD) in the SSA/P was classified into the following four types: (1) conventional adenoma-like dysplasia, (2) serrated dysplasia with eosinophilic cytoplasm, (3) serrated dysplasia without eosinophilic dysplasia, and (4) "cryptal dysplasia (tentative name)." Conventional adenoma-like dysplasia was defined as dysplasia that cytologically looked similar to a conventional tubular or tubulovillous adenoma. Serrated dysplasia was subclassified into two types according to the presence or absence of prominent eosinophilic cytoplasm. Serrated dysplasia with eosinophilic cytoplasm was defined as dysplasia that cytologically looked similar to a TSA with prominent eosinophilic cytoplasm. Serrated dysplasia without eosinophilic cytoplasm was defined as dysplasia that cytologically looked similar to a TSA but exhibited no prominent eosinophilic cytoplasm.

Previously unreported type of CD localized in the crypt base was detected that could neither be classified as conventional adenoma-like dysplasia nor serrated dysplasia in some cases. Such cryptal dysplasia shows high Ki-67 index occasionally associated with abnormality in p53.

These diseases also may be a target of endoscopic therapy as second or third carcinoma in the aging society in the future. Lesions with over 10 mm of hyperplastic polyp-like appearance (IIa/LST) in the right side colon is the point of diagnosis in elderly person.

1.5.3.2 IBD Dysplasia/Carcinoma

Inflammatory Bowel Disease (IBD) associated with carcinoma/dysplasia (IBD dysplasia/carcinoma) is one of problems for pathological diagnosis. It is unlikely that characteristic histological findings of dysplasia (noninvasive tumor lesion associated with IBD) and cancer have become generalized.

These are sometimes called dysplasia/dysplasia-associated lesions and masses: DALMs, also taking into account macroscopic images.

IBD cancer includes standard differentiated adenocarcinoma, but has more poorly differentiated adenocarcinoma (por) or neuroendocrine cell carcinoma (NEC) than normal carcinoma. Even mucinous adenocarcinoma (muc) or Signet-ring cell carcinoma (sig) is sometimes seen [11]. The terms such as in situ anaplasia or pancellular type neoplasia has been proposed by Riddell et al. [12, 13]. There are several patterns for the form of dysplasia.

While nuclear atypia of adenomatous type neoplasia has similar form to standard adenoma (sporadic adenoma: SA), structural atypia has villious or club-shaped villi different from SA. Some patients show invasion in crypt. The invasion mode is also different from SA in terms of proliferation being different between cortical layer and deep part. Basal cell type neoplasia is not common and sometimes diagnosed as regenerating epithelium. As the features, stratified nuclei or nucleus rotundus called beluga caviar like nucleus rotundus associated with cascade nucleus without disorder of polarity should be focused on. Regarding clear cell type neoplasia, which can be regarded as serrated lesion, it is difficult to consider where the tumor lesion starts, similar to diagnosis of serrated lesions. It may be diagnosed as hyperplastic mucosa in some cases, possibly already associated with the invasion in the deep part. Additionally,

structural or cellular atypia associated with IBD cancer/dysplasia includes crawling glands and dystrophic goblet cells. There are problems with pathological diagnosis affecting the treatment option [14]. Clinicopathological efforts are required for uniform accessibility in the future. If increase in IBD cancer is expected, genetic diagnosis should be considered to narrow down subjects with complication of cancer (high-risk group) [15, 16].

On the other hand, malignant transformation of Crohn's disease (CD cancer) is still at the stage of case report in Japan. Recent statistics reported that the cumulative incidence rate of UC cancer is 2% in 10 years, 2.5–8% in 20 years, and 8–18% in 30 years of duration of illness as average data. In Japan, 5% in 10 year and 10% in 20 years according to the report. On the other hand, regarding CD cancer, there is report as 2–3% in 10 years, 5–6% in 20 years, and 8–9% in 30 years. The number of subjects is small in Japan with 1% or less. Historically, UC cancer has been reported in 1925 by Crohn and Rosenberg [17] for the first time and CD cancer has been reported in 1948 by Warren et al. [18] for the first time. In Japan, the number of subjects with long-term follow-up for IBD is increasing, indicating the possibility of increase in IBD cancer.

It has been demonstrated that the mode of carcinogenesis of UC cancer is different from that of sporadic colorectal cancer. A *p53* genetic mutation occurs at a relatively early stage, resulting in multiple premalignant lesions called dysplasia (tumor). The *p53* genetic mutation may occur in mucosa which cannot be morphologically diagnosed [19]. Subsequently, genetic abnormality involved in dysplasia-invasive carcinoma is added. The mechanism mediated reactive oxygen or nitrogen is considered as the cause of genetic mutation. Recently, a gene editing enzyme inducing mutation to DNA or RNA has been identified and it has been demonstrated that especially activation-induced cytidine deaminase (AID) develops *p53* genetic mutation at a high rate because of the persistent expression [20]. The results from the future research are required together with abnormal methylation of DNA and inflammatory carcinogenesis [21]. These early-stage lesions will be target for endoscopic therapy (for purpose of diagnosis and treatment).

1.5.3.3 Clinical Evaluation and Treatment of T1-Ip Type Carcinoma [3]

The subclassification of early carcinoma (0 type; superficial type) is as follows: I: Protruding type (Ip: pedunculated, Isp: subpedunculated, Is: sessile) and II: Superficial type (IIa: Slightly elevated type, IIb: Superficial and flat type, IIc: Slightly depressed type). The superficial type represents lesions possibly including Tis (intramucosal carcinoma), T1 carcinoma (submucosal invasive carcinoma). For macroscopic judgment of superficial type, endoscopic findings are taken priority for large intestine. There is even a term called LST (laterally spreading tumor) for laterally spreading tumor with a diameter of 10 mm or more [22].

Regarding Ip type carcinoma, disrupted muscularis mucosae in some cases cannot be measured the invasion depth. In reports on metastases to lymph nodes of Ip carcinomas [23], 384 cases were tabulated from multiple centers to investigate the rate of metastasis to lymph node/recurrence from observation period for 44 months in average. The rate of metastasis to lymph nodes in all cases was 3.5% and metastasis to lymph nodes and recurrence of head invasion cases were zero; however, the rate of metastasis to lymph nodes was 6.2% and the rate of recurrence was 0.8% in the pedicle invasion cases.

This is the reason why head invasion is clinically regarded as intramucosal invasive carcinoma. For T1 colorectal carcinomas only associated with head invasion, the rate of metastasis to lymph node/recurrence was extremely low, resulting in the conclusion that it is likely to be completely cured by endoscopic therapy.

This is clinically relevant for diagnosis of head invasion. Although T1 cancer (Ip) is a lesion which can be completely cured by endoscopic therapy, sufficient accuracy control of endoscopic excision and pathological diagnosis is necessary. In the future, in case of diagnosis made for Ip type carcinoma, a strategy to directly

measure from level 2 line as intramucosal carcinoma for head invasion, and SM (T1) carcinoma for pedicle invasion is important to consider additional surgery.

1.6 Conclusion

In this issue, we have discussed the early carcinomas of EGI tracts and several problems and Japanese topics related to the pathological diagnosis.

We hope that this English textbook will be widely accepted and used worldwide to bring about improvements in quality of diagnosis, treatment, and prognosis of patients with early carcinomas in EGI tracts.

Acknowledgments The author thanks Dr. W, Sano (Sano Hospital, Division of Internal Medicine) for data analysis of SSA/P with cytological dysplasia, and Dr. K, Ichikawa, Dr. T. Tashiro, Ms. Y. Nishikawa and all staff of Shinko Hospital, Division of Pathology Department, for pathological analysis, and Ms. A. Kikuchi and Mr. Y. Nagata, staff of Medical Management Company (All drafts of manuscripts were typed by them).

References

1. Japanese Classification of Esophageal Cancer. Japan Esophageal Society. 10th ed. Tokyo: Kanehara; 2008.
2. Japanese Classification of Gastric Carcinoma, Japanese Research Society for Gastric Cancer. Tokyo: Kanehara; 1995.
3. Japanese Classification of Colorectal Carcinoma, Japanese Society for Cancer of the Colon and Rectum. 2nd ed. Tokyo: Kanehara; 2009.
4. Watanabe T, Itabashi M, Shimoda T, et al. Japanese Society for Cancer of the colon and Rectum (JSCCR). Guideline 2014 for treatment of colorectal cancer. Int J Clin Oncol. 2015;20:207–39.
5. Kitajima K, Fujimori T, Fujii S, et al. Correlations between lymph node metastasis and depth of submucosal invasion in submucosal invasive colorectal carcinoma: a Japanese collaborative study. J Gastroenterol. 2004;39:534–43.
6. Ueyama H, Yao T, Nakashima Y, et al. Gastric adenocarcinoma of fundic gland type (chief cell predominant type): proposal for a new entity of gastric adenocarcinoma. Am J Surg Pathol. 2010;34: 609–19.
7. Leggett B, Whitehall V. Role of the serrated pathway in colorectal cancer pathogenesis. Gastroenterology. 2010;138:2088–100.
8. Gaiser T, Meinhardt S, Hirsch D, et al. Molecular patterns in the evolution of serrated lesion of the colorectum. Int J Cancer. 2013;132:1800–10.
9. Burgess NG, Tutticci NJ, Pellise M, Bourke MJ. Sessile serrated adenoma/polyps with cytologic dysplasia: a triple threat for interval cancer. Gastrointest Endosc. 2014;80:307–10.
10. Rex DK, Ahnen DJ, Baron JA, Batts KP, Burke CA, Burt RW, et al. Serrated lesions of the colorectum: review and recommendations from an expert panel. Am J Gastroenterol. 2012;107:1315–29.
11. Tomita S, Fujii S, Fujimori T. Pathological issues of ulcerative colitis/dysplasia. In: Miskovitz P, editor. Colonoscopy. Croatia: Intechweb.Org; 2011. p. 139–52.
12. Riddell RH. The precarcinomatous phase of ulcerative colitis. Curr Top Pathol. 1976;63:179–219.
13. Riddell RH, Goldman H, Ransohoff DF, et al. Dysplasia in inflammatory bowel disease: standardized classification with provisional clinical applications. Hum Pathol. 1983;14:931–68.
14. Fujimori T, Fujii S, Saito N, et al. Pathological diagnosis of early colorectal carcinoma and its clinical implications. Digestion. 2009;79:40–51.
15. Issa JP, Ahuja N, Toyota M, et al. Accelerated age-related CpG island methylation in ulcerative colitis. Cancer Res. 2001;61:3573–7.
16. Fujii S, Fujimori T, Chiba T, et al. Efficacy of surveillance and molecular markers for detection of ulceractive colitis-associated colorectal neoplasia. J Gastroenterol. 2003;28:1117–25.
17. Crohn BB, Rosenberg H. The sigmoidoscopic picture of chronic ulcerative colitis (non-specific). Am J Med Sci. 1925;170:220–8.
18. Warren S, Sommers SC. Cicatrizing enteritis as a pathologic entity; analysis of 120 cases. Am J Pathol. 1948;24:475–501.
19. Fujii S, Fujimori T, Chiba T. Usefulness of analysis of p 53 alteration and observation of surface microstructure for diagnosis of ulcerative colitis-associated colorectal neoplasia. J Exp Clin Cancer Res. 2003;22:107–15.
20. Endo Y, Marusawa H, Kou T, et al. Activation-induced cytidine deaminase links between inflammation and the development of colitis-associated colorectal cancers. Gastroenterolgy. 2008;135:889–98, e1–3.
21. Tominaga K, Fujii S, Mukawa K, et al. Prediction of colorectal neoplasia by quantitative methylation analysis of estrogen receptor gene in nonneoplastic epithelium from patients with ulcerative colitis. Clin Cancer Res. 2005;11:8880–5.
22. Kudo S, Lambert R, Allen JI, et al. Nonpolypoid neoplastic lesions of the colorectal mucosa. Gastrointest Endosc. 2008;68:S3–S47.
23. Matsuda T, Fukuzawa M, Uraoka T, et al. Risk of lymph node metastasis in patients with pedunculated type early invasive colorectal cancer: a retrospective multicenter study. Cancer Sci. 2011;102: 1693–7.

Morphological Description of Early GI Neoplasia

2

Shinji Tanaka

The Paris classification has been widely used as a macroscopic classification of superficial neoplastic lesion in colon (Fig. 2.1) [1]. In brief, it is divided into polypoid and non-polypoid (superficial) lesion. In this classification, the height of the 0-Is lesion is clearly defined in each organ. As for neoplasia in the columnar epithelium (Barrett's esophagus, stomach and colon), 0-Is lesion is determined to be higher than 2.5 mm (the height of the closed biopsy forceps). On the other hand, regarding neoplasia in the squamous cell epithelium, 0-Is lesion is determined to be higher than 1 mm. The reason for this is based on the fact that esophageal squamous carcinoma higher than 1 mm shows high frequency of submucosal invasion.

In Japan, in esophagus and stomach 0-Ip and 0-Is are got together into 0-I. Because of the difficulty in exact measuring of the height of the lesion in clinical practice, gastric 0-Is is determined to be higher than about 2–3 mm. However, regarding neoplasia in the squamous cell epithelium, 0-I lesion is determined to be higher than 1 mm as well as Paris classification. As for colorectal lesion in Japan, polypoid type is divided three subtypes: 0-Ip, 0-Isp (subpedunculated) and 0-Is (Fig. 2.2). Also, the absolute height is not defined and macroscopic type emphasize the real shape of the lesion based on the reason I mentioned above. As there are no acid and peptic ulcer, Japanese classification does not include 0-III in early colorectal neoplasia.

The term "laterally spreading tumor" (LST) was originally proposed by Kudo for colorectal tumors that tend to extend laterally and circumferentially, rather than vertically along the colonic wall [2]. Recently, the concept of LST has been accepted not only in Japan but also in Western countries (Fig. 2.3) [3]. LSTs are divided into two subtypes based on their detailed endoscopic appearance: granular type (LST-G), which has even or uneven nodules on the surface, and non-granular type (LST-NG), which has a smooth surface. Furthermore, each type has two subtypes: LST-G has a "homogeneous type" and a "nodular mixed type," while LST-NG has a "flat elevated type" and "pseudodepressed type."

Besides, the term "LST" is not the terminology for morphologic classification [3]. The term LST is a nickname for superficially spreading tumor [3]. Relationship between macroscopic classification and LST subclassification is described in Fig. 2.3. Generally, LST-G homogeneous type has a lower malignant potential than LST-G nodular mixed type, and that LST-G homogeneous type has a very low frequency of submucosal invasion [4, 5]. On the other hand, LST-NG, pseudodepressed type shows a higher

S. Tanaka (✉)
Endoscopy and Medicine, Graduate School of Biomedical & Health Sciences, Hiroshima University, Hiroshima, Japan
e-mail: colon@hiroshima-u.ac.jp

P. W. Y. Chiu et al. (eds.), *Endoscopy in Early Gastrointestinal Cancers, Volume 1*,
https://doi.org/10.1007/978-981-10-6769-3_2

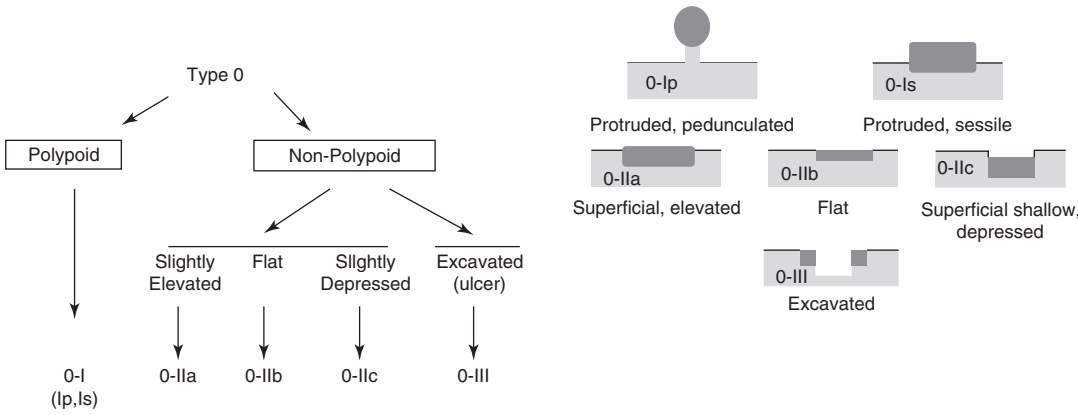

Fig. 2.1 The Paris endoscopic classification of superficial neoplastic lesions; esophagus, stomach, and colon. November 30–December 1, 2002, Participants in the Paris Workshop, Paris, France

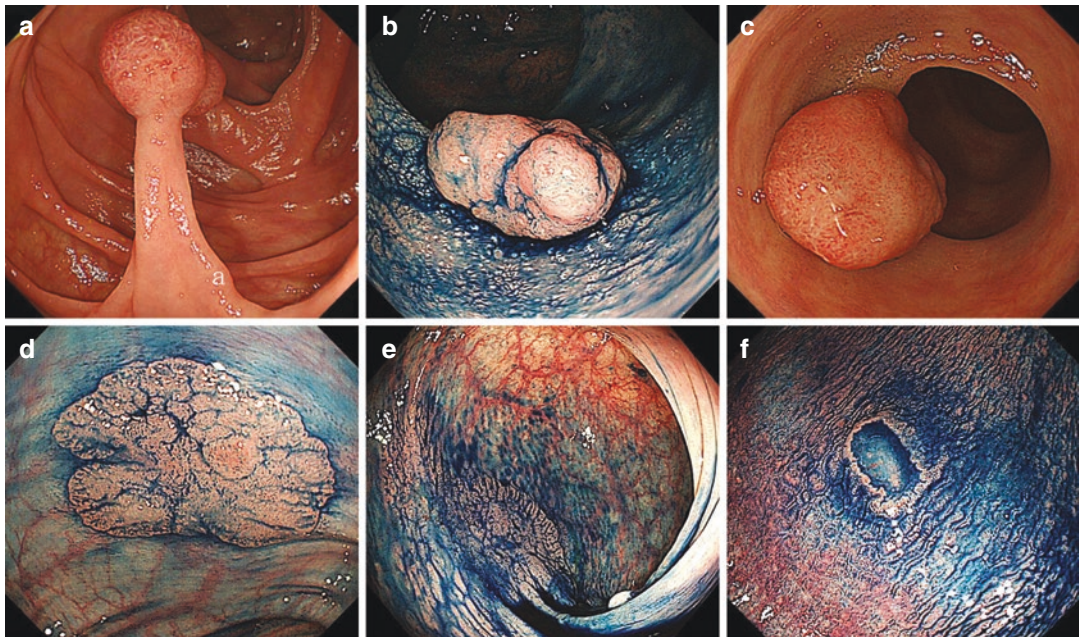

Fig. 2.2 Each lesion among macroscopic classification (colorectal tumor). (**a**) 0-Ip type, polyp with distinct stalk, (**b**) 0-Isp type, subpedunculated shape (globular shape), (**c**) 0-Is type, broad based polypoid lesion, (**d**) 0-IIa type, superficial flat elevated shape, (**e**) 0-IIb type, height of the lesion is almost equal to surrounding normal mucosa, (**f**) 0-IIc type, superficial depressed shape often accompanied by slight marginal elevation (reactive hyperplasia)

malignant potential and has a very high frequency of submucosal invasion, often multifocally [4, 5].

The recognition of detailed gross appearance and its classification is very important in daily endoscopic examination. Although there are few reports in this point of view [6], for recognition of the detailed gross appearance contrast chromoendoscopy such as indigo carmine dye spraying is useful. Staining chromoendoscopy such as crystal violet or methylene blue staining is useful in detailed observation of lesion surface pattern (pit pattern) using magnification; however, it is not suitable for diagnosis of gross appearance, especially for shallow depressed area and concavity and convexity.

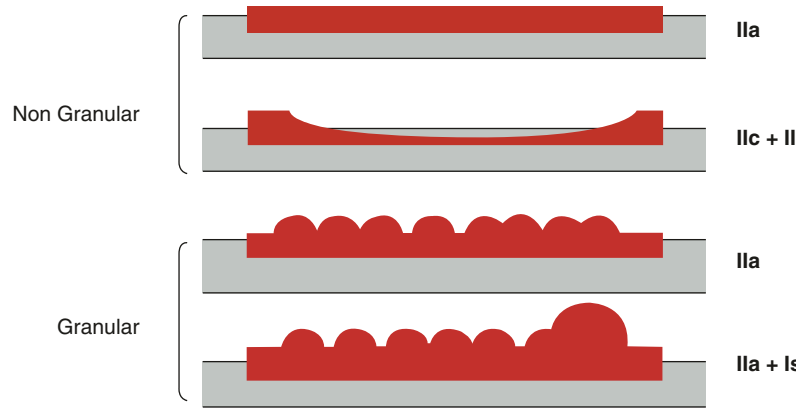

Fig. 2.3 Relationship between macroscopic classification and LST subclassification. Cited from Kudo S, et al. Nonpolypoid neoplastic lesions of the colorectal mucosa. *Gastrointest Endosc* 68, 2008 (Suppl)

TABLE 2. Subtypes of LST lesions: morphologic classification of LST lesion and their correspondance the Paris-Japanese classification*

Subtypes of LST	Classification in type 0
LST granular	
Homogenous type	0-IIa
Nodular mixed type	0-IIa, 0-Is + IIa, 0-IIa + Is
LST nongranular	
Elevated type	0-IIa
Pseudodepressed type	0-IIa + IIc, 0-IIc +IIa

* the term " laterally spreading type (LST)" refers to the lateral growth of lesions at least 10 mm in diameter; this is in opposition to traditional polypoid (upward growth) or flat and depressed lesions (downward growth).

References

1. Lambert R, Lightdale CJ. The Paris endoscopic classification of superficial neoplastic lesions: esophagus, stomach, and colon. Gastrointest Endosc. 2003;58(Suppl):S3–S27.
2. Kudo S. About laterally spreading tumor. Early Colorectal Cancer. 1998;2:477–81 (in Japanese with English abstract).
3. Kudo S, Lambert R, Allen JI, et al. Nonpolypoid neoplastic lesions of the colorectal mucosa. Gastrointest Endosc. 2008;68(Suppl):S3–S47.
4. Uraoka T, Saito Y, Matsuda T, et al. Endoscopic indications for endoscopic mucosal resection of laterally spreading tumours in the colorectum. Gut. 2006;55:1592–7.
5. Oka S, Tanaka S, Kanao H, et al. Therapeutic strategy for colorectal laterally spreading tumor. Dig Endosc. 2009;21(Suppl 1):S43–6.
6. Shigita K, Oka S, Tanaka S, et al. Clinical significance and validity of the subclassification for colorectal laterally spreading tumor granular type. J Gastroenterol Hepatol. 2016;31:973–9.

3 Endoscopic Diagnosis of Superficial Esophageal Neoplasia

Pankaj Shrimal, Rupa Banerjee, and Philip W. Y. Chiu

3.1 Introduction

Esophageal cancer is an aggressive tumor with high mortality rate and most patients who present with symptomatic tumor have poor prognosis despite best of the standard care.

As per Globocan 2012 data [1] oesophageal cancer is the eighth most common cancer worldwide, with approximately 455,000 new cases in 2012 and age standardized rates of 5.9 per 100,000. It is the sixth most common cause of cancer-related death, with an estimated 400,000 cases in 2012 and age standardized rates of 5.0 per 100,000.

Generally, esophageal cancers consisted of squamous cell carcinoma (ESCC) developing from the esophageal epithelium and adenocarcinoma (EAC) developing from reflux related metaplastic Barrett's epithelium. Both the histologic types have different risk factors, location in esophagus, and geographic distribution. EAC is the predominant type of esophageal cancer in North America and Europe, especially among white men [2], while ESCC is more common in the so-called "esophageal cancer belt" which extends from northern Iran through the central Asian republics to North-Central China [3]. Barrett's esophagus is a known precursor for oesophageal adenocarcinoma especially when associated with high-grade dysplasia. A meta-analysis [4] which included 57 studies showed that pooled annual incidence of EAC in patients with nondysplastic Barrett's esophagus was as low as 0.33% (95% CI 0.28–0.38%), while another meta-analysis [5] which included 24 studies showed that the pooled annual incidence rates of EAC in patients with BE with low-grade dysplasia (LGD) was 0.5% (95% CI 0.3–0.8) and for high-grade dysplasia (HGD) and/or EAC combined was 1.7% (95% CI 1.0–2.5). The risk of EAC for patients with HGD was examined in a meta-analysis [6] of four studies including 236 patients. The weighted annual incidence rate was 7% (95% CI 5–8).

The overall prognosis of oesophageal malignancy depends to a large extent on the timing of diagnosis. The five-year survival rate for oesophageal SCC can be up to 70% for early superficial neoplasia, while it is only 15% for advanced stage cancers [7]. In a long-term follow-up study in China, the 5 years, 10 years, and 20 years' survival rates for patients discovered by screening were found to be 86%, 75%, and 64% respectively [8].

Cancer detection at an early stage provides opportunity for endoscopic treatment, obviates need for morbid surgical procedure of

P. Shrimal · R. Banerjee (✉)
Asian Institute of Gastroenterology, Hyderabad, India

P. W. Y. Chiu
Department of Surgery, Faculty of Medicine, The Chinese University of Hong Kong, Hong Kong, Hong Kong

P. W. Y. Chiu et al. (eds.), *Endoscopy in Early Gastrointestinal Cancers, Volume 1*,
https://doi.org/10.1007/978-981-10-6769-3_3

esophagectomy and thus improves prognosis. Endoscopic resection has shown good results for tumors limited to mucosal layer as the risk of lymph node metastasis has been found to be very low.

3.2 Superficial Esophageal Neoplasia

Superficial esophageal neoplasia is defined as cancer confined to mucosa and submucosa without lymphatic spread and distant metastasis. Tumors at this early stage are usually asymptomatic. However, these are the lesions which are amenable to cure by endoscopic resection.

Standard white light endoscopy (WLI) may miss the subtle lesions of superficial oesophageal neoplasia [9]. This is because the early cancer lesions are usually flat and may appear isochromatic to surrounding mucosa on WLI. Advanced endoscopic imaging technologies like chromoendoscopy, autofluorescence imaging (AFLI), and narrow band imaging (NBI) are therefore a useful adjunct to detect these early lesions of esophagus which are potential targets for endoscopic curative resection.

Chromoendoscopy was the first enhancement technique used. This combines endoscopy with spraying of various dyes on the mucosa in order to facilitate visualization of benign versus cancerous mucosal changes. Several staining agents have been described that can broadly be categorized as absorptive (vital) stains, contrast stains, and reactive stains. Absorptive stains (e.g., Lugol's iodine solution and methylene blue) diffuse or are preferentially absorbed across specific epithelial cell membranes; Contrast stains (e.g., indigo carmine) highlight surface topography and mucosal irregularities by permeating mucosal crevices and Reactive stains (e.g., Congo red and phenol red) undergo chemical reactions with specific cellular constituents, resulting in a color change.

Chromoendoscopy is an excellent technique to detect early esophageal cancer (EEC) and has been widely used. However, the technique is often operator dependent and time consuming. It requires additional instruments like the spray catheter and the dye may not spread evenly across the mucosal surface. Additionally switching between white light view and chromoendoscopic view is not possible. The vascular microstructure is difficult to assess after spraying dye and can be distorted by the use of dyes like acetic acid which causes vascular congestion. Moreover, the risks of aspiration pneumonitis particularly in sedated elderly patients limits its usage.

Image Enhanced Endoscopy (IEE) using technologies such as narrow band imaging (NBI) or fuji intelligent chromoendoscopy (FICE) can overcome most of these limitations and is now preferred in clinical practice particularly for the early detection of early squamous esophageal cancers. This chapter aims to discuss the role of NBI in the detection of superficial oesophageal neoplasia.

3.3 Technology of Narrow Band Imaging

In conventional WLI, the image is captured with a CCD (charge-coupled device) chip, transmitted electronically, and displayed on a video monitor. NBI uses special set of filters which is interposed after the light source to restrict the incident light in two narrow bands of wavelengths (blue at 415 nm and green at 540 nm).

Usefulness of NBI in detecting micro-surface and microvessels morphology depends on two factors. First the penetration depth and scattering of light. This is dependent on its wavelength with visible blue light having lower wavelength and less scattering thereby penetrating only superficial areas of tissue and visible red light with longer wavelength penetrating deeper in the tissues and more likely to be scattered when directed at the tissue. Second, hemoglobin in the tissues is a chromophore while other tissues like nuclei and fibrous tissues do not have color, so the color of mucosa is dependent on the absorption of light by hemoglobin.

The narrow band light used in NBI covers the wavelength for its peak absorption. Thus vessels in superficial layer appear brownish color and

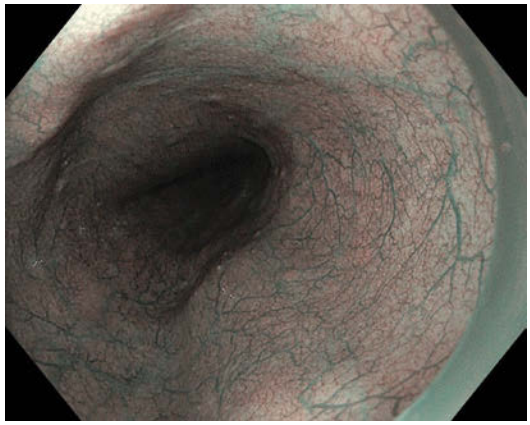

Fig. 3.1 Normal squamous esophageal mucosa under non-magnifying NBI

deeper submucosal layer appear cyan in color (Fig. 3.1). The selective reflection of the NBI light by the superficial layers of the mucosa improves the definition of the surface; while its selective absorption by hemoglobin enhances the contrast of the vascular network.

With the addition of magnification NBI, the magnifying power of the optical zoom can reach up to ×150, but usually ×80 is enough for most indications and delineates finer mucosal details brilliantly. When the zoom is activated, the focal distance between the objective and the mucosal surface decreases in proportion to the power of magnification; therefore, the tip of the instrument is placed at a very short distance of the target and a small area of the mucosa is explored. A transparent hood, fixed at the tip of the endoscope, helps to maintain an adequate and focused distance, particularly in the cardia region.

3.4 Strategy for Endoscopic Diagnosis of Early Esophageal Neoplasia

Diagnosis of early esophageal neoplasia can be optimized with systematic approach. There are two steps in endoscopic diagnosis: detection of an abnormal mucosal lesion and then characterization by detailed evaluation of the micro-surface architectural changes.

3.5 Pre-procedure Preparation and Premedication

Despite the availability of high quality and advanced imaging technology, the unclean mucosal surface of the esophagus can make these high-end pieces of equipment virtually useless. Defoaming agents like simethicone as oral solution should be used 15–30 min before procedure and can be used as frequent flushing as required during endoscopic procedure.

In general, after detecting the abnormal lesion with standard WLI or NBI, mucosal changes should be evaluated in detail with use of magnification NBI. Characterization relies on the following elements:

Configuration of the Lesion The lesion is classified according to Paris classification [10] for superficial neoplastic lesions as polypoidal (0-1) or non-polypoidal which includes slightly elevated, flat, and slightly depressed lesions (0-IIa, 0-IIb, and 0-IIc, respectively) and excavated (0-IIIc). Secondly, under narrow band imaging the demarcation line of the lesion can be recognized with a distinct color changes from background mucosa as a dark brownish appearance of superficial esophageal neoplasia (Fig. 3.2a). This is related to the prominent dilated and tortuous IPCL pattern.

Microvascular Network Evaluation of superficial vessels in subepithelial region is important as these vessels are close to the epithelial cells having high mitotic activity. In squamous esophageal mucosa, these superficial vessels are represented as intra-papillary capillary loops (IPCL). Increased in capillary diameter, tortuosity and density in these neoplastic lesions are often the first changes observed during evolving of neoplasia from LGID to HGID to cancer. The superficial blood vessels appear brownish on NBI and various changes in patterns have been described which predict histology and depth of tumor invasion.

Micro-surface Structure Fine structure of the epithelium is best explored with NBI with magnification or with dye-based chromoendoscopy. In

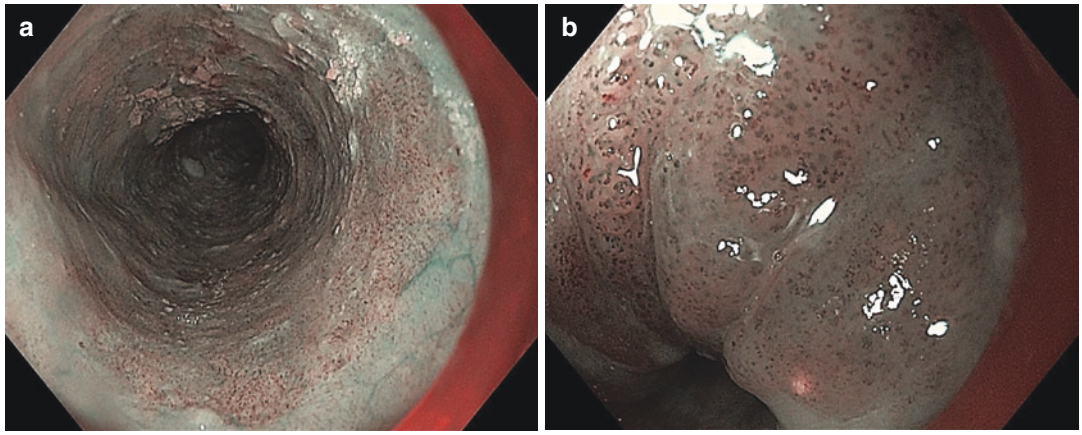

Fig. 3.2 Schema of diagnostic endoscopy for superficial esophageal neoplasia. (**a**) Detection of abnormal brownish/darken areas under NBI. (**b**) Characterization of the irregular IPCL pattern under NBI magnifying endoscopy

columnar epithelium various pit patterns have been described which correlate with depth of invasion. While in stratified squamous epithelium, pit pattern is absent and various morphology of intra-papillary capillary loops (IPCLs) have been correlated with depth of invasion (Fig. 3.2b). Hence, the changes in micro-surface structural pattern is more relevant to Barrett's esophagus related neoplasia as most of superficial squamous esophageal neoplasia only had changes in IPCL pattern.

3.6 Detection of ESCC Using NBI

Determining the T stage of esophageal cancer is of prime importance in selecting mode of treatment as well as prognosis. Studies have shown that the rate of lymph node metastases is low (2–3%) in mucosal carcinomas, but much higher (37–53%) in cases of submucosal invasion [11].

In the esophagus the surface of the normal stratified squamous epithelium has a smooth appearance with a clear pink color and no pit pattern. The diagnosis of early ESCC is based on configuration of intra-papillary capillary loops (IPCLs). IPCL are microvessels which arise perpendicularly from branching vessels in submucosal layer and are observed beneath the basement membrane of the epithelium. In the imaging with conventional endoscopy, IPCLs are usually shown as red dot-like structures with regular intervals of about 100 μm in esophageal mucosa. Under magnified imaging, normal IPCL are hairpin shaped and small in diameter. Under magnification endoscopy with NBI they appear as brown loops. Morphological changes and irregular arrangement of IPCLs are associated with inflammation and neoplasia of esophagus. The four characteristic changes of magnified appearance in squamous cell carcinoma are dilation, tortuosity, caliber change, and varying shapes of IPCLs. Based on these IPCL changes, various classifications have been proposed to predict vertical depth of neoplasia and lymph node metastasis.

3.7 Classification of IPCL Patterns: Inoue Classification

Inoue et al. [12] first described five types of IPCL patterns upon observation under magnifying endoscopy. The five different IPCL patterns (Table 3.1) have been described in association with histopathology, from normal mucosa to modified mucosa due to inflammation, dysplasia or cancer. Type I IPCL are normal looking IPCL with loop shaped, aligned in one direction without dilatation (Fig. 3.3). Type II IPCL shows slight elongation with mild dilatation (Fig. 3.3). Type III IPCL shows no changes or minimal changes (Fig. 3.4). Type IV IPCL are usually rep-

Table 3.1 Inoue original IPCL classification

IPCL types	Description	Pathology
Type I	Smooth running, small diameter capillaries	Normal
Type II	Dilatation and elongation of Type I capillaries	Inflammation
Type III	Normal IPCL within a brownish lesion	Inflammation/ LGD
Type IV	Increased vessel caliber and elongation of IPCL toward the epithelial surface	LGD/HGD
Type V1	Nonuniform, irregularly dilated IPCL	M1
Type V2	Elongation of Type V1 capillaries	M2
Type V3	Loss of loop configuration and spread to horizontal plane	M3/SM1
Type Vn	Vessel caliber 3x larger than V3—new tumor vessels	SM2

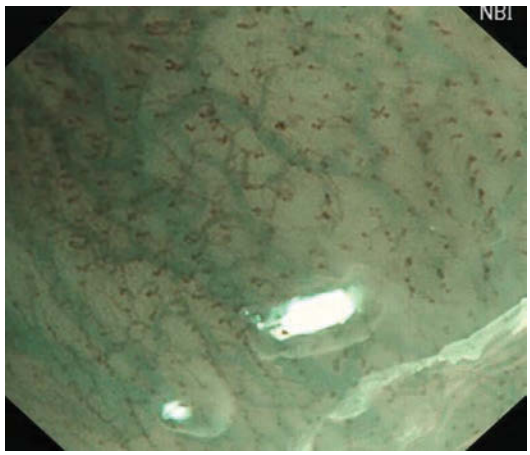

Fig. 3.3 IPCL Type I/II; Inoue Group 1; JES Type A

resented by presence of dilatation with increased in caliber, and tortuous pattern. Type V IPCL demonstrate all four characteristic changes including dilatation, tortuous weaving, caliber changes, with different shapes in each of the IPCL. Type V IPCL is further classified into V1, 2, 3, and Vn. In Type V1, IPCL appears in tortuous and dilated pattern with increased in caliber (Fig. 3.5), while in type V2, IPCL changes with tortuous, dilated loops with an elongated pattern (Fig. 3.6). In Type V3, IPCL loses its loop configuration and a there is horizontal spread of

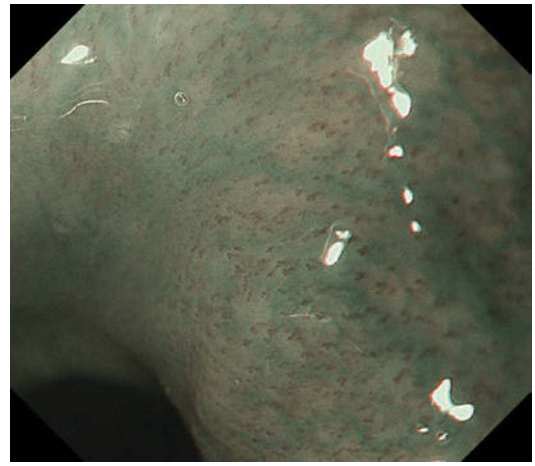

Fig. 3.4 IPCL Type III/Inoue Group 2/JES Type A

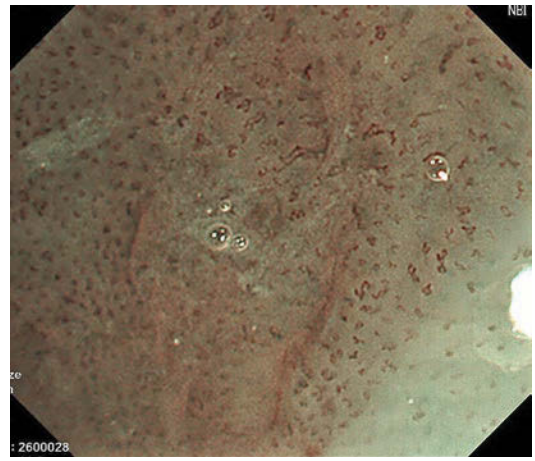

Fig. 3.5 IPCL Type V1/Inoue Group 3A/JES B1

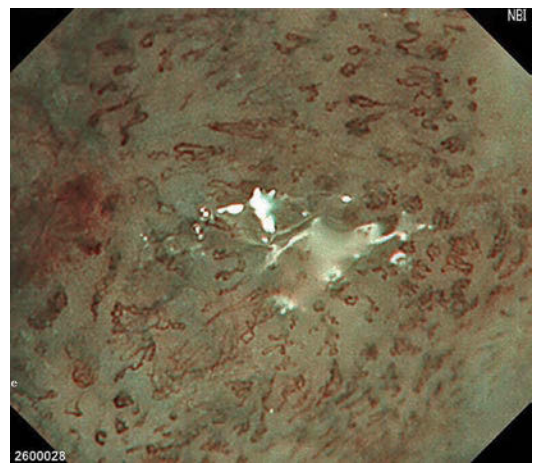

Fig. 3.6 IPCL Type V2; Inoue Group 3A; JES Type B2

these changes. Type V3 pattern was further subclassified into Type V3a where all vessels run on a horizontal plane and in IPCL 3b these changes extend perpendicularly in a deeper mucosa. V1 correlates with m1 and V2 correlates with m2 lesions where risk of lymph node metastasis is low, and hence these lesions are best candidates for endoscopic resection (EMR/ESD).

The major criterion for differentiating IPCL-V3 and -Vn is that of vessel caliber. IPCL-Vn vessels, which appear in massively invasive submucosal carcinoma, have a caliber approximately three times larger than that found in IPCL-V3 (Fig. 3.7). IPCL-Vn is observed as large green vessels, whereas IPCL-V1 to -V3 are observed as small brown vessels.

These IPCL patterns have been correlated with histopathological diagnosis. Type I corresponds to normal mucosa, type II to inflammation, type III corresponds to borderline lesions, often related to low-grade intraepithelial neoplasia, type IV and V corresponds to high-grade intraepithelial neoplasia (HGIN) or carcinoma [13]. In one study, IPCL V3b as compared to V3a has shown relatively higher risk of SM invasion: IPCL-V3a correlated with M2 disease in 60%, M3SM1 disease in 40%, while, IPCL-V3b correlated with M3SM1 disease in 70% and SM2 disease in 30%, respectively [14].

According to Inoue classification, Kumagai et al. reported the accuracy rate of 83.1% in diagnosing depth of superficial esophageal cancers on the basis of NBI with magnification endoscopy [15].

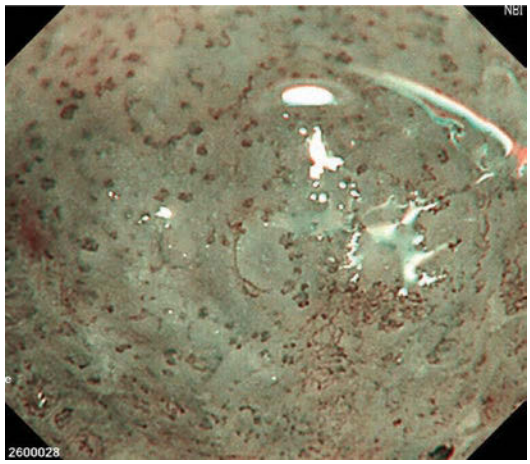

Fig. 3.7 IPCL Type Vn; Inoue Group 3B; JES Type B3

3.8 Classification of IPCL Pattern: Arima Classification

Arima et al. [16] reported their classification of microvascular patterns using magnifying endoscopy. Type 1 was characterized by thin, linear capillaries in subepithelial papillae, similar to the normal mucosa. Type 1 vessels are seen in normal mucosa. Type 2 was characterized by dilated, regularly arranged vessels with preserved capillary structure in subepithelial papillae. Type 2 vessels are seen in inflammatory lesions. Type 3 was characterized by destruction of vessels in subepithelial papillae, spiral vessels of irregular caliber, and crushed vessels with red spots. Type 3 vessels are seen in severe dysplasia and m1/m2 cancers. Type 4 was characterized by irregular multilayered, irregularly branched, reticular vessels. The size of avascular areas (AVA) surrounded by distended type 4 vessels is related to the depth of tumor invasion. Reticular vessels are commonly seen in poorly differentiated cancers.

3.9 Classification of IPCL Pattern: Simplified Inoue Classification

As there is certainly difficulty in clinical application of the conventional IPCL classification, Inoue et al. (Table 3.2) proposed a simplified classification for planning of treatment for early ESCC. They combined original five titer IPCL types into three groups: Group 1 (nonneoplastic: IPCL I, II), Group 2 (borderline: IPCL III, IV), Group 3 (cancer: IPCL V). Group 1 lesions (Fig. 3.3) require no treatment; group 2 (Fig. 3.4) mandates careful follow-up or prophylactic therapy; and group 3 definitely demands therapy.

For more precise histopathological correlation these groups can be subdivided: Group IA (normal tissue, IPCL I); IB (inflammation, IPCL II);

Table 3.2 Inoue IPCL simplified classification

Groups	IPCL pattern	Management
Group 1	Nonneoplastic (IPCL-I, -II)	No treatment
Group 2	Borderline (IPCL-III, -IV)	Careful follow-up or prophylactic therapy
Group 3	Cancer (IPCL-V)	Treatment is required
3A	Intramucosal cancer (IPCL-V1, -V2)	
3A'	Deep M or superficial SM cancer (IPCL-V3)	
3B	Submucosal cancer (IPCL-VN)	

II (low-grade dysplasia, IPCL III, IV); and III (cancer, IPCL V).

Group 3 can then be subdivided into two main subcategories, each according to its characteristic microvascular appearance. Group 3A (Fig. 3.5) has both loop-like vessels which correspond to M1 and M2 lesions (IPCL V1/2). In group 3A' (Fig. 3.6) the distorted vessel which has already lost loop-like figure (IPCL V3) is usually related both deep mucosal and superficial SM invasion. Group 3B (Fig. 3.7) corresponds almost exclusively to submucosal cancer, being characterized by large abnormal vessels (IPCL VN), which are three times the caliber of Group-3A vessels.

According to the Japanese guidelines for diagnosis and treatment of esophageal cancer, T1a-EP or T1a-LPM SCC is considered an absolute indication for Endoscopic resection; T1a-MM or T1b-SM1, a relative indication; and T1b-SM2, an investigative stage (functionally speaking, a contraindication).

3.10 Classification of IPCL Pattern: Japan Esophageal Society (JES) Classification

To simply clinical decision making regarding endoscopic resection of early ESCC, recently Japan Esophageal Society (JES) proposed simplified classification [17] of microvessel morphology based on magnifying endoscopy. According to JES, the microvascular irregularity is evaluated for the presence or absence of each of the following morphological factors: weaving (i.e., tortuosity), dilatation, irregular caliber, and different shape (i.e., various shapes). Microvessels are classified as type A if they have three or fewer factors and type B if they have all four. Type B is then subclassified into B1, B2, and B3 based on the running pattern or degree of dilatation of severely irregular microvessels (Table 3.3).

Type A: Normal IPCL or abnormal microvessels without severe irregularity (Figs. 3.3 and 3.4).

Type B: Abnormal microvessels with severe irregularity or highly dilated abnormal vessels.

B1 is defined as type B vessels with a loop-like formation (Fig. 3.5). The B1 vessels normally appear as dot-like microvessels in a target area (e.g., a brownish area) under NBI endoscopic observation with low or no magnification. B2 is defined as type B vessels without a loop-like formation that have a stretched and markedly elongated transformation (Fig. 3.6). The B2 vessels often show a multilayered arrangement or an irregularly branched/running pattern. B3 is defined as highly dilated abnormal vessels whose caliber appears to be more than three times that of the usual B2 vessels and the B3 vessels often appear green in color (Fig. 3.7).

When target lesions have only type B1 vessels, the histological invasion depth is predicted as T1a-EP or T1a-LPM. When B2 and B3 vessels are seen in target lesions, the histological invasion depth is predicted as T1a-MM or T1b-SM1 and T1b-SM2 or deeper, respectively.

3.11 NBI at the EG Junction and in Barrett's Esophagus

Normal esophageal mucosa is lined with stratified squamous epithelium which is featureless and appears pale and glossy on conventional WLI. Barrett's esophagus is defined as an area of metaplastic columnar epithelium extending above the EGJ and appears reddish and velvet-like texture on conventional WLI. Barrett's esophagus is clinically asymptomatic but is a known precursor to esophageal adenocarcinoma and carcinogenesis occurs through a sequential process of metaplasia to dysplasia to carcinoma.

Table 3.3 JES classification in relation to clinical state of the early squamous esophageal cancer

TNM staging			Lymph node metastasis	Indication for endoscopic resection	JES IPCL types
T1a, Tumor invades mucosa (M)	EP	Carcinoma in situ (Tis)	0–3.3%	Absolute	B1
	LPM	Tumor invades lamina propria mucosa (LPM)			
	MM	Tumor invades lamina muscularis mucosa (MM)	0–12.2%	Relative	B2
T1b, Tumor invades submucosa (SM)	SM1	Tumor invades the submucosa to a depth of 200 μm or less from the muscularis mucosa	8–26.5%		
	SM2	Tumor invades the submucosa to a depth more than 200 μm	22–61%	Investigative stage (Contraindication)	B3

This provides an opportunity to detect neoplasia at early stage during screening endoscopy or when surveillance endoscopies are performed in patients with confirmed BE and potential for endoscopic resection.

Standard method to detect high-grade dysplasia or early cancer in BE, is to biopsy morphologically distinct lesions, like plaques, nodules, or ulcers, and take random four quadrant biopsies every 1–2 cm (Seattle protocol) for entire length of Barrett's esophagus. This method has been described as "hit and miss" approach as the dysplasia in BE can be small and patchy. Moreover, taking multiple blind biopsies is time consuming and has been shown to sample only 4–5% of Barrett's epithelium [18, 19]

Furthermore, the sensitivity and positive predictive value of standard upper endoscopy for diagnosing BE have been reported to be only 82% and 34%, respectively [20]

NBI facilitates the detection of dysplasia by enhancing mucosal microstructure and take targeted biopsies and thus minimizing number of biopsies to detect HGD/early EAC. Various classifications have been proposed to detect dysplasia on the basis of mucosal micro-surface and microvessel architecture.

Sharma et al. (Kansas classification) [21], did a prospective study to assess the ability of NBI to accurately predict histology during screening and surveillance of BE patients. They described three specific mucosal patterns and two distinct vascular patterns based on correlation with histology in their prospective study.

Mucosal Patterns:

1. Ridge/villous pattern: presence of uniform, longitudinally aligned ridges (darker lines) alternating with a villiform pattern (lighter lines).
2. Circular pattern: presence of circular and/or oval areas arranged in a regular fashion.
3. Irregular/distorted pattern: significant distortion and irregularity of the ridge and villous pattern.

Vascular Patterns

Normal pattern: fine capillary pattern showing normal size, shape, and distribution of small blood vessels.

Abnormal pattern: increased number, and tortuous, dilated, corkscrew-type small blood vessels.

In this study, the correlation between the mucosal/vascular patterns and the histology results was very good. The sensitivity, specificity, and positive predictive value of ridge/villous pattern for diagnosis of IM without HGD were 93.5%, 86.7%, and 94.7%, respectively. The sensitivity, specificity, and positive predictive value of irregular/distorted pattern for HGD were 100%, 98.7%, and 95.3%, respectively. However, the NBI patterns did not differ significantly between nondysplastic intestinal metaplasia and LGD.

Kara et al. (Amsterdam classification) [22] designed classification system which described mucosal and vascular pattern as regular versus irregular and look for the presence of normal versus abnormal blood vessels. They simplified the

classification by grouping villous and gyrus-forming structures of various shapes and sizes into one category. They found that the regularity of the pattern is more important than a precise description of the shapes and sizes of the mucosal pits and crests. Three factors were found to be important in differentiating HGIN from nondysplastic tissues: (1) the irregularity of the mucosal pattern, (2) the irregularity of the vascular pattern, and (3) the presence of abnormal blood vessels. In all areas with HGIN, at least one of these abnormalities was present, and, in 85% of cases, two or more of these factors were detected. The frequency of these mucosal morphology abnormalities increased from nondysplastic SIM through LGIN to HGIN. As per their classification, magnified NBI images had a sensitivity of 94%, a specificity of 76%, a positive predictive value of 64%, and a negative predictive value of 98% for diagnosing HGIN.

They proposed a hierarchical (multistep) classification of the mucosal morphology in BE. First mucosal pattern should be determined followed by determination of its regularity/irregularity, because irregular patterns may be associated with a higher chance of dysplasia/cancer. The next step is the detection of the vascular pattern and determination of its regularity/irregularity, because it forms an integral and clinically relevant part of the mucosal morphology. Subsequently, the mucosa should be evaluated for the presence of abnormal blood vessels, because their presence is one of the three abnormalities that may raise a suspicion for dysplasia/cancer. Finally, the abnormal blood vessels should be described.

R Singh et al. (Nottingham classification) [23] described mucosal morphology into four different types: Type A: Round pits with regular microvasculature, Type B: Villous/ridge pits with regular microvasculature, Type C: Absent pits with regular microvasculature, and Type D: Distorted pits with irregular microvasculature. The PPV and NPV for type A pattern (columnar mucosa without intestinal metaplasia) were 100% and 97%, respectively; for types B and C (intestinal metaplasia) they were 88% and 91%, respectively; and for type D (high-grade dysplasia) 81% and 99%, respectively. Overall they found high accuracy and the "substantial to good" interobserver and intraobserver agreement exhibited by both the NBI expert and the non-NBI expert endoscopists in differentiating the mucosal classification (Table 3.4).

Recently, Barrett's International NBI Group (BING) [24] developed new classification based on magnification NBI. Mucosal and vascular patterns were classified as regular or irregular. Regular mucosal patterns were classified as circular, ridged/villous, or tubular patterns, and irregular mucosa were classified as absent or irregular surface patterns. Regular vascular patterns were defined by blood vessels situated regularly along or between mucosal ridges and/or those showing normal, long, branching patterns; irregular vascular patterns were marked by focally or diffusely distributed vessels not following the normal architecture of the mucosa. Images not readily identified as regular or irregular were classified as "uncertain."

The BING criteria can be used to predict the presence or absence of dysplasia in BE based on the

Table 3.4 Classification of Barrett's esophagus and related neoplasia

Classification systems		
Kansas	Amsterdam	Nottingham
Mucosal pattern Ridge/villous Circular Irregular/distorted	*Mucosal pattern* Regular Irregular	*Type A*: Round/oval pits with regular microvasculature *Type B*: Villous/ridge/linear pits with regular microvasculature *Type C*: Absent pits with regular microvasculature *Type D*: Distorted pits with irregular microvasculature
Vascular pattern Normal Abnormal	*Vascular pattern* Regular Irregular	
	Abnormal vessels ±	

simple classification of mucosal and vascular patterns as regular (nondysplastic) or irregular (dysplastic). The BING criteria identified patients with dysplasia with 85% overall accuracy, 80% sensitivity, 88% specificity, 81% positive predictive value, and 88% negative predictive value. When dysplasia was identified with a high level of confidence, these values were 92%, 91%, 93%, 89%, and 95%, respectively. The overall strength of interobserver agreement was substantial ($k = 0.681$).

These various classifications systems based on the mucosal and vascular architecture, were able to identify high-grade dysplasia in BE with high accuracy, but, the NBI patterns were not found to be significantly different between nondysplastic intestinal metaplasia and LGD. Although, this may not be of much significance as the diagnosis of LGD itself is almost always contentious, with high interobserver variability seen even among expert pathologists and natural progression of LGD in BE is found to be controversial. In a large database of information on BE patients, LGD regressed or remained stable in most patients and progressed to HGD/EAC in only 10.3% and adenocarcinoma in 3.2% of patients [25]

3.12 Summary

Novel imaging technologies including Narrow Band imaging (NBI) have enabled early detection and accurate characterization of superficial esophageal malignancy. With increasing availability of therapeutic procedures including endoscopic mucosal resection (EMR) and endoscopic submucosal dissection (ESD) superficial oesophageal neoplasia is potentially curable with minimal chances of lymph node metastasis.

References

1. International Agency for Research on Cancer. GLOBOCAN 2012, estimated cancer incidence, mortality and prevalence worldwide in 2012. Geneva: World Health Organization; 2012.
2. Enzinger PC, Mayer RJ. Esophageal cancer. N Engl J Med. 2003;349:2241–52.
3. Jemal A, Bray F, Center MM, et al. Global cancer statistics. CA Cancer J Clin. 2011;61:69–90.
4. Desai TK, Krishnan K, Samala N, et al. The incidence of oesophageal adenocarcinoma in non-dysplastic Barrett's oesophagus: a meta-analysis. Gut. 2012;61:970–6.
5. Singh S, Manickam P, Amin AV, et al. Incidence of esophageal adenocarci- noma in Barrett's esophagus with low-grade dysplasia: a systematic review and meta-analysis. Gastrointest Endosc. 2014;79:897–909.
6. Rastogi A, Puli S, El-Serag HB, et al. Incidence of esophageal adenocarcinoma in patients with Barrett's esophagus and high-grade dysplasia: a meta-analysis. Gastrointest Endosc. 2008;67:394–8.
7. Rice TW, Rusch VW, Ishwaran H, Blackstone EH, Worldwide Esophageal Cancer, C. Cancer of the esophagus and esophagogastric junction: data-driven staging for the seventh edition of the American Joint Committee on Cancer/International Union Against Cancer Cancer Staging Manuals. Cancer. 2010;116:3763–73. https://doi.org/10.1002/cncr.25146.
8. Wang GQ, et al. Long-term results of operation for 420 patients with early squamous cell esophageal carcinoma discovered by screening. Ann Thorac Surg. 2004;77:1740–4. https://doi.org/10.1016/j.athoracsur.2003.10.098.
9. Kodama T. Kakegawa. Treatment of *superficial* cancer of the esophagus: a summary of responses to a questionnaire on *superficial* cancer of the esophagus in Japan. Surgery. 1998;123(4):432–9.
10. Lambert R, Lightdale CJ. The Paris endoscopic classification of superficial neoplastic lesions: esophagus, stomach, and colon: November 30 to December 1, 2002. Gastrointest Endosc. 2003;58:S3–43.
11. Tajima Y, Nakanishi Y, Ochiai A, Tachimori Y, Kato H, Watanabe H, Yamaguchi H, Yoshimura K, Kusano M, Shimoda T. Histopathologic findings predicting lymph node metastasis and prognosis of patients with *superficial* esophageal carcinoma: analysis of 240 surgically resected tumors. Cancer. 2000;88(6):1285–93.
12. Inoue H. Magnification endoscopy in the esophagus and stomach. Dig Endosc. 2001;13:S40–1.
13. Yoshida T, Inoue H, Usui S, Satodate H, Fukami N, Kudo SE. Narrow-band imaging system with magnifying endoscopy for superficial esophageal lesions. Gastrointest Endosc. 2004;59(2):288–95.
14. Inoue H, Kaga M, Sato Y, et al. Magnifying endoscopic diagnosis of tissue atypia and cancer invasion depth in the area of pharyngo- esophageal squamous epithelium by NBI enhanced magnification image: IPCL pattern classification. In: Cohen J, editor. Advanced digestive endoscopy: Comprehensive atlas of high resolution endoscopy and narrow band imaging. Oxford: Blackwell; 2007. p. 49–66.
15. Kumagai Y, Inoue H, Kawano T. Magnifying endoscopic observation of superficial esophageal carcinoma. Dig Endosc. 2004;16:277–81.

16. Arima M. Evaluation of microvascular patterns of superficial esophageal cancers by magnifying endoscopy. Esophagus. 2005;2:191–7.
17. Oyama T, Inoue H, et al. Prediction of the invasion depth of superficial squamous cell carcinoma based on microvessel morphology: magnifying endoscopic classification of the Japan Esophageal Society. Esophagus. 2017;14:105–12.
18. Levine DS, Blount PL, Rudolph RE, et al. Safety of a systematic endoscopic biopsy protocol in patients with Barrett's esophagus. Am J Gastroenterol. 2000;95:1152–7.
19. Sharma P, McQuaid K, Dent J, et al. A critical review of the diagnosis and management of Barrett's esophagus: the AGA Chicago Workshop. Gastroenterology. 2004;127:310–30.
20. Eloubeidi MA, Provenzale D. Does this patient have Barrett's esophagus? The utility of predicting Barrett's esophagus at the index endoscopy. Am J Gastroenterol. 1999;94:937–43.
21. Sharma P, Bansal A, et al. The utility of a novel narrow band imaging endoscopy system in patients with Barrett's esophagus. Gastrointest Endosc. 2006;64(2):167–75.
22. Kara MA, Ennahachi M, et al. Detection and classification of the mucosal and vascular patterns (mucosal morphology) in Barrett's esophagus by using narrow band imaging. Gastrointest Endosc. 2006;64(2):155–66.
23. Singh R, Anagnostopoulos GK, et al. Narrow−band imaging with magnification in Barrett's esophagus: validation of a simplified grading system of mucosal morphology patterns against histology. Endoscopy. 2008;40:457–63.
24. Sharma P, Bergman JJ, et al. Development and validation of a classification system to identify high-grade dysplasia and esophageal adenocarcinoma in Barrett's esophagus using narrow-band imaging. Gastroenterology. 2016;150:591–8.
25. Sharma P. Low-grade dysplasia in Barrett's esophagus. Gasteroenterology. 2004;127:1233–8.

4 Diagnosis of Superficial Esophageal Neoplasia: Classification

Rajvinder Singh, Leonardo Zorron Cheng Tao Pu, and Kun Cheong Choi

4.1 Introduction

According to the World Health Organization (GLOBOCAN 2012), esophageal cancer is the eighth leading cancer in incidence (3.2%) and sixth leading cancer in mortality (4.9%) in the world [1]. There are mainly two types of neoplasia which arise from the mucosal layer: squamous cell carcinoma (SCC) and esophageal adenocarcinoma (EAC). The former affects mainly the proximal two-thirds of the esophagus and is highly associated with smoking and alcohol intake. The latter is found mainly in the distal esophagus and gastroesophageal junction (GEJ) and has been mainly attributed to a precursor lesion: the Barrett's esophagus (BE) [2]. BE is commonly associated with gastroesophageal reflux disease and is defined as metaplastic change of columnar type epithelium. The presence of specialized intestinal metaplasia is required by most but not all Gastroenterology Societies [3–7]. BE and EAC diagnosis will be further discussed in Chap. 7.

Early morphological and topographical changes in the surface structure and vasculature have been used to characterize grades of dysplasia, superficial and deep cancer during endoscopy. Severe cytologic atypia which occurs up to the basement membrane is regarded as high-grade dysplasia (HGD) in the West, or carcinoma in situ by the Japanese Esophageal Society (JES). Intramucosal cancer is defined as a cancer breaching the basement membrane and extending up to the muscularis mucosa. A superficial submucosal esophageal cancer can be defined as malignancy which penetrates the submucosa, up to the sm1 layer (the upper one-third of the submucosa), or a depth of infiltration of up to 200 μm in SCC. In this chapter, all these definitions will be considered as superficial esophageal neoplasia which will be used interchangeably with early esophageal cancer.

4.2 Endoscopic Imaging

Although a number of methods have been proposed through the years to screen for esophageal cancer (e.g., brush, balloon, sponge cytology), endoscopy still remains as the gold standard [8]. In order to make a diagnosis during endoscopy, it is important to use all aides available to optimize the detection of inconspicuous change.

R. Singh (✉)
Gastroenterology Department,
Lyell McEwin Hospital Gastroenterology Department, Adelaide, SA, Australia
e-mail: Rajvinder.Singh@sa.gov.au

L. Zorron Cheng Tao Pu
The University of Adelaide, Adelaide, Australia

Nagoya University, Nagoya, Japan

K. C. Choi
The University of Adelaide, Adelaide, Australia

P. W. Y. Chiu et al. (eds.), *Endoscopy in Early Gastrointestinal Cancers, Volume 1*,
https://doi.org/10.1007/978-981-10-6769-3_4

These include using high-definition endoscopes and techniques that allow better visualization of mucosal and vascular patterns such as stains and light filters. This section will focus on the different vital stains and virtual chromoendoscopy methods for the diagnosis of squamous neoplasia.

4.2.1 Vital Stain

For characterization of superficial SCC, the main stain used is Lugol's iodine. The exact concentration for its use is debatable. The most common concentration recommended varies from 1 to 3%. As the use of iodine in the esophagus leads to the increase in contractions, lower concentrations are advisable if one is to perform an endoscopic resection after its use. It is important to note that the contractions caused by the agent can be partially addressed with sodium thiosulfate solution (e.g., 3%), which acts as an antidote/buffer.

Once Lugol's iodine is applied to the mucosa, glycogen within the cells takes up the stain. The normal surface becomes dark brown while neoplastic tissue retains a yellowish discoloration. The rationale of this reaction is that as neoplastic tissue has increased metabolism, it holds less glycogen compared to normal squamous epithelium. This leads to the paler color of SCC compared to the brownish discoloration of normal esophageal epithelium (Fig. 4.1). After a few minutes, the initial pale area which is suspicious for neoplasia may present a specific sign known as the "pink color sign." This has been suggested to be due to the loss of the keratinous layer in the area harboring neoplasia [9]. It is important to note that chemical pneumonitis is a risk when using Lugol's iodine. Special care is hence needed when staining the upper esophagus to prevent aspiration.

4.2.2 Virtual Chromoendoscopy

All mainstream virtual chromoendoscopy modalities work in similar ways. They narrow the spectrum of light which enhances the visibility of mucosal and vascular patterns. However, classifications have been mostly studied with Narrow Band Imaging (NBI). Superficial neoplasia in SCC usually presents on NBI without magnification as a darker/brownish discoloration compared to the surroundings. However, it is within the vascular pattern assessed under magnification that the identification of superficial neoplasia resides. Initially described by Inoue et al. [10], the intrapapillary capillary loop (IPCL) has been studied by several authors and culminated as a classification which has been endorsed by the JES in 2017 [11]. Initially, the use of non-magnified NBI can highlight a suspicious area where either a mucosal irregularity or a darker area is detected. IPCLs can then be interrogated further with magnified NBI. The regularity and thickness of IPCLs become increasingly distorted as the pathway to cancer progresses.

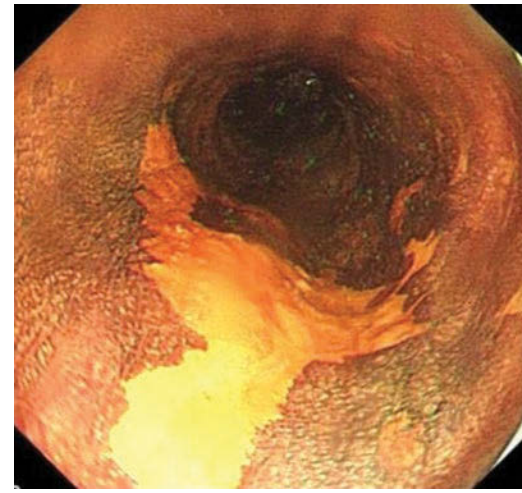

Fig. 4.1 Lugol-voiding area

4.2.3 JES Classification for Superficial SCC

The JES classification describes four types of IPCL patterns. The normal appearance of an IPCL (small regular coiled vessels) and inflammatory pattern IPCL (slightly irregular/engorged coiled vessels) initially described by Inoue have been merged into the type A pattern (Fig. 4.2). Neoplasia can be detected when type B IPCLs

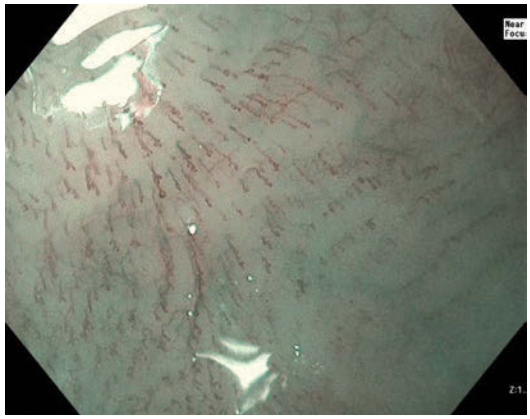

Fig. 4.2 Type A IPCL

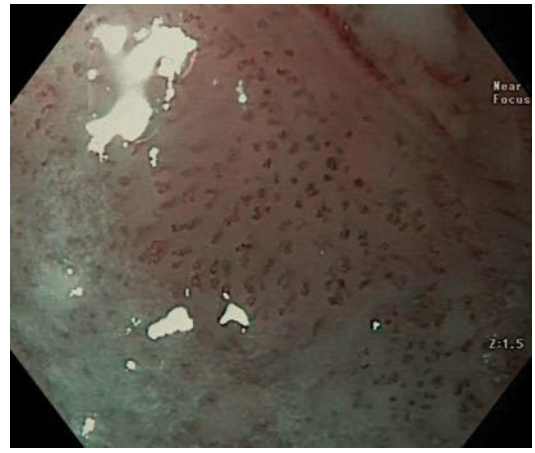

Fig. 4.4 Type B2 IPCL

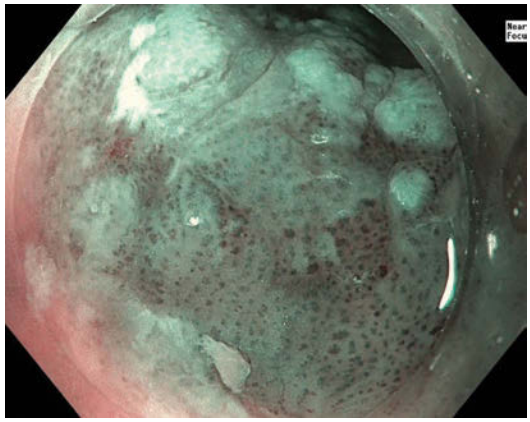

Fig. 4.3 Type B1 IPCL

are found (i.e., abnormal microvessels with different degrees of irregularity and caliber change or dilated abnormal neo vasculature). Type B is further subdivided into three subcategories. Type B1 (Fig. 4.3) occurs when the loop formation is still present, type B2 (Fig. 4.4) is found when the loop formation is lost, and type B3 corresponds to a vessel caliber with a large diameter (more than three times the normal caliber). Type B IPCLs have been shown to correspond to increasing depth of invasion, from HGD to deep submucosal cancer.

In addition to the above, JES has proposed auxiliary criteria for its classifications, based on the extent of the avascular area (AVA) found within the area of interest. This has been proposed to be used for further differentiation of types B2 and B3 patterns [12]. The AVA can be classified into three types: small (<0.5 mm in diameter), medium (≥0.5 and <3 mm), and large (≥3 mm). Any type of AVA surrounded by B1 vessels are suggestive of invasion up to the lamina propria. AVA-medium surrounded by B2 or B3 suggests mucosal or superficial submucosal invasion, while AVA-large surrounded by the same type of vessels suggests invasion up to or beyond the sm2 layer [13]. The JES classification with AVA auxiliary criteria is summarized in Table 4.1.

The JES evaluated their classification in a study across five centers in Japan, enrolling 211 patients. Accurate diagnosis was possible in 97.5% of lesions for B1 type, 75% for B2 type and 55% for B3 type. Underestimation occurred for 7.6% of type B1 lesions (4.1% and 3.5% should have been B2 and B3, respectively), while for B2 lesions 14.3% were over and 10.7% were underestimated. All lesions deemed as B3 were accurately diagnosed. As the majority of lesions were diagnosed as type B1 (81.5% of the cohort), the overall accuracy (Acc) of the JES classification was 90.5%, even though accuracy for B2 was lower. The sensitivity/specificity (Sn/Sp) of B1, B2, and B3 were 97.5/72.9%; 75.0/96.2%; and 55/100%, respectively [11].

Although its initial accuracy has been reported as over 90%, a validation study on 70 superficial

Table 4.1 JES IPCL classification with AVA auxiliary criteria for superficial SCC

	A		B1	B2	B3
Type	Small coiled vessels		Severe irregularity/highly dilated abnormal vessels		
Vascular finding	Normal	Slightly irregular	Loop vessel maintained	Non-loop vessel	Thick green vessel
					
Epithelial finding	Not applicable		AVA-small (<0.5 mm)	AVA-medium (0.5-2.9mm)	AVA-large (≥3mm)
					
Most likely pathology	Non-neoplasm		Neoplasm		
	Normal	Inflammatory	m1-2	m3-sm1	>sm2
ER	No	No	Yes	Relative	No

ER Endoscopic resection

SCCs found it to be lower (78.6%) [14]. Kim and colleagues found types B1, B2, and B3 with an Acc of 88.6%, 78.6%, and 75.0%, respectively. The Sn/Sp were 71.4/100%, 94.4/54.8%, and 75.0/97.8%, respectively. B1 type accurately detected all m1–m2 lesions. However, B2 diagnosis was overestimated in 8 (11.4%) and underestimated 6 (8.6%) lesions. Type B3 diagnosis overestimated 1 lesion (5.3%). Kim and colleagues also evaluated the interobserver agreement which was found to be excellent (0.87). It is important to note that no type A lesions or deep invasive cancers were included in these studies as the study was conducted only on patients referred for endoscopic resection. Nonetheless, the JES classification is presently the gold standard for advanced virtual chromoendoscopy imaging in superficial SCC.

4.3 Conclusion

The use of stains and virtual chromoendoscopy are useful to detect and further interrogate suspicious areas, enabling early diagnosis and hence targeted treatment of superficial squamous neoplasia in the esophagus. The main components of superficial SCCs are the presence of type B IPCLs on NBI, which should be further interrogated and classified according to the JES classification to determine optimal management strategies.

References

1. Organization WH. GLOBOCAN 2012: Estimated cancer incidence, mortality and prevalence worldwide in 2012. http://globocan.iarc.fr/Pages/fact_sheets_cancer.aspx. Accessed 20/08/2018.
2. Wong MCS, Hamilton W, Whiteman DC, Jiang JY, Qiao Y, Fung FDH, et al. Global incidence and mortality of oesophageal cancer and their correlation with socioeconomic indicators temporal patterns and trends in 41 countries. Sci Rep. 2018;8(1):4522. https://doi.org/10.1038/s41598-018-19819-8.
3. Weusten B, Bisschops R, Coron E, Dinis-Ribeiro M, Dumonceau JM, Esteban JM, et al. Endoscopic management of Barrett's esophagus: European Society of Gastrointestinal Endoscopy (ESGE) position statement. Endoscopy. 2017;49(2):191–8. https://doi.org/10.1055/s-0042-122140.
4. Thosani N, Abu Dayyeh BK, Sharma P, Aslanian HR, Enestvedt BK, Komanduri S, et al. ASGE technology committee systematic review and meta-analysis assessing the ASGE preservation and incorporation of valuable endoscopic innovations thresholds for adopting real-time imaging-assisted endoscopic targeted biopsy during endoscopic surveillance of Barrett's esophagus. Gastrointest Endosc. 2016;83(4):684–98e7. https://doi.org/10.1016/j.gie.2016.01.007.
5. Whiteman DC, Appleyard M, Bahin FF, Bobryshev YV, Bourke MJ, Brown I, et al. Australian clinical practice guidelines for the diagnosis and management of Barrett's esophagus and early esophageal adenocarcinoma. J Gastroenterol Hepatol. 2015;30(5):804–20. https://doi.org/10.1111/jgh.12913.
6. Fitzgerald RC, di Pietro M, Ragunath K, Ang Y, Kang JY, Watson P, et al. British Society of Gastroenterology guidelines on the diagnosis and management of Barrett's oesophagus. Gut. 2014;63(1):7–42. https://doi.org/10.1136/gutjnl-2013-305372.

7. Kuwano H, Nishimura Y, Oyama T, Kato H, Kitagawa Y, Kusano M, et al. Guidelines for diagnosis and treatment of carcinoma of the esophagus April 2012 edited by the Japan Esophageal Society. Esophagus. 2015;12:1–30. https://doi.org/10.1007/s10388-014-0465-1.
8. di Pietro M, Canto MI, Fitzgerald RC. Clinical endoscopic management of early adenocarcinoma and squamous cell carcinoma of the esophagus (screening, diagnosis and therapy). Gastroenterology. 2018;154(2):421–36. https://doi.org/10.1053/j.gastro.2017.07.041.
9. Ishihara R, Kanzaki H, Iishi H, Nagai K, Matsui F, Yamashina T, et al. Pink-color sign in esophageal squamous neoplasia, and speculation regarding the underlying mechanism. World J Gastroenterol. 2013;19(27):4300–8.
10. Inoue H, Honda T, Nagai K, Kawano T, Yoshino K, Takeshita K, et al. Ultra-high magnification endoscopic observation of carcinoma in situ of the esophagus. Digest Endosc. 1997;9(1):16–8. https://doi.org/10.1111/j.1443-1661.1997.tb00453.x.
11. Oyama T, Inoue H, Arima M, Momma K, Omori T, Ishihara R, et al. Prediction of the invasion depth of superficial squamous cell carcinoma based on microvessel morphology: magnifying endoscopic classification of the Japan esophageal society. Esophagus. 2017;14(2):105–12. https://doi.org/10.1007/s10388-016-0527-7.
12. Arima M, Tada M, Arima H. Evaluation of microvascular patterns of superficial esophageal cancers by magnifying endoscopy. Esophagus. 2005;2(4):191–7. https://doi.org/10.1007/s10388-005-0060-6.
13. Ogo T, Kawada K, Nakajima Y, Tokairin Y, Ito T, Kawano T. Comparative analysis of avascular areas in superficial esophageal squamous cell carcinomas using in vivo and ex vivo magnifying endoscopy. Endosc Int Open. 2017;5(10):E999–e1004. https://doi.org/10.1055/s-0043-117956.
14. Kim SJ, Kim GH, Lee MW, Jeon HK, Baek DH, Lee BE, et al. New magnifying endoscopic classification for superficial esophageal squamous cell carcinoma. World J Gastroenterol. 2017;23(24):4416–21.

5 Endoscopic Diagnosis of Early Gastric Cancer

T. Kanesaka and Noriya Uedo

5.1 Introduction

Gastric cancer is the fifth most common malignancy and the third leading cause of cancer death worldwide in 2018 [1]. More than one million cases of gastric cancer newly occurred in a year (1,033,701 cases in 2018) [1]. Early gastric cancer was defined by The Japanese Society of Gastroenterological Endoscopy in 1962 as an adenocarcinoma confined to the mucosa or submucosa regardless of the lymph node metastasis. A 5-year survival rate of the patients who underwent gastrectomy with lymph node dissection for early gastric cancer was over 95% [2]. The rate of lymph node metastasis of intramucosal gastric cancer is less than 3% [3, 4], and it is practically 0% when it fulfills the following histopathological characteristics: ≤2 cm in size, differentiated type, and absence of ulcerative findings (UL) [4]. Moreover, the expanded indication for endoscopic resection have been confirmed to have a sufficient therapeutic effect [5]. Thus, early gastric cancer is expected to have a favorable prognosis if proper treatment is given.

T. Kanesaka (✉)
Department of Gastrointestinal Oncology, Osaka International Cancer Institute, Chuo-ku, Osaka, Japan

N. Uedo
Department of Gastrointestinal Oncology, Endoscopy Training and Learning Center, Osaka Medical Center for Cancer & Cardiovascular Diseases, Higashinari-ku, Osaka, Japan

Detection and evaluation of the suspicious lesion using upper gastrointestinal endoscopy are the essential first steps in the early treatment of gastric cancer [6, 7]. In Korea, screening endoscopy was reported to be less likely to die from gastric cancer than upper gastrointestinal series; odds ratio was 0.53 (95% confidence interval [CI], 0.51–0.56) for endoscopy and 0.98 (95% CI, 0.95–1.01) for upper gastrointestinal series [8]. Routine endoscopy is mainly performed by a conventional white light endoscopy [9]. However, magnifying endoscopy and image-enhanced endoscopy (e.g., narrow-band imaging, blue laser imaging) are recently available and the high diagnostic abilities for early gastric cancer are reported [10, 11].

5.2 Risk Factors for Gastric Cancer

Age-standardized incidence rates in men are twofold greater than women [1]. Gastric cancer is well known to develop generally in patients with chronic *Helicobacter pylori* (*H. pylori*) infection [12]. As described later, extent of atrophic gastritis is associated with the development of gastric cancer. In Japan, Matsuo et al. reported that *H. pylori*-negative cases was 0.66% (95% CI, 0.41–1.01) of the entire cases with gastric cancer [13]. Moreover, presence of gastric xanthelasma, which is characterized by the accumulation of lipid in histiocytic foam cells, is also associated

P. W. Y. Chiu et al. (eds.), *Endoscopy in Early Gastrointestinal Cancers, Volume 1*,
https://doi.org/10.1007/978-981-10-6769-3_5

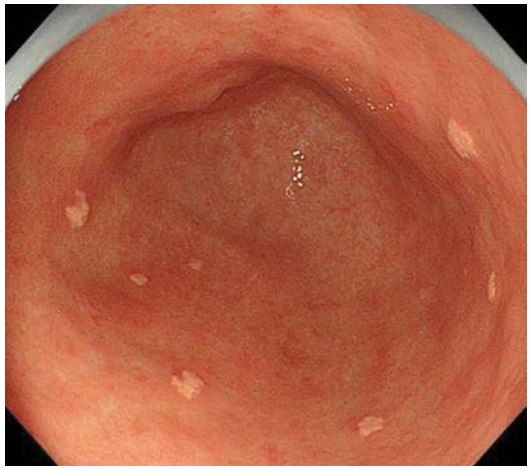

Fig. 5.1 Gastric xanthelasmas

with the development of early gastric cancer (Fig. 5.1) [14].

5.3 Preparation

If mucus and bubbles remained on the gastric mucosal surface, the detection and characterization of early gastric cancer are disturbed. It is therefore recommended that the subject takes water with mucolytic and antifoaming agents before the procedure [15], i.e., 20,000 U pronase, 1 g sodium bicarbonate, and 10 ml dimethylpolysiloxane. Taking pronase 20 min before endoscopy significantly improves visibility of the lesion and reduces the frequency of water injection during endoscopy [16].

Recently, routine upper gastrointestinal endoscopy is often undergone without any anticholinergic agents in Japan. If the peristalsis should be suppressed, an anticholinergic agent (e.g., 10–20 mg scopolamine butylbromide or 1 mg glucagon) is used. Glucagon is used instead of scopolamine butylbromide for the patients with cardiovascular diseases, glaucoma or prostatic hyperplasia, because scopolamine butylbromide makes those diseases worse. Whereas, L-menthol is also used to suppress gastric peristalsis [17]. Spraying L-menthol on the gastric mucosa during endoscopy is easier than the intravenous or intramuscular injection of other anticholinergic agents.

5.4 Evaluation of Gastric Mucosa

5.4.1 Normal Gastric Mucosa

Yagi et al. proposed that "regular arrangement of collecting venules (RAC)" observed in the lesser curvature of lower gastric body was a sensitive and specific (93.8% and 96.2%, respectively) sign for normal gastric mucosa without *H. pylori* infection [18, 19]. Although RAC was proposed as a finding of magnifying endoscopy but it can be identified even by conventional non-magnifying endoscopy (Fig. 5.2). RAC is rarely detected in the stomach after successful eradication (19%) [20]. Moreover, in the *H. pylori*-negative cases, red streak, hemorrhagic erosion, and bleeding spot are looked in entire stomach, and fundic gland polyposis and raised erosions are looked in gastric body and antrum, respectively [21].

5.4.2 Atrophic Gastritis

In the patients with chronic *H. pylori* infection, lesser curvature of gastric body looks pale and the visibility of vessels increased (Fig. 5.3a) [22]. As the mucosal atrophy spreads, gastric folds diminish (Fig. 5.3b). The extent of mucosal atrophy was classified by Kimura et al. (Fig. 5.4) [22]. A sensitivity and specificity of the visible vessels for a diagnosis of moderate-to-severe histological mucosal atrophy are 48% and 87%, respectively, whereas those of the absence of gastric folds are 67% and 85%, respectively [23]. The relative risk for the development of gastric cancer are 1.7 (95% CI, 0.8–3.7) in moderate atrophy and 4.9 (95% CI, 2.8–19.2) in severe atrophy [12]. Shichijo et al. demonstrated that the cumulative incidences of gastric cancer in group A (no intestinal metaplasia), B (intestinal metaplasia in only antrum), and C (intestinal metaplasia in body with or without antrum) were 0.3%, 0%, and 5.6% at 1 year; 1.5%, 3.7%, and 9.8% at 5 years; and 1.5%, 11%, and 16% at 10 years, respectively [24].

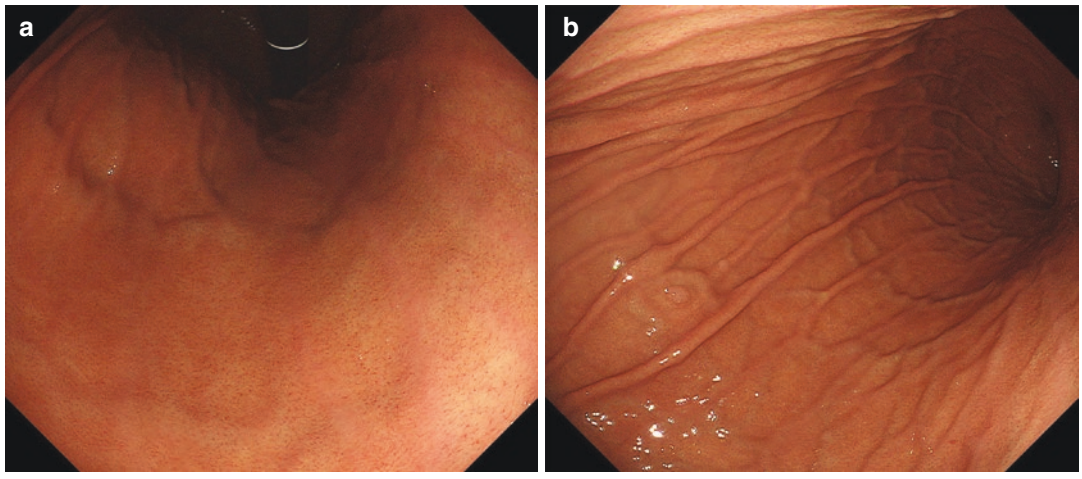

Fig. 5.2 Normal gastric body without *H. pylori* infection. (**a**) A retroflex view of gastric body in white light endoscopy. Regular arrangement of collecting venules (RAC) is shown as starfish-like. (**b**) A forward view of gastric body in white light endoscopy

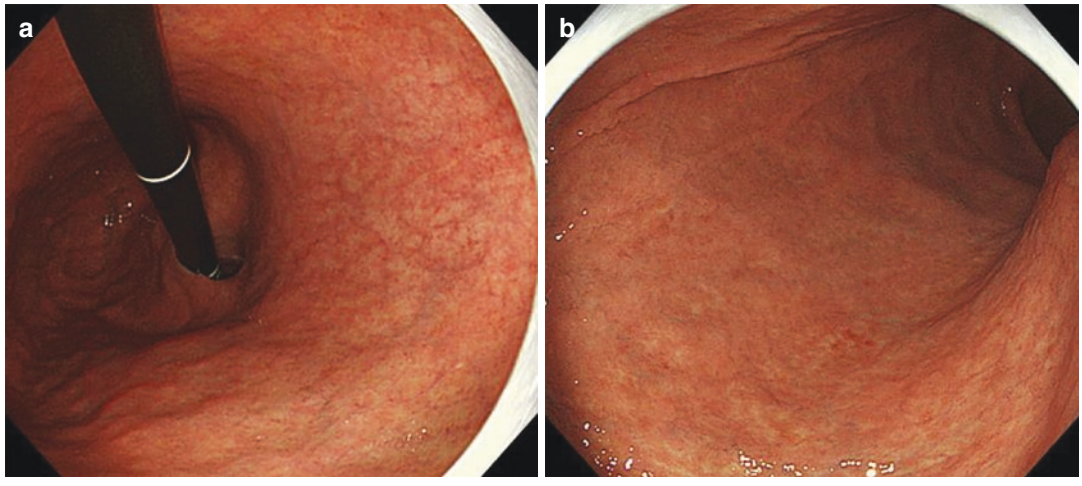

Fig. 5.3 *H. pylori*-related atrophic gastritis. (**a**) A retroflex view of gastric body in white light endoscopy. (**b**) A forward view of gastric body in white light endoscopy

5.4.3 Intestinal Metaplasia

Gastric mucosa is slowly changed into the intestinal phenotype with chronic *H. pylori* infection [25]. Intestinal metaplasia mucosa shows various endoscopic findings, e.g., slightly elevated with whitish patches [26] and mottled reddish depression [27].

5.5 Evaluation of Early Gastric Cancer

5.5.1 Macroscopic Type

"Type 0" is a macroscopic type corresponding to early gastric cancer stated in the Japanese Gastric Cancer Association Classification (Fig. 5.5) [28]

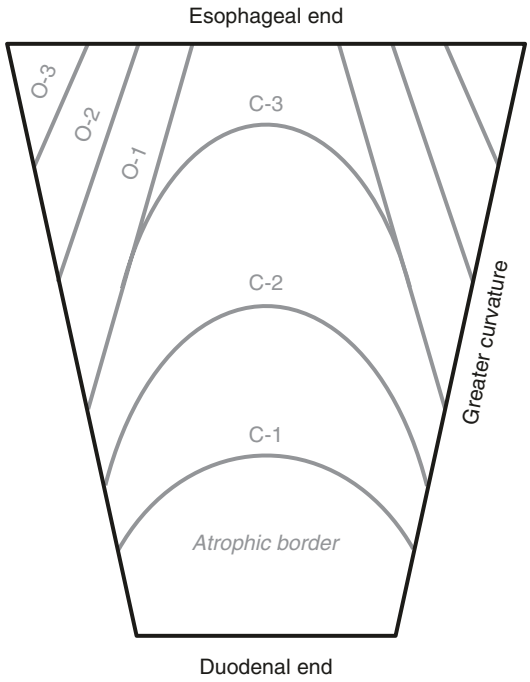

Fig. 5.4 Kimura–Takemoto classification. Citation from [22]. C-1: the atrophic findings are not visible in the gastric body; C-2: the atrophic border on the lesser curvature is observed at a lower gastric body; C-3: the atrophic border on the lesser curvature is observed at the upper gastric body; O-1: the atrophic border is observed between the lesser curvature and the anterior wall; O-2: the atrophic border is observed between the anterior wall and the greater curvature; O-3: the atrophic border on the greater curvature is observed proximal to the lower gastric body

or the Paris classification [29]. Type 0-I (protruding), Type 0-II (superficial), and Type 0-III (excavated) are the subclassification of Type 0. Type 0-II is further divided into three types: Type 0-IIa (superficial elevated), Type 0-IIb (superficial flat), and Type 0-IIc (superficial depressed). Type 0-IIc is the major macroscopic type (78%) of early gastric cancer and Type 0-IIa is the second most common (17%) (Figs. 5.6 and 5.7) [28]. Whereas, the remains are small number (0-I, 3%; 0-IIb, 0.4%; or 0-III, 2%). If two or more components are contained in a lesion, both should be stated, e.g., 0-IIa + IIc, 0-IIc + III, etc. Using uniform terminology enables common recognition in discussing and describing endoscopic appearances.

5.5.2 Detection

Most early gastric cancers show only subtle endoscopic findings in color and mucosal height. Disappearance of the background vessels (Fig. 5.8a) or spontaneous bleeding (Fig. 5.8b) can be also a clue of the detection of early gastric cancer. Although the superiority of chromoendoscopy using indigo carmine to white light endoscopy has not been proven yet, it is widely done in the clinical practice in Japan for the detection and characterization of early gastric cancer.

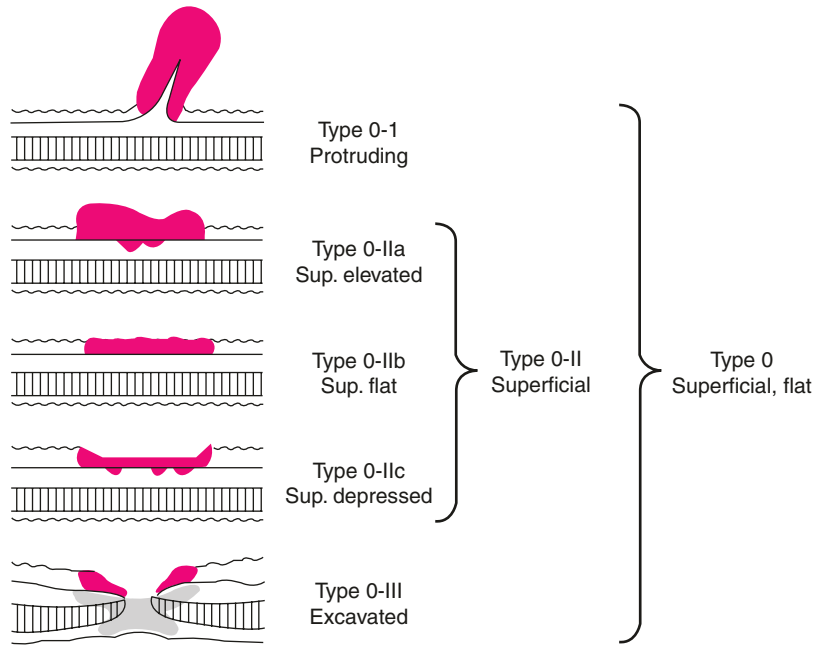

Fig. 5.5 Macroscopic type of early gastric cancer in the Japanese Gastric Cancer Association Classification. Citation from the Japanese classification of gastric carcinoma: 3rd English edition [28]

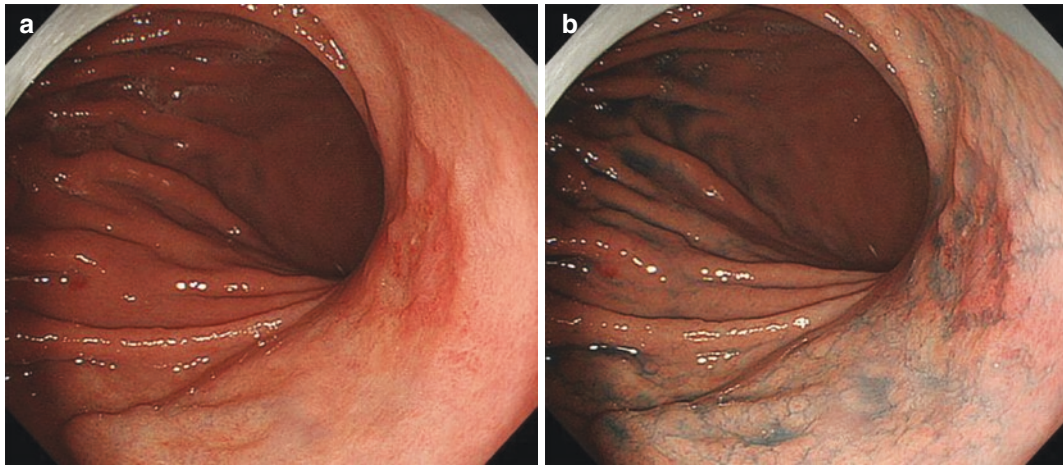

Fig. 5.6 Type 0-IIc lesion. The histopathological diagnosis was differentiated-type early gastric cancer. (**a**) An image of white light endoscopy. (**b**) An image of chromoendoscopy

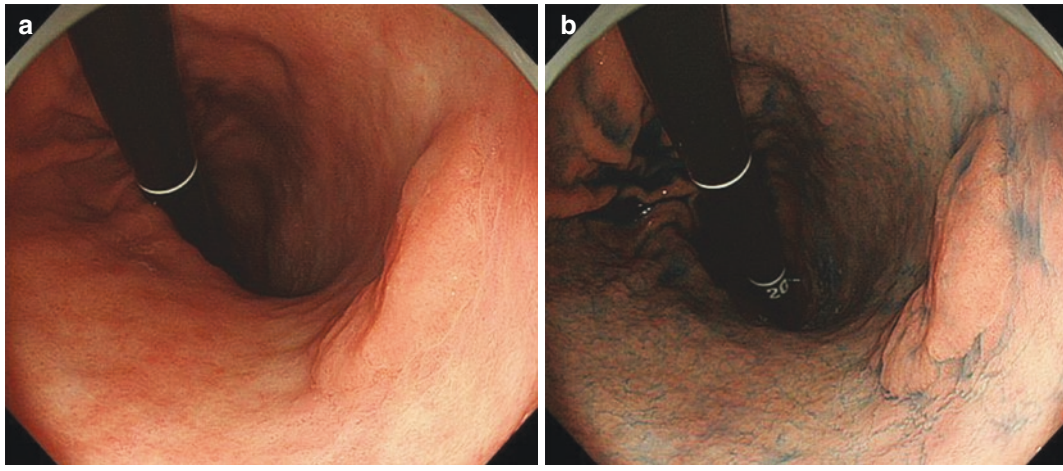

Fig. 5.7 Type 0-IIa lesion. The histopathological diagnosis was differentiated-type early gastric cancer. (**a**) An image of white light endoscopy. (**b**) An image of chromoendoscopy

5.5.3 Differentiation of Cancer from Noncancerous Lesions

Early gastric cancer shows the well-demarcated area with an irregularity in color and/or mucosal pattern [30, 31]. Use of indigo carmine can enhance the surface patterns and magnifying narrow-band imaging provides the additional information (the details are described in the other Chapters).

5.5.4 Endoscopic Staging

Tumor size, depth of tumor invasion, and presence of UL (i.e., fold convergence) are assessed and the forceps biopsy is taken to diagnose the histological type of cancer. These findings are associated with the likelihood of lymph node metastasis and are essential to determine the indication of endoscopic resection [32].

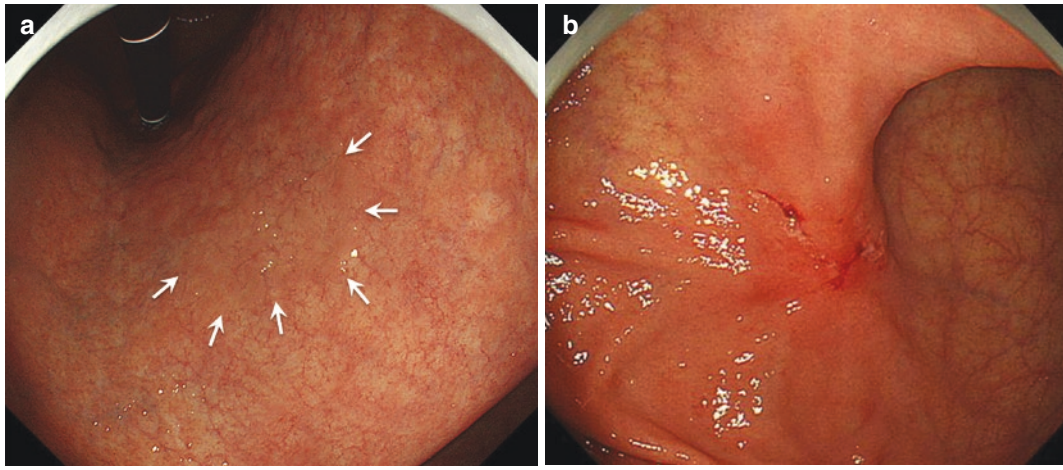

Fig. 5.8 (**a**) Background vessels is not shown in an early gastric cancer (differentiated-type, arrows). (**b**) Spontaneous bleeding is shown on an early gastric cancer (undifferentiated type)

Table 5.1 Histological classification of gastric cancer (only common type)

Papillary adenocarcinoma (pap)
Tubular adenocarcinoma (tub)
Well-differentiated (tub1)
Moderately differentiated (tub2)
Poorly differentiated adenocarcinoma (por)
Solid type (por1)
Non-solid type (por2)
Signet-ring cell carcinoma (sig)
Mucinous adenocarcinoma (muc)

Citation from the Japanese classification of gastric carcinoma: 3rd English edition [28]

5.5.5 Histological Type

"Common type" of histological type of gastric cancer are shown in Table 5.1 [28]. Those are divided into differentiated and undifferentiated types according to the presence or absence of glandular formation (Fig. 5.9). These correspond to the intestinal and diffuse types in Lauren's classification, respectively [33]. The risk of lymph node metastasis in the undifferentiated type is higher than that in the differentiated type [4, 34, 35]. Differentiated-type early gastric cancer is significantly associated with older age (≥72 years), male, and elevated type (Type 0-I, 0-IIa) compared with the undifferentiated type [36]. Especially, a specificity of the elevated type for the differentiated-type was 99% (95% CI, 92 – 100%). Differentiated-type early gastric cancer tend to appears reddish compared with the undifferentiated type due to the difference in hemoglobin content [37]. Whereas, some superficial elevated-type early gastric cancer and gastric adenoma look whitish, because the lipid droplets are accumulated in the superficial part of mucosa in those lesions [38].

5.5.6 Tumor Extent

Horizontal boundary is evaluated according to the difference in color and mucosal pattern between the lesion and the surrounding area (e.g., irregular margin, spiny depressed area [10]). It can be identified even by white light endoscopy. However, subsequent chromoendoscopy and/or magnifying narrow-band imaging is useful for the more accurate diagnosis [39]. However, undifferentiated-type cancer frequently develops in intermediate layer of mucosa and the evaluation of tumor extent is therefore difficult [40]. Taking negative biopsies from the surrounding mucosa can be required to determine the exact tumor boundary for such cases [11].

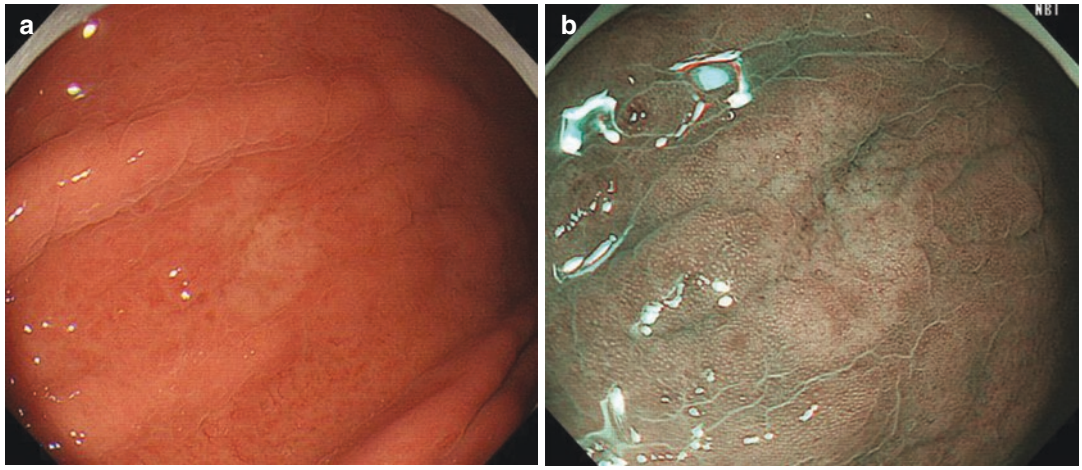

Fig. 5.9 Undifferentiated-type early gastric cancer. (**a**) An image of white light endoscopy. (**b**) An image of narrow-band imaging

5.5.7 Depth of Tumor Invasion

Histological examination of the resected specimen is the gold standard in the diagnosis of tumor invasion depth. The possibility of additional surgery depending on the results of the histology should be explained to the patient before endoscopic resection is performed. In most Japanese institutions, the tumor invasion depth is estimated mainly based on the findings on white light endoscopy and chromoendoscopy. If the lesion is large (>30 mm) and appears pronounced redness, uneven surface features, and marginal elevation, a sensitivity, specificity, and accuracy for the submucosal invasion are 57.3%, 86.2%, and 81.1%, respectively [41]. Choi et al. reported that sensitivity, specificity, and accuracy of white light endoscopy by experienced endoscopists for distinguishing intramucosal cancer from submucosal cancer were 85.5%, 73.9%, and 78.0%, respectively [42]. Nagahama et al. demonstrated that "non-extension sign" was a sign of massive submucosal invasion [43]. When the gastric wall is fully distended by insufflation of a large volume of air, the invasive area is not extended and the thickness remains: a sensitivity, specificity, and accuracy for submucosal invasion are 92.0%, 97.7%, and 96.9%, respectively.

The usefulness of endoscopic ultrasound (EUS) is controversial in the diagnosis of tumor invasion depth of early gastric cancer. In a meta-analysis about staging of gastric cancer by using EUS, a sensitivity and specificity of EUS for distinguishing intramucosal cancer from submucosal cancer were 83% and 79%, respectively [44]. Choi et al. proposed that accuracy of white light endoscopy outperformed EUS in differential diagnosis between intramucosal and submucosal cancers (73.7% vs. 67.4%, $P < 0.001$) [45]. Tsujii et al. recommended EUS for lesions estimated as submucosal cancer by white light endoscopy to salvage over-diagnosed cancers [46].

5.5.8 Ulcerative Findings

UL is histologically diagnosed based on the disruption of muscularis mucosa [32]. However, endoscopic findings are also taken into consideration in a conclusive diagnosis (Fig. 5.10). A forceps biopsy causes a fibrosis restricted to small areas. If it cannot be distinguished from the original ulcer scar, it should be classified as UL positive.

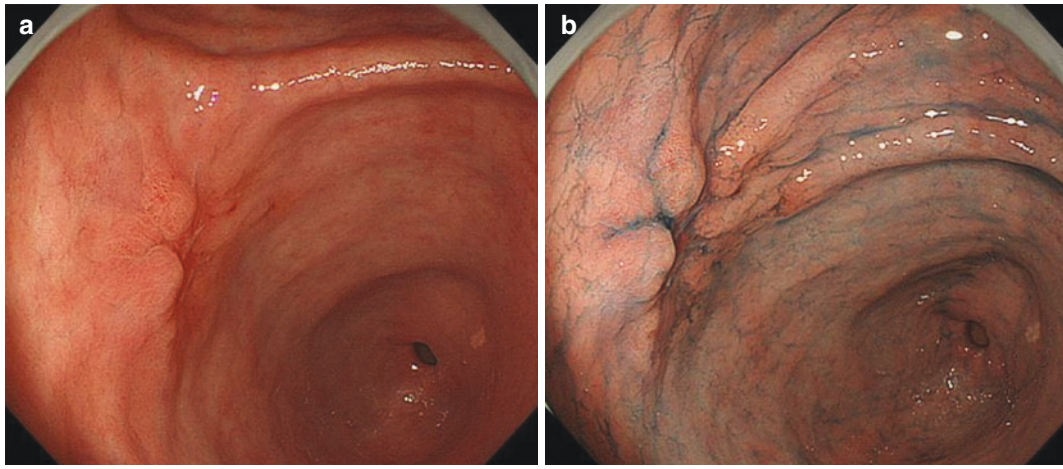

Fig. 5.10 Ulcerative finding is shown as a fold convergence. (**a**) An image of white light endoscopy. (**b**) An image of chromoendoscopy

5.6 Summary

- Early gastric cancers expected to have a favorable prognosis if proper treatment is given.
- *H. pylori* infection is the most important risk factor of gastric cancer. Gastric atrophy and xanthelasma are the endoscopic markers for predicting the development of gastric cancer.
- When the detected lesion was diagnosed as cancer, tumor size, depth of invasion, presence of UL, and the histological type of cancer should be assessed. Those are necessary to confirm the indication of endoscopic resection.

References

1. Bray F, Ferlay J, Soerjomataram I, et al. Global cancer statistics 2018: GLOBOCAN estimates of incidence and mortality worldwide for 36 cancers in 185 countries. CA Cancer J Clin. 2018;68:394–424.
2. Yamazaki H, Oshima A, Murakami R, et al. A long-term follow-up study of patients with gastric cancer detected by mass screening. Cancer. 1989;63:613–7.
3. Sano T, Kobori O, Muto T. Lymph node metastasis from early gastric cancer: endoscopic resection of tumour. Br J Surg. 1992;79:241–4.
4. Gotoda T, Yanagisawa A, Sasako M, et al. Incidence of lymph node metastasis from early gastric cancer: estimation with a large number of cases at two large centers. Gastric Cancer. 2000;3:219–25.
5. Hasuike N, Ono H, Boku N, et al. A non-randomized confirmatory trial of an expanded indication for endoscopic submucosal dissection for intestinal-type gastric cancer (cT1a): the Japan Clinical Oncology Group study (JCOG0607). Gastric Cancer. 2018;21:114–23.
6. Allum WH, Blazeby JM, Griffin SM, et al. Guidelines for the management of oesophageal and gastric cancer. Gut. 2011;60:1449–72.
7. Thrumurthy SG, Chaudry MA, Hochhauser D, et al. The diagnosis and management of gastric cancer. BMJ. 2013;347:f6367.
8. Jun JK, Choi KS, Lee HY, et al. Effectiveness of the Korean National Cancer Screening Program in reducing gastric cancer mortality. Gastroenterology. 2017;152:1319–28.
9. Uedo N, Fujishiro M, Goda K, et al. Role of narrow band imaging for diagnosis of early-stage esophagogastric cancer: current consensus of experienced endoscopists in Asia-Pacific region. Dig Endosc. 2011;23(Suppl 1):58–71.
10. Ezoe Y, Muto M, Uedo N, et al. Magnifying narrowband imaging is more accurate than conventional white-light imaging in diagnosis of gastric mucosal cancer. Gastroenterology. 2011;141:2017–25.
11. Yao K, Doyama H, Gotoda T, et al. Diagnostic performance and limitations of magnifying narrow-band imaging in screening endoscopy of early gastric cancer: a prospective multicenter feasibility study. Gastric Cancer. 2014;17:669–79.
12. Uemura N, Okamoto S, Yamamoto S, et al. Helicobacter pylori infection and the development of gastric cancer. N Engl J Med. 2001;345:784–9.
13. Matsuo T, Ito M, Takata S, et al. Low prevalence of Helicobacter pylori-negative gastric cancer among Japanese. Helicobacter. 2011;16:415–9.
14. Sekikawa A, Fukui H, Sada R, et al. Gastric atrophy and xanthelasma are markers for predicting the

development of early gastric cancer. J Gastroenterol. 2016;51:35–42.
15. Fujii T, Iishi H, Tatsuta M, et al. Effectiveness of premedication with pronase for improving visibility during gastroendoscopy: a randomized controlled trial. Gastrointest Endosc. 1998;47:382–7.
16. Lee GJ, Park SJ, Kim SJ, Kim HH, Park MI, Moon W. Effectiveness of premedication with pronase for visualization of the mucosa during endoscopy: a randomized, controlled trial. Clin Endosc. 2012 Jun;45(2):161–4.
17. Hiki N, Kaminishi M, Yasuda K, et al. Antiperistaltic effect and safety of L-menthol sprayed on the gastric mucosa for upper GI endoscopy: a phase III, multicenter, randomized, double-blind, placebo-controlled study. Gastrointest Endosc. 2011;73:932–41.
18. Yagi K, Nakamura A, Sekine A. Characteristic endoscopic and magnified endoscopic findings in the normal stomach without Helicobacter pylori infection. J Gastroenterol Hepatol. 2002;17:39–45.
19. Yagi K, Aruga Y, Nakamura A, et al. Regular arrangement of collecting venules (RAC): a characteristic endoscopic feature of Helicobacter pylori-negative normal stomach and its relationship with esophago-gastric adenocarcinoma. J Gastroenterol. 2005;40:443–52.
20. Kato M, Terao S, Adachi K, et al. Changes in endoscopic findings of gastritis after cure of H. pylori infection: multicenter prospective trial. Dig Endosc. 2013;25:264–73.
21. Kato T, Yagi N, Kamada T, et al. Diagnosis of Helicobacter pylori infection in gastric mucosa by endoscopic features: a multicenter prospective study. Dig Endosc. 2013;25:508–18.
22. Kimura K, Takemoto T. An endoscopic recognition of the atrophic border and its significance in chronic gastritis. Endoscopy. 1969;1:87–97.
23. Redeen S, Petersson F, Jonsson KA, Borch K. Relationship of gastroscopic features to histological findings in gastritis and Helicobacter pylori infection in a general population sample. Endoscopy. 2003;35:946–50.
24. Shichijo S, Hirata Y, Niikura R, et al. Histologic intestinal metaplasia and endoscopic atrophy are predictors of gastric cancer development after Helicobacter pylori eradication. Gastrointest Endosc. 2016;84:618–24.
25. Busuttil RA, Boussioutas A. Intestinal metaplasia: a premalignant lesion involved in gastric carcinogenesis. J Gastroenterol Hepatol. 2009;24:193–201.
26. Kaminishi M, Yamaguchi H, Nomura S, et al. Endoscopic classification of chronic gastritis based on a pilot study by the research society for gastritis. Dig Endosc. 2002;14:138–51.
27. Nagata N, Shimbo T, Akiyama J, et al. Predictability of gastric intestinal metaplasia by mottled patchy erythema seen on endoscopy. Gastroenterol Res. 2011;4:203–9.
28. Japanese Gastric Cancer Association. Japanese classification of gastric carcinoma: 3rd English edition. Gastric Cancer. 2011;14:101–12.
29. Participants in the Paris Workshop. The Paris endoscopic classification of superficial neoplastic lesions: esophagus, stomach, and colon: November 30 to December 1, 2002. Gastrointest Endosc. 2003;58(6 Suppl):S3–43.
30. Yao K. The endoscopic diagnosis of early gastric cancer. Ann Gastroenterol. 2013;26:11–22.
31. Yao K, Iwashita A, Yao T, et al. Quantitative method to characterize electronic endoscopic color images of early gastric carcinomas, using index of hemoglobin. Gastraenterol Endosc. 1997;39:2253–63. Japanese with English abstract.
32. Japanese Gastric Cancer Association. Japanese gastric cancer treatment guidelines 2014 (ver.4). Gastric Cancer. 2017;20:1–19.
33. Lauren P. The two histological main types of gastric carcinoma: diffuse and so-called intestinal-type carcinoma. Acta Pathol Microbiol Scand. 1965;64:31–49.
34. Hirasawa T, Gotoda T, Miyata S, et al. Incidence of lymph node metastasis and the feasibility of endoscopic resection for undifferentiated-type early gastric cancer. Gastric Cancer. 2009;12:148–52.
35. Sekiguchi M, Oda I, Taniguchi H, et al. Risk stratification and predictive risk-scoring model for lymph node metastasis in early gastric cancer. J Gastroenterol. 2016;51:961–70.
36. Kanesaka T, Nagahama T, Uedo N, et al. Clinical predictors of histologic type of gastric cancer. Gastrointest Endosc. 2018;87:1014–22.
37. Yao K, Yao T, Matsui T, Iwashita A, Oishi T. Hemoglobin content in intramucosal gastric carcinoma as a marker of histologic differentiation: a clinical application of quantitative electronic endoscopy. Gastrointest Endosc. 2000;52:241–5.
38. Yao K, Iwashita A, Tanabe H, et al. White opaque substance within superficial elevated gastric neoplasia as visualized by magnification endoscopy with narrow-band imaging: a new optical sign for differentiating between adenoma and carcinoma. Gastrointest Endosc. 2008;68:574–80.
39. Nagahama T, Yao K, Uedo N, et al. Delineation of the extent of early gastric cancer by magnifying narrow-band imaging and chromoendoscopy: a multicenter randomized controlled trial. Endoscopy. 2018;50:566–76.
40. Okada K, Fujisaki J, Kasuga A, et al. Diagnosis of undifferentiated type early gastric cancers by magnification endoscopy with narrow-band imaging. J Gastroenterol Hepatol. 2011 Aug;26(8):1262–9.
41. Abe S, Oda I, Shimazu T, et al. Depth-predicting score for differentiated early gastric cancer. Gastric Cancer. 2011;14:35–40.
42. Choi J, Kim SG, Im JP, et al. Endoscopic prediction of tumor invasion depth in early gastric cancer. Gastrointest Endosc. 2011;73:917–27.

43. Nagahama T, Yao K, Imamura K, et al. Diagnostic performance of conventional endoscopy in the identification of submucosal invasion by early gastric cancer: the “non-extension sign” as a simple diagnostic marker. Gastric Cancer. 2017;20:304–13.
44. Mocellin S, Marchet A, Nitti D. EUS for the staging of gastric cancer: a meta-analysis. Gastrointest Endosc. 2011;73:1122–34.
45. Choi J, Kim SG, Im JP, et al. Comparison of endoscopic ultrasonography and conventional endoscopy for prediction of depth of tumor invasion in early gastric cancer. Endoscopy. 2010;42:705–13.
46. Tsujii Y, Kato M, Inoue T, et al. Integrated diagnostic strategy for the invasion depth of early gastric cancer by conventional endoscopy and EUS. Gastrointest Endosc. 2015 Sep;82(3):452–9.

6 Diagnosis of Early Gastric Cancer: Endoscopic Diagnosis and Classification: VS Classification System for the Diagnosis of Early Gastric Cancer by Magnifying Endoscopy

Kenshi Yao and Akinori Iwashita

6.1 Microanatomies Visualized by Magnifying Endoscopy in the Stomach

In this section, we describe which microanatomies are visualized by optical magnifying endoscopy (ME). Instead of using a special term for description of ME findings, we need to employ anatomical term since the modern optical magnifying endoscopy has enough resolution to dissect capillary, which is the smallest unit in the human vessels [1].

6.1.1 Magnified Endoscopic Findings of Normal Gastric Mucosa

In the normal gastric mucosa, each microanatomical component in the stomach visualized by ME is common. However, microvascular architecture and microsurface structure are different depending upon the part of the stomach, that is, gastric fundic glandular mucosa or gastric pyloric glandular mucosa [2, 3].

6.1.1.1 Gastric Fundic Glandular Mucosa (Fig. 6.1.)

As for microvascular architecture, the morphology of the capillary shows a dark brown polygonal closed loop. These loops anastomose repeatedly with each other, forming a regular honeycomb-like subepithelial capillary network (SECN) pattern. The SECN drains into a cyan-colored CV.

As for microsurface structure, the epithelial morphology is visualized as semitransparent white belt-like structures, showing a circular or oval shape. This is the marginal crypt epithelium (MCE). In the center, the brown oval crypt opening (CO) is surrounded by the MCE (epithelium within vessel pattern).

6.1.1.2 Gastric Pyloric Glandular Mucosa (Fig. 6.2)

As for microvascular architecture, the morphology of the capillary is that of a dark brown coil-shaped open loop. Although it has been shown anatomically that these loops anastomose repeatedly with each other under the epithelial surface, subepithelial anastomoses are not often visualized. In contrast to the gastric fundic glandular

K. Yao (✉)
Department of Endoscopy, Fukuoka University Chikushi Hospital,
Fukuoka, Japan
e-mail: yao@fukuoka-u.ac.jp

A. Iwashita
Department of Pathology, Fukuoka University Chikushi Hospital,
Fukuoka, Japan

P. W. Y. Chiu et al. (eds.), *Endoscopy in Early Gastrointestinal Cancers, Volume 1*,
https://doi.org/10.1007/978-981-10-6769-3_6

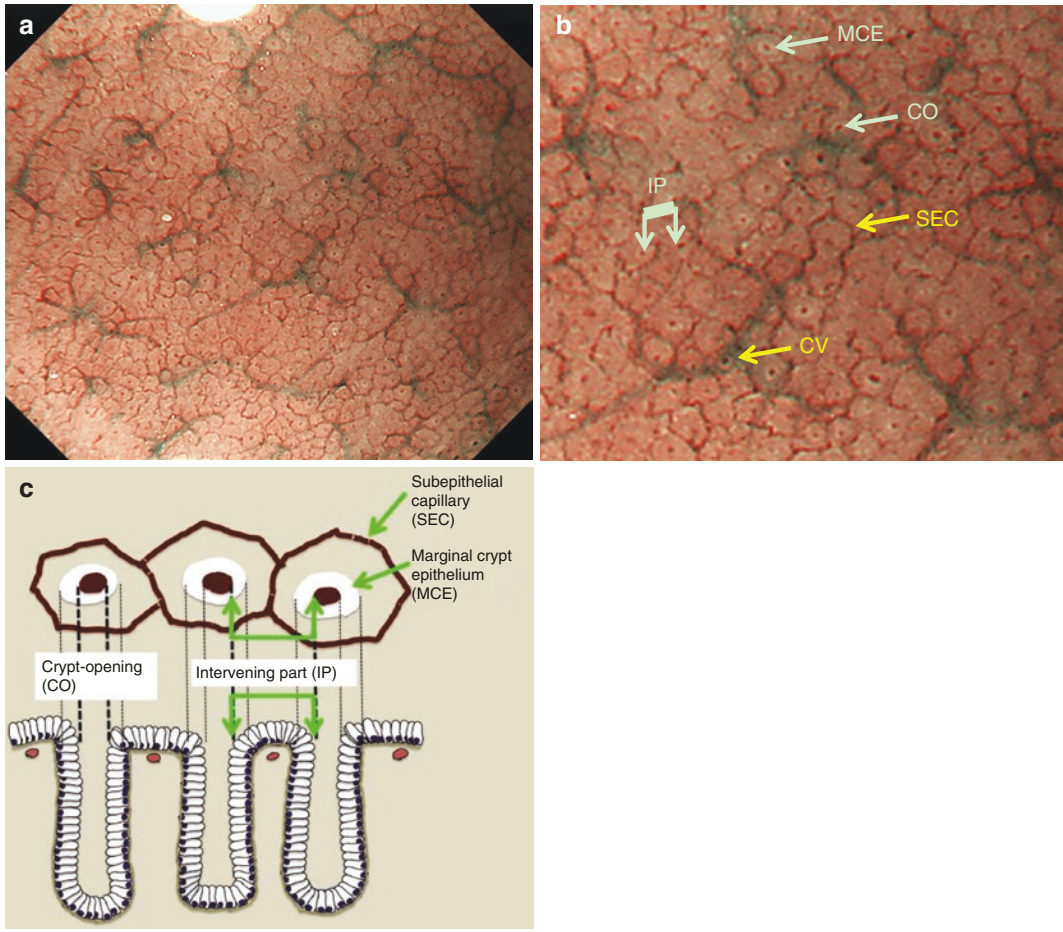

Fig. 6.1 (**a**) M-NBI findings of the normal gastric fundic gland mucosa. V (MV architecture): Regular honeycomb-like subepithelial capillary network (SECN) pattern with regular collecting venule (CV) pattern present. S (MS structure): Regular oval crypt opening (CO) pattern and circular marginal crypt epithelium (MCE) pattern. (**b**) Anatomical components visualized by M-NBI in the normal gastric fundic gland mucosa. *SEC* subepithelial capillary, *CV* collecting venule, *MCE* marginal crypt epithelium, *CO* crypt opening, *IP* intervening part between crypts. (**c**) Correlation between visualized micro-anatomies by M-NBI (upper part) and histological finings (lower part) in the superficial part of the gastric fundic glandular mucosa

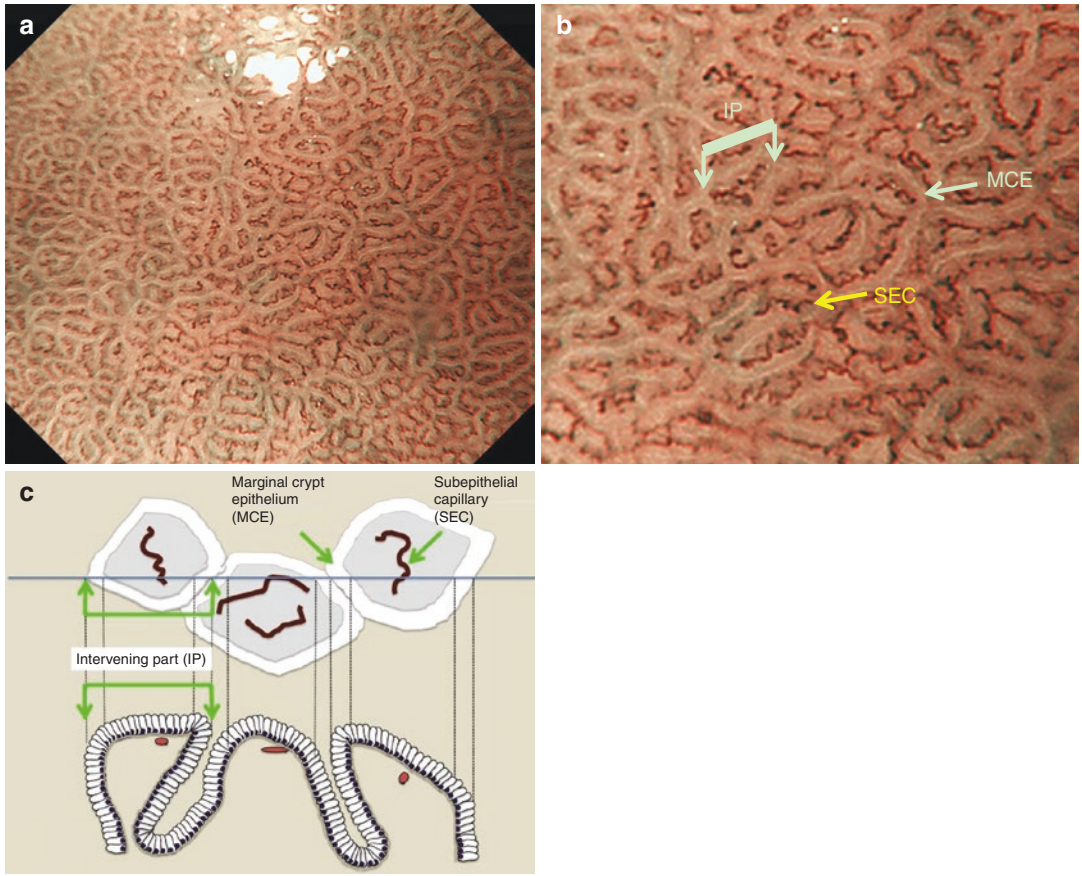

Fig. 6.2 (**a**) M-NBI findings of the normal gastric pyloric gland mucosa. V (MV architecture): Regular coil-shaped SECN pattern but regular CV pattern absent. S (MS structure): Regular polygonal or curved MCE pattern. (**b**) Anatomical components visualized by M-NBI in the normal gastric fundic gland mucosa. SEC, subepithelial capillary; MCE, marginal crypt epithelium; IP, intervening part between crypts. (**c**) Correlation between visualized microanatomies by M-NBI (upper part) and histological finings (lower part) in the superficial part of the gastric pyloric glandular mucosa

mucosa, CVs are rarely observed since they are located at the deeper part of the mucosa.

As for microsurface structure, the shape of MCE shows curved or polygonal shape. Different from the fundic gland mucosa, the SEC is surrounded by MCE (vessel within epithelium pattern).

6.1.2 Other Microanatomical Components for Microsurface Pattern: Optical Markers for Intestinal Metaplasia with Chronic Gastritis and Epithelial Neoplasia in the Stomach

6.1.2.1 Light Blue Crest (LBC) (Fig. 6.3a)

The LBC is a specific phenomenon that can only be visualized using narrow-band imaging (NBI). It was discovered by Uedo et al. and reported by them in 2005 [4]. The LBC is defined as "a fine, blue, white line on the crests of epithelial surface/gyri." Using ME with NBI, it is identified as a light blue (light cyan colored) linear light reflections at the edge of the MCE. The LBC is one of optical markers for predicting histological intestinal metaplasia in gastric mucosa with chronic gastritis. Bio-optically, this phenomenon involves strong reflection of short wavelength narrow-band blue light (400–430 nm), with a central wavelength of 415 nm. We can infer that the short wavelength narrow-band light is reflected by the microvilli of brush borders of the area of intestinal metaplasia. A similar phenomenon is seen in the epithelial margins of the duodenal mucosa. If LBC is visualized by ME with NBI, it can be one of the components for microsurface pattern.

6.1.2.2 White Opaque Substance (WOS) (Fig. 6.3b)

The WOS is visualized by ME with both white-light and narrow-band imaging. It was reported by us for the first time in 2008 [5]. The WOS is defined white substance in the superficial part of gastric mucosa that obscures subepithelial microvascular architecture. The nature of the WOS is the phenomenon caused by reflections/strong scattering of whole projected lights due to lipid microdroplets accumulated in the surface epithelium of the intervening part [6]. Human eye thus recognizes reflected light/scattering as white color. The WOS is optical marker for predicting intestinal metaplasia as well as the LBC [7]. The WOS can be an alternative marker for making a diagnosis of early gastric cancer (EGC) when the subepithelial microvascular (MV) pattern is obscured by the WOS. Accordingly, the WOS can be one of the components for microsurface pattern.

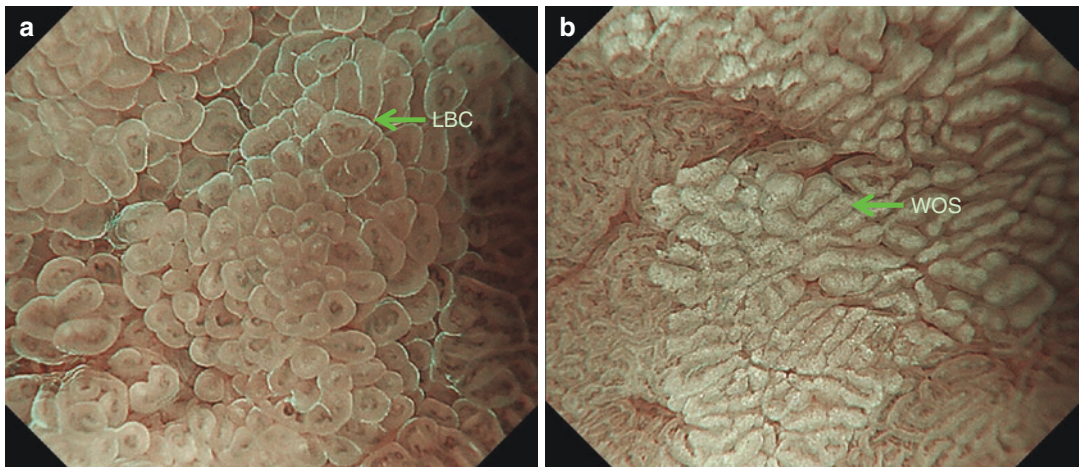

Fig. 6.3 (**a**) M-NBI finings of light blue crest (LBC) in gastric mucosa with intestinal metaplasia. Fine light blue (light cyan colored) linear reflections are located on the epithelial margins, visualized using M-NBI. (**b**) M-NBI finings of white opaque substance (WOS) in gastric mucosa with intestinal metaplasia. White opaque substance visualized by reflections/strong scattering of whole projected lights located in the surface epithelium of the intervening part (IP)

6.1.3 Terminology for Analyzing Microanatomies as Visualized by Magnifying Endoscopy

- V: microvascular pattern
  - Subepithelial capillary (SEC)
  - Collecting venule (CV)
  - Pathological microvessels (MV)
- S: microsurface pattern
  - Marginal crypt epithelium (MCE)
  - Crypt opening (CO)
  - Intervening part (IP) between crypts
  - Light blue crest (LBC)
  - White opaque substance (WOS)

6.2 VS (Vessel Plus Surface) Classification System for the Diagnosis of Early Gastric Cancer (EGC) by Magnifying Endoscopy

6.2.1 Descriptions and Principles

The VS (Vessels plus surface) classification system for the analysis of ME findings was developed by Yao et al. [1, 8, 9]. This diagnostic system has proven to be very useful for correctly diagnosing superficial (0-II) cancer [10–12] and delineating the margins of EGC [13, 14]. This VS classification system is a well-accepted systematic method worldwide for the diagnosis of EGC using magnifying endoscopy.

Anatomical terms are used to define the MV and MS patterns as visualized by ME. The MV pattern comprises a subepithelial capillary, a collecting venule, and pathological microvessels, whereas the MS pattern is identified by an MCE, a crypt opening, an intervening part between crypts, LBC, and WOS.

On principle, the MV and MS patterns need to be determined separately.

6.2.2 Definitions and Diagnostic Criteria

6.2.2.1 Demarcation Line

The definition of a DL is a border between the lesion and non-lesion areas, discernible through an abrupt change in MV and/or MS patterns. If magnifying endoscopic findings of the lesion border show gradual changes in MV and/or MS patterns, demarcation line is determined to be absent [1, 15].

VS Classification

There are three categories of MV and MS patterns including regular, irregular, and absent [1, 15] (Fig. 6.4).

1. Microvascular pattern
   (a) Regular MV pattern: Mucosal capillaries have a uniform shape that can be closed-looped (polygonal) or open-looped with a homogeneous morphology, symmetrical distribution, and regular arrangement.
   (b) Irregular MV pattern: the vessels are closed-looped (polygonal), open-looped, tortuous, branched, or bizarrely shaped, with or without a network, and have a heterogeneous morphology, asymmetrical distribution, and irregular arrangement.
   (c) Absent MV pattern: The subepithelial microvascular pattern is obscured by the presence of a white opaque substance (WOS) within the superficial part of the mucosa.
2. Microsurface pattern
   (a) Regular MS pattern: The morphology of the marginal crypt epithelium shows a uniform linear/curved/oval/circular structure. It shows a homogeneous morphology, symmetrical distribution, and regular arrangement. When WOS is present, regular WOS can be an additional marker of a regular microsurface pattern, defined as

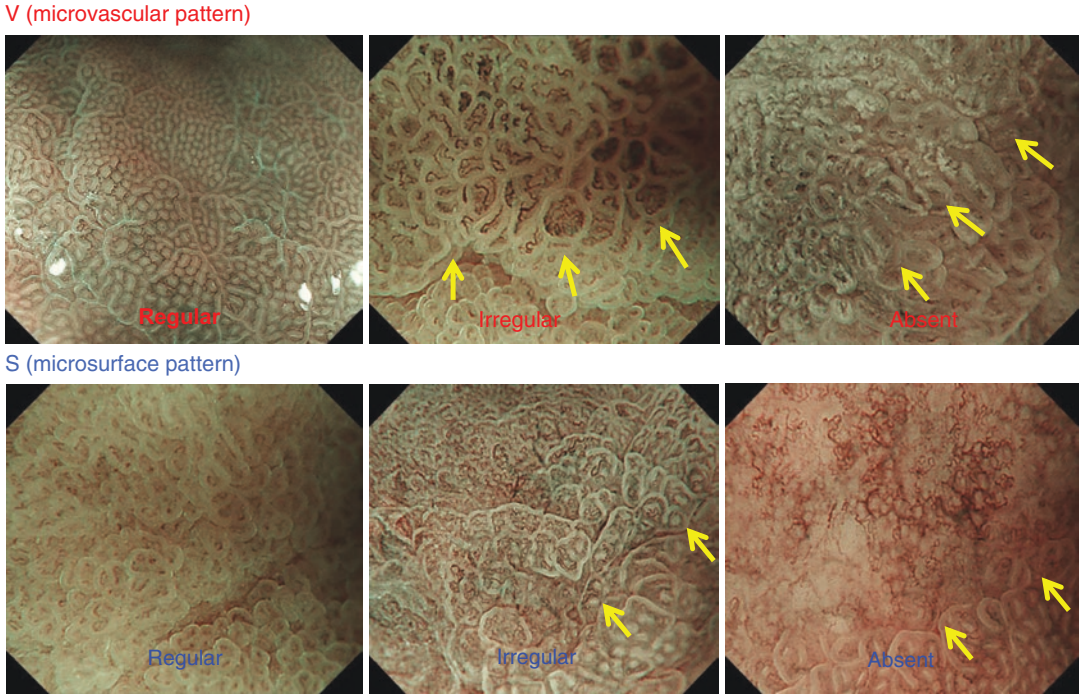

Fig. 6.4 VS classification

a well-organized and symmetrical distribution of WOS in a regular reticular/maze-like/speckled pattern.

(b) Irregular MS pattern: The morphology of the marginal crypt epithelium shows an irregular linear/curved/oval/circular/villous structure. It shows a heterogeneous morphology, asymmetrical distribution, and irregular arrangement. When WOS is present, irregular WOS can be an additional marker of an irregular microsurface pattern, defined as a disorganized and asymmetrical distribution of WOS in an irregular reticular/speckled pattern.

(c) Absent MS pattern: Neither the marginal crypt epithelial structure nor WOS are visible using M-NBI.

According to the VS classification system, the characteristic M-NBI findings of early gastric cancer are a clear demarcation line between the background noncancerous mucosa and the cancerous mucosa, and an irregular microvascular pattern and/or irregular microsurface pattern within the demarcation line [1]. Accordingly, we set the criteria for making a diagnosis of gastric cancer as follows:

1. Presence of an irregular microvascular pattern with a demarcation line.
2. Presence of an irregular microsurface pattern with a demarcation line.

If the endoscopic findings fulfill either or both, we make the diagnosis of cancer, and we make the diagnosis of noncancer if neither is fulfilled. According to our investigations, 97% of early gastric cancers fit the above criteria [1].

6.3 Magnifying Endoscopy Simple Diagnostic Algorithm for Early Gastric Cancer (MESDA-G) (Fig. 6.5)

A unified algorithm for general use in the clinical setting is necessary for enhancing the efficacy of ME diagnosis of EGC has been proposed as multi-society consensus [15]. The Japan Gastroenterological Endoscopy Society (JGES),

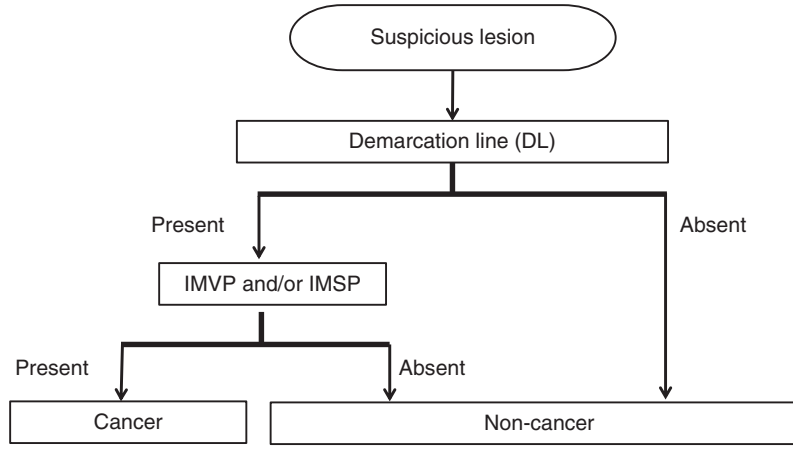

Fig. 6.5 Magnifying Endoscopy Simple Diagnostic Algorithm for Early Gastric Cancer (MESDA-G)

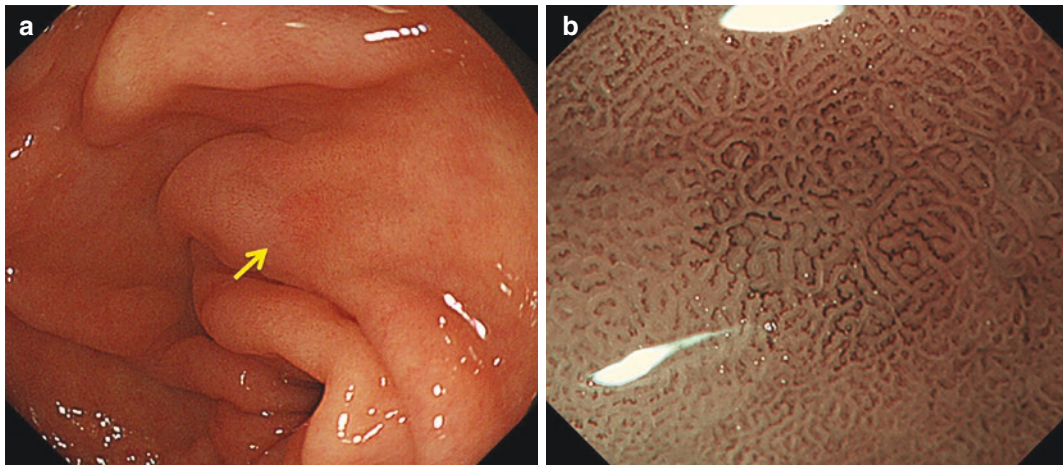

Fig. 6.6 An example of absent demarcation line. (**a**) A flat reddened lesion (arrow) is detected at the gastric antrum by conventional white light endoscopy. (**b**) M-NBI findings shows that the microvascular pattern (subepithelial capillary network) are gradually dilated from the background mucosa to the lesion. The microsurface pattern (marginal crypt epithelium/white zone) has no abrupt change between the lesion and the background mucosa. Accordingly, no demarcation line is detected between the lesion and the background mucosa. Therefore, this lesion is diagnosed as non-cancer according to MESDA-G

the Japanese Gastric Cancer Association (JGCA), and the World Endoscopy Organization (WEO) jointly devised a unified international algorithm for ME using an evidence-based approach. This is named as magnifying endoscopy simple diagnostic algorithm for early gastric cancer (MESDA-G).

This algorithm was constructed based on VS classification system since VS classification system was proved to be most commonly accepted diagnostic system and to be used to demonstrated usefulness of magnifying endoscopy with the highest evidence level.

According to this algorithm, to diagnose EGC, one has to identify any suspicious lesion that is potentially a neoplasm. To recognize such a lesion, we carefully observe the color change (whitish or reddish) or morphological change (elevated, flat, or depressed) on the gastric mucosal surface. If we detect a suspicious lesion, identification of a demarcation line (DL) between the lesion and the background mucosa is the first step in distinguishing EGC from a noncancerous lesion. If a DL is absent, the diagnosis of a benign lesion may be made (Fig. 6.6). If a DL is present, the subsequent presence of an irregular microvascular (MV) pattern and an irregular microsurface (MS) pattern should be determined (Figs. 6.7 and 6.8). If irregular MV and/or irregular MS patterns

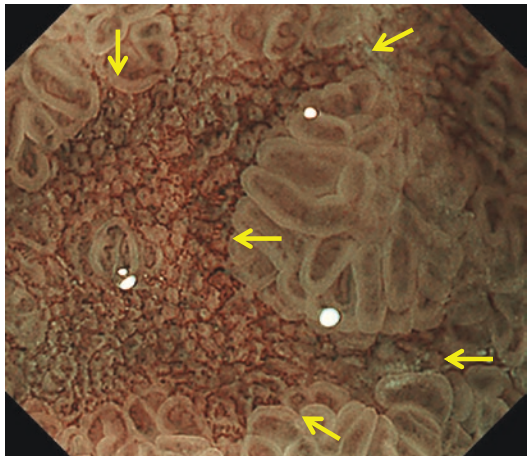

Fig. 6.7 An example of present demarcation line and absent irregular MV pattern and/or irregular MS pattern. A distinct demarcation line is detected between the background mucosa and the depressed lesion. Within the demarcation line, it shows regular MV pattern plus regular MS pattern based on VS classification. According to MESDA-G, this lesion is diagnosed as non-cancer since both irregular MV pattern and irregular MS pattern are absent. Histological findings of biopsy specimen showed noncancerous lesion (chronic gastritis with intestinal metaplasia)

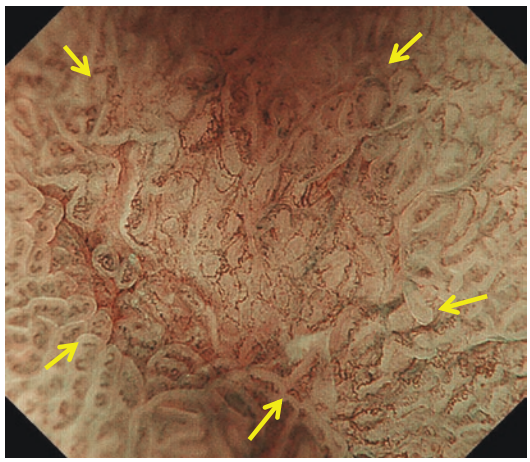

Fig. 6.8 An example of present demarcation line and irregular MV pattern and irregular MS pattern. A demarcation line is present between the background mucosa and the lesion. Within the demarcation line, irregular MV pattern plus irregular MS pattern are identified. According to MESDA-G, this lesion is diagnosed as cancer. Histological findings of endoscopically resected specimens demonstrated well-differentiated adenocarcinoma (2 mm in diameter)

are present within the demarcation line, the diagnosis of EGC can be made. Both irregular MV nor irregular MS patterns are absent, the diagnosis of noncancerous lesion is made.

6.4 Clinical Applications of Magnifying Endoscopy Based on VS Classification System

6.4.1 Characterization of Subtle Mucosal Lesions in Screening Endoscopy

Making a differential diagnosis of slightly depressed lesion between focal gastritis and small depressed cancer used to be one of the limitations of conventional white light imaging (C-WLI). We investigated the real-time diagnostic yield of the C-WLI compared to the M-NBI in a multicenter, prospective, randomized controlled trial of patient with undiagnosed depressed lesions ≤10 mm in diameter detected during screening esophagogastroduodenoscopy [11]. With regard to the diagnostic performance of C-WLI versus M-NBI for small, depressed gastric lesions, the accuracy, and specificity of M-NBI were greater than with C-WLI, although the difference in sensitivity was not significant (Table 6.1). The combination of C-WLI and M-NBI significantly enhanced performance compared with the C-WLI alone (Table 6.2). These outcomes clearly demonstrate that carry-

Table 6.1 Diagnostic performance of C-WLI and M-NBI for gastric small depressed lesions

	C-WLI (n = 176)	M-NBI (n = 177)	P-value[a]
Accuracy (%) [95% CI]	65 [57–72]	90 [85–94]	*<0.001*
Sensitivity (%) [95% CI]	40 [19–64]	60 [36–81]	0.34
Specificity(%) [95% CI]	68 [60–75]	94 [89–97]	*<0.001*

[a]Chi-square test

Table 6.2 Diagnostic performance of C-WLI plus M-NBI for gastric small depressed lesions

	C-WLI (n = 176)	C-WLI plus M-NBI (n = 176)	P-value[a]
Accuracy (%) [95% CI]	65 [57–72]	97 [94–99]	*<0.001*
Sensitivity (%) [95% CI]	40 [19–64]	95 [75–100]	*<0.001*
Specificity (%) [95% CI]	68 [60–75]	97 [93–99]	*<0.001*

[a]Chi-square test

ing out M-NBI after careful C-WLI has sufficient diagnostic accuracy for determining a correct endoscopic diagnosis even for gastritis-like cancer. Furthermore, we demonstrated that the M-NBI has greater sensitivity and reproducibility than chromoendoscopy (CE) for the diagnosis of minute (≤5 mm diameter) gastric cancers [16]. Nevertheless, in clinical practice, taking a biopsy cannot be omitted, because the histological findings, such as histological type, are needed for a diagnosis of cancer. However, using the M-NBI and the VS classification system could contribute toward minimization of the number of biopsies of noncancerous lesions taken in order to rule out gastritis-like cancer. In fact, we have demonstrated the advantages in cost-effectiveness of M-NBI, in particular, M-NBI may contribute to reducing the number of biopsies required to detect a cancer in screening endoscopy [12].

The limitations of M-NBI in screening endoscopy was reported by a prospective multicenter feasibility study [12]. As shown in Fig. 6.9, a pale depressed lesion by C-WLI is characteristic of a signet-ring cell or undifferentiated carcinoma. However, by M-NBI, it is only visualized as a regular MV pattern and of M-NBI in screening endoscopy since signet-ring cell carcinoma invades underneath the surface epithelium without any destruction of MCE or SEC. Accordingly, a pale flat, or depressed mucosal lesion is set as one of the limitations of M-NBI. If we limit a good indication of M-NBI to a non-pale lesion, the M-NBI can be considered an optical biopsy [12].

6.4.2 Determining the Horizontal Extent of EGC for Successful Endoscopic Submucosal Dissection

Magnifying endoscopy enables reliable delineation of the horizontal extent of EGCs prior to endoscopic submucosal dissection (ESD) [13, 14]. In our previous studies, we have reported the advantages of M-NBI over C-WLI with dye spraying CE [13]. We investigated the usefulness and limitations of ME with

NBI when CE could not be used to determine the horizontal extent of an EGC. A series of 350 consecutive EGCs resected en bloc using ESD were included in the study. Approximately 18.9% (66/350) of cases showed unclear margins using CE. Of these, 62 of 66 cancers were examined using M-NBI. According to the VS classification system, the entire margins were successfully delineated in 72.6% (45/62) of the lesions with unclear margins using CE (Fig. 6.10).23 However, the diagnostic success rate for undifferentiated cancers was 0%, significantly lower than that for differentiated lesions (p<0.001). Accordingly, M-NBI using the VS classification system is an excellent modality for identifying the entire margin of EGCs when the margins are unclear using CE. However, it is still difficult to assess the lateral extent of the EGC of an undifferentiated type using endoscopic findings alone because the cancer cell infiltrates laterally in the lamina propria deep to the glandular neck. M-NBI of the surface cannot detect any cancer with specific irregular MV or MS patterns. Thus, the endoscopic diagnostic strategy to be adopted depends on the histological type, as shown in Fig. 6.11. In difficult cases, we recommend that the clinical strategy should be to take biopsy samples from the apparently noncancerous tissue around the lesion and then determine the resec-

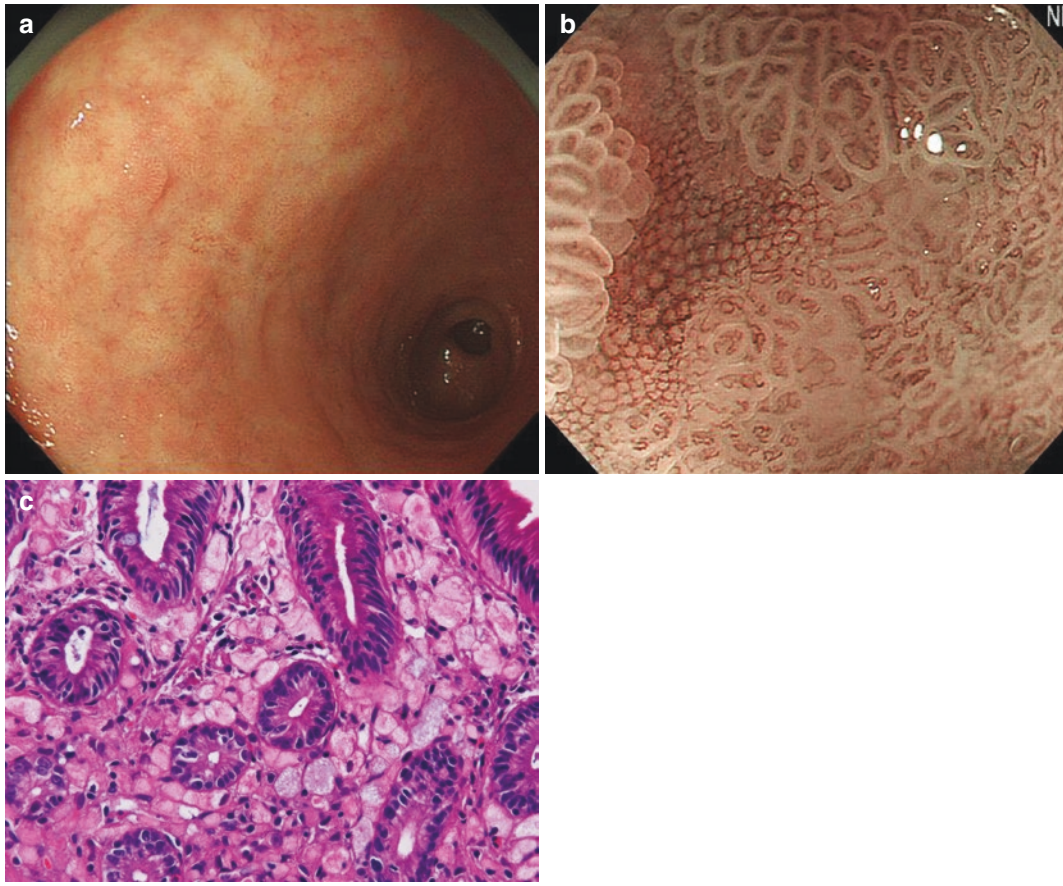

Fig. 6.9 A good example of limitations of M-NBI in screening endoscopy. (**a**) C-WLI shows a slightly depressed pale lesion in the gastric antrum. (**b**) M-NBI demonstrate regular MV pattern plus regular MS pattern with a demarcation line. (**c**) The histological findings of the biopsy specimen shows signet-ring cell carcinoma

tion margins after histopathologically confirming the absence of cancerous invasion in the biopsy specimens.

Further evidence was reported recently. According to the well-designed multicenter randomized controlled study comparing CE and M-NBI for accurate delineation, CE and M-NBI appeared to be clinically equivalent [14]. Accordingly, standard CE and advanced M-NBI can be both useful for determining the horizontal extent of EGC for successful endoscopic submucosal dissection.

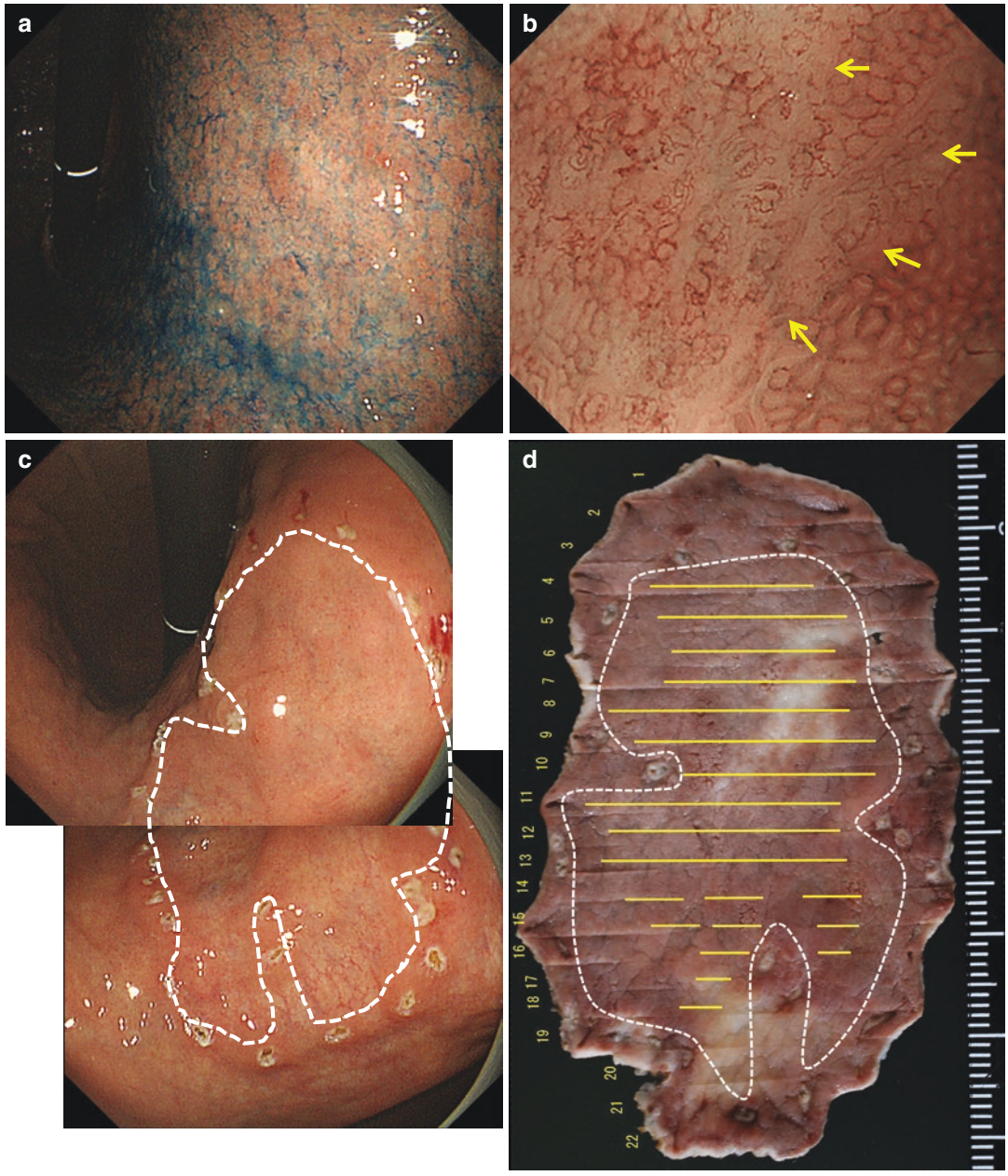

Fig. 6.10 Usefulness of M-NBI for determining the horizontal extent of early gastric cancer when there is an unclear margin by CE. (**a**) CE findings of a differentiated 0-IIb type early gastric cancer. The margins of lateral extent cannot be clearly delineated, let alone the presence of cancer. (**b**) M-NBI findings of oral margin of the cancer. Using M-NBI, a clear demarcation line was identified. Within the demarcation line, irregular MV pattern plus absent MS pattern were present. Therefore, we successfully determined cancer specific margin. (**c**) Because we determined the cancer-specific margins all the way around the cancer by M-NBI, we placed the markings just outside the demarcation lines according to ME with NBI findings. (**d**) The en bloc resected specimen by endoscopic submucosal dissection. According to the histopathological findings, the extent of the carcinoma (yellow lines) was reconstructed on the macroscopic photograph. The preoperative markings were clearly identified all the way around the carcinoma as shown by the white dotted line. Therefore, the lesion had been successfully delineated by M-NBI

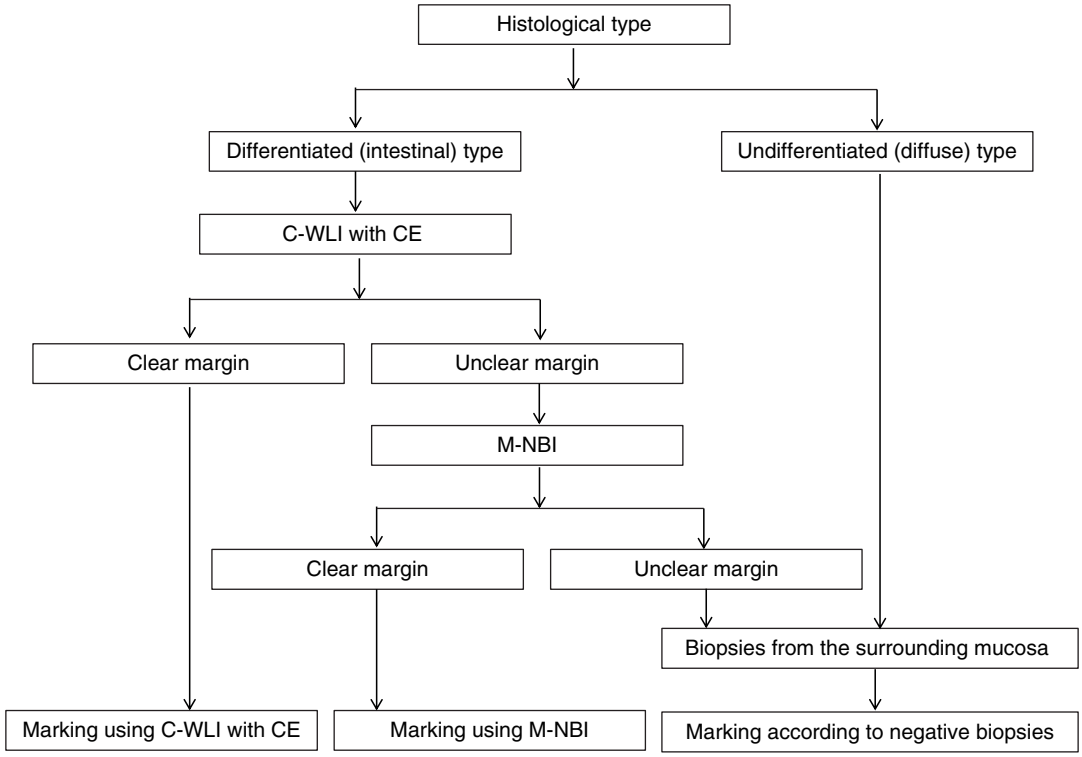

Fig. 6.11 A strategy for determining the lateral extent of early gastric cancer, for curative endoscopic resection. C-WLI, conventional white-light imaging; CE, chromoendoscopy; M-NBI, magnifying endoscopy with narrow-band imaging

6.5 Conclusion

VS classification system for making a correct diagnosis of early gastric cancer now become the standard diagnostic system approved by multi-society consensus based on evidence-based medicine.

2. VS (vessel plus surface classification system)
   1) Principles
   2) Definitions and Diagnostic criteria
      (1) Demarcation line
      (2) Microvascular pattern
         (a) Regular MV pattern
         (b) Irregular MV pattern
         (c) Absent MV pattern
      (3) Microsurface pattern
         (d) Regular MS pattern
         (e) Irregular MS pattern
         (f) Absent MS pattern
   3) Magnifying endoscopy simple diagnostic algorithm for early gastric cancer (MESDA-G)

References

1. Yao K, Anagnostopoulos GK, Ragunath K. Magnifying endoscopy for diagnosing and delineating early gastric cancer. Endoscopy. 2009;41:462–7. https://doi.org/10.1055/s-0029-1214594.
2. Yao K, Oishi T. Microgastroscopic findings of mucosal micorvacular architecture as visualized by magnifying endoscopy. Dig Endosc. 2001;13(Suppl):S27–33.
3. Yao K. Microanatomies as visualized using magnifying endoscopy with narrow band imaging in the stomach: Which microanatomical structures can we visualize in the glandular epithelium using narrow band imaging, and how is this achieved? In: Yao K, editor. Zoom gastroscopy. 1st ed. Tokyo: Springer; 2013. p. 57–69.
4. Uedo N, Ishihara R, Iishi H, et al. A new method of diagnosing gastric intestinal metaplasia: narrow-band

imaging with magnifying endoscopy. Endoscopy. 2006;38:819–24.
5. Yao K, Iwashita A, Tanabe H, Nishimata N, et al. White opaque substance within superficial elevated gastric neoplasia as visualized by magnification endoscopy with narrow-band imaging: a new optical sign for differentiating between adenoma and carcinoma. Gastrointest Endosc. 2008;68:574–80. https://doi.org/10.1016/j.gie.2008.04.011.
6. Yao K, Iwashita A, Nambu M, et al. Nature of white opaque substance in gastric epithelial neoplasia as visualized by magnifying endoscopy with narrow-band imaging. Dig Endosc. 2012;24(6):419–25. https://doi.org/10.1111/j.1443-1661.2012.01314.x.
7. Kanemitsu T, Yao K, Nagahama T, et al. Extending magnifying NBI diagnosis of intestinal metaplasia in the stomach: the white opaque substance marker. Endoscopy. 2017;49:529–35. https://doi.org/10.1055/s-0043-103409.
8. Yao K, Oishi T, Matsui T, Yao T, et al. Novel magnified endoscopic findings of microvascular architecture in intramucosal gastric cancer. Gastrointest Endosc. 2002;56:279–84.
9. Yao K. The proposed vessels plus surface (VS) classification system: Principles for interpretation of magnifying endoscopy with narrow-band imaging (M-NBI) findings. In: Yao K, editor. Zoom gastroscopy. 1st ed. Tokyo: Springer; 2013. p. 71–2.
10. Yao K, Iwashita A, Tanabe H, et al. Novel zoom endoscopy technique for diagnosis of small flat gastric cancer: a prospective, blind study. Clin Gastroenterol Hepatol. 2007;5:869–78.
11. Ezoe Y, Muto M, Uedo N, et al. Magnifying narrowband imaging is more accurate than conventional white-light imaging in diagnosis of gastric mucosal cancer. Gastroenterology. 2011;141:2017–25. https://doi.org/10.1053/j.gastro.2011.08.007.
12. Yao K, Doyama H, Gotoda T, et al. Diagnostic performance and limitations of magnifying narrow-band imaging in screening endoscopy of early gastric cancer: a prospective multicenter feasibility study. Gastric Cancer. 2014;17:669–79. https://doi.org/10.1007/s10120-013-0332-0.
13. Nagahama T, Yao K, Maki S, et al. Usefulness of magnifying endoscopy with narrow-band imaging for determining the horizontal extent of early gastric cancer when there is an unclear margin by chromoendoscopy (with video). Gastrointest Endosc. 2011;74:1259–67. https://doi.org/10.1016/j.gie.2011.09.005.
14. Nagahama T, Yao K, Uedo N, et al. Delineation of the extent of early gastric cancer by magnifying narrow-band imaging and chromoendoscopy: a multicenter randomized controlled trial. Endoscopy. 2018;50:566–76. https://doi.org/10.1055/s-0044-100790.
15. Muto M, Yao K, Kaise M, et al. Magnifying endoscopy simple diagnostic algorithm for early gastric cancer (MESDA-G). Dig Endosc. 2016;28:379–93. https://doi.org/10.1111/den.12638.
16. Fujiwara S, Yao K, Nagahama T, et al. Can we accurately diagnose minute gastric cancers (≤5 mm)? Chromoendoscopy (CE) vs magnifying endoscopy with narrow band imaging (M-NBI). Gastric Cancer. 2015;18:590–6. https://doi.org/10.1007/s10120-014-0399-2.

7 Diagnosis of Early Colorectal Carcinoma: Endoscopic Diagnosis and Classification

Han Mo Chiu

7.1 Introduction

Analysis of 109,953 CRC cases in the United States Surveillance, Epidemiology, and End Results (SEER) database, the risk of lymph node metastasis in T1 CRC is around 10% [1, 2]. Surgical resection has traditionally been the standard treatment of T1 CRC, but recent studies have suggested that endoluminal resection might be feasible if there were no unfavorable histological findings such as deep invasion, poor differentiation, budding, or lymphovascular invasion [3]. Endoscopic resection of early CRC confined to the mucosal layer (Tis) and superficial submucosal layer (superficial T1) without unfavorable histology is considered curative, and can avoid over-surgery and improved quality of life after treatment as compared with surgical resection. On the contrary, underestimation of invasion depth may result in post-colonoscopy CRC with a potentially poor prognosis. A recent Dutch study showed that once recurrence occurs the risk of mortality could be as high as 40% [4]. Nevertheless, a recent Japanese study showed there was no increased risk of lymph node metastasis or recurrence after secondary surgery (attempted endoscopic resection followed by surgery if the histological findings were unfavorable) as compared with primary surgery [5]. This finding is consistent with later studies showing the similar results [6, 7].

Modern endoscopic methods, especially image-enhanced endoscopic technologies, such as narrow band imaging (NBI) or chromoendoscopy (CE), are able to demonstrate the surface and/or capillary characteristics of lesions, which assists in making an accurate endoscopic diagnosis (Fig. 7.1).

7.2 Risk of Lymph Node Metastasis in T1 Colorectal Cancers

Data of the lymph node metastasis rate in CRC is primarily from studies analyzing surgically resected specimens. Gunderson et al. examined SEER 1992–2004 data, and reported that the overall lymph node metastasis rate was 10% in 16,864 T1 CRCs, and the risk was higher in rectal rather than in colonic T1 cancers. (12.3 vs. 8.9%, respectively). A meta-analysis summarizing 17 studies showed that the overall risk of lymph node metastasis was 11.4%, with the risk in rectal T1 cancers higher than that in colonic T1 cancers (risk ratio = 1.37). This is clinically relevant, as radical surgery for rectal cancer is usually associated with higher invasiveness, and increased risk of complications making local excision an attractive alternative treatment option. The higher risk of lymph

H. M. Chiu (✉)
Department of Internal Medicine, National Taiwan University Hospital, Taipei, Taiwan

Department of Internal Medicine, College of Medicine, National Taiwan University, Taipei, Taiwan
e-mail: hanmochiu@ntu.edu.tw

P. W. Y. Chiu et al. (eds.), *Endoscopy in Early Gastrointestinal Cancers, Volume 1*,
https://doi.org/10.1007/978-981-10-6769-3_7

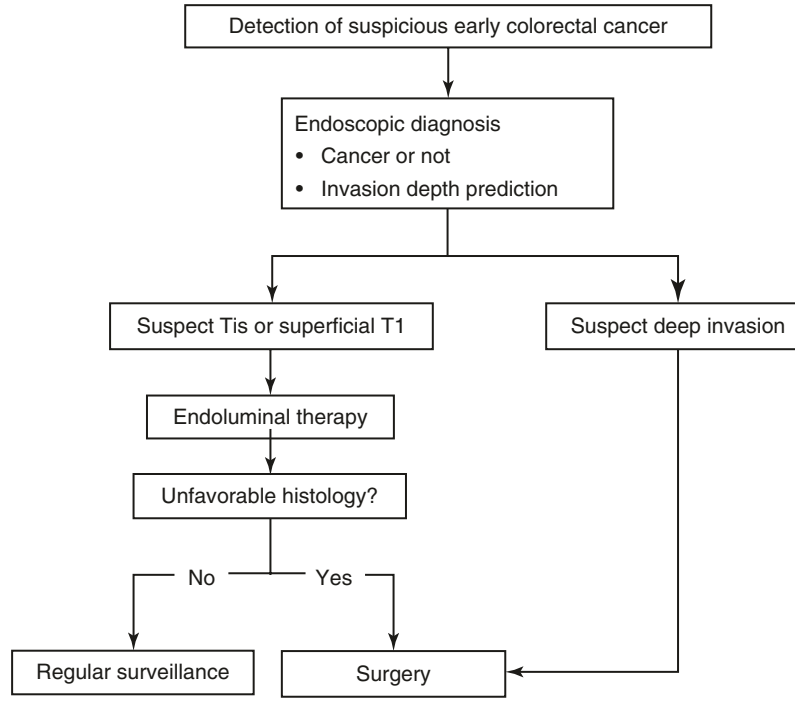

Fig. 7.1 Conceptual framework of managing patients with suspected early colorectal cancer

node metastasis in rectal T1 cancer, however, should be carefully considered when offering this option to patients (Tables 7.1 and 7.2).

Table 7.1 Risk of lymph node metastasis in T1 colorectal cancer (SEER, 1999–2004; adopted from: Gunderson et al. *J Clin Oncol. 2010*;28:264–71) [2]

N Stage	Number	%
N0	15,196	90.1
N1a	962	5.7
N1b	509	3.0
N2a	141	0.8
N2b	56	0.33
Total	16,864	

Table 7.2 Comparison of the risk of lymph node metastasis in T1 colon and rectal cancer (SEER, 1999–2004; adopted from: Gunderson et al. *J Clin Oncol.* 2010;28:256–63) [1]

	Colon		Rectum	
N Stage	Number	%	Number	%
N0	10,930	91.1	4266	87.7
N1a	643	5.4	319	6.6
N1b	325	2.7	184	3.8
N2a	77	0.6	64	1.3
N2b	27	0.2	29	0.6
Total	12,002	100	4862	100

7.3 Endoscopic Methods Used for the Diagnosis of Early Colorectal Cancer

Step-by-step application of different endoscopic methods is necessary for establishing an accurate diagnosis, and excluding the presence of deep invasive cancer, which is contraindicated for endoscopic resection. When lesions are detected, white light endoscopy (WLE) is used first to evaluate the gross morphology and color under normal magnification. Then, NBI is used to enhance the surface and capillary pattern under both normal and high magnification. Chromoendoscopy can then be performed with indigo-carmine (IC) dye to delineate the macroscopic morphology of the lesion under normal magnification. A pit pattern can be visualized under high-magnification CE. When a malignant lesion is suspected, greater delineation of subtle surface characteristics (Kudo's type V pit pattern) is necessary, and it usually requires crystal violet staining and high-magnification observation. Such a step-by-step approach can facilitate qualitative (presence of malignancy) and qualitative (invasion depth) evaluation of the lesion.

– *White light endoscopy*:

Nevertheless there already exist several IEE (Image enhanced endoscopy) modalities for clinical use, observation with ordinary WLE remains the most basic and important first step for diagnosing early CRC. In fact, many deeply invasive T1 cancers can be diagnosed with WLE alone. Magnified observation with NBI or CE plays the role of confirming the diagnosis made by WLE, which increase the diagnostic accuracy. The following features observed under WLE suggestive of a deeply invasive malignancy:

- Fold convergence (Fig. 7.2a)
- Stiffness of the surface (Fig. 7.2b)
- Bleeding during irrigation (Fig. 7.2c)
- Bulging tumor surface (Fig. 7.2d)

Using the abovementioned features of deeply invasive cancers, the accuracy in predicting invasion depth (differentiating deep vs. superficial invasive cancers) can be as high as 70–80%.

– *Narrow band imaging.*

NBI enhances the capillary network within the mucosal layer. It has been reported that the morphology of the capillary network in cancerous lesions is closely associated with invasion depth [8]. Observation under magnification is usually

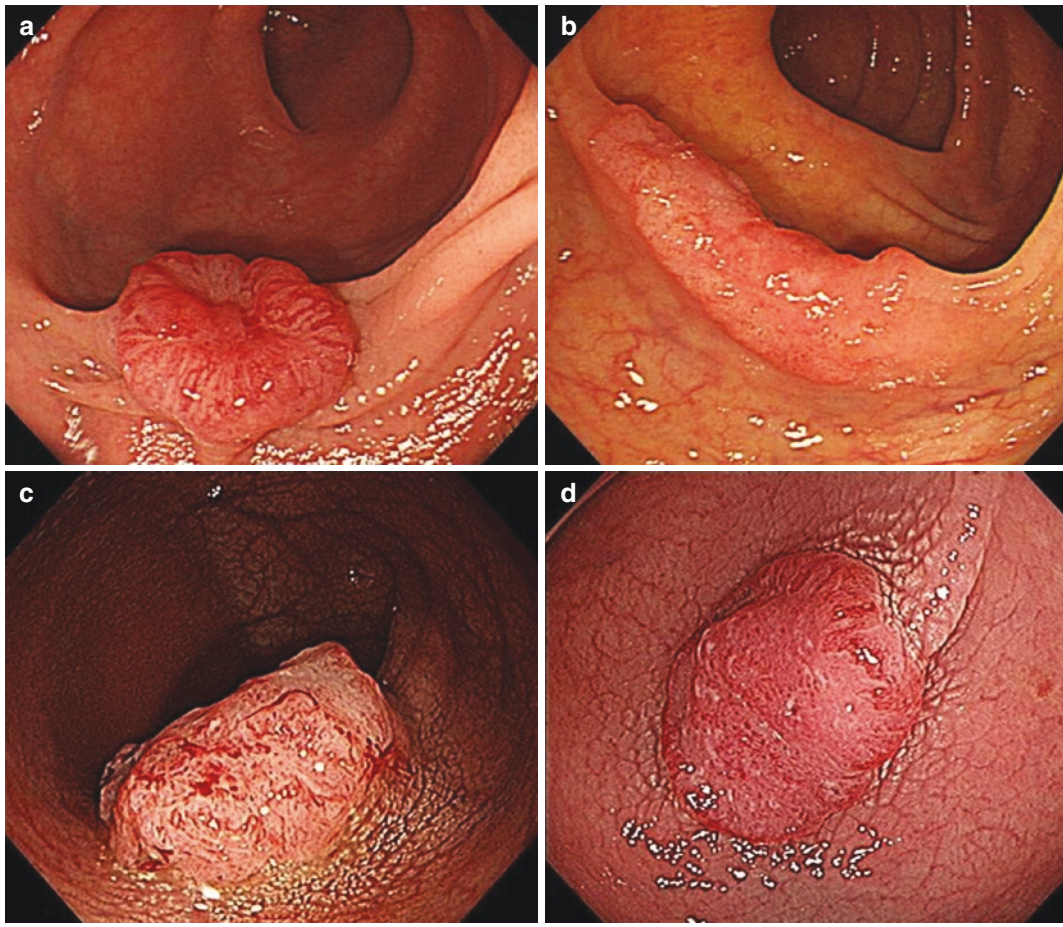

Fig. 7.2 Endoscopic characteristics indicating deep invasion. (**a**) Fold convergence, (**b**) Surface stiffness, (**c**) Easy bleeding, (**d**) bulging of tumor surface

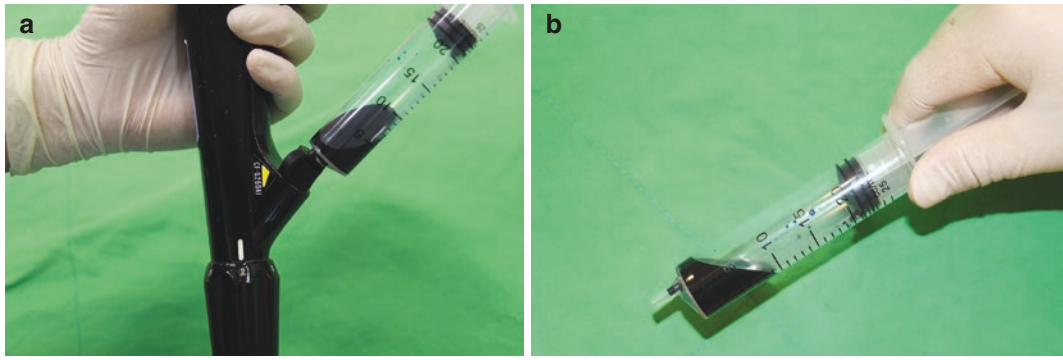

Fig. 7.3 Chromoendoscopy: Indigo-carmine dye spraying with syringe. (**a**) Dye is sprayed with the syringe by connecting to the working channel of the endoscope. (**b**) 5 mL of indigo-carmine dye is put into the 25 mL syringe and fill the remaining space with air

necessary for better visualization of the capillary network appearance.

– Chromoendoscopy [9].
  - Indigo-carmine (IC). IC is a non-absorbing contrast dye that accumulates in the mucosal crypts, and thereby enhances the contrast of crypts and the surface of the colonic mucosa. Typically, 0.4% IC dye is used for observation of colorectal lesions. During colonoscopy, it is convenient to put 5 mL of IC dye in a 25 mL syringe, fill the remaining space with air, and then deliver the dye via the working channel of the colonoscope. The air pushes the dye into the colon lumen, and helps to avoid using too much dye, which may darken the visual field (Fig. 7.3a). IC dye is useful for defining lesion morphology, and can assist in visualization of Kudo's pit pattern under magnification. Usually, a type I–IV pit pattern can be easily enhanced and visualized with IC dye. In our endoscopic unit (National Taiwan University Hospital), we usually prepare IC dye solution twice a week to guarantee good color quality of the dye, as discoloration may occur after a period of 3–4 days.
  - Crystal violet (CV): CV is a dye used to stain and delineate subtle structural changes on the mucosal surface. A concentration of 0.05% is usually used, and it is an indispensable tool for the observation of Kudo's type V pit pattern (type V_I and V_N), as well as for evaluating the invasion depth of early CRCs. When observing the Kudo type V pit pattern, the tip of the colonoscopy has to be about 2 mm from the lesion surface. Special attention should be paid to avoid contact bleeding, because once bleeding occurs during the process of staining the observation of subtle mucosal changes is very difficult. CV is applied in a different manner from IC dye. A nontraumatic catheter is typically used for spraying the dye. The catheter has a roundish tip with a flushing hole, and its use can avoid trauma and resultant bleeding from the surface of the lesion during staining (Fig. 7.4). Using a nontraumatic catheter can also limit the amount of CV sprayed during the proce-

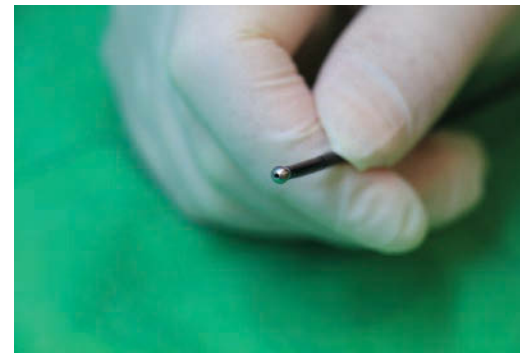

Fig. 7.4 Chromoendoscopy: Crystal violet staining with nontraumatic catheter

dure, as too much can significantly darken the visual field by adhering to the surrounding colonic mucosa, and also helps to adjust the orientation of the lesion to facilitate observation. Gentle irrigation of the mucus adherent to the mucosal surface followed by repeated CV staining (stain 2–3 times, 30–60 s each time) is the key to obtaining a clear and informative magnified CE view.

7.4 Endoscopic Morphology

Though larger lesion size is associated with increased risk of invasive cancer, the gross morphology of a colorectal neoplasm is even more important for evaluating the risk of malignant transformation and/or deep invasion [10]. There are specific morphological characteristics that are associated with a higher risk of invasive cancer [11]. Studies have shown that a depressed neoplasm (0-IIc, 0-IIa + IIc or 0-IIc + IIa) (Fig. 7.5) has an extraordinarily high risk of being an invasive cancer at a relatively small size as compared with polypoid neoplasms or a laterally spreading tuamor (LST) [12, 13]. Within the LST category, a nongranular type LST has a much higher risk of being an invasive cancer, or even a multifocal invasive cancer, especially a nongranular type LST with pseudo-depression (LST-NG-PD) morphology [14]. The various morphologies of LSTs are shown in Fig. 7.6. Uraoka et al. reported that 28% of submucosal invasion was multifocal, and en bloc resection is warranted to provide a more complete specimen for comprehensive pathological analysis [15]. In this context, endoscopic submucosal dissection (ESD) is necessary to achieve en bloc resection [16]. A lesion with 0-Is+IIc or 0-IIc + Is morphology (Fig. 7.7) is usually a deeply invasive cancer. The polypoid (0-Is) portion of the lesion arises from the depressed portion of its precursor 0-IIc or 0-IIa + IIc lesion [11].

Chromoendoscopy with IC dye is the criterion standard for defining gross morphology. For depressed neoplasms, the depressed area is sometimes difficult to delineate with WLE or even with NBI, although the latter can enhance the lesion itself (Fig. 7.8). If the morphology indicates a depressed or LST-NG-PD, then detailed observation under magnification after CV staining may be helpful for diagnosing malignant changes and deep invasion. Depressed lesions with 0-IIa + IIc or 0-Is+IIc morphology are considered as originated and progressed from 0-IIc lesion, carrying even higher risk of invasive cancers; therefore, endoscopists should pay special attention during observation.

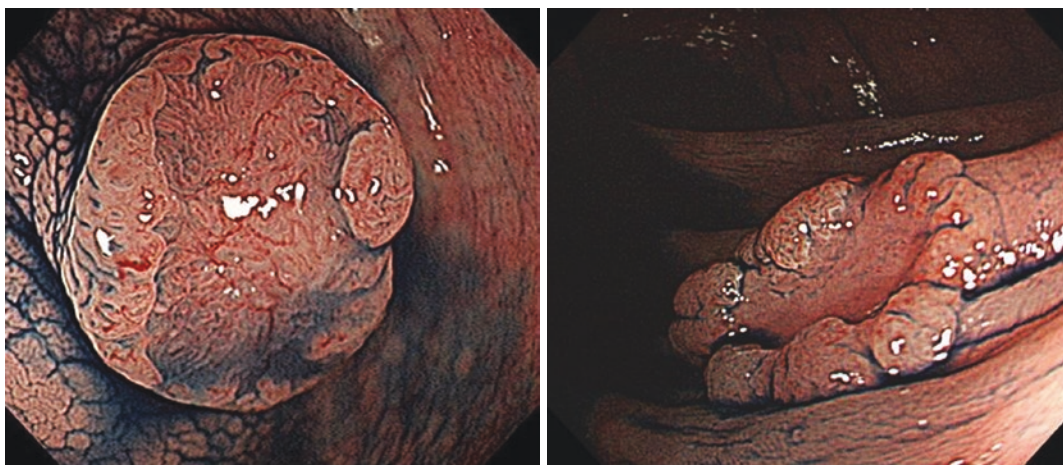

Fig. 7.5 Depressed colorectal neoplasm

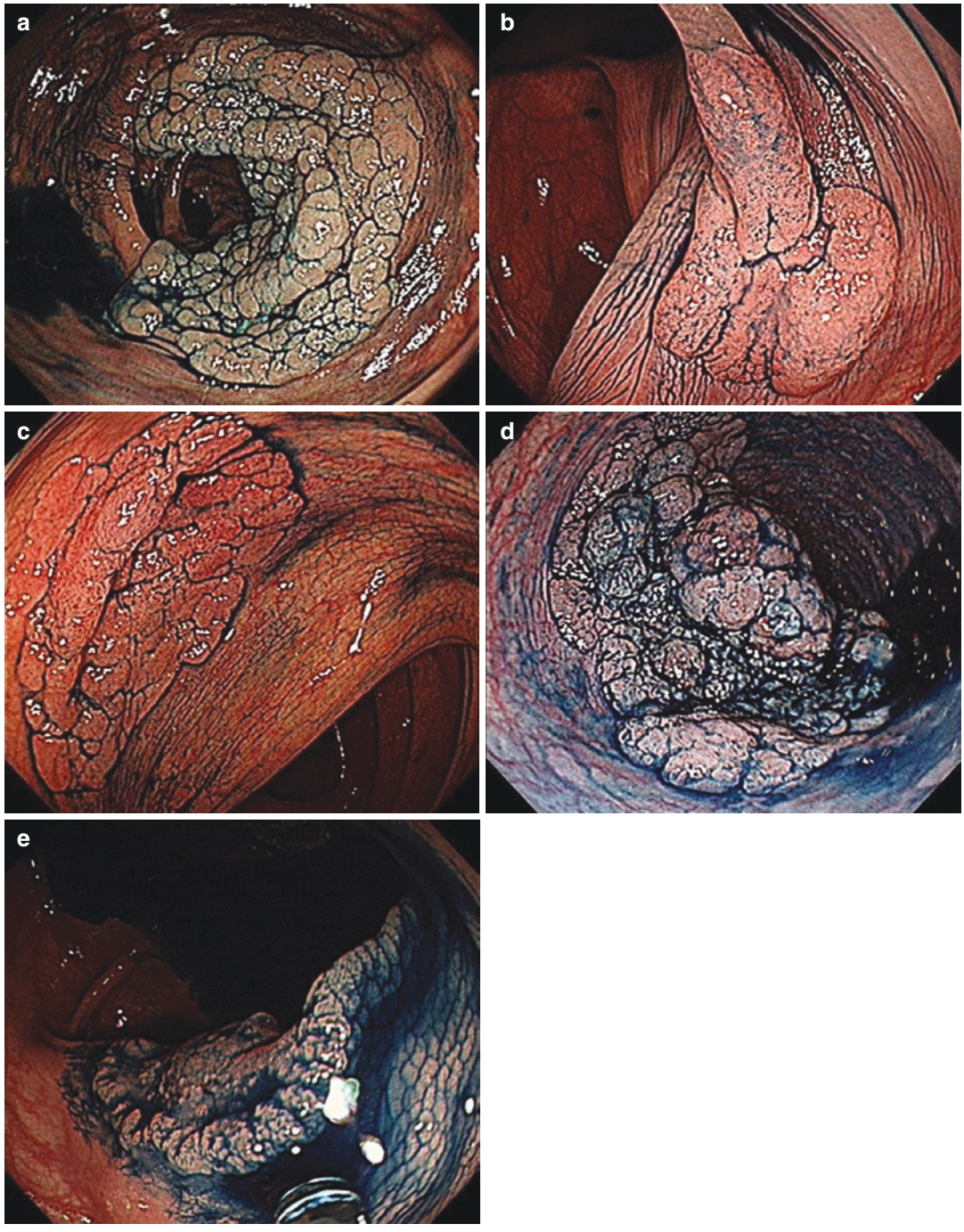

Fig. 7.6 Different morphological types of laterally spreading tumor (LST). (**a**) homogenous granular type (LST-G-H), (**b**) and (**c**) flat elevated nongranular type (LST-NG-FE), (**d**) mixe nodular granular type (LST-G-NM), (**e**) pseudo-depressed nongranular type (LST-NG-PD)

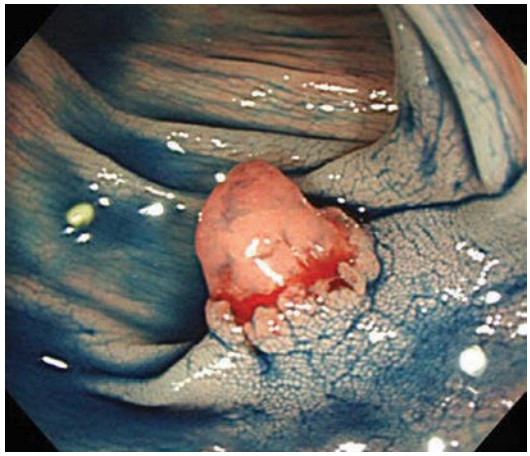

Fig. 7.7 Type 0-Is+IIc lesion. The 0-Is part (polypoid) of such lesion is considered as arisen from the depressed portion (cancerous part) of its precursor 0-IIc or 0-IIa + IIc lesion

7.5 Narrow Band Imaging Findings

The NICE (NBI International Colorectal Endoscopic) classification has been introduced for classifying neoplastic and nonneoplastic colorectal lesions, and studies have shown that it is highly accurate. Among neoplastic capillary patterns, NICE type 3 usually refers to deep invasive cancers that should be surgically resected. NICE type 2, however, contains heterogeneous groups of neoplasms, including benign adenoma, adenoma with high-grade dysplasia (or Tis), shallow or even deep invasive cancers [17]. This classification is, therefore, not considered discriminatory for deep and superficial invasive cancers. The JNET (Japanese NBI Expert Team) classification system was sub-

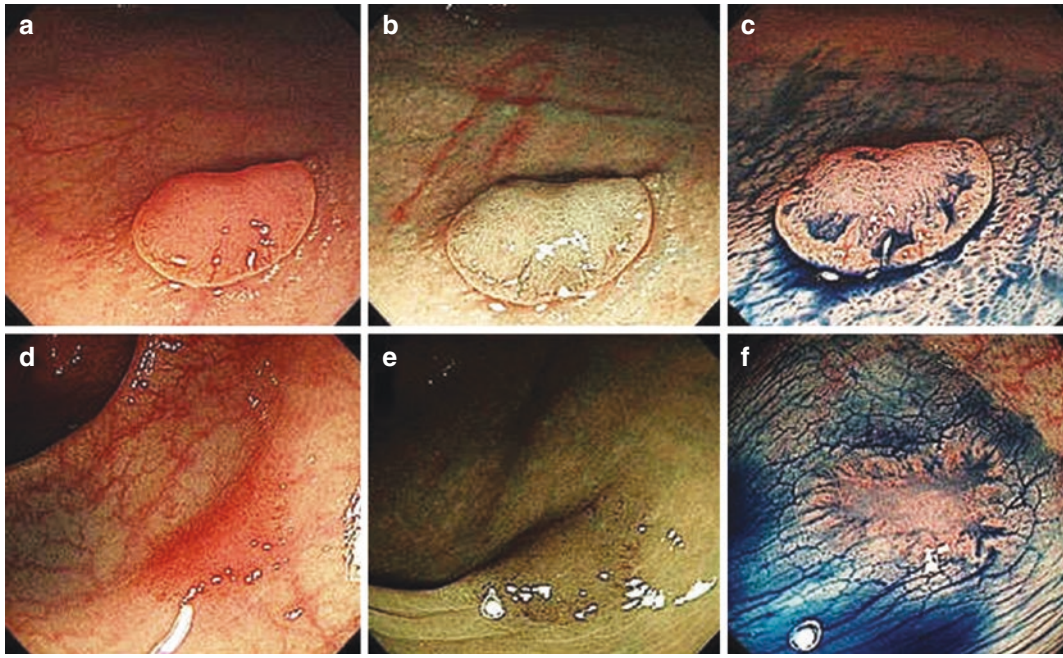

Fig. 7.8 Enhancing macroscopic morphology of colorectal neoplasms with IEE modalities. (**a**) 0-IIa + IIc lesion, WLE, (**b**) 0-IIa + IIc lesion, NBI, (**c**) 0-IIa + IIc lesion, chromoendoscopy with IC, (**d**) LST-NG-PD, WLE, (**e**) LST-NG-PD, NBI, (**f**) LST-NG-PD, chromoendoscopy with IC

sequently proposed to improve treatment guidance [18]. JNET type 2A usually refer to an adenoma with low-grade dysplasia, and 2B refers to HGD/Tis or superficially invasive T1 cancers. JNET type 3 is basically equivalent to NICE type 3, which indicates deeply invasive cancers for which endoluminal treatment is contraindicated [19]. A validation study using this system is now still ongoing (2017). The details of these two classification systems will be described in latter sections of this chapter. Some examples are shown in Fig. 7.9.

7.6 Chromoendoscopic Findings

The Kudo pit pattern is the most widely used system for CE diagnosis of colorectal lesions [20, 21]. Magnifying CE is useful for discriminating neoplastic from nonneoplastic lesions, and also useful for prediction of invasion depth of malignancies. Kudo type V pit patterns (V_I and V_N) usually indicate a malignant lesion (Fig. 7.10). Of them, the type V_N pit pattern refers to massively invasive cancers, which cannot be resected endoscopically. The type V_I pit pattern generally represents noninvasive cancers (Tis/high-grade dysplasia, or superficially invasive cancer), which can be resected endoscopically. However, some highly irregular V_I pit patterns may represent deeply invasive cancer and endoscopists should be aware of this possibility. It is worthwhile to note that V_I pit pattern located within a demarcated area is a sign of deep invasion, which has a very high diagnostic accuracy [22].

7.7 NBI or CE for Prediction of Invasion Depth

Both NBI and CE have been demonstrated to be useful for predicting invasion depth of early CRC. However, there is a paucity of direct comparisons of the two methods [23]. Nevertheless, many countries do not have CV dye available for endoscopic use, and thus are limited to using only NBI to predict depth of invasion. NBI has the advantage of a relatively simple dye staining process, which usually requires approximately 5 min. There are some concerns, however, when using NBI for predicting invasion depth. First, if touch bleeding of the lesion occurs during endoscopic observation, NBI observation may become extremely difficult. Second, the NBI classification system for differentiating deep invasive cancer from superficially invasive cancer or Tis (the JNET system) is still under validation. Third, Sakamoto et al. reported that the accuracy of using NBI or CV for predicting invasion depth were similar, but CE and CV staining had superior interobserver agreement as compared with NBI using the Sano classification system [24]. Further study is warranted in this aspect.

7.8 Role of Endoscopic Ultrasound (EUS) in Diagnosing Early Colorectal Cancer

Endoscopic ultrasound is commonly used for evaluating invasion depth of various gastrointestinal tract malignancies, such as esophageal and gastric cancers. Previous meta-analysis revealed that the diagnostic accuracy of EUS in predicting invasion depth of CRC is T stage specific, with 87.8% sensitivity for T1 rectal cancer, which is significantly lower than the sensitivity of 95.4% for T4 cancer [25]. Thus, EUS has yet to become a standard procedure for diagnosing invasion depth of early CRCs prior to the endoscopic resection. In Japan, magnified CE with CV staining is more popular than EUS for evaluating the invasion depth of early CRCs. Currently, there are only a few studies directly comparing the diagnostic performance of EUS and CE using CV. An early study from Japan demonstrated that CE with CV dye had superior diagnostic accuracy than EUS [26]. Owing to the convenient one-touch operation, CE with magnification is recommended over EUS for determining the invasion depth of CRC.

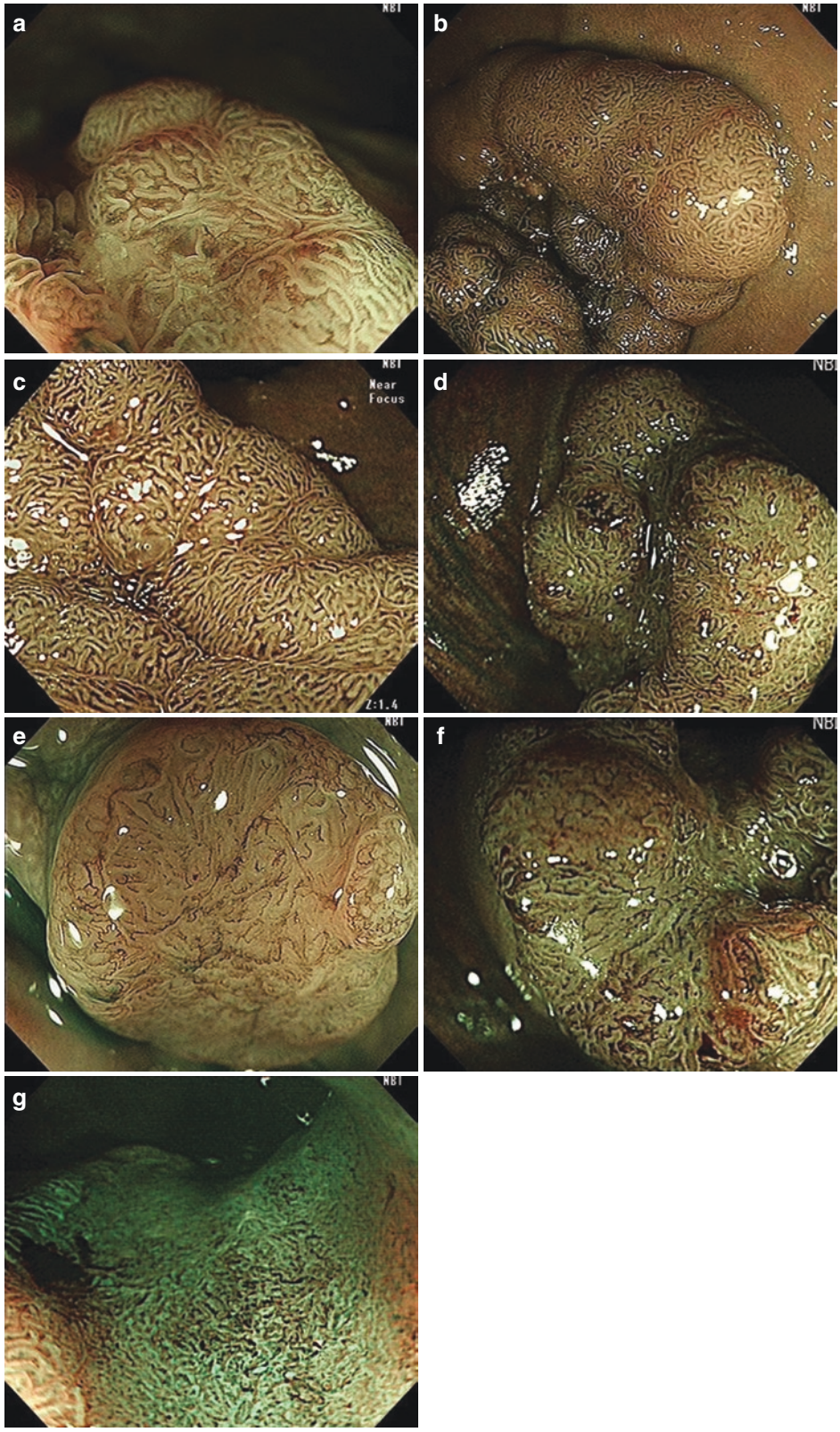

Fig. 7.9 Some examples of JNET type 2 and type 3. (**a**)–(**c**) type 2A, (**d**)–(**e**) 2B, (**f**)–(**g**) type 3

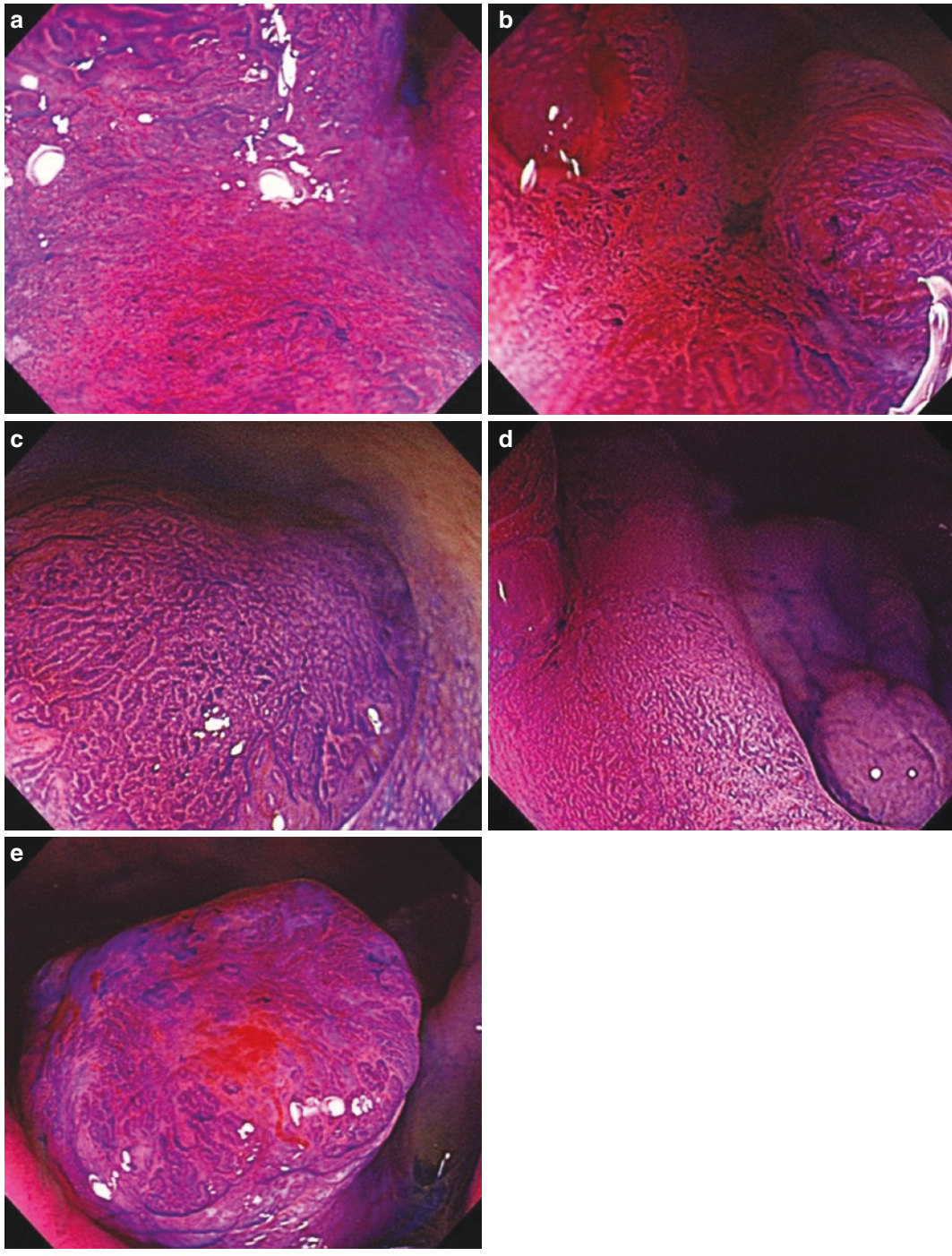

Fig. 7.10 Examples of type V Kudo pit pattern (type V_I or V_N) (**a**)–(**d**): type V_I; (**e**) type V_N

7.9 Summary

Endoscopic diagnosis of invasion depth is of utmost important for clinical decision-making when treating early CRC. IEE modalities, including digital enhancement (e.g., NBI) or CE with IC or CV dye with magnification are very helpful tools. Endoscopists should master these techniques in order to determine invasion depth with a high level of accuracy, which can avoid undertreatment (endoscopic resection for deep invasive cancer) as well as overtreatment (surgery for T_{is} or superficial T1 cancers).

References

1. Gunderson LL, Jessup JM, Sargent DJ, et al. Revised tumor and node categorization for rectal cancer based on surveillance, epidemiology, and end results and rectal pooled analysis outcomes. J Clin Oncol. 2010;28:256–63.
2. Gunderson LL, Jessup JM, Sargent DJ, et al. Revised TN categorization for colon cancer based on national survival outcomes data. J Clin Oncol. 2010;28: 264–71.
3. Bosch SL, Teerenstra S, de Wilt JH, et al. Predicting lymph node metastasis in pT1 colorectal cancer: a systematic review of risk factors providing rationale for therapy decisions. Endoscopy. 2013;45:827–34.
4. Backes Y, de Vos Tot Nederveen Cappel WH, van Bergeijk J, et al. Risk for incomplete resection after macroscopic radical endoscopic resection of T1 colorectal cancer: a multicenter cohort study. Am J Gastroenterol. 2017;112:785–96.
5. Ikematsu H, Yoda Y, Matsuda T, et al. Long-term outcomes after resection for submucosal invasive colorectal cancers. Gastroenterology. 2013;144:551–9. quiz e14
6. Yoshii S, Nojima M, Nosho K, et al. Factors associated with risk for colorectal cancer recurrence after endoscopic resection of T1 tumors. Clin Gastroenterol Hepatol. 2014;12:292–302. e3
7. Tamaru Y, Oka S, Tanaka S, et al. Long-term outcomes after treatment for T1 colorectal carcinoma: a multicenter retrospective cohort study of Hiroshima GI Endoscopy Research Group. J Gastroenterol. 2017;52:1169–79.
8. Ikematsu H, Matsuda T, Emura F, et al. Efficacy of capillary pattern type IIIA/IIIB by magnifying narrow band imaging for estimating depth of invasion of early colorectal neoplasms. BMC Gastroenterol. 2010;10:33.
9. Fujii T, Hasegawa RT, Saitoh Y, et al. Chromoscopy during colonoscopy. Endoscopy. 2001;33:1036–41.
10. Matsuda T, Saito Y, Fujii T, et al. Size does not determine the grade of malignancy of early invasive colorectal cancer. World J Gastroenterol. 2009;15:2708–13.
11. Lambert R, Kudo SE, Vieth M, et al. Pragmatic classification of superficial neoplastic colorectal lesions. Gastrointest Endosc. 2009;70:1182–99.
12. Chiu HM, Lin JT, Chen CC, et al. Prevalence and characteristics of nonpolypoid colorectal neoplasm in an asymptomatic and average-risk Chinese population. Clin Gastroenterol Hepatol. 2009;7:463–70.
13. Matsuda T, Saito Y, Hotta K, et al. Prevalence and clinicopathological features of nonpolypoid colorectal neoplasms: should we pay more attention to identifying flat and depressed lesions? Dig Endosc. 2010;22(Suppl 1):S57–62.
14. Kim BC, Chang HJ, Han KS, et al. Clinicopathological differences of laterally spreading tumors of the colorectum according to gross appearance. Endoscopy. 2011;43:100–7.
15. Uraoka T, Saito Y, Matsuda T, et al. Endoscopic indications for endoscopic mucosal resection of laterally spreading tumours in the colorectum. Gut. 2006;55:1592–7.
16. Yamada M, Saito Y, Sakamoto T, et al. Endoscopic predictors of deep submucosal invasion in colorectal laterally spreading tumors. Endoscopy. 2016;48:456–64.
17. Hayashi N, Tanaka S, Hewett DG, et al. Endoscopic prediction of deep submucosal invasive carcinoma: validation of the narrow-band imaging international colorectal endoscopic (NICE) classification. Gastrointest Endosc. 2013;78:625–32.
18. Sano Y, Tanaka S, Kudo SE, et al. Narrow-band imaging (NBI) magnifying endoscopic classification of colorectal tumors proposed by the Japan NBI Expert Team. Dig Endosc. 2016;28:526–33.
19. Sumimoto K, Tanaka S, Shigita K, et al. Diagnostic performance of Japan NBI Expert Team classification for differentiation among noninvasive, superficially invasive, and deeply invasive colorectal neoplasia. Gastrointest Endosc. 2017;86:700–9.
20. Kudo S, Lambert R, Allen JI, et al. Nonpolypoid neoplastic lesions of the colorectal mucosa. Gastrointest Endosc. 2008;68:S3–47.
21. Kudo S, Rubio CA, Teixeira CR, et al. Pit pattern in colorectal neoplasia: endoscopic magnifying view. Endoscopy. 2001;33:367–73.
22. Matsuda T, Fujii T, Saito Y, et al. Efficacy of the invasive/non-invasive pattern by magnifying chromoendoscopy to estimate the depth of invasion of early colorectal neoplasms. Am J Gastroenterol. 2008;103:2700–6.
23. Backes Y, Moss A, Reitsma JB, et al. Narrow band imaging, magnifying chromoendoscopy, and gross morphological features for the optical diagnosis of

T1 colorectal cancer and deep submucosal invasion: a systematic review and meta-analysis. Am J Gastroenterol. 2017;112:54–64.
24. Sakamoto T, Saito Y, Nakajima T, et al. Comparison of magnifying chromoendoscopy and narrow-band imaging in estimation of early colorectal cancer invasion depth: a pilot study. Dig Endosc. 2011;23:118–23.
25. Puli SR, Bechtold ML, Reddy JB, et al. How good is endoscopic ultrasound in differentiating various T stages of rectal cancer? Meta-analysis and systematic review. Ann Surg Oncol. 2009;16:254–65.
26. Fu KI, Kato S, Sano Y, et al. Staging of early colorectal cancers: magnifying colonoscopy versus endoscopic ultrasonography for estimation of depth of invasion. Dig Dis Sci. 2008;53:1886–92.

8 NBI International Colorectal Endoscopic (NICE) Classification

Mineo Iwatate, Daizen Hirata, and Yasushi Sano

8.1 History

Narrow-band imaging (NBI) is one of the most frequently used optical digital methods of image-enhanced endoscopy that allows endoscopists to characterize colorectal lesions by enhancing the vessel and surface structure on the lesions [1, 2]. Diagnosis based on the vessel morphological change would be ideal for early detection and accurate diagnosis of colorectal polyps because angiogenesis reflects the growth of tumors critically [3]. In Japan, Sano et al., the initial developer of the NBI system, found the specific differences of vessel morphology on the surface to distinguish each pathological type of colorectal polyps. In normal mucosa or hyperplastic polyp, there are hexagonal thin vessels surrounding crypts which cannot be visualized by magnifying NBI due to lacking resolution power in current system. In adenomatous polyp, these hexagonal vessels uniformly become thicker, and hence they are observable on magnifying NBI, known as meshed capillary (MC) vessels. In harboring cancer, MC vessels are more irregular and dense, which eventually proceed to completely destructed structure of vessels (disruption of thick vessel or avascular) in deep (≥1000 μm) submucosal invasive cancer. He originally reported these vessel patterns for corresponding histology as the Sano classification in 2006, which was validated by several studies [4–7]. Based on the Sano classification, multiple NBI classifications of colorectal lesions with or without optical magnification has been proposed worldwide [8–12]. Although the overall diagnostic performance of these NBI classifications have been shown, the validity of their component criteria has not been established. Therefore, endoscopists around the world needed a universal simple NBI classification available even without magnification for the potential of international use.

Under these circumstances, the Colon Tumor NBI Interest Group (CTNIG) was set up in 2009, with an aim to develop a simplified NBI endoscopic classification of colorectal polyps that can be used with or without optical magnification. The CTNIG consisted of the following six members: Tanaka S (Chair, Japan); Sano Y (Japan); Rex DK (USA); Soetikno RM (USA); Ponchon T (France); and Saunders BP (UK) (Fig. 8.1). In 2009, the CTNIG proposed an NBI classification based on international validation studies [13, 14]. This classification was named as NBI International Colorectal Endoscopic (NICE) classification by Sano Y at London in February 2010 and approved by the members of the CTNIG (Fig. 8.2) [15].

M. Iwatate (✉) · D. Hirata
Gastrointestinal Center, Sano Hospital, Kobe, Japan

Institute of Minimally-Invasive Endoscopic Care (iMEC), Sano Hospital, Kobe, Japan

Y. Sano
Gastrointestinal Center & Institute of minimally-invasive endoscopic care (iMEC), Sano Hospital, Kobe, Hyogo, Japan

P. W. Y. Chiu et al. (eds.), *Endoscopy in Early Gastrointestinal Cancers, Volume 1*,
https://doi.org/10.1007/978-981-10-6769-3_8

8.2 Development of the NICE Classification

Six experienced endoscopists (Japan [Y.S. and S.T.], U. S [D.K.R and R.S] and Europe [B.P.S and T.P]) assessed the reliability of NBI prediction on corresponding histopathology including hyperplastic polyp, adenoma, and deep submucosal invasive cancer. All endoscopists viewed still NBI images of colorectal polyps on a high-definition monitor and predicted their histology with a level of confidence to the prediction (high or low). High-confidence prediction was made when participants had ≥90% certainty of the diagnosis [16]. Combined performance characteristics of high-confidence prediction for adenoma and deep submucosal invasive cancer by international experts are shown in Table 8.1. The accuracy, sensitivity, specificity, positive predictive value (PPV), and negative predictive value (NPV) were 98.9%, 98.0%, 100%, 97.7%, and 100%, respectively, for lesions predicted as adenoma with high confidence, 84.1%, 86.8%, 81.5%, 86.9%, and 81.4%, respectively, for lesions predicted as deep submucosal invasive cancer with high confidence [13, 14].

Fig. 8.1 The Colon Tumor NBI Interest Group (CTNIG)

Following to the confirmation of accurate diagnosis of each histological types of polyps by the experienced endoscopists, CTNIG finally developed the NICE classification after struc-

	Type 1	Type 2	Type 3
Color	Same or lighter than background	Browner relative to background (verify color arises from vessels)	Brown to dark brown relative to background; sometimes patchy whiter areas
Vessels	None, or isolated lacy vessels may be present coursing across the lesion	Brown vessels surrounding white structures**	Has area(s) of disrupted or missing vessels
Surface pattern	Dark or white spots of uniform size, or homogeneous absence of pattern	Oval, tubular or branched white structures** surrounded by brown vessels	Amorphous or absent surface pattern
Most likely pathology	**Hyperplastic & sessile serrated polyp (SSP) *** **	**Adenoma**** **	**Deep submucosal invasive cancer**
Endoscopic image	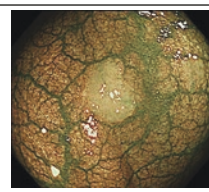	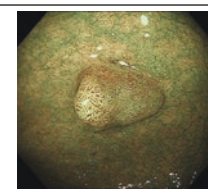	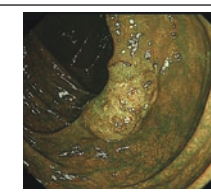

* Can be applied using colonoscopes with/ without optical (zoom) magnification

** These structures (regular or irregular) may represent the pits and the epithelium of the crypt opening.

*** In the WHO classification, sessile serrated polyp and sessile serrated adenoma are synonymous.

**** Type 2 consists of Vienna classification types 3, 4 and superficial 5 (all adenomas with either low or high grade dysplasia, or with superficial submucosal carcinoma). The presence of high grade dysplasia or superficial submucosal carcinoma may be suggested by an irregular vessel or surface pattern, and is often associated with atypical morphology (e.g., depressed area).

Fig. 8.2 The NICE classification

tured discussions and voting using modified Delphi method to achieve a consensus [17]. This classification is divided into three categories for corresponding histology (Type 1, hyperplastic or sessile serrated polyp; Type 2, adenoma; Type 3, deep submucosal invasive cancer) and has three components criteria (color, vessel pattern, and surface pattern).

8.3 Validation of the NICE Classification

First, performance characteristics of individual criterion (color, vessel, surface) was validated by novice or untrained students and summarized in Table 8.2 [13, 14]. Each component was highly associated with corresponding histopathology. Color criterion was worth incorporating to the NICE classification because the specificity of color was as high as that of vessel or surface, and anyone could evaluate it easily and quickly. Then, the CTING validated the whole classification in two studies and obtained the performance characteristics for high-confidence prediction of adenoma (NICE 1 vs 2) and deep submucosal cancer (NICE 2 vs 3) (Table 8.3) [13, 14].

In the prior study, two experts made a prospective evaluation in differentiating adenoma from hyperplastic polyp during colonoscopy. They assessed 236 consecutive subcentimeter colorectal polyps using NBI including 192 diminutive (≤5 mm) and 44 small (6–9 mm) polyps. Of 236

Table 8.1 Combined performance characteristics of high-confidence prediction by international experts

Prediction	Adenoma	Deep submucosal invasive cancer
Polyp (n)	118	80
Performance, % (95% CI)		
Accuracy	99 (98–100)	84 (79–88)
Sensitivity	98 (95–99)	87 (79–92)
Specificity	100 (98–100)	82 (74–88)
PPV	100 (99–100)	81 (74–88)
NPV	98 (95–99)	87 (80–92)

CI confidence interval, *PPV* positive predictive value, *NPV* negative predictive value

Table 8.3 Performance characteristics of the NICE classification for high-confidence prediction

	NICE 1 vs 2	NICE 2 vs 3
Prediction	Adenoma	Deep submucosal invasive cancer
Rater, n	Experts, 2	Medical students, 5
Polyps (n)	236	400
Evaluation	Real time during colonoscopy	Still images
Performance, % (95% CI)		
Accuracy	89 (83–93)	90 (85–93)
Sensitivity	98 (94–100)	92 (87–95)
Specificity	69 (55–80)	88 (84–92)
PPV	87 (80–92)	88 (83–91)
NPV	95 (84–99)	92 (87–95)
HC rate, %	75	50

Table 8.2 Performance characteristics of individual criterion when validated by novice or untrained students

Prediction	Adenoma			Deep submucosal invasive cancer		
Participants (n)	44			5		
Criterion	Color	Vessel	Surface	Color	Vessel	Surface
Accuracy, % (95% CI)	71 (68–74)	86 (84–88)	86 (83–89)	71 (67–75)	79 (75–82)	77 (73–81)
Sensitivity, % (95% CI)	49 (42–56)	80 (74–85)	83 (75–88)	71 (66–76)	88 (84–92)	73 (68–77)
Specificity, % (95% CI)	93 (91–95)	92 (90–95)	90 (87–94)	71 (67–75)	72 (68–74)	81 (77–84)
PPV, % (95% CI)	88 (86–91)	92 (90–94)	91 (88–93)	66 (61–70)	71 (67–74)	75 (70–79)
NPV, % (95% CI)	65 (62–68)	83 (79–87)	85 (80–89)	76 (72–80)	89 (84–92)	79 (75–83)

polyps, 149 (63%) were adenoma with a mean size of 4.6 mm (range, 1–9) and 87 (37%) were non-adenomatous lesions with a mean size of 3.2 mm (range, 1–8). 75% of all polyps were predicted with high confidence (82% in adenomas; and 64% in hyperplastic polyps). The diagnostic performance with high-confidence prediction reached 89% in accuracy, and 95% in negative predictive value for all polyps, 88% in accuracy and 95% in negative predictive value for diminutive polyps. These diagnostic performances potentially met the thresholds for adopting real-time endoscopic assessment of the histology of diminutive colorectal polyps established by the American Society of Gastroenterology [18, 19].

In the latter study, five trained medical students assessed the performance characteristics of NICE 3 lesions for deep submucosal invasive cancer by using a high-definition still NBI image library of consecutive colorectal tumors, which consisted of 22 tubular adenomas with low-grade dysplasia, 23 adenomatous lesions with high-grade dysplasia or superficial (<1000 μm) submucosal invasive cancer, and 35 deep submucosal invasive cancers. The mean size of the lesions was 21.2 ± 10.3 mm (range 6–60 mm). All images were taken using high-definition colonoscopes without optical magnification (CF-H260AZI; Olympus, Tokyo, Japan). The five trained medical students made a high-confidence prediction in 50% of all polyps. Among the lesions with high-confidence prediction, the students achieved 90% of accuracy, 92% of sensitivity, 88% of specificity, 88% of positive predictive value, and 92% of negative predictive value.

The CTNIG confirmed that the NICE classification is valid for real-time NBI diagnosis of adenoma in clinical practice and for diagnosis of deep submucosal cancer using still images without optical magnification.

8.4 Treatment Strategy Using the NICE Classification in Clinical Practice

When you diagnose a polyp as NICE 1, the corresponding histopathology of the polyp is either hyperplastic polyp (HP) or sessile serrated polyp (SSP). There are several endoscopic findings and classifications which may be useful to differentiate SSP from HP; however, the diagnostic performance of these were unsatisfactory in terms of accuracy and sensitivity [20–22]. The main reason for this is the low concordance rate of its diagnosis among pathologists. As there is no standard consensus or diagnostic criteria for SSP, the treatment strategy of NICE 1 lesions depends on its location and size. Sano W et al. reported the proportion of SSP 5 mm or less in size was 1.8% in proximal colon and 0.9% in distal colon and that of SSP 6–9 mm in size was 43.8% and 22.2% among polyps with hyperplastic features [23]. Based on these data, NICE 1 lesions greater than 6 mm in size should be resected.

NICE 2 lesions predictive of adenoma should basically be treated by endoscopic resection. This category includes benign low-grade adenomas as well as high-grade adenomas and submucosal invasive cancer with malignant behavior (Fig. 8.3). These two types should be diagnosed individually in terms of choosing correct treatment strategy. The former is basically benign and can be treated by polypectomy or piecemeal resection. The latter is malignant and should be treated by en bloc deep resection such as EMR or ESD to examine correct invasion depth of cancer for deciding curative or non-curative resection. The Japan NBI expert team (JNET) divided type 2 category into type 2A (low grade adenoma) and 2B (high grade adenoma and submucosal cancer) using magnifying endoscopy. They have developed advanced classification called the JNET classification based on the NICE classification [15, 24].

For NICE 3 category predictive for deep submucosal cancer, the diagnostic performance of NICE 3 achieved high accuracy of 90% when diagnosed with high confidence. If you diagnose NICE 3 with high confidence, surgical resection is recommended. However, in case of NICE 3 with low confidence, prior endoscopic resection should be considered carefully before surgical resection because the diagnostic performance of NICE 3 with low confidence are not high, hence curative therapy may be achieved endoscopically.

	NICE 2	
Most likely pathology	Low grade adenoma	High grade adenoma~SM Cancer
Endoscopic image	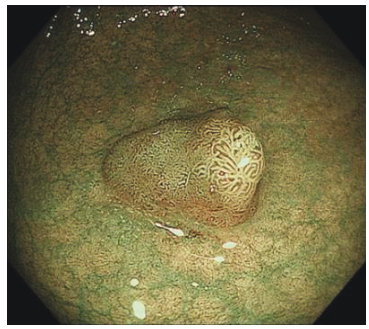	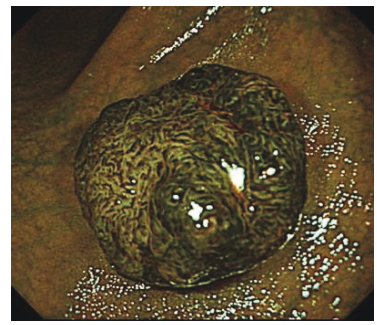
Treatment	Polypectomy (piecemeal resection: acceptable)	EMR/ESD (*En bloc* resection)

Fig. 8.3 NICE 2 category

The NICE classification is the simple and validated classification developed by international experts. This classification has been established and disseminated in many countries where magnifying endoscopy is not available.

References

1. Gono K, Obi T, Yamaguchi M, et al. Appearance of enhanced tissue features in narrow-band endoscopic imaging. J Biomed Opt. 2004;9:568–77.
2. Tajiri H, Niwa H. Recent advances in electronic endoscopes: image-enhanced endoscopy. Jpn Med Assoc J. 2008;51:199–203.
3. Konerding MA, Fait E, Gaumann A. 3D microvascular architecture of pre-cancerous lesions and invasive carcinomas of the colon. Br J Cancer. 2001;84:1354–62.
4. Sano Y, Ikematsu H, Yoshida S, et al. Meshed capillary vessels using narrow band imaging for differential diagnosis of small colorectal polyps. Gastrointest Endosc. 2008;23:278–83.
5. Katagiri A, Fu KI, Yoshida S, et al. Narrow band imaging with magnifying colonoscopy as a diagnostic tool for predicting the histology of early colorectal neoplasia. Aliment Pharmacol Ther. 2008;27:1269–74.
6. Ikematsu H, Matsuda T, Sano Y, et al. Efficacy of capillary pattern type IIIA/IIIB by magnifying narrow band imaging for estimating depth of invasion of early colorectal neoplasms. BMC Gastroenterol. 2010;10:33.
7. Sano Y, Horimatsu T, Fu KI, et al. Magnifying observation of microvascular architecture of colorectal lesions using a narrow band imaging system. Dig Endosc. 2006;18:S44–51.
8. Tanaka S, Hirata M, Oka S, et al. Clinical significance of narrow band imaging (NBI) in diagnosis and treatment of colorectal tumor. Gastroenterol Endosc. 2008;50:1289–97.
9. Wada Y, Kudo S, Kashida H, et al. Diagnosis of colorectal lesions with the magnifying narrow-band imaging system. Gastrointest Endosc. 2009;70:522–31.
10. Nikami T, Saito S, Tajiri H, et al. The evaluation of histological atypia and depth of invasion of colorectal lesions using magnified endoscopy with narrow-band imaging. Gastroenterol Endsc. 2009;51:10–9.
11. East JE, Suzuki N, Bassett P, et al. Narrow band imaging with magnification for the characterization of small and diminutive colonic polyps: pit pattern and vascular pattern intensity. Endoscopy. 2008;40:811–7.
12. Rastogi A, Keighley J, Singh V, et al. High accuracy of narrow band imaging without magnification for the real-time characterization of polyp histology and its comparison with high-definition white light colonoscopy: a prospective study. Am J Gastroenterol. 2009;104:2422–30.
13. Hewett DG, Kaltenbach T, Sano Y, et al. Validation of a simple classification system for endoscopic diagnosis of small colorectal polyps using narrow-band imaging. Gastroenterology. 2012;143:599–607.

14. Hayashi N, Tanaka S, Hewett DG, et al. Endoscopic prediction of deep submucosal invasive carcinoma: validation of the narrow-band imaging international colorectal endoscopic (NICE) classification. Gastrointest Endosc. 2013;78:625–32.
15. Sano Y, Tanaka S, Kudo SE, et al. Narrow-band imaging (NBI) magnifying endoscopic classification of colorectal tumors proposed by the Japan NBI expert team. Dig Endosc. 2016;28:526–33.
16. Rex DK. Narrow-band imaging without optical magnification for histologic analysis of colorectal polyps. Gastroenterology. 2009;136:1174–81.
17. Milholland AV, Wheeler SG, Heieck JJ. Medical assessment by a Delphi group opinion technic. N Engl J Med. 1973;288:1272–5.
18. Rex DK, Kahi C, O'Brien M, et al. The American Society for Gastrointestinal Endoscopy PIVI (preservation and incorporation of valuable endoscopic innovations) on real-time endoscopic assessment of the histology of diminutive colorectal polyps. Gastrointest Endosc. 2011;73:419–22.
19. Abu Dayyeh BK, Thosani N, Konda V, et al. ASGE Technology Committee systematic review and meta-analysis assessing the ASGE PIVI thresholds for adopting real-time endoscopic assessment of the histology of diminutive colorectal polyps. Gastrointest Endosc. 2015;81:502.e1–502.e16.
20. Kimura T, Yamamoto E, Yamano HO, et al. A novel pit pattern identifies the precursor of colorectal cancer derived from sessile serrated adenoma. Am J Gastroenterol. 2012;107:460–9.
21. Yamada M, Sakamoto T, Otake Y, et al. Investigating endoscopic features of sessile serrated adenomas/polyps by using narrow-band imaging with optical magnification. Gastrointest Endosc. 2015;82:108–17.
22. IJspeert JE, Bastiaansen BA, van Leerdam ME, et al. Development and validation of the WASP classification system for optical diagnosis of adenomas, hyperplastic polyps and sessile serrated adenomas/polyps. Gut. 2016;65:963–70.
23. Sano W, Sano Y, Iwatate M, et al. Prospective evaluation of the proportion of sessile serrated adenoma/polyps in endoscopically diagnosed colorectal polyps with hyperplastic features. Endosc Int Open. 2015;3:E354–8.
24. Iwatate M, Sano Y, Tanaka S, et al. Validation study for development of the Japan NBI expert team classification of colorectal lesions. Dig Endosc. 2018;30:642–51.

9 The Japan Narrow-Band Imaging Expert Team (JNET) Classification for the Characterization of Colorectal Lesion Using Magnifying Endoscopy

Yasushi Sano, Shinji Tanaka, and Yutaka Saito

9.1 History of Development of Magnifying NBI Classification for Colorectal Lesions

Narrow-band imaging (NBI) was initially developed by Yasushi Sano, Manabu Muto, and Hirokazu Gono et al., under the supervision of Dr. Shigeaki Yoshida at the National Cancer Center Hospital East in 1999 [1, 2]. A prototype short-wavelength narrow-band RGB filter was successfully created in 2001 (monochrome NBI) [1, 2], and the microvascular architecture of the gastrointestinal tract and tumor surface structure were successfully visualized in color using 415 and 540 nm short- and medium-wavelength filters in 2003 [3].

In 2004, Sano et al. reported the usefulness of observing the pit pattern and the usefulness of vascular classification using NBI [3], and reported the first classification of the capillary pattern (so-called "Sano classification") using NBI magnifying colonoscopy in 2006 [4–8]. Thereafter, the Magnifying Endoscopy Study Groups of the Ministry of Health, Labor and Welfare (Sin-ei Kudo, Yasushi Sano, and Haruhiro Inoue groups) discussed the usefulness of NBI classification based on the findings of NBI magnifying endoscopy, which led to the proposal of new classifications (Hiroshima [9, 10], Showa [11], and Jikei [12] classifications) based on the capillary pattern from several institutions.

A number of validation studies of NBI magnifying endoscopic classifications proposed in Japan have reported the usefulness of NBI magnifying endoscopy in the qualitative and quantitative diagnosis of colorectal lesions. However, clinical studies have raised the following issues: (1) existence of multiple terms for the same or similar magnifying findings, (2) the necessity of including the surface patterns in magnifying endoscopic classifications, and (3) differences in the NBI magnifying findings in elevated and superficial lesions. To resolve the aforementioned issues, the necessity of developing a universal classification was discussed.

Y. Sano (✉)
Gastrointestinal Center & Institute of minimally-invasive endoscopic care (iMEC), Sano Hospital, Kobe, Hyogo, Japan

S. Tanaka
Department of Endoscopy at Hiroshima University Hospital, Hiroshima University Hospital, Hiroshima, Japan

Y. Saito
Gastrointestinal Endoscopy Division, National Cancer Hospital, Tokyo, Japan

P. W. Y. Chiu et al. (eds.), *Endoscopy in Early Gastrointestinal Cancers, Volume 1*,
https://doi.org/10.1007/978-981-10-6769-3_9

9.2 The Universal NBI Magnifying Endoscopic Classification of Colorectal Tumors: The Japan NBI Expert Team (JNET) Classification

To establish a universal NBI magnifying endoscopic classification of colorectal tumors, the Japan NBI Expert Team (JNET), consisting of 38 members, mainly specialists in colonoscopy from throughout Japan, was formed within the "Research Group of the National Cancer Center Research and Development Fund" (Yutaka Saito Group) in 2011 (Fig. 9.1).

First, it was necessary to establish common evaluation criteria, and a working group mainly consisting of young but experienced researches from six institutions, including the institution to which the member who first proposed establishment of a classification belonged to, was organized to hold discussions. Consequently, normal/hyperplastic lesions/sessile serrated polyp were classified as type 1, low-grade adenomas as type 2A, high-grade adenomas as type 2B, and deep submucosal invasive cancers as type 3, and a magnifying NBI scale including the vascular and surface patterns was created (Fig. 9.2a, b) [13].

To scientifically evaluate the NBI scale and determine the NBI findings and diagnostic criteria used in the universal classification, a web image interpretation study was conducted by NBI specialists in colonoscopy belonging to the JNET in 2013 (Principal investigator: Yasushi Sano) [14]. Twenty-five expert colonoscopists in the JNET viewed 100 still NBI images with and without magnification on the web to evaluate the NBI findings and necessity of each criterion (vessel pattern and surface pattern) which was counted when the criterion gave a great contribution to the final diagnosis. We found that surface pattern in magnifying NBI images was necessary for diagnosis of polyps in more than 60% of cases, whereas vessel pattern was required in around 90%. Univariate/multivariate analysis among five candidate findings of type 3 in the NBI scale identified three findings (loose vessel area, interruption of thick vessel, and amorphous areas of surface pattern) significantly associated with deep submucosal cancer (Table 9.1). Evaluation of the diagnostic performance for these three findings in combination showed that the sensitivity was highest (54.7%), and the specificity was acceptable (97.4%) when any one of the three findings was evident (Table 9.2). Similarly, three findings of type 2B (variable caliber of vessels, irregular distribution of vessels, and irregular or obscure surface pattern) were identified and the presence of any one of the three type 2B findings

Fig. 9.1 Main member of Japan expert team (Tokyo, 2106)

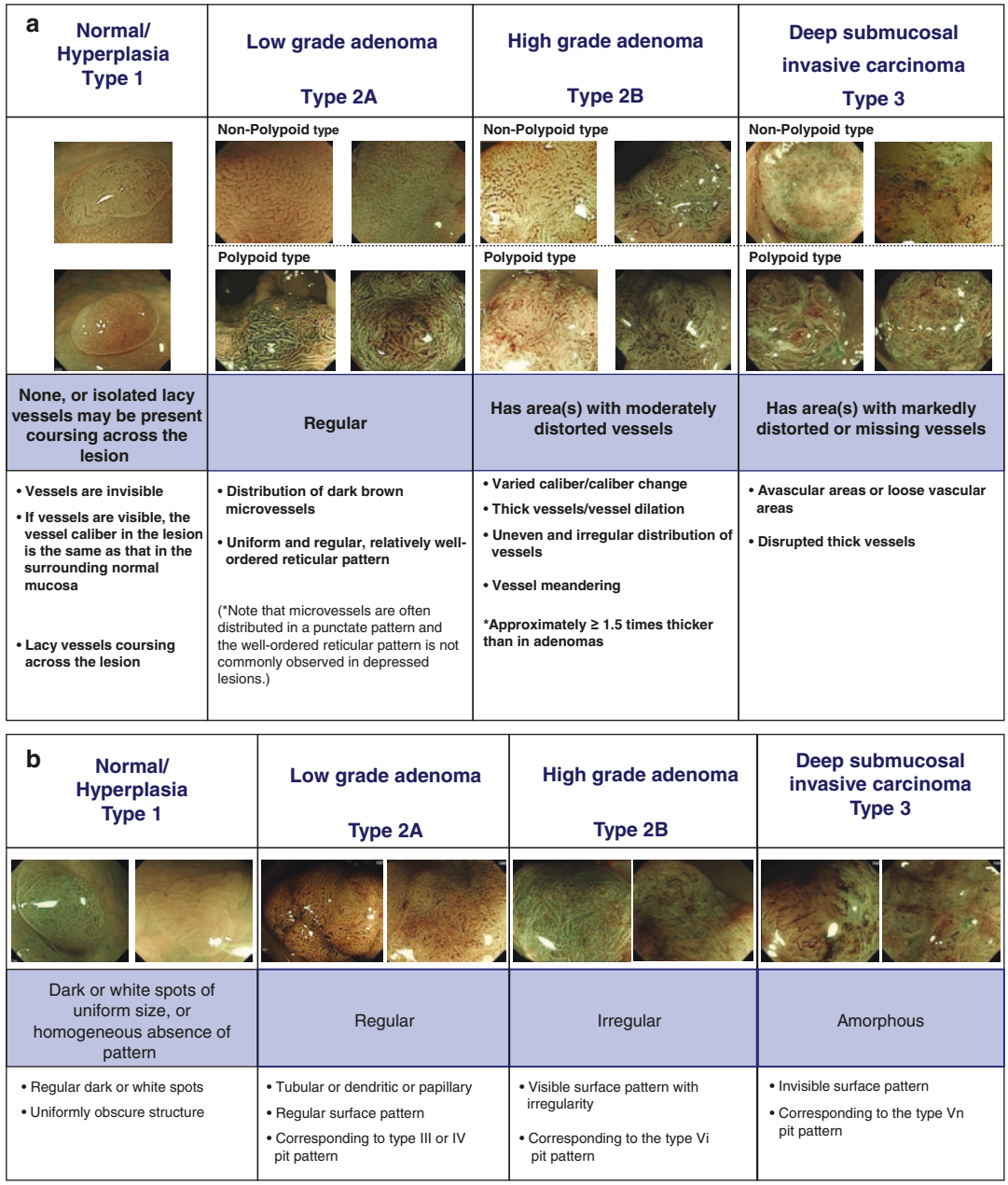

Fig. 9.2 Magnifying NBI scale (**a**) NBI scale and definition for vascular pattern. (**b**) NBI scale and definition for surface pattern

yielded the highest sensitivity of 44.9%, which could diagnose malignant polyps the most. Furthermore, we found that the macroscopic type (polypoid or non-polypoid) had only a little influence on the key diagnostic performance of types 2B and 3.

Based on these data obtained from the present study, the Saito Group meeting on June 6, 2014 reached a consensus on the universal NBI magnifying endoscopic classification of colorectal tumors based on scientific grounds using a modified Delphi method (Fig. 9.3).

Table 9.1 Prevalence and univariate/multivariate analysis of the five candidate type 3 findings for deep submucosal invasive cancer

Type 3 candidate findings	D-SMC (n = 500) no. (%)	S-SMC/ HGIN or LGIN (n = 1000) no. (%)	Univariate analysis OR (95% CI)	Multivariate analysis OR (95% CI)
Loose vessel area	124 (24.8%)	13 (1.3%)	30.5 (16.9–54.9)	5.4 (1.6–18.0)
Interruption of thick vessels	124 (24.8%)	7 (0.7%)	57.0 (26.2–123.8)	12.1 (2.4–61.3)
Scattered vessels	106 (21.2%)	8 (0.8%)	39.5 (19.0–82.2)	2.0 (0.57–6.8)
Thick, linearized/meandering atypical vessels in the tumor	45 (9.0%)	5 (0.5%)	21.6 (8.5–54.9)	0.6 (0.08–3.8)
Amorphous areas of surface pattern	107 (21.4%)	10 (1.0%)	47.6 (24.3–93.2)	4.0 (1.29–12.4)

Table 9.2 Performance characteristics of diagnostic criteria of type 3 in combination with three NBI findings for deep submucosal invasive cancer

Type 3 criteria in combination with three findings[a]		Sensitivity (%)	Specificity (%)
1	Any one of three findings	54.7	97.4
2	Any two of three findings	50.5	98.6
3	All three findings	23.4	99.5

[a]Three findings: loose vessel area, interruption of thick vessel, and amorphous areas of surface pattern

The JNET classification consists of four categories of vessel and surface patterns, i.e., Types 1, 2A, 2B, and 3. Types 1, 2A, 2B, and 3 are correlated with the histopathological findings of hyperplastic polyp/sessile serrated polyp (SSP), low-grade adenoma, high-grade adenoma, and deep submucosal invasive cancer, respectively [15].

Magnifying endoscopy with NBI has been widely used not only in distinction between non-neoplasia and neoplasia, but also, in the differential diagnosis of deep submucosal colorectal cancers from superficial submucosal cancers and intramucosal neoplasms. However, resent systematic review and meta-analysis showed that magnifying NBI and magnifying chromoendoscopy had comparable specificities in diagnosing deep submucosal colorectal cancers, but the sensitivity of M-NBI was slightly lower than that of magnifying chromoendoscopy. Therefore, a detail observation using magnifying chromoendoscopy is recommended, when the lesion is showing JNET type 2B [16].

9.3 Application of the NICE and the JNET Classification

The NICE classification [17, 18] and the JNET classification are compatible with each other because the two classifications both contain three main categories predictive for the same histology (Fig. 9.4). When magnifying endoscopy is not available, the NICE classification should be used in clinical practice. While, the JNET classification is more advanced in selecting the correct therapeutic strategy based on precise diagnosis when magnifying endoscopy is available. A video article introducing the JNET classification with typical cases of each category will help you understand this classification easily in short time [19].

	Type 1	Type 2A	Type 2B	Type 3
Vessel pattern	・Invisible*1	・Regular caliber ・Regular distribution (meshed/spiral pattern)*2	・Variable caliber ・Irregular distribution	・Loose vessel areas ・Interruption of thick vessels
Surface pattern	・Regular dark or white spots ・Similar to surrounding normal mucosa	・Regular (tubular/branched/papillary)	・Irregular or obscure	・Amorphous areas
Most likely histology	Hyperplastic polyp/ Sessile serrated polyp	Low grade intramucosal neoplasia	High grade intramucosal neoplasia/ Shallow submucosal invasive cancer*3	Deep submucosal invasive cancer
Endoscopic image	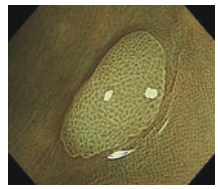	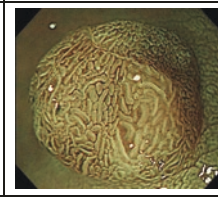		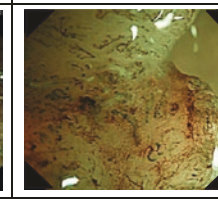

*1. If visible, the caliber in the lesion is similar to surrounding normal mucosa.

*2. Micro-vessels are often distributed in a punctate pattern and well-ordered reticular or spiral vessels may not be observed in depressed lesions.

*3. Deep submucosal invasive cancer may be included.

Fig. 9.3 JNET classification (NBI magnifying endoscopic classification of colorectal tumors)

	Type 1	Type 2	Type 3
Color	Same or lighter than background	Browner relative to background (verify color arises from vessels)	Brown to dark brown relative to background; sometimes patchy whiter areas
Vessels	None, or isolated lacy vessels may be present coursing across the lesion	Brown vessels surrounding white structures**	Has area(s) of disrupted or missing vessels
Surface pattern	Dark or white spots of uniform size, or homogeneous absence of pattern	Oval, tubular or branched white structures** surrounded by brown vessels	Amorphous or absent surface pattern
Most likely pathology	**Hyperplastic & sessile serrated polyp (SSP)*** **	**Adenoma**** **	**Deep submucosal invasive cancer**

* Can be applied using colonoscopes with / without optical (zoom) magnification

** These structures (regular or irregular) may represent the pits and the epithelium of the crypt opening.

*** In the WHO classification, sessile serrated polyp and sessile serrated adenoma are synonymous. SSPs often demonstrate some dark, dilated crypt orifices.

**** Type 2 consists of Vienna classification types 3, 4 and superficial 5 (all adenomas with either low or high grade dysplasia, or with superficial submucosal carcinoma). The presence of high grade dysplasia or superficial submucosal carcinoma may be suggested by an irregular vessel or surface pattern, and is often associated with atypical morphology (e.g., depressed area).

Fig. 9.4 NICE classification

References

1. Sano Y, Kobayashi M, Kozu T, et al. Development and clinical application of a narrow band imaging (NBI) system with built-in narrow-band RGB filters. Stomach Intestine. 2001;36:1283–7.
2. Sano Y. NBI story. Early Colorectal Cancer. 2007;11:91–2.
3. Machida H, Sano Y, Hamamoto Y, et al. Narrow band imaging for differential diagnosis of colorectal mucosal lesions: a pilot study. Endoscopy. 2004;36:1094–8.
4. Sano Y, Horimatsu T, Fu KI, et al. Magnifying observation of microvascular architecture of colorectal lesions using a narrow band imaging system. Dig Endosc. 2006;18:S44–51.
5. Sano Y, Ikematsu H, Fu KI, et al. Meshed capillary vessels by use of narrow-band imaging for differential diagnosis of small colorectal polyps. Gastrointest Endosc. 2009;69:278–83.
6. Katagiri A, Fu KI, Sano Y, et al. Narrow band imaging with magnifying colonoscopy as a diagnostic tool for predicting the histology of early colorectal neoplasia. Aliment Pharmacol Ther. 2008;27:1269–74.
7. Ikematsu H, Matsuda T, Emura F, et al. Efficacy of capillary pattern type IIIA/IIIB by magnifying narrow band imaging for estimating depth of invasion of early colorectal neoplasms. BMC Gastroenterol. 2010;10:33.
8. Higashi R, Uraoka T, Kato J, et al. Diagnostic accuracy of narrow-band imaging and pit pattern analysis significantly improved for less-experienced endoscopists after an expanded training program. Gastrointest Endosc. 2010;72:127–35.
9. Tanaka S, Hirata M, Oka S, et al. Clinical significance of narrow band imaging (NBI) in diagnosis and treatment of colorectal tumor. Gastroenterol Endosc. 2008;50:1289–97.
10. Kanao H, Tanaka S, Oka S, et al. Narrow band imaging magnification predicts the histology and invasion depth of colorectal tumors. Gastrointest Endosc. 2009;69:631–6.
11. Wada Y, Kudo S, Kashida H, et al. Diagnosis of colorectal lesions with the magnifying narrow-band imaging system. Gastrointest Endosc. 2009;70:522–31.
12. Nikami T, Saito S, Tajiri H, et al. The evaluation of histological atypia and depth of invasion of colorectal lesions using magnified endoscopy with narrow-band imaging. Gastroenterol Endosc. 2009;51:10–9.
13. Saito Y, Wada Y, Ikematsu H, et al. Multicenter trial to unify magnified NBI classification using Web test system. Intestine. 2013;17:223–31.
14. Iwatate M, Sano Y, Tanaka S, et al. Validation study for development of the Japan NBI Expert Team classification of colorectal lesions. Dig Endosc. 2018;30:642–51.
15. Sano Y, Tanaka S, Kudo SE, et al. Narrow-band imaging (NBI) magnifying endoscopic classification of colorectal tumors proposed by the Japan NBI expert team. Dig Endosc. 2016 Jul;28(5):526–33.
16. Sumimoto K, Tanaka S, Shigita K, et al. Clinical impact and characteristics of the narrow-band imaging magnifying endoscopic classification of colorectal tumors proposed by the Japan NBI expert team. Gastrointest Endosc. 2017;85(4):816–21.
17. Hewett DG, Kaltenbach T, Sano Y, et al. Validation of a simple classification system for endoscopic diagnosis of small colorectal polyps using narrow-band imaging. Gastroenterology. 2012;143:599–607.
18. Hayashi N, Tanaka S, Hewett DG, et al. Endoscopic prediction of deep submucosal invasive carcinoma: validation of the narrow-band imaging international colorectal endoscopic (NICE) classification. Gastrointest Endosc. 2013;78:625–32.
19. Sano Y, Hirata D, Saito Y. Japan NBI Expert Team classification: Narrow-band imaging magnifying endoscopic classification of colorectal tumors. Dig Endosc. 2018;30(4):543–45.

ESD for the Esophagus

10

Rajvinder Singh, Leonardo Zorron Cheng Tao Pu, Florencia Leiria, and Philip W. Y. Chiu

10.1 Introduction

The traditional approach to esophageal cancer consists of open or thoraco-laparoscopic surgery, chemoradiotherapy or both. Surgery has consistently been associated with increased morbidity and mortality. An older large cohort study famously reported fairly high esophagectomy mortality rates ranging from 9.5 to 15.3% [1]. These numbers have improved drastically since the introduction of minimally invasive transthoracic esophagectomy. In a multicenter cohort study of over 1000 procedures, mortality from surgery ranged between 1.0 and 4.6% [2]. The benefits of endoscopic resection over surgery have been reported in a study by Zhang and colleagues who evaluated the perioperative mortality of esophagectomy compared to ESD in 596 patients with T1a or T1b esophageal cancers. The mortality of surgery was five times higher than that of ESD [3]. In addition, esophagectomy was associated with higher episodes of severe adverse events (27.7 versus 15.2% for surgery and ESD, respectively). In a median follow-up of 21 months, the all-cause mortality and cancer recurrence/metastasis was similar across both cohorts (10.9 versus 7.4% and 8.9 versus 9.1%, respectively, for surgery and ESD). Current data do suggest similar efficacy when ESD is compared to surgery not only in the esophagus but also in the stomach and colon [4, 5]. Nevertheless, ESD is an advanced endoscopic resection technique and has one of the highest complication rates in therapeutic endoscopy. As with other procedures requiring manual dexterity, the complication rate is inversely associated with procedural volume. Odagiri and colleagues reported an average complication rate of 3.3% for esophageal ESD. Perforation or perforation associated complication rates varied almost fourfold depending on hospital's ESD volume per year: very low volume centers (≤8 cases) having a complication rate of 4.8%; low volume (9–17 cases), 4.5%; high volume (18–38 cases), 2.5%; and very high volume (≥39 cases), 1.3% [6]. As opposed to perforation, post-ESD bleeding appears to be very rare (0–0.7%) [7]. However, even when these complications occur, surgery is rarely needed [8].

R. Singh (✉)
Gastroenterology Department, Lyell McEwin Hospital Gastroenterology Department, Adelaide, SA, Australia
e-mail: Rajvinder.Singh@sa.gov.au

L. Zorron Cheng Tao Pu
The University of Adelaide, Adelaide, Australia

Nagoya University, Nagoya, Japan

F. Leiria
The University of Adelaide, Adelaide, Australia

P. W. Y. Chiu
Department of Surgery, Faculty of Medicine, The Chinese University of Hong Kong, Hong Kong
Hong Kong

P. W. Y. Chiu et al. (eds.), *Endoscopy in Early Gastrointestinal Cancers, Volume 1*,
https://doi.org/10.1007/978-981-10-6769-3_10

10.2 Indication

Although a higher en bloc resection is achieved with ESD, there may be little clinically proven advantages of this method compared to a less complex procedure, Endoscopic Mucosal Resection (EMR) [9]. Currently, EMR may be considered for lesions that are <1 cm in size and deemed to be restricted to the mucosa by advanced imaging techniques.

ESD is indicated for larger superficial neoplasia that cannot be resected en bloc using the EMR technique and/or when invasion is predicted to reach the superficial submucosal layer. Before proceeding with the ESD, an in-depth understanding of advanced imaging techniques is paramount (please refer to Volume 1 for details on Endoscopic Imaging of superficial esophageal neoplasia). Occasionally, it may be difficult to totally rely on endoscopic imaging alone. Therefore, endoscopic resection (either ESD or EMR) is now also used as a "staging procedure."

The Japanese Esophageal Society (JES) guidelines for ESD state that endoscopic resection is deemed sufficient as treatment of early esophageal cancer for T1a lesions up to the lamina propria and affecting less than two-thirds of the circumference of the organ. A broadened criterion (relative indication) includes invasion up to 200 μm into the submucosa (sm1, 10]. The ESGE guidelines have a slightly different approach toward curative ESD and recommends that it should be confined to the superficial mucosa and not have lymphovascular invasion [11]. The ESGE also recognizes that for SCC, invasion up to 200 μm is most likely curative if there are no other high-risk criteria. The JES highlights that their guidelines are mostly based on SCC which has a higher lymph node metastasis rate compared to esophageal adenocarcinoma (EAC). In line with this, a Japanese study looking at EAC has proposed similar thresholds as the ESGE for EAC which has as relative indication for submucosal invasive tumors extending up to 500 μm into the submucosa [12]. The indications according to ESGE and JES for both SCC and EAC have been summarized in Table 10.1.

Finally, it is important to touch on the use of antithrombotic agents and its influence on procedural bleeding. It has been shown that aspirin may not influence bleeding during or after ESD in contrast to other antiplatelet and anticoagulant agents [7]. One should liaise with the patients' general practitioner and/or specialist in order to discuss the risks and benefits of discontinuing these medications prior to performing an ESD. Using CO_2 is mandatory in ESDs.

10.3 ESD Procedure

10.3.1 Preparation

As in all therapeutic endoscopic procedures, most ESDs are performed under General Anesthesia (GA). This prevents aspiration and provides better overall control for the proceduralist. The sedation duration should ideally be tailored to patient and lesion characteristics (e.g., ESD in larger lesions could last for several hours, complicated by more intraprocedural bleeding and require numerous reinsertions of the endoscope).

10.3.2 Marking

This step begins with the clear delineation of the margin of the lesion. Either or both virtual chromoendoscopy (e.g., narrow band imaging—NBI) and vital stain (e.g., Lugol iodine) can be used (Fig. 10.1). The type of accessory used to perform the marking largely depends on personal experience and the equipment available but usually consists of either argon plasma coagulation or the same knife that will be used for incision/submucosal dissection (e.g., ERBE knife, dual knife J, triangular tip knife J), in the "coagulation mode." This should be performed on normal mucosa surrounding the lesion with at least a 2 mm normal margin "clearance" (Fig. 10.2). It is advisable that on the oral extremity, an additional marking be placed to make the orientation of the specimen easier after the procedure is completed. Therefore, one can inform the pathologist of the orientation

Table 10.1 Endoscopic submucosal dissection in esophagus—standard and extended indication flowchart

Indication for esophageal ESD		ESGE guidelines		JES guidelines[a]	
		Standard	Extended	Standard	Extended
Squamous	Size	Any	Any	<2/3rds of circumference	Any
Cell	Depth	m2	m3/sm1 (≤200 μm)	T1a (up to lamina propria)	sm1 (≤200μm)
Carcinoma	Histology	Any	Well-differentiated	Any	Any
	Lymphovascular invasion	No	No	Unclear[b]	Unclear[b]
Esophageal	Size	Any	Any	≤3 cm	–
Adeno	Depth	m3	sm1 (≤500μm)	sm1 (≤500μm)	–
Carcinoma	Histology	Any	Not poorly differentiated	Not poorly differentiated	–
	Lymphovascular invasion	No	No	No	–

[a]Indication for esophageal adenocarcinoma based on Ishihara et al. [12]
[b]Unclear if lymphovascular invasion status alone determines whether the lesion was completely resected or not [13]

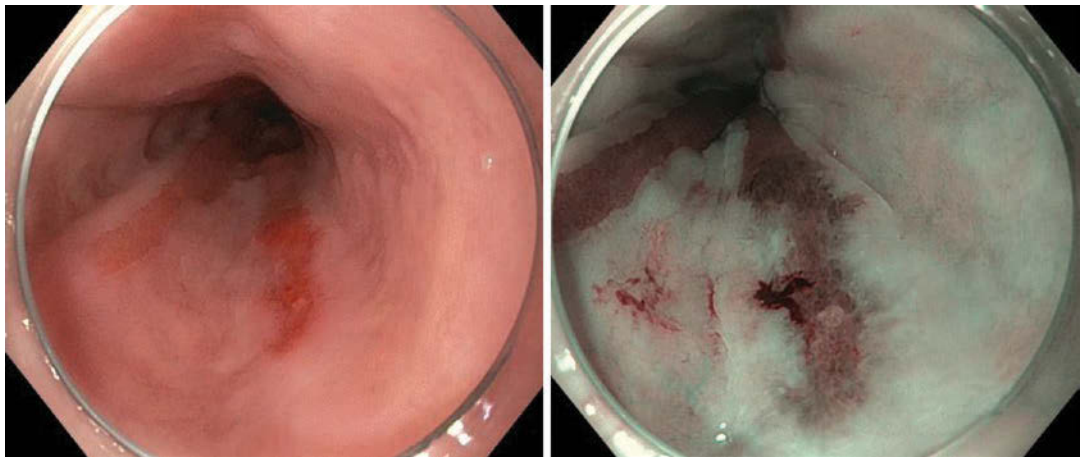

Fig. 10.1 Area of interest on white light and NBI

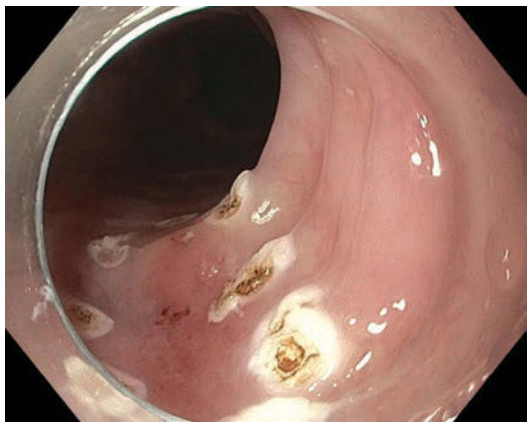

Fig. 10.2 Marking

of the specimen, which could be crucial when margins are compromised. In accordance with this, one must note that the marking line should not be breached during mucosal incision.

10.3.3 Submucosal Injection

Submucosal injection solution customarily consists of a saline/colloid mix with adrenaline and a small amount of coloring agent such as indigo carmine or methylene blue. The colloid generally used is Gelofusine® (succinylated fluid gelatin), MucoUp® (hyaluronic acid), or mannitol. The exact amount of

each is debatable, but a common mix used in the East consists of 100 mL of saline + 1 mg of adrenaline (1:100,000 solution) + 100 mL of hyaluronic acid + 0.4 mL of indigo carmine. This is usually injected with a 25G needle in 2–5 mL aliquots per injection (5–10 mL syringe).

10.3.4 Incision

There are different approaches used for the initial mucosal incision. For instance, for small lesions it is possible to perform an all-round mucosal incision prior to the submucosal dissection. For larger lesions, a 2–3 cm incision on the proximal edge is sufficient, followed by submucosal dissection. As the endoscopist is proceeding with the submucosal dissection, it may sometimes become difficult to progress due to restrain provided by the "un-incised" mucosa. The mucosal incision can then be extended on either side and dissection continued until the mucosal incision on either side are connected at the anal extremity. A number of alternative methods to tackle specific/difficult situations have also been developed, such as the pocket creation method. This consists of a smaller initial mucosal incision and tunneling the submucosa until the anal extremity if reached. The mucosal incisions are then "joined" on either side of the pocket after most of submucosal dissection has taken place.

Whenever possible, the mucosal incision should be extended to the depth of the deepest submucosal layer (Fig. 10.3). This will enable the endoscopist to cut the border loose during submucosal dissection as opposed to further "digging" underneath the incision line (which could be carried out blindly leading to complications). This is optimally and safely achieved in an angled approach (45–60 degrees). Avoiding a 90-degree angle helps in preventing perforations.

10.3.5 Submucosal Dissection

As per anatomic particularities (e.g., thinner wall, absence of serosa), the esophagus requires more "gentle" knives than the stomach. The most common knives available in the market that can be used for esophageal ESD are the IT knife nano, dual knife (1.5 mm), flush knife (1.5 mm), SB knife Jr, and the ERBE hybrid knife. All of these have their advantages and disadvantages.

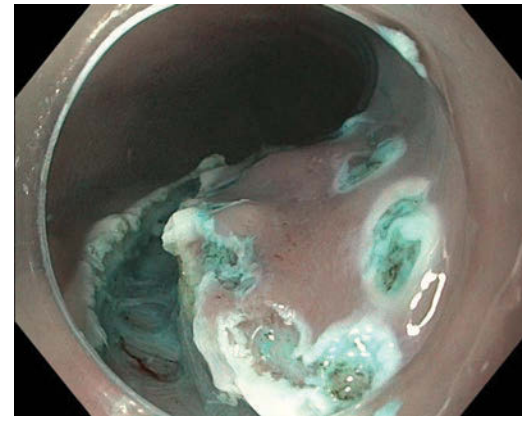

Fig. 10.3 Mucosal incision extended up to deep submucosa

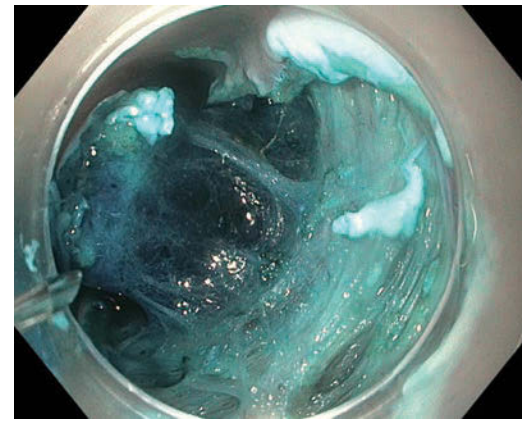

Fig. 10.4 Submucosal dissection

The ability to visualize the muscular plane is one of the most important (and maybe one of the most difficult) steps (Fig. 10.4). This could be a drawback of the SB knife Jr. This device requires the assistant to rotate the knife to meet the parallel plane of dissection, hence requiring at least two operators who are experienced in ESD. However, it is thought to lead to less complications, especially for nonexperts as it provides more controlled cutting with a "scissor-type" action.

The IT knife nano (and other insulated tip knives) have the peculiarity of needing a mucosal breach before initiating its use (e.g., with a needle knife). This knife does offer additional protection to prevent perforation when compared to the non-insulated tip types. With the IT knife nano, the incision and dissection should be preferably performed in a retrograde or "pulling" fashion (i.e., from anal to oral) or sideways.

Other knives such as the Dual knife J, the triangular tip knife and the ERBE hybrid knife can be used as sole devices, although they do require an injection prior. With the latter knives, incision and dissection should be preferably performed in an antegrade fashion (i.e., from oral to anal) or sideways.

A thin wall, surrounding vital structures (e.g., aorta, mediastinum) and absence of serosa layer make the esophagus a site for particular concern for perforation. When a muscular defect is suspected, the patient vitals should be monitored closely and endoscopic closure of the defect attempted using standard endoscopic clips. If this is successful and the patient is stable, one could continue with the procedure with extra caution. If this is unsuccessful and/or the patient vitals deteriorate, an endoscopy-guided nasogastric tube must be swiftly placed and the procedure aborted. Depending on the endoscopist expertise with advanced endoscopy, other closure devices could be used to deal with the perforation (e.g., Over The Scope Clip-OTSC®, fully covered stents, endoscopic suturing using the OverStitch™).

Another difficulty one may find during esophageal ESD is related to the adequate presentation of the submucosa to the knife. This sometimes can be made easier with the traction technique. It can only be used when a mucosal incision and at least some submucosal dissection has been performed. This technique consists of tying a line (e.g., dental floss) to an endoscopic clip which is advanced through the working channel prior to scope insertion (scope withdrawn, outside the patient). The line should pass outside the scope to enter the distal end of the working channel. After the line is tied, the clip is closed and withdrawn into the working channel. The scope is then introduced into the patien t. The clip should then be deployed on the submucosal face of the to-be specimen, on its proximal edge. Once deployed, the clip and hence the specimen will be connected to the line which can be separately captured outside the patient's oral cavity. An assistant could apply proximal and downward traction which is likely to allow easier access to the submucosa. A snare and clip technique could also be used which may help with both pushing and pulling. Although specialized through-the-scope clips with traction capability have been developed (e.g., S-O clip—Zeon Medical, Tokyo, Japan), this are mostly used for colonic and gastric ESD as they require a broad lumen for optimal performance. Therefore, the manually prepared traction system described above is still preferred for esophageal ESD.

After the completion of resection, the specimen should be retrieved and fixed on a flat surface (e.g., cork with pins) before formalin is added, and then sent for histological evaluation (Fig. 10.5). The pathologist should be informed of the specimen's orientation (e.g., different color pin on the proximal extremity), especially if the margins are not clear. It is also advisable to extensively photo document the resected specimen and the resection bed for future reference. Once the ESD is complete and the specimen retrieved, a final assessment of the ulcer/bed should be done carefully, applying hemostatic forceps (e.g., Coagrasper™) to any visible vessels and clipping any muscular breaches.

As per variations in the abovementioned ESD technique, there are multiple different techniques

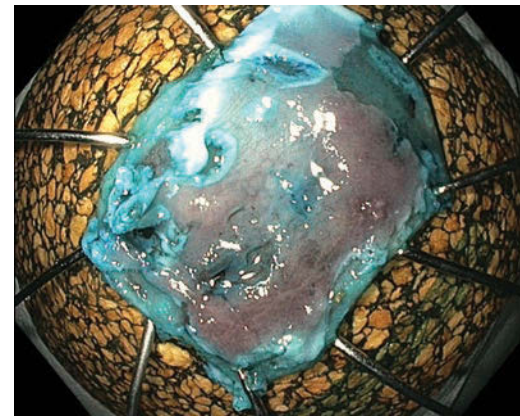

Fig. 10.5 Specimen fixed on cork

and devices that could be used and hence should be tailored to the Endoscopist's experience.

10.3.6 Training

It is contentious how many procedures are required to achieve competency as previous experience can have a big impact on the learning curve. Full proficiency with both diagnostic and therapeutic gastroscopy and colonoscopy must be achieved before attempting ESD. In addition, watching a number of ESDs performed by experts is of utmost importance. However, the exact number of observed and mentored ESDs and the site where to start is debatable.

In the East, it is advised that one should begin with 50 gastric antral ESDs before proceeding with more complex areas such as the esophagus. This is mainly because the stomach has thicker submucosa and muscularis propria layers. It is also a common site for early neoplastic lesions in the East, making it a feasible target for early training. In the West however, this site is difficult to use for training mainly due to the low incidence of early gastric cancers. Therefore, in the West, rectal lesions are generally targeted before progressing to the colon and esophagus [14]. In addition, the availability of mentoring for ESD is much more limited in the West as opposed to the East. These make the consensus of a minimum standard difficult to reach.

It is important to note that familiarity with other endoscopic resection techniques (e.g., EMR) influences the learning curve. Therefore, teaching should be individualized and tailored to the availability of cases and mentoring in each center. In addition, practice on animal models (in vivo or ex vivo) and observation of ESDs in high-volume centers is advised [11].

10.4 Conclusion

ESD of the esophagus is a complex therapeutic endoscopic procedure that allows even large superficial neoplasms to be resected in an en bloc fashion. Special attention must be given prior to the procedure to ensure it is performed for the correct indication; and during the procedure ensuring the lesion is clearly demarcated and cautiously dissected. Attention should also be focused on intra-procedural complications such as bleeding and perforation. In addition, sufficient training is necessary to achieve optimal proficiency.

References

1. Birkmeyer JD, Stukel TA, Siewers AE, Goodney PP, Wennberg DE, Lucas FL. Surgeon volume and operative mortality in the United States. N Engl J Med. 2003;349(22):2117–27. https://doi.org/10.1056/NEJMsa035205.
2. Schmidt HM, Gisbertz SS, Moons J, Rouvelas I, Kauppi J, Brown A, Asti E, Luyer M, Lagarde SM, Berlth F, Philippron A, Bruns C, Holscher A, Schneider PM, Raptis DA, van Berge Henegouwen MI, Nafteux P, Nilsson M, Rasanen J, Palazzo F, Rosato E, Mercer S, Bonavina L, Nieuwenhuijzen G, Wijnhoven BPL, Schroder W, Pattyn P, Grimminger PP, Gutschow CA. Defining benchmarks for transthoracic esophagectomy: a multicenter analysis of total minimally invasive esophagectomy in low risk patients. Ann Surg. 2017;266(5):814–21. https://doi.org/10.1097/sla.0000000000002445.
3. Zhang Y, Ding H, Chen T, Zhang X, Chen WF, Li Q, Yao L, Korrapati P, Jin XJ, Zhang YX, Xu MD, Zhou PH. Outcomes of endoscopic submucosal dissection vs esophagectomy for T1 esophageal squamous cell carcinoma in a real-world cohort. Clin Gastroenterol Hepatol. 2018;71:73–81.e3. https://doi.org/10.1016/j.cgh.2018.04.038.
4. Jeon HK, Kim GH, Lee BE, Park DY, Song GA, Kim DH, Jeon TY. Long-term outcome of endoscopic submucosal dissection is comparable to that of surgery for early gastric cancer: a propensity-matched analysis. Gastric Cancer. 2018;21(1):133–43. https://doi.org/10.1007/s10120-017-0719-4.
5. Gamaleldin M, Benlice C, Delaney CP, Steele S, Gorgun E. Management of the colorectal polyp referred for resection: a case-matched comparison of advanced endoscopic surgery and laparoscopic colectomy. Surgery. 2018;163(3):522–7. https://doi.org/10.1016/j.surg.2017.10.057.
6. Odagiri H, Yasunaga H. Complications following endoscopic submucosal dissection for gastric, esophageal, and colorectal cancer: a review of studies based on nationwide large-scale databases. Ann Transl Med. 2017;5(8):189. https://doi.org/10.21037/atm.2017.02.12.
7. Kataoka Y, Tsuji Y, Sakaguchi Y, Minatsuki C, Asada-Hirayama I, Niimi K, Ono S, Kodashima

S, Yamamichi N, Fujishiro M, Koike K. Bleeding after endoscopic submucosal dissection: risk factors and preventive methods. World J Gastroenterol. 2016;22(26):5927–35. https://doi.org/10.3748/wjg.v22.i26.5927.
8. Wang WP, Ni PZ, Yang JL, Wu JC, Yang YS, Chen LQ. Esophagectomy after endoscopic submucosal dissection for esophageal carcinoma. J Thorac Disord. 2018;10(6):3253–61. https://doi.org/10.21037/jtd.2018.05.143.
9. Terheggen G, Horn EM, Vieth M, Gabbert H, Enderle M, Neugebauer A, Schumacher B, Neuhaus H. A randomised trial of endoscopic submucosal dissection versus endoscopic mucosal resection for early Barrett's neoplasia. Gut. 2017;66(5):783–93. https://doi.org/10.1136/gutjnl-2015-310126.
10. Bhatt A, Abe S, Kumaravel A, Vargo J, Saito Y. Indications and techniques for endoscopic submucosal dissection. Am J Gastroenterol. 2015;110:784. https://doi.org/10.1038/ajg.2014.425.
11. Pimentel-Nunes P, Dinis-Ribeiro M, Ponchon T, Repici A, Vieth M, De Ceglie A, Amato A, Berr F, Bhandari P, Bialek A, Conio M, Haringsma J, Langner C, Meisner S, Messmann H, Morino M, Neuhaus H, Piessevaux H, Rugge M, Saunders BP, Robaszkiewicz M, Seewald S, Kashin S, Dumonceau JM, Hassan C, Deprez PH. Endoscopic submucosal dissection: European Society of Gastrointestinal Endoscopy (ESGE) guideline. Endoscopy. 2015;47(9):829–54. https://doi.org/10.1055/s-0034-1392882.
12. Ishihara R, Oyama T, Abe S, Takahashi H, Ono H, Fujisaki J, Kaise M, Goda K, Kawada K, Koike T, Takeuchi M, Matsuda R, Hirasawa D, Yamada M, Kodaira J, Tanaka M, Omae M, Matsui A, Kanesaka T, Takahashi A, Hirooka S, Saito M, Tsuji Y, Maeda Y, Yamashita H, Oda I, Tomita Y, Matsunaga T, Terai S, Ozawa S, Kawano T, Seto Y. Risk of metastasis in adenocarcinoma of the esophagus: a multicenter retrospective study in a Japanese population. J Gastroenterol. 2017;52(7):800–8. https://doi.org/10.1007/s00535-016-1275-0.
13. Kuwano H, Nishimura Y, Oyama T, Kato H, Kitagawa Y, Kusano M, Shimada H, Takiuchi H, Toh Y, Doki Y, Naomoto Y, Matsubara H, Miyazaki T, Muto M, Yanagisawa A. Guidelines for diagnosis and treatment of carcinoma of the esophagus April 2012 edited by the Japan Esophageal Society. Esophagus. 2015;12:1–30. Epub 2014 Nov 11.
14. Bourke MJ, Neuhaus H, Bergman JJ. Endoscopic submucosal dissection: indications and application in Western endoscopy practice. Gastroenterology. 2018;154(7):1887–1900.e1885. https://doi.org/10.1053/j.gastro.2018.01.068.

11 Diagnosis of Early Neoplasia and Dysplasia in Inflammatory Bowel Disease

Moe Kyaw and Siew C. Ng

11.1 Introduction

Colorectal cancer (CRC) is one of the major causes of morbidity and mortality worldwide, representing the second most common cancer among females and the third among males [1]. Patients with inflammatory bowel disease (IBD) are at an increased risk for CRC and the risk increases with the duration and extent of the disease [2]. The earliest meta-analysis on risk of IBD-associated CRC concluded that the cumulative probability of CRC was 2% by 10 years, 8% by 20 years, and 18% by 30 years after the diagnosis of IBD [3]. A more recent meta-analysis reported a lower cumulative risk of CRC at 1.2% by 15 years, 1.7% by 20 years, and 2.6% by 25 years of disease duration [4]. Yet, there remains a 2.4-fold increased risk of CRC in patients with IBD compared to those without IBD [4] and this risk increases to 4.8-fold in patients with concomitant primary sclerosing cholangitis [5].

IBD-associated CRC and sporadic CRC (CRC in patients without any predisposition) differ in their pathological pathways. Unlike sporadic CRC that develops mostly from the standard adenoma-carcinoma sequence, IBD-associated CRCs develop from a background of inflammation and regeneration [6]. In addition, unlike the adenoma precursor in sporadic CRC, the precancerous lesion in IBD is cellular dysplasia arising from flat mucosa that may not be readily seen by standard white light endoscopy.

Surveillance colonoscopy should be performed approximately 8–10 years after the onset of ulcerative colitis or Crohn's colitis (involving at least one-third of the colon). Traditionally, it has been agreed that a minimum of 32 random biopsies (non-targeted) should be performed at each surveillance colonoscopy by obtaining 4-quadrant biopsies every 10 cm, with each quartet placed in a separate specimen container [7]. This technique is time-consuming and random biopsies only cover a minute fraction of the entire colon. The rational for the random biopsies is based on the observation that dysplasia in IBD is invisible or difficult to detect. With recent advances in endoscopic technology, those dysplasia that was thought to be "invisible" with standard white light endoscopy has become identifiable. In this chapter, we describe the endoscopic imaging techniques currently available for the detection of IBD-associated neoplasia.

M. Kyaw · S. C. Ng (✉)
Department of Medicine and Therapeutics, Institute of Digestive Disease, The Chinese University of Hong Kong, Shatin, Hong Kong
e-mail: siewchienng@cuhk.edu.hk

P. W. Y. Chiu et al. (eds.), *Endoscopy in Early Gastrointestinal Cancers, Volume 1*,
https://doi.org/10.1007/978-981-10-6769-3_11

11.2 Image Enhanced Endoscopy: Chromoendoscopy

11.2.1 Preparation and Technique of Chromoendoscopy

Three types of dyes are available to perform chromoendoscopy: indigo carmine (a contrast dye), methylene blue (an absorptive dye), and cristal violet.

If a suspicious lesion is identified, a selective spray of a more concentrated solution of dye can be helpful to enhance the border and surface tomography of the lesion.

11.2.2 Detection and Characterization of Lesions

During the inspection, the endoscopist should look for areas that appear to be different from surrounding mucosa in terms of the following characteristics: (1) color (discolored or reddened); (2) level of elevation (elevated, or depressed); (3) vascular pattern (obscure vascular pattern); and (4) surface pit pattern (Kudo pit pattern). The endoscopist should not ignore the presence of surrounding mucosal inflammation or inflammatory polyps as these findings increase the risk for dysplasia.

The Paris and Kudo classification can used to describe lesion morphology and pit pattern similar to sporadic polyps. Using the Paris classification, lesions are described as polypoid or non-polypoid lesions. Polypoid lesions are easier to detect and if deemed resectable should be removed by polypectomy or endoscopic mucosal resection or endoscopic submucosal dissection. Additional biopsy specimen should be taken from normal appearing mucosa surrounding the lesion to exclude dysplasia in the surrounding area.

It is more challenging to detect non-polypoid lesions. Targeted biopsies of any suspicious appearing lesions remains a reasonable alternative if the yield of chromoendoscopy is reduced by significant underlying inflammation, inflammatory polyps, in any area of poorly visualized mucosa or the endoscopist is uncertain of the presence of a definitive lesion [8]. Targeted biopsies should also be taken of any unresectable abnormality visualized through chromoendoscopy to diagnose dysplasia [9]. Tattooing should be considered for any suspicious dysplastic lesions arising from a flat mucosa or those not amenable to endoscopic removal.

If biopsies for dysplasia are not done at a specific segment, two random biopsies in each bowel segment may be reasonable to document microscopic disease activity. Microscopic inflammation has been shown to affect disease outcome in UC including risk of CRC and surgery [10, 11]. If no biopsies for dysplasia were taken, there should still be a total of eight random biopsies (two from caecum, two from transverse, two from descending colon, and two from rectum) after each colonoscopy.

11.2.3 Barriers to Effective Chromoendoscopy

The following factors can reduce the effectiveness of surveillance chromoendoscopy and should be optimized accordingly. Quality of bowel preparation should be good and ideally excellent. Appropriate time should be allocated in endoscopy lists to permit chromoendoscopy and for meticulous mucosal inspection. The British Society of Gastroenterology recommends adding 15 min per procedure [12]. Active inflammation during chromoendoscopy makes differentiation from dysplastic areas very challenging. In such cases it may be best to perform random biopsies every 10 cm in the bowel segments of inflammation (Fig. 11.1).

11.3 Image Enhanced Endoscopy: NBI, i-scan, FICE, and AFI

11.3.1 Narrow-Band Imaging (NBI)

NBI can be used to identify dysplastic lesions in patients with IBD; however, guidelines have not recommended this technique as an alternative to

dye-based chromoendoscopy [9] (Fig. 11.1). This recommendation is based on results of four randomized studies, which have not shown a significant difference in the detection in number of patients with dysplasia between NBI and dye-based chromoendoscopy [13–16]. Nonetheless, the studies do not document a benefit of chromoendoscopy over NBI. Inconclusive findings from these studies are likely due to small sample size and a lack of power to address the superiority of CE over NBI. Furthermore, in all the studies, an older generation of NBI was tested, most likely limited by the inadequate brightness of the images (LUCERA SPECTRUM or EXERA II). With the latest generation of NBI (LUCERA ELITE or EXERA III) being widely available in most centers, providing brighter and improved image resolution, whether CE is truly superior to NBI in detection of dysplasia in IBD patients remains to be determined.

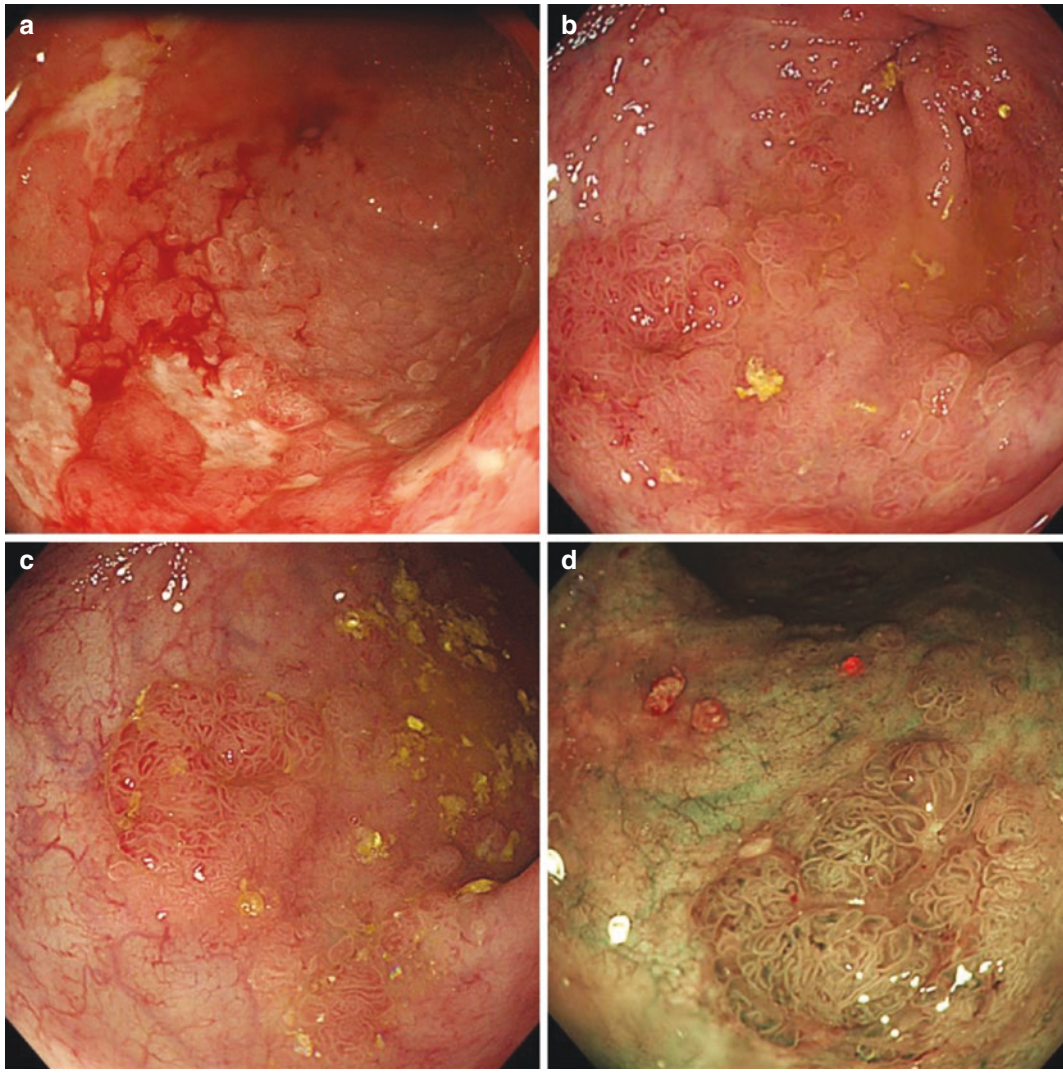

Fig. 11.1 (**a**) A patient with active ulcerative colitis—random biopsies from inflamed segment suggestive of low-grade dysplasia. (**b**, **c**) Follow-up colonoscopy after treatment of ulcerative colitis, multifocal non-polypoid lesions detected at white light endoscopy, low-grade dysplasia from histology of lesion. (**d**) NBI images of the non-polypoid lesion

11.3.2 i-scan

i-scan is a type of digital chromoendoscopy. It has three modes of image enhancement: (1) surface enhancement (SE), (2) contrast enhancement (CE), and (3) tone enhancement (TE) [17]. The three modes can be switched with a press of a button. Furthermore, SE mode and CE mode has three enhancement levels (low, medium, and high), and three different TE modes are available to examine esophagus, stomach, or colon.

Currently, there is a lack of evidence to support the use i-scan for surveillance endoscopy in patients with IBD. Few studies have explored the use of i-scan in patients with IBD. For detection of dysplasia, a randomized study concluded no additional benefit of i-scan over high-definition (HD) white light endoscopy or chromoendoscopy. The study published in abstract form only (96 patients in total) did not provide a detection rate for i-scan [18]. A recent case–control study published in abstract form reported that the detection of dysplasia with i-scan (12.5%, 2/16) was comparable with chromoendoscopy (21%, 4/19, $P = 0.336$) [19]. The only fully published randomized trial of the use of i-scan in IBD patients was for assessing inflammation. It reported that i-scan significantly improves the diagnosis of the severity and extent of mucosal inflammation in patients with IBD in comparison to HD white light endoscopy [20].

11.3.3 Fujinon Intelligent Color Enhancement (FICE)

Similar to i-scan, with FICE, each components of the white light image is converted along its tone curve followed by resynthesis of the three components to reconstruct a new digital image. The number of combinations is endless but FICE is equipped with 10 filters with predefined absorption wavelengths, which can be activated by a press of the button or changed using the keyboard.

To our knowledge, there are no data as yet on the use of FICE for surveillance endoscopy in patients IBD, although a trial of FICE for the surveillance of IBD patients is registered on Clinicaltrials.gov (identifier NCT01882205).

11.3.4 Autofluorescence Imaging (AFI)

AFI is performed with an endoscope (Lucera, Olympus, Tokyo, Japan), which has an additional charge-coupled device allowing differentiating normal tissue from neoplastic tissue. All tissues will exhibit autofluorescence when excited by ultraviolet (>400 nm) or short visible light (400–550 nm) [21]. Autofluorescence is produced by fluorophores (biomolecules such as collagen, elastin) emitting a fluorescent light of longer wavelength. AFI is influenced by tissue architecture, absorption of light (determined by absorptive capability of neoplastic neovascularization), and concentration of fluorophores. With AFI, neoplastic tissue appears as purple color on a green fluorescence background of normal tissue [22].

Limited data exists on the use of AFI for surveillance in patients with IBD. In the only randomized trial (prospective crossover trial) in patients receiving AFI first, 10 lesions in 25 patients were detected and the subsequent white light endoscopy did not detect additional lesions. In the patients receiving white light endoscopy first, three lesions were detected in 25 patients, and AFI detected an additional three lesions. This resulted in a miss rate of 50% in the white light endoscopy group versus 0% in the AFI group ($P = 0.036$) [23]. Larger studies are required to investigate the potential role of AFI for surveillance of patients with IBD.

11.4 Endomicroscopy

11.4.1 Confocal Laser Endomicroscopy

Confocal laser endomicroscopy (CLE) provides histologic real time in vivo imaging at subcellular level. After topical (acriflavine hydrochloride, cresyl violet) or intravenous administration (fluorescein sodium) of contrast agents, CLE emits a low power blue laser light onto the tissue. The light reflected from the tissue is refocused by the detecting system, resulting in a 1000-fold magnification [24]. The key mechanism of CLE being blue laser

is focused at specific depth, and only light reflected back from that plane is refocused through a pinhole to the detector. Light emitting outside the plane of interest is not detected. Thus, the illumination and detection system are at the same focal plane and are, therefore, termed "confocal."

Currently there are two types of CLE which are FDA-approved: (1) probe-based CLE (Cellvizio, Mauna Kea Technologies, Paris, France) and (2) integrated CLE (Pentax, Tokyo, Japan). With probe-based CLE, there are specific probes available for each area of the gastrointestinal tract (GastroFlex [300 cm length], Coloflex, [400 cm length]), which are advanced through the working channel of the endoscope. With integrated CLE, the CLE device is attached to the end of a high-resolution endoscope. The advantage of integrated-CLE is that imaging plane depth can be adjusted by the endoscopist (0–250 μm) and biopsy can be taken simultaneously.

CLE has been shown to be effective in detecting neoplasia and CLE patterns for neoplasia has been described. The value of CLE has been shown in a randomized trial where CLE combined with dye-based chromoendoscopy increased the detection of neoplasia by 5.75-fold compared to white light endoscopy [25]. From a meta-analysis of 15 studies (719 patients) with either sporadic polyps or IBD-associate neoplasia, CLE can distinguish neoplasm and non-neoplastic tissue with a sensitivity of 83% and a specificity of 90% [26]. CLE pattern classification to predict colorectal neoplasm has been described in the Mainz criteria [25] (Table 11.1). Generally, dysplasia in CLE is characterized by dark cells with crypt density attenuation, ridged-lined irregular epithelial layer with irregular or loss of crypts, and distorted blood vessels with leakage (Fig. 11.2). In contrast, inflammation is characterized by dilated crypt openings, enlarged spaces between crypts, and leakage of fluorescein into the crypt lumen, making the lumen brighter than the surrounding epithelium. Inflammation can be described using Chang-Qing Scale, a CLE-based rating scale for inflammation [27] (Table 11.2). CLE can also be used to predict disease relapse in patients with ulcerative colitis [28].

It would not be practical to use CLE as a primary examination of the entire surface area of the colon as required for IBD surveillance. Instead, its potential role would be in characterization of lesions identified during surveillance [9]. Furthermore, it may be useful in cases where it is difficult to differentiate between active colitis and underlying dysplasia.

11.4.2 Endocytoscopy

Endocytoscopy (Olympus, Tokyo, Japan) uses an ultra-high magnification (up to 1390-fold) to allow in vivo microscopic imaging of the gastrointestinal tract [29]. It uses a high-power fixed-focus objective lens. Preparation for endocytoscopy includes initial treatment with a mucolytic agent (10% N-acetylcysteine) followed by application of 1% methylene blue (which stain the nucleus) or 0.1% crystal violet (which stain both the nucleus and cytoplasm). Similar to CLE, endocytoscopy is available as probe-based endocytoscopy and integrated endocytoscopy. There are two different probe-based endocytoscopy with either 450-fold magnification (XEC 300F) or 1390-fold magnification (XEC 120 U). The

Table 11.1 Mainz criteria for neoplasia; CLE pattern classification to predict colorectal neoplasm [25]

Grading	Crypt architecture	Vessel architecture
Normal	Regular lumen opening and distribution of crypts Homogenous layer of epithelial cells and goblet cells	Hexagonal, honeycomb appearance that presents a network of capillaries outlining opening of crypts
Regeneration	Star-shaped luminal crypt opening or focal aggregation of regular-shaped crypts with a regular or reduced amount of goblet cells	Hexagonal, honeycomb appearance with no or mild increase in number of capillaries
Neoplasia	Rigid-lined irregular epithelial layer Loss of crypts and goblet cells Irregular cell architecture with little or no mucin	Dilated and distorted vessels with increase leakage, irregular architecture with little or no orientation to adjacent tissue

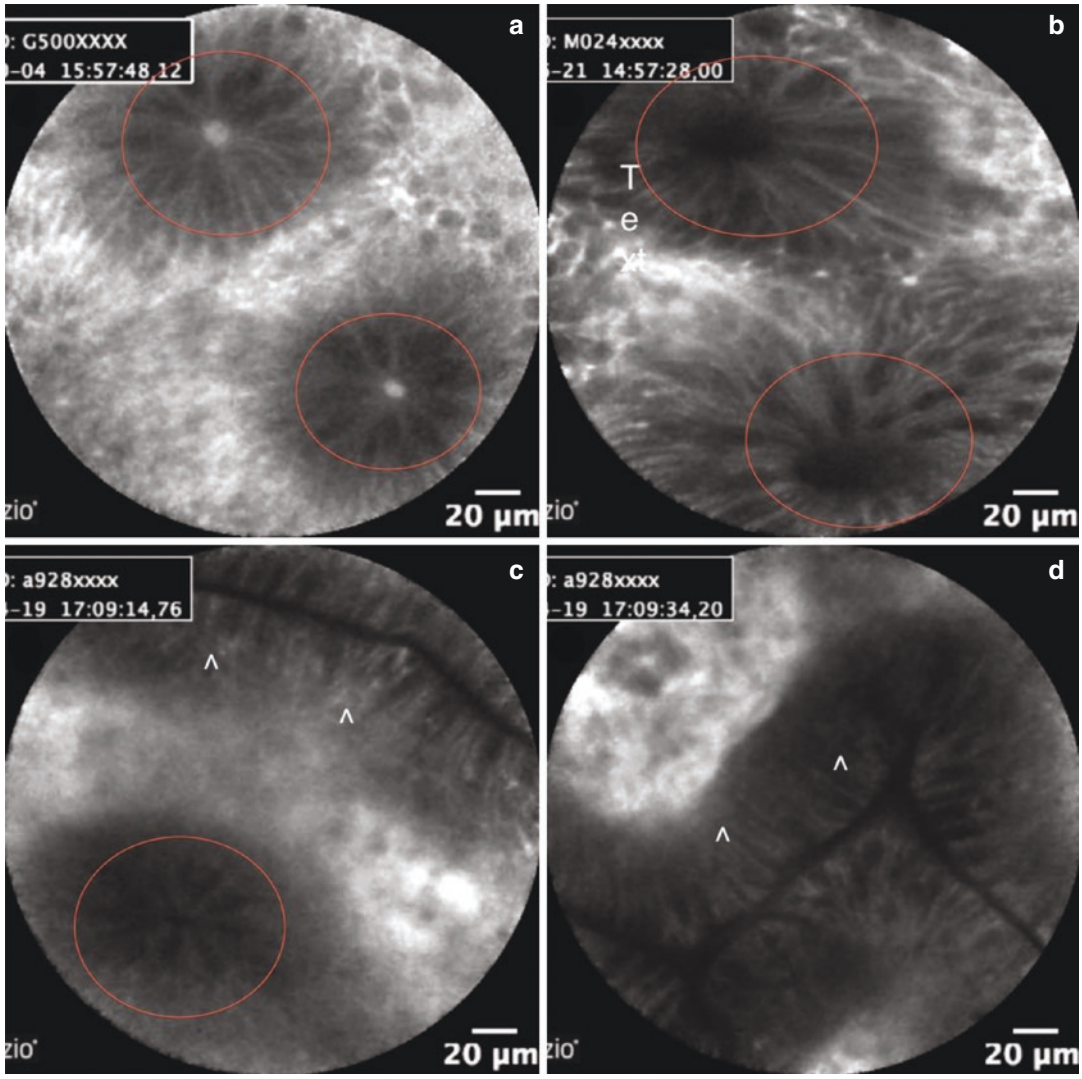

Fig. 11.2 (**a**, **b**) Confocal endomicroscopy—Normal: Regular lumen opening and distribution of crypts (circle). (**c**) Dysplasia: Rigid-lined irregular epithelial layer (arrow) next to one normal appearing crypt (circle). (**d**) Dysplasia: Rigid-lined irregular epithelial layer (arrow), loss of crypts, and leakage of fluorescein

Table 11.2 Chang-Qing scale; CLE-based rating scales for inflammation [27]

Grading	Crypt architecture
(A) No inflammation	Regular arrangement and size of the crypts, Lumen of crypts shown as dark spots without fluorescein leakage
(B) Chronic inflammation	Irregular arrangement of crypts and enlarged space between the crypts, fluorescein leakage into spaces among epithelial cells but not into crypt lumen (lumen of crypts is still free of fluorescein)
C) Acute inflammation	The arrangement of crypts is more irregular and spaced between the crypts are more enlarged than in grade B, fluorescein leakage into crypt lumen (white appearance)
D) Acute inflammation	Crypt destruction and/crypt abscesses, fluorescein leakage into crypt lumen (white appearance)

recent second-generation integrated endocystoscope (GIF-Y0002) allows a zoom from conventional endoscopy level to 380-fold with the use of a hand lever. With the additional digital magnification (X 1.6) the maximum zoom can reach to 600-fold allowing continuous magnification from standard level to subcellular level.

Compared to CLE, there are fewer studies on the use of endocytoscopy in patients with IBD. The use of endocytoscopy in patients with IBD has only been reported for assessing inflammation [30, 31]. Also, it has been demonstrated that endocytoscopy not only can visualize different cellular structures within the mucosa by can visualize and identify single inflammatory cells [30]. In addition, it has been reported that endocytoscopy can identify dysplasia in aberrant crypt foci of the colorectum [32]. Yet, there has been no studies reporting the role of endocytoscopy in detecting IBD-associated neoplasia.

11.5 Interval for Colonoscopic Surveillance

The management of patients and time interval for subsequent colonoscopy depends on the endoscopy findings and patient's risk factors. Below is a summary of the recommendations for management of IBD-associated neoplasia, and surveillance intervals from various existing guidelines [7, 33, 34]. It is important to note that recommended surveillance intervals come from expert opinions, and not based on robust evidence. Importantly, the optimal surveillance interval should be applied after a risk–benefit discussion with individual patients.

Low-grade dysplasia found—if a visible dysplastic lesion is found, the lesion is completely resected, and surrounding mucosa is found to be non-dysplastic, repeat surveillance in 6 months should be recommended. If the dysplastic lesion is found to be unresectable or the surrounding mucosa is found to be dysplastic, discussion should be made with patient for options of repeat surveillance in 3 months or a colectomy.

High-grade dysplasia found—If a visible dysplastic lesion is found, the lesion is completely resected, and surrounding mucosa is found to be non-dysplastic—repeat surveillance in 6 months should be recommended. If the dysplastic lesion is found to be unresectable or surrounding mucosa is found to be dysplastic, discussion should be made to consider colectomy.

No dysplasia found—After risk stratification of patient, surveillance colonoscopy of 1 year, 3 year, or 5 year will be recommended [33]. Risk factors include the presence of active inflammation, extent of inflammation, primary sclerosing cholangitis, family history of colorectal cancer, colonic stricture, multiple inflammatory polyps, and history of dysplasia.

References

1. Ferlay J, Soerjomataram I, Dikshit R, Eser S, Mathers C, Rebelo M, et al. Cancer incidence and mortality worldwide: sources, methods and major patterns in GLOBOCAN 2012. Int J Cancer. 2015;136:E359–86.
2. Herrinton LJ, Liu L, Levin TR, Allison JE, Lewis JD, Velayos F. Incidence and mortality of colorectal adenocarcinoma in persons with inflammatory bowel disease from 1998 to 2010. Gastroenterology. 2012;143:382–9.
3. Eaden JA, Abrams KR, Mayberry JF. The risk of colorectal cancer in ulcerative colitis: a meta-analysis. Gut. 2001;48:526–35.
4. Jess T, Simonsen J, Jorgensen KT, Pedersen BV, Nielsen NM, Frisch M. Decreasing risk of colorectal cancer in patients with inflammatory bowel disease over 30 years. Gastroenterology. 2012;143:375–81. e1; quiz e13-4.
5. Soetikno RM, Lin OS, Heidenreich PA, Young HS, Blackstone MO. Increased risk of colorectal neoplasia in patients with primary sclerosing cholangitis and ulcerative colitis: a meta-analysis. Gastrointest Endosc. 2002;56:48–54.
6. Itzkowitz SH, Yio X. Inflammation and cancer IV. Colorectal cancer in inflammatory bowel disease: the role of inflammation. Am J Physiol Gastrointest Liver Physiol. 2004;287:G7–17.
7. Farraye FA, Odze RD, Eaden J, Itzkowitz SH, McCabe RP, Dassopoulos T, et al. AGA medical position statement on the diagnosis and management of colorectal neoplasia in inflammatory bowel disease. Gastroenterology. 2010;138:738–45.
8. Murthy SK, Kiesslich R. Evolving endoscopic strategies for detection and treatment of neoplastic lesions in inflammatory bowel disease. Gastrointest Endosc. 2013;77:351–9.
9. Laine L, Kaltenbach T, Barkun A, McQuaid KR, Subramanian V, Soetikno R. SCENIC Guideline

Development Panel. SCENIC international consensus statement on surveillance and management of dysplasia in inflammatory bowel disease. Gastrointest Endosc. 2015;81:489–501.e26.
10. Rutter M, Saunders B, Wilkinson K, Rumbles S, Schofield G, Kamm M, et al. Severity of inflammation is a risk factor for colorectal neoplasia in ulcerative colitis. Gastroenterology. 2004;126:451–9.
11. Gupta RB, Harpaz N, Itzkowitz S, Hossain S, Matula S, Kornbluth A, et al. Histologic inflammation is a risk factor for progression to colorectal neoplasia in ulcerative colitis: a cohort study. Gastroenterology. 2007;133:1099–105; quiz 1340-1.
12. Beintaris I, Rutter M. Advanced imaging in colonoscopy: contemporary approach to dysplasia surveillance in inflammatory bowel disease. Frontline Gastroenterol. 2016;7:308–15.
13. Pellise M, Lopez-Ceron M, Rodriguez de Miguel C, Jimeno M, Zabalza M, Ricart E, et al. Narrow-band imaging as an alternative to chromoendoscopy for the detection of dysplasia in long-standing inflammatory bowel disease: a prospective, randomized, crossover study. Gastrointest Endosc. 2011;74:840–8.
14. Efthymiou M, Allen PB, Taylor AC, Desmond PV, Jayasakera C, De Cruz P, Kamm MA. Chromoendoscopy versus narrow band imaging for colonic surveillance in inflammatory bowel disease. Inflamm Bowel Dis. 2013;19:2132–8.
15. Feitosa F, Carlos A, Nogueira J. Narrow-band imaging and chromoendoscopy for the detection of colonic dysplasia in inflammatory bowel disease: a prospective and randomized study. Inflamm Bowel Dis. 2011;17:S14–5.
16. Bisschops R, Bessissow T, Baert F, Ferrante M, Balle TV, Willekens H, Rutgeerts P. Chromo-endoscopy versus narrow band imaging in ulcerative colitis: a prospective randomized controlled trial. Gastrointest Endosc. 2012;75:AB148.
17. Kodashima S, Fujishiro M. Novel image-enhanced endoscopy with i-scan technology. World J Gastroenterol. 2010;16:1043–9.
18. Iacucci M, Gasia F, Urbanski S, Minoo P, Kaplan G, Panaccione R, Ghosh S. Detection and characterization of colonic dysplastic lesions in IBD surveillance colonoscopy—a randomised comparison of high definition alone with high definition dye spraying and electronic virtual chromoendoscopy using iSCAN 2015; ECCO Poster 146.
19. López-Serrano A, Paredes JM, Polanco A, García C, Hervás J, Amurrio C et al. Virtual chromoendoscopy with i-Scan as alternative to dye-spray chromoendoscopy for dysplasia detection in long-standing colonic inflammatory bowel disease 2017; ECCO Poster 224.
20. Neumann H, Vieth M, Gunther C, Neufert C, Kiesslich R, Grauer M, et al. Virtual chromoendoscopy for prediction of severity and disease extent in patients with inflammatory bowel disease: a randomized controlled study. Inflamm Bowel Dis. 2013;19:1935–42.
21. DaCosta RS, Wilson BC, Marcon NE. Optical techniques for the endoscopic detection of dysplastic colonic lesions. Curr Opin Gastroenterol. 2005;21:70–9.
22. Matsumoto T, Nakamura S, Moriyama T, Hirahashi M, Iida M. Autofluorescence imaging colonoscopy for the detection of dysplastic lesions in ulcerative colitis: a pilot study. Color Dis. 2010;12:e291–7.
23. van den Broek FJ, Fockens P, van Eeden S, Reitsma JB, Hardwick JC, Stokkers PC, Dekker E. Endoscopic tri-modal imaging for surveillance in ulcerative colitis: randomised comparison of high-resolution endoscopy and autofluorescence imaging for neoplasia detection; and evaluation of narrow-band imaging for classification of lesions. Gut. 2008;57:1083–9.
24. Kiesslich R, Burg J, Vieth M, Gnaendiger J, Enders M, Delaney P, et al. Confocal laser endoscopy for diagnosing intraepithelial neoplasias and colorectal cancer in vivo. Gastroenterology. 2004;127:706–13.
25. Kiesslich R, Goetz M, Lammersdorf K, Schneider C, Burg J, Stolte M, et al. Chromoscopy-guided endomicroscopy increases the diagnostic yield of intraepithelial neoplasia in ulcerative colitis. Gastroenterology. 2007;132:874–82.
26. Su P, Liu Y, Lin S, Xiao K, Chen P, An S, et al. Efficacy of confocal laser endomicroscopy for discriminating colorectal neoplasms from non-neoplasms: a systematic review and meta-analysis. Color Dis. 2013;15:e1–12.
27. Li CQ, Xie XJ, Yu T, Gu XM, Zuo XL, Zhou CJ, et al. Classification of inflammation activity in ulcerative colitis by confocal laser endomicroscopy. Am J Gastroenterol. 2010;105:1391–6.
28. Li CQ, Liu J, Ji R, Li Z, Xie XJ, Li YQ. Use of confocal laser endomicroscopy to predict relapse of ulcerative colitis. BMC Gastroenterol. 2014;14:45–230X-14-45.
29. Neumann H, Fuchs FS, Vieth M, Atreya R, Siebler J, Kiesslich R, Neurath MF. Review article: in vivo imaging by endocytoscopy. Aliment Pharmacol Ther. 2011;33:1183–93.
30. Neumann H, Vieth M, Neurath MF, Atreya R. Endocytoscopy allows accurate in vivo differentiation of mucosal inflammatory cells in IBD: a pilot study. Inflamm Bowel Dis. 2013;19:356–62.
31. Bessho R, Kanai T, Hosoe N, Kobayashi T, Takayama T, Inoue N, et al. Correlation between endocytoscopy and conventional histopathology in microstructural features of ulcerative colitis. J Gastroenterol. 2011;46:1197–202.
32. Cipolletta L, Bianco MA, Rotondano G, Piscopo R, Meucci C, Prisco A, et al. Endocytoscopy can identify dysplasia in aberrant crypt foci of the colorectum: a prospective in vivo study. Endoscopy. 2009;41:129–32.
33. Cairns SR, Scholefield JH, Steele RJ, Dunlop MG, Thomas HJ, Evans GD, et al. Guidelines for colorectal cancer screening and surveillance in moderate and high risk groups (update from 2002). Gut. 2010;59:666–89.
34. Annese V, Daperno M, Rutter MD, Amiot A, Bossuyt P, East J, et al. European evidence based consensus for endoscopy in inflammatory bowel disease. J Crohns Colitis. 2013;7:982–1018.

Chromoendoscopy

12

Noboru Hanaoka and Noriya Uedo

12.1 Introduction

Endoscopic treatment such as endoscopic mucosal resection (EMR), argon plasma coagulation (APC), radiofrequency ablation (RFA), etc. for gastrointestinal (GI) tract neoplasm is currently available as an option of minimally invasive treatment all around the world. Moreover, recently developed endoscopic submucosal dissection (ESD) technique enables us to remove superficial neoplasms in the GI tract that were difficult to be removed en bloc by conventional EMR. In general, identification of superficial GI tract neoplasms are difficult because its color and morphological changes are usually very subtle. However, if superficial GI neoplasms are detected in an early stage without risk of lymph node metastasis, local treatment with endoscopy can be offered to the patients. Moreover, accurate diagnosis of lesion extent is mandatory for endoscopic treatment because the lesion must be completely removed by local endoscopic resection, and the lesion size is related to risk of lymph node metastasis, thus indication for endoscopic resection.

Chromoendoscopy was initially developed in the 1960s as a method to improve detection, characterization, and staging of early GI neoplasms. Since then, several types of chromoendoscopy have been developed and their usefulness has been reported. Recently, instead of dye-based image enhanced endoscopy (IEE), equipment-based IEE, i.e., narrow-band imaging (NBI), flexible spectral imaging color enhancement (FICE), iScan, Blue LASER imaging (BLI), etc. has developed and implemented in clinical practice in some countries. Equipment-based IEE is a novel imaging technology that enhances both surface and vascular patterns of the superficial mucosa without dye spraying. Equipment-based IEE, particularly in combination with magnifying endoscopy, shows significant improvement in characterization of neoplastic lesions in the GI tract. However, the equipment-based IEE or magnifying endoscopy is not always available in all institutions, and the clinical usefulness have remained controversial in some aspect. Therefore, the chromoendoscopy is still worthwhile to implement in clinical practice because of its significant improvement on diagnostic yield for endoscopic detection and characterization of superficial GI tract neoplasms compared to conventional white light endoscopy. In this chapter, the currently available methods of chromoendoscopy in the GI tract are introduced.

N. Hanaoka
Department of Gastrointestinal Oncology, Osaka International Cancer Institute, Osaka, Japan

Department of Gastroenterology and Hepatology, Osaka Red Cross Hospital, Osaka, Japan

N. Uedo (✉)
Department of Gastrointestinal Oncology, Endoscopy Training and Learning Center, Osaka Medical Center for Cancer & Cardiovascular Diseases, Higashinari-ku, Osaka, Japan

P. W. Y. Chiu et al. (eds.), *Endoscopy in Early Gastrointestinal Cancers, Volume 1*,
https://doi.org/10.1007/978-981-10-6769-3_12

12.2 General Information

12.2.1 Classification

Chromoendoscopy is classified according to the mechanisms of dye application as contrast, absorptive, and reactive methods, and representative reagents for each method are listed in Table 12.1. In contrast method, dye retains in the depressed part of the mucosa, thus the mucosal pits or grooves are represented as dye-stained (pooled) areas (Fig. 12.1, left). In the absorptive method, dye stains epithelium by absorption or diffusion across the cell membrane, thus the mucosal pits or grooves are represented as dye-non-stained area (Fig. 12.1, middle). Recently, absorptive method is also used for nuclear staining for endocytoscopic observation. In the reactive method, dye undergoes chemical reactions, i.e., iodine–glycogen reaction, etc. with specific cellular constituents, resulting in a color change (Fig. 12.1, right).

12.2.2 Preparation

Before dye application, it is important to remove mucous and bubble on the surface of the mucosa (Fig. 12.2a). When the mucosa is covered by the mucous or bubble, the dye does not reach to the mucosal surface and neither contrast nor absorptive chromoendoscopic effect is achieved (Fig. 12.2b).

Pronase mixture: 40–60 ml of water with 20,000 U pronase (Kaken Pharmaceutical, Tokyo, Japan), 1 g sodium bicarbonate, and 2–3 ml (20 mg/ml) of dimethylpolysiloxane (Gascon drop, Horii Pharmaceutical Inc., Osaka Japan) is administered before the insertion of the scope if it is available [1]. In a place where pronase is not available, acetylcysteine mixture: 40–60 ml of water, 2 ml of acetylcysteine (200 mg/ml, Parvolex, Celltech, UK, or Mucomyst, Bristol-Myers Squibb, USA), and 0.5 ml of (40 mg/ml) activated dimethicone (Infacol, Forest Laboratories, Slough, Berkshire, UK) can be used as an alternative to pronase solution [2]. Even just simple syringe flushing with dimethylpolysiloxane solution before mucosal observation can facilitate detailed characterization of the mucosa and improve accuracy of chromoendoscopy.

Dyes for chromoendoscopy can be purchased from several vendors of pharmaceutic companies but none of the dye are specifically marketed for chromoendoscopy. Therefore, preparation and

Table 12.1 Types of chromoendoscopy

Method	Representative dyes and concentration			Organ	Indications	
	Reagent	Color	Concentration		Detection	Characterization
Contrast	Indigo carmine	Blue	0.04–0.2%	Barrett's esophagus, stomach, colon (columnar epithelium)	○	○
	Methylene blue	Blue	0.05%			○
Absorptive	Methylene blue	Blue	0.2–1.0%	Barrett's esophagus, stomach, Colorectum (columnar epithelium)		○
	Crystal violet	Violet	0.05%	Colorectum (columnar epithelium)		○
	Toluidine blue	Dark blue	0.25%–1%	Oropharynx, Esophagus (squamous epithelium)	○	
Reactive	Iodine	Reddish brown	Iodine concentration of 1.0–3.0%	Esophagus (squamous epithelium)	○	○
	Congo red	pH 3: Blue-black、pH 5: Red	0.3%	Stomach	○	

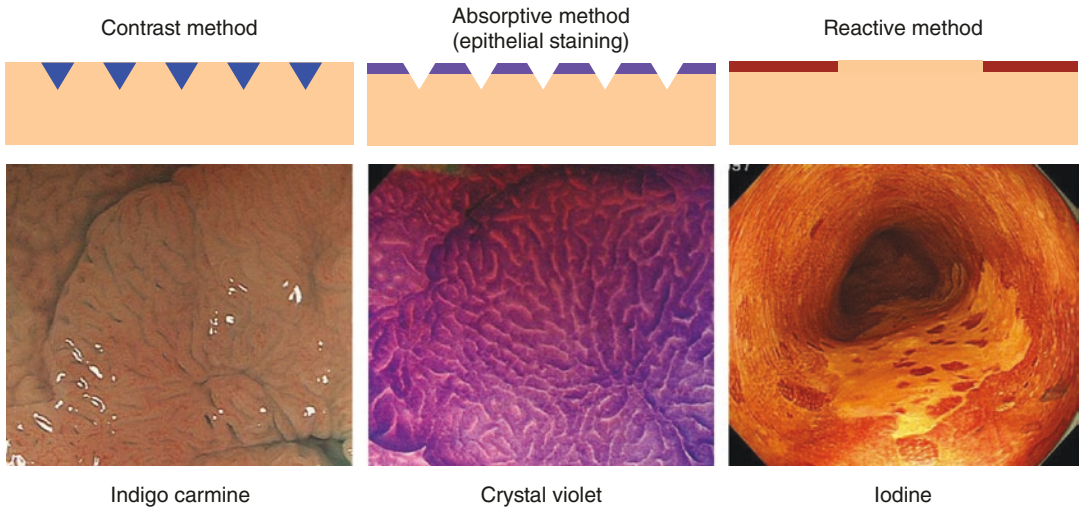

Fig. 12.1 Classification of chromoendoscopy. In contrast method, pits are seen as dye pooled areas and the intervening parts are seen as dye-shed areas (Left). In absorptive method, pits are seen as non-stained areas and the intervening parts are seen as stained areas (Middle). In reactive method (iodine chromoendoscopy), a neoplastic area is seen as non-stained area and surrounding mucosa are seen as stained (iodine–glycogen reaction) areas (Right)

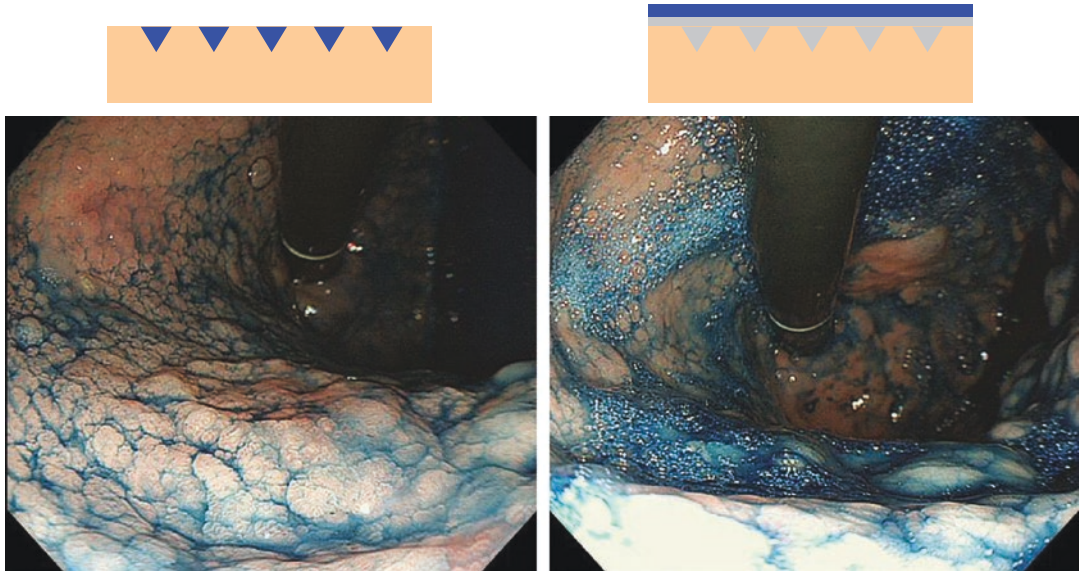

Fig. 12.2 After removal of the mucous or bubble, mucosal characteristics is well-enhanced by chromoendoscopy (Left). Without removal of the mucous or bubble, dyes applied on the surface of the mucous or bubble only masks mucosal appearance (Right)

dilution of the stock dye solution must be done in house. As all the solutions do not contain preservative, it is recommended to prepare the stock dye solution every day. Otherwise, the solution could be stored in a refrigerator and should be spent within a few days.

In contrast method, low-concentration dye solution is generally suitable for observation of gross morphological appearance and original color of lesions (Fig. 12.3a and b). Whereas, high-concentration dye solution is suitable for observation of fine microstructure or pit pattern

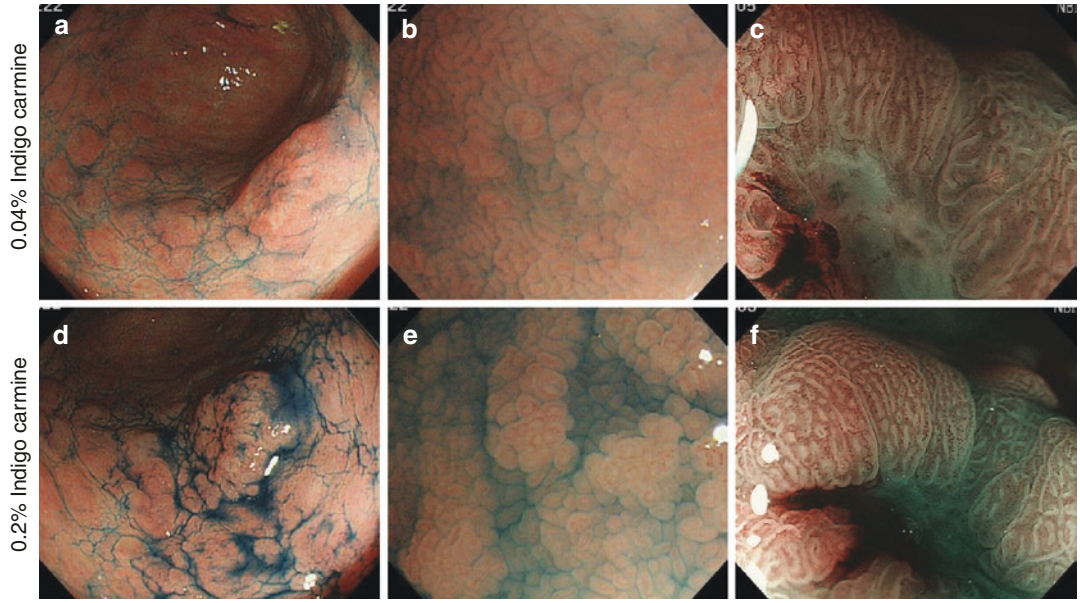

Fig. 12.3 Low-concentration (0.04%) indigo carmine (**a**, **b**, and **c**) facilitate evaluating gross morphology and original color of the lesion (whitish lesion color appears better in **a** than in **d**). While high-concentration (0.2%) indigo carmine (**d**, **e**, and **f**) contrast fine mucosal surface structure better than low-concentration dye. Even high-concentration indigo carmine does not interfere observation of the surface structure and vasculature in magnifying NBI (**c** and **f**)

of the mucosa using magnifying observation (Fig. 12.3b and e). Even application of low and high concentration of contrast dye solution, narrow-band imaging observation is not affected (Fig. 12.3c and f).

For iodine chromoendoscopy, around 50–60% of patients complain adverse symptom such as retrosternal pain, discomfort, or nausea, and administration of sodium thiosulfate solution relieve the symptoms [3]. High-concentration iodine solution stains the mucosa better than low-concentration solution (Fig. 12.4a), but it increases adverse symptoms such as retrosternal discomfort or pain, or nausea, etc. Moreover, superficial or small lesions are obscured by mucosal irritation caused by iodine. Recently, therefore, low-concentration (<1.5%) iodine solution (Fig. 12.4b) is preferred to high-concentration solution in clinical practice. When staining is weak or is faded early, dye solution is applied repeatedly with syringe flushing.

12.2.3 Application

For lesion detection or evaluation of wide areas (panchromoendoscopy), the dye is better to be applied with spraying catheter (PW-205V, PW-5L-1, PW-6P-1, Olympus Medical Systems. Tokyo, Japan; S2816, Fine jet, Top Corp. Tokyo, Japan). The tip of catheter is protruded from the scope and the dye solution is sprinkled onto the entire lumen with scope maneuvering (Fig. 12.5a). For colonic panchromoendoscopy, dye is diluted into the bottle of water jet pump and the solution can be applied via scope waterjet [4].

For lesion characterization (target chromoendoscopy), the dye is applied to a suspicious area in standard endoscopic observation such as an area with uneven surface, discoloration, disappeared vascular network of the background mucosa, or spontaneous bleeding. Syringe flush is commonly used for topical application of dye solution. It is important to apply the dye solution

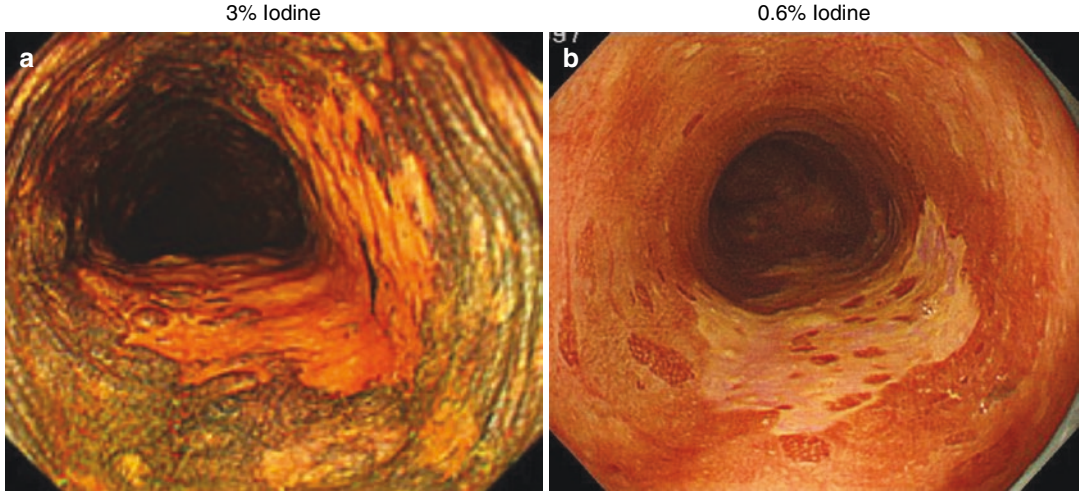

Fig. 12.4 High-concentration (3%) iodine solution (**a**) stains the mucosa better than low-concentration (0.6%) iodine solution (**b**), but it is likely to cause unpleasant symptoms

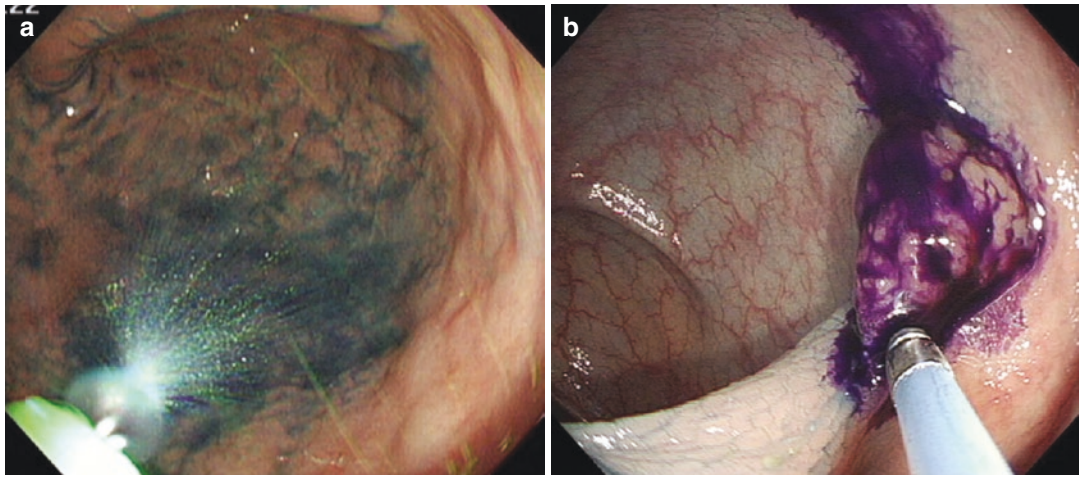

Fig. 12.5 Indigo carmine solution is sprinkled onto the gastric mucosa (**a**). Only tip of the spraying catheter is protruded from the working channel, and endoscope is maneuvered to be kept in the center of the lumen because close dye sprinkling to the mucosa may cause bleeding. Crystal violet is topically applied to the colonic adenoma using non-traumatic catheter (6233064, Olympus Medical Systems) (**b**)

not only to the lesion but also surrounding mucosa because lesion characterization is often carried out in comparison with finding of the surrounding mucosa. Moreover, GI naoplasms are often accompanied by superficial lesion extension, thus it can be a chance to detect the lateral extent of the lesion. The syringe flush can be used for wide areal application of dye solution as well. In this case, more than 20 mL of dye solution is administered into the lumen and is applied onto the wide luminal surface by collapse of the lumen with air suction.

Highly targeted dye application is performed with nontraumatic catheter (6233064, Olympus Medical Systems. Tokyo, Japan, Fig. 12.5b). This method is used for pit pattern analysis of colorec-

tal neoplasms using magnifying colonoscopy and nuclear observation using endocytoscopy (GIF-H290EC, CF-H29ECI, Olympus Medical Systems. Tokyo, Japan).

12.3 Specific Information

12.3.1 Contrast Method

12.3.1.1 Indigo Carmine

Indigo carmine blue dye pools in mucosal grooves and depressed areas and contrast mucosal surface topography (Fig. 12.6). Superficial neoplasms often have shallower and narrower crypts, and this likely to contribute to the lesion having less dye on its surface (Fig. 12.7). In this method, a 0.04–2.0% solution of indigo carmine is applied onto the mucosa. It is widely used in the columnar epithelium, i.e., Barrett's esophagus, stomach, and colorectum. Use of 0.1–0.5% indigo carmine pancolonic chromoendoscopy with targeted biopsies is recommended for neoplasia surveillance in patients with long-standing colitis [5]. Zhao et al. reported the pooled sensitivity, specificity, and area under the curve of indigo carmine chromoendoscopy for diagnostic of early gastric cancer were 0.90, 0.82, and 0.94, respectively [6], and the diagnostic accuracy of chromoendoscopy was higher than that of standard white light endoscopy. Nagahama T, et al. indicated that indigo carmine chromoendoscopy showed the clinically equivalent accuracy for lesion delineation of early gastric cancer compared to magnifying narrow-band imaging [7].

12.3.1.2 Methylene Blue

0.05% methylene blue can be also used as a contrast method, but it requires vigorous washing of the mucosal surface before application because it stains the mucous well.

12.3.2 Absorptive (Vital Staining) Methods

12.3.2.1 Methylene Blue

Methylene blue is absorbed by intestinal type epithelium such as the normal small intestinal and colorectal mucosa, or intestinal type metaplasia in the stomach or the esophagus.

0.5% methylene blue is used for staining of the specialized intestinal metaplasia (SIM) in the esophagus, facilitating diagnosis of Barrett's esophagus and detection of dysplasia and carcinoma in the Barrett's esophagus. Some investigators proposed classifications of pit patterns of columnar esophageal mucosa [8–10], and indicated excellent diagnostic accuracy (sensitivity of 95% and specificity of 97%) for detection of

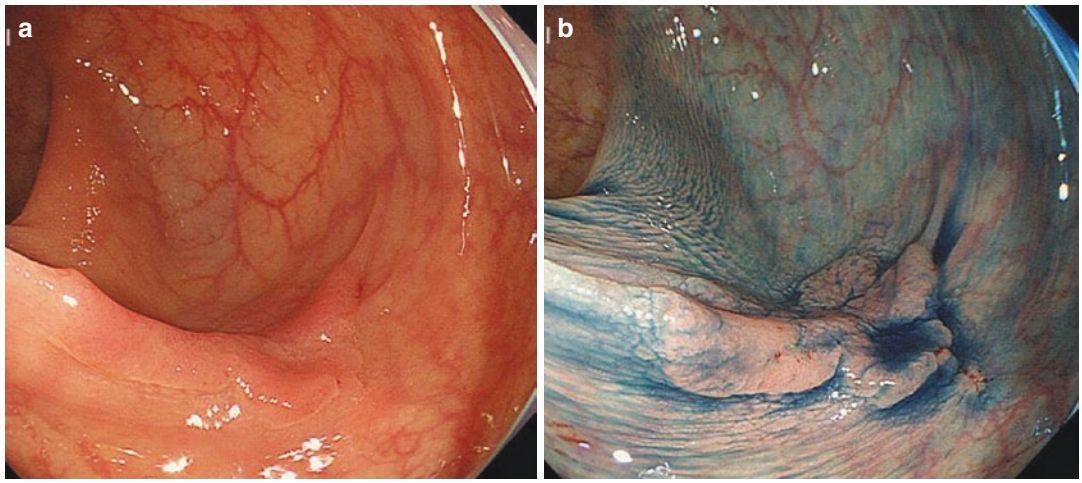

Fig. 12.6 Laterally spreading tumor in the transverse colon (**a**). After application of 0.2% indigo carmine solution, tumor morphology became apparent (**b**)

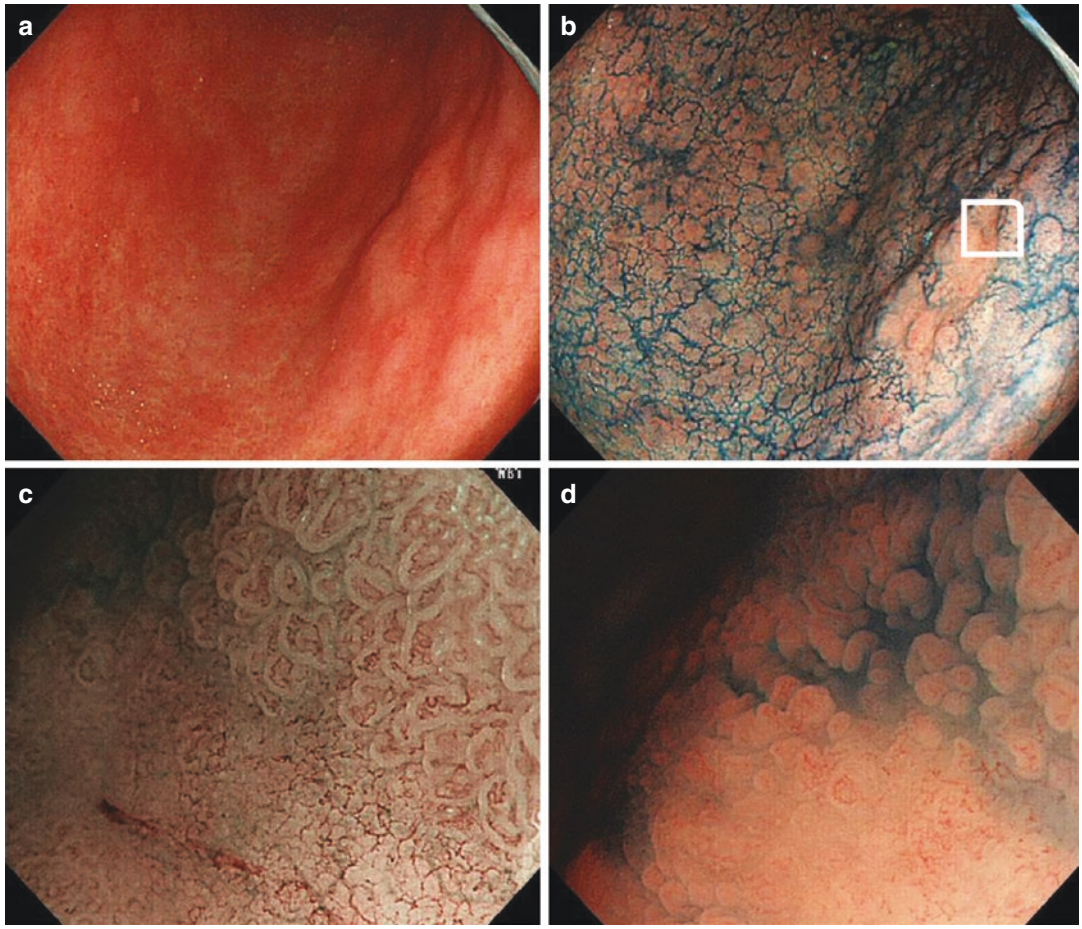

Fig. 12.7 Small superficial depressed type early gastric cancer in the posterior wall of the lower gastric body (**a**). After spraying 0.2% indigo carmine solution, the lesion looked as a dye shed area (**b**). Because cancerous pits are usually shallower and narrower than surrounding mucosa, surface structure in the cancerous mucosa looks absent (**c**), therefore the dye does not retain in the cancerous area (**d**)

SIM. Ragunath et al., in their randomized crossover trial, demonstrated methylene blue-directed biopsy had significantly better accuracy for detection of SIM, but not for dysplasia or carcinoma, in the Barrett's esophagus compared to conventional random biopsy [11].

Dinis-Ribeiro M. et al. used 1% methylene blue magnifying chromoendoscopy for diagnosis of gastric intestinal metaplasia and dysplasia, and indicated diagnostic accuracy of 84 and 83%, respectively [12].

1% Methylene blue stains nuclei, and can be used for nuclear observation of the squamous epithelium in combination with endocytoscopy [13, 14].

12.3.2.2 Crystal Violet

Crystal violet, which is also known as a topical antimicrobial agent, is absorbed by the epithelium and stain it. It is used for detection of intestinal metaplasia and dysplasia in the Barrett's esophagus [15] and for enhancing visualization of the pit patterns in the colon [16, 17]. For colonic pit pattern analysis, small amount (1–2 ml) of 0.05–0.1% crystal violet solution is usually applied with a catheter to avoid excessive darkened staining of the surrounding mucosa. Based on stereomicroscopic investigation, the pit patterns of colonic tumors are classified according to the shape of crypt openings (Type I, round pits; Type II, stellar or papillary pits; Type III_L,

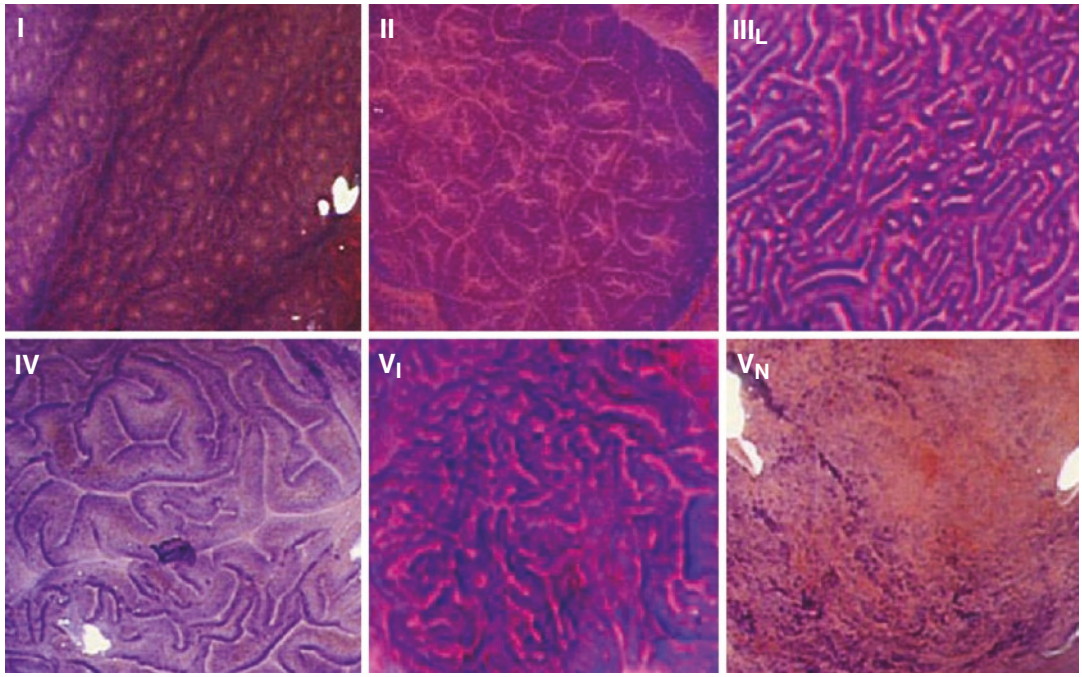

Fig. 12.8 Kudo's pit pattern classification. Type I, round pits; Type II, stellar pits; Type III_L, large tubular pits; Type IV, branch- and gyrus-like pits; Type V_I, irregular pits; and Type V_N, nonstructural pits

large tubular pits; Type III_S, small tubular pits; Type IV, branch- and gyrus-like pits; and Type V, irregular or nonstructural pits), which correlate with histological finding of the lesions (Fig. 12.8). The pit patterns observed in magnifying chromoendoscopy were fundamentally similar to those in stereomicroscopic images. When the diagnosis by magnifying endoscopy was compared with the stereomicroscopic diagnosis, the concordance rate was 81.5% (1130 of 1387 lesions). Later, Kudo's pit pattern Type V was divided into Type V_I: irregular pits and V_N, nonstructural pits. Matsuda et al. indicated as "invasive pattern" that include Type V_I pits within demarcated area and Type V_N pits showed sensitivity of 86% and specificity of 99% for deep (≥1000 μm) submucosal invasive colorectal cancers [18].

0.05% crystal violet is used for staining of cytoplasm in endocytoscopy [14, 19].

12.3.2.3 Toluidine Blue

Toluidine blue is an absorptive dye, and it was initially used for the detection of squamous dysplasia and carcinoma of the oral cavity [20].

0.5% Toluidine blue stains cell nucleus in the stomach and the colon better than 1% methylene blue, and is used for endocytoscopic observation [14].

12.3.3 Reactive Method

12.3.3.1 Iodine

When 1–3% iodine solution is applied, normal squamous epithelium turns the color into brown because of chemical reaction between iodine and glycogen which is contained in the normal squamous epithelium (Figs. 12.3 and 12.9). Besides, the neoplastic squamous epithelium appears yel-

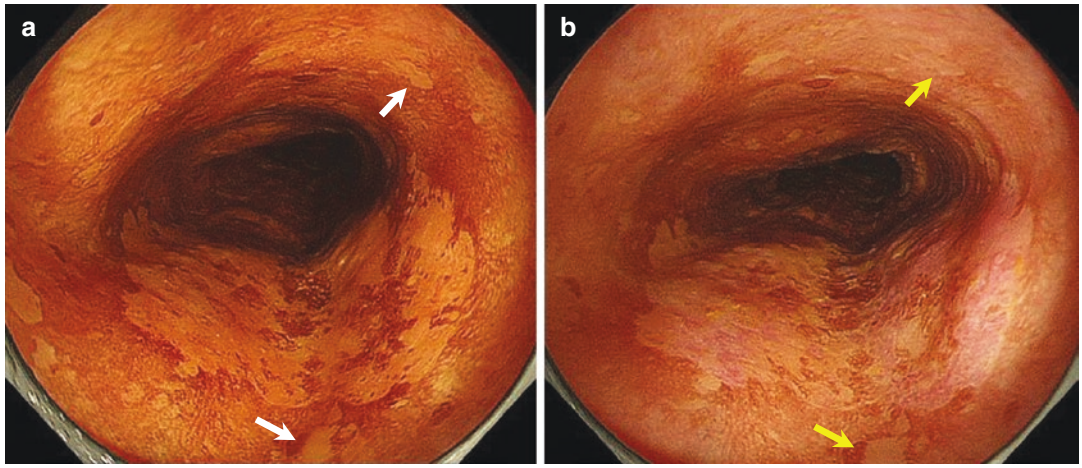

Fig. 12.9 After application of iodine solution, the normal esophageal mucosa turns the color into brownish, whereas squamous cell carcinoma does not change the color (**a**). Multiple Lugol voiding areas (white arrows in **a**) is associated with risk of squamous cell carcinoma in the esophagus, head and neck. After 30 s to 1 min, a cancerous non-stained area turns the color into pinkish (**b**), while noncancerous non-stained areas remain yellowish (yellow arrows in **b**)

lowish non-stained areas because glycogen in the cancerous epithelium is consumed by excessive glycolytic metabolism.

Iodine non-stained areas, especially when the lesion is small, include not only high-grade dysplasia or squamous cell carcinoma but also low-grade neoplasia or even normal mucosa. Hence, Iodine chromoendoscopy is a highly sensitive (91–100%) but not very specific (40–95%) for detecting squamous cell carcinoma. However, the diagnostic accuracy of iodine chromoendoscopy for squamous cell carcinoma is improved by additional assessment of pinkish color change, so-called pink-color sign, of the non-stained area (sensitivity and specificity of 91.9 and 94%, respectively, Fig. 12.9) [21].

Multiple Lugol voiding lesions in iodine chromoendoscopy is associated with risk of synchronous esophageal squamous cell carcinoma in patients with head and neck cancer [22], and a strong predictor for development of metachronous esophageal, head and neck squamous carcinoma in patients received endoscopic resection of superficial esophageal squamous cell carcinoma (Fig. 12.9) [23].

12.3.3.2 Congo Red

Congo red dye is a pH indicator and it changes the color from red to dark blue-black under acidic conditions (<pH 3). Congo red chromoendoscopy technique involves stimulation of acid secretion with 250 mg of intravenous pentagastrin, application of 0.5% sodium bicarbonate solution followed by 0.3% Congo red solution. This method has been used for mapping acid-secreting normal fundic (oxyntic) mucosa. Areas where acid secretion is impaired by chronic fundic gastritis are seen as non-discolored areas (red color) in Congo red chromoendoscopy (Fig. 12.10).

A double staining technique using methylene blue and Congo red has been used to identify early gastric cancers as non-discolored or "bleached" areas of mucosa (Fig. 12.10) [24]. Iishi et al. demonstrated that Congo red methylene blue chromoendoscopy detected synchronous early

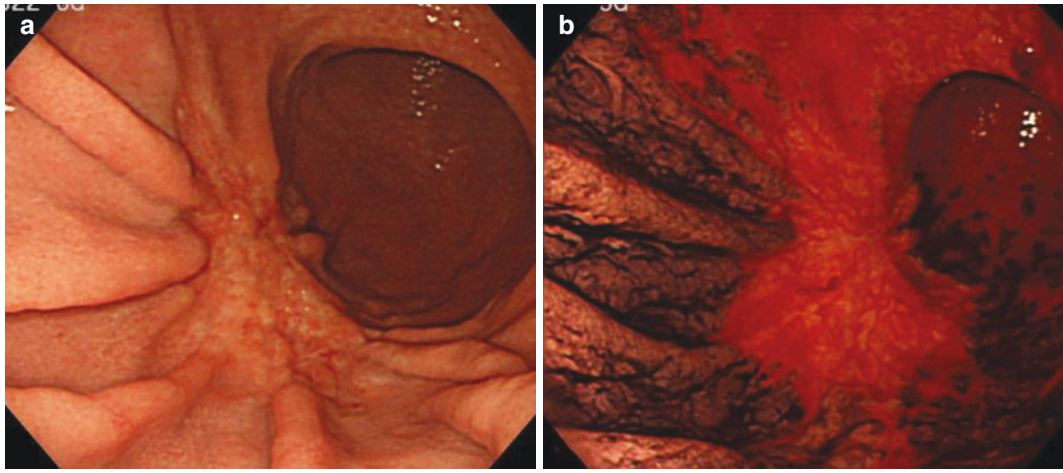

Fig. 12.10 Superficial depressed type early gastric cancer in the lower gastric body (**a**). In Congo red chromoendoscopy, mucosa in the corpus greater curvature are seen as discolored area (blue-black mucosa) indicating presence of normal oxyntic mucosa, while the mucosa in the lesser curvature are seen as non-discolored area (red mucosa) because of loss of oxyntic glands by atrophic gastritis. The early gastric cancer remains as non-discolored areas (red color, **b**)

gastric cancers better (89%) than standard white light endoscopy (28%) [25].

12.3.4 Others

12.3.4.1 Acetic Acid

Acetic acid alters tertiary structure of cytoplasmic proteins and causes transient whitening of the surface epithelium. Acetic acid is not regarded as chromoendoscopy because the acetic acid is not a dye, but the actual effect is similar to that achieved in an absorptive method. Acetic acid endoscopy was first used to observe the specialized columnar epithelium in the Barrett's esophagus [26], and was then adopted for the diagnosis of gastric [27] of colorectal neoplasms [28]. 10–20 mL of 1.5–3% acetic acid is applied onto the mucosal surface. Use of magnification endoscopy and narrow-band imaging enhances observation of detailed micro-surface structure (Fig. 12.11a and d).

12.3.4.2 Combination of Indigo Carmine with Acetic Acid

When acetic acid and indigo carmine are applied together, the surrounding noncancerous mucosa stained blueish but the cancerous mucosa does not stained, showing as a well-contrasted reddish area (Fig. 12.11c and d). The method is originally performed as administration of mixture solution (0.6% acetic acid–0.4% indigo carmine mixture, AIM) [29], but latterly it is also performed by subsequent administration of 1% acetic acid and 1% indigo carmine solution [30].

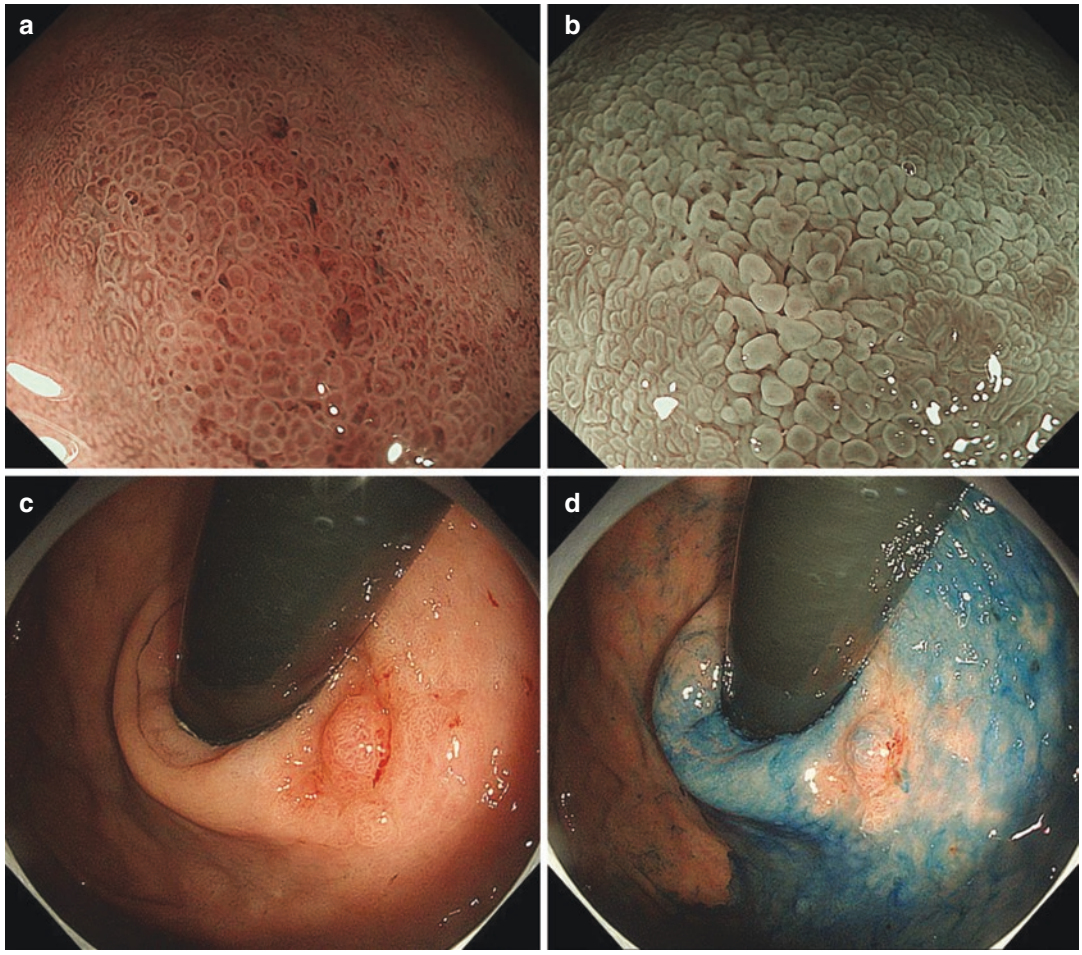

Fig. 12.11 A superficial flat type early gastric cancer (**a**). Mucosal surface is whitened by 3% acetic acid application (**b**). A superficial depressed type early gastric cancer near the cardia (**c**). After application of 3% acetic acid and 0.2% indigo carmine, the lesion is seen as a well-contrasted reddish area (**d**)

12.4 Summary

Chromoendoscopy enhances mucosal morphology and color, and improves diagnostic yield of endoscopy for detection and characterization of superficial neoplasms in the digestive tract. In contrast to equipment-based IEE, chromoendoscopy requires extra time and effort for preparation and application of the method. However, in other words, if a little effort is taken, significant

benefit in clinical practice is achieved even with conventional endoscopy systems. The equipment and reagents for chromoendoscopy are widely available at reasonable price around the world. Implementation of this method in clinical practice is at endoscopists' discretion.

References

1. Fujii T, Iishi H, Tatsuta M, Hirasawa R, Uedo N, Hifumi K, Omori M. Effectiveness of premedication with pronase for improving visibility during gastroendoscopy: a randomized controlled trial. Gastrointest Endosc. 1998;47(5):382–7.
2. Monrroy H, Vargas JI, Glasinovic E, Candia R, Azúa E, Gálvez C, Rojas C, Cabrera N, Vidaurre J, Álvarez N, González J, Espino A, González R, Parra-Blanco A. Use of N-acetylcysteine plus simethicone to improve mucosal visibility during upper GI endoscopy: a double-blind, randomized controlled trial. Gastrointest Endosc. 2018;87(4):986–93.
3. Kondo H, Fukuda H, Ono H, Gotoda T, Saito D, Takahiro K, Shirao K, Yamaguchi H, Yoshida S. Sodium thiosulfate solution spray for relief of irritation caused by Lugol's stain in chromoendoscopy. Gastrointest Endosc. 2001;53:199–202.
4. Soetikno R, East J, Suzuki N, et al. Endoscopic submucosal dissection for nonpolypoid colorectal dysplasia in patients with inflammatory bowel disease: in medias res. Gastrointest Endosc. 2018;87:1085–94.
5. Kamiński MF, Hassan C, Bisschops R, et al. Advanced imaging for detection and differentiation of colorectal neoplasia: European Society of Gastrointestinal Endoscopy (ESGE) Guideline. Endoscopy. 2014;46:435–49.
6. Zhao Z, Yin Z, Wang S, et al. Meta-analysis: The diagnostic efficacy of chromoendoscopy for early gastric cancer and premalignant gastric lesions. J Gastroenterol Hepatol. 2016;31:1539–45.
7. Nagahama T, Yao K, Uedo N, et al. Delineation of the extent of early gastric cancer by magnifying narrow-band imaging and chromoendoscopy: a multicenter randomized controlled trial. Endoscopy. 2018;50:566–76.
8. Endo T, Awakawa T, Takahashi H, et al. Classification of Barrett's epithelium by magnifying endoscopy. Gastrointest Endosc. 2002;55:641–7.
9. Guelrud M, Ehrlich E. Endoscopic classification of Barrett's esophagus. Gastrointest Endosc. 2004;59:58–65.
10. Canto MI, Setrakian S, Petras RE, et al. Methylene blue selectively stains intestinal metaplasia in Barrett's esophagus. Gastrointest Endosc. 1996;44:1–7.
11. Ragunath K, Krasner N, Raman VS, et al. A randomized, prospective cross-over trial comparing methylene blue-directed biopsy and conventional random biopsy for detecting intestinal metaplasia and dysplasia in Barrett's esophagus. Endoscopy. 2003;35:998–1003.
12. Dinis-Ribeiro M, da Costa-Pereira A, Lopes C, et al. Magnification chromoendoscopy for the diagnosis of gastric intestinal metaplasia and dysplasia. Gastrointest Endosc. 2003;57:498–504.
13. Kumagai Y, Monma K, Kawada K. Magnifying chromoendoscopy of the esophagus: in-vivo pathological diagnosis using an endocytoscopy system. Endoscopy. 2004;36:590–4.
14. Kodashima S, Fujishiro M, Takubo K, et al. Ex-vivo study of high-magnification chromoendoscopy in the gastrointestinal tract to determine the optimal staining conditions for endocytoscopy. Endoscopy. 2006;38:1115–21.
15. Amano Y, Kushiyama Y, Ishihara S, et al. Crystal violet chromoendoscopy with mucosal pit pattern diagnosis is useful for surveillance of short-segment Barrett's esophagus. Am J Gastroenterol. 2005;100:21–6.
16. Kudo S, Tamura S, Nakajima T, et al. Diagnosis of colorectal tumorous lesions by magnifying endoscopy. Gastrointest Endosc. 1996;44:8–14.
17. Kudo S, Rubio CA, Teixeira CR, Kashida H, Kogure E. Pit pattern in colorectal neoplasia: endoscopic magnifying view. Endoscopy. 2001;33:367–73.
18. Matsuda T, Fujii T, Saito Y, et al. Efficacy of the invasive/non-invasive pattern by magnifying chromoendoscopy to estimate the depth of invasion of early colorectal neoplasms. Am J Gastroenterol. 2008;103:2700–6.
19. Ichimasa K, Kudo S, Mori Y, et al. Double staining with crystal violet and methylene blue is appropriate for colonic endocytoscopy: an in vivo prospective pilot study. Dig Endosc. 2014;26:403–8.
20. Epstein JB, Feldman R, Dolor RJ, et al. The utility of tolonium chloride rinse in the diagnosis of recurrent or second primary cancers in patients with prior upper aerodigestive tract cancer. Head Neck. 2003;25:911–21.
21. Shimizu Y, Omori T, Yokoyama A, et al. Endoscopic diagnosis of early squamous neoplasia of the esophagus with iodine staining: high-grade intraepithelial neoplasia turns pink within a few minutes. J Gastroenterol Hepatol. 2008;23:546–50.
22. Muto M, Hironaka S, Nakane M, et al. Association of multiple Lugolvoiding lesions with synchronous and metachronous esophageal squamous cell carcinoma in patients with head and neck cancer. Gastrointest Endosc. 2002;56:517–21.
23. Katada C, Yokoyama T, Yano T, et al. Alcohol consumption and multiple dysplastic lesions increase risk of squamous cell carcinoma in the esophagus, head, and neck. Gastroenterology. 2016;151:860–9.
24. Song LMWK, Adler DG, Chand B, et al. Chromoendoscopy. Gastrointest Endosc. 2007;66:639–49.
25. Iishi H, Tatsuta M, Okuda S. Diagnosis of simultaneous multiple gastric cancers by the endoscopic Congo red methylene blue test. Endoscopy. 1988;20:78–82.

26. Guelrud M, Herrera I. Acetic acid improves identification of remnant islands of Barrett's epithelium after endoscopic therapy. Gastrointest Endosc. 1998;47:512–5.
27. Toyoda H, Tanaka K, Hamada Y, et al. Magnification endoscopic view of an early gastric cancer using ascetic acid and Narrow-Band Imaging System. Dig Endosc. 2006;18:S41–3.
28. Kawamura YJ, Togashi K, Sasaki J, et al. Acetic acid spray in colonoscopy: an alternative to chromoendoscopy. Gut. 2005;54(2):313.
29. Kawahara Y, Takenaka R, Okada H, et al. Novel chromoendoscopic method using an acetic acid-indigocarmine mixture for diagnostic accuracy in delineating the margin of early gastric cancers. Dig Endosc. 2009;21:14–9.
30. Iizuka T, Kikuchi D, Hoteya S, et al. The acetic acid + indigocarmine method in the delineation of gastric cancer. J Gastroenterol Hepatol. 2008;23:1358–61.

Narrow-Band Imaging

13

James Weiquan Li and Tiing Leong Ang

13.1 Introduction

Image-enhanced endoscopy (IEE) is widely used in many centers for the detection and characterization of gastrointestinal (GI) lesions found in various parts of the GI tract, namely the esophagus, stomach, and large colon. IEE includes chromoendoscopy, optical filtering and digital filtering, and the features can further be enhanced with high magnification.

Narrow-band imaging (NBI) represents the most commonly used optical digital method of IEE currently. This form of imaging was first conceptualized in the 1990s, and its feasibility was soon reported in the literature where it was demonstrated to increase the contrast between vascular patterns and intervening mucosa on the underside of the tongue [1]. In collaboration with Sano, an NBI system for GI endoscopy was developed, and in 2006, the first such system was launched in the form of the EXERA II (Olympus CLV-180 EVIS EXERA II xenon light source, Olympus CV-180 EVIS EXERA II video system center).

This chapter aims to outline the principles behind the use of NBI and its utility in the field of GI endoscopy.

13.2 Principles of NBI

Light is an electromagnetic wave consisting of wavelengths in the ultraviolet, visible light, and infrared spectra. Within the visible spectrum of light, the primary colors are represented in increasing order of wavelengths by blue, green, and red light, respectively. Blue light, with its shorter wavelength, is scattered and reflected in the superficial mucosa, while the longer red wavelength penetrates deeper into the tissue layers. When normal white light hits tissues, some of it reflects off the surface while others diffuse in a three-dimensional manner, which results in light scattering. The extent to which this occurs differs according to the wavelengths within the visible spectrum of light making contact with the tissue. As a result, unfiltered white light has the tendency to mask details of the surface pattern of the mucosa along with its vascular structures.

J. W. Li · T. L. Ang (✉)
Department of Gastroenterology and Hepatology, Changi General Hospital, Singapore, Singapore
e-mail: ang.tiing.leong@singhealth.com.sg; tiing_leong_ang@cgh.com.sg

P. W. Y. Chiu et al. (eds.), *Endoscopy in Early Gastrointestinal Cancers, Volume 1*,
https://doi.org/10.1007/978-981-10-6769-3_13

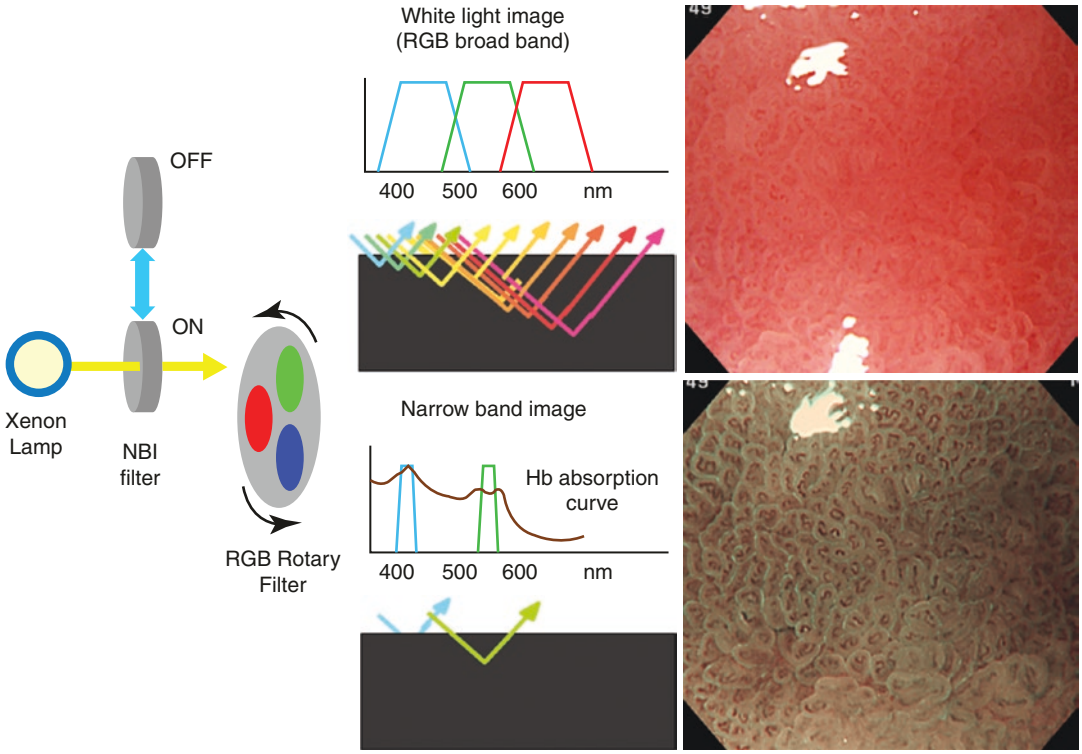

Fig. 13.1 Mechanism of NBI

NBI utilizes the following two phenomena about the visible spectrum of light to enhance the contrast between blood vessels and the surface mucosa, which enables the operator to characterize lesions in greater detail with regards to mucosal surface architecture and vascular patterns (Fig. 13.1):

1. The wavelengths of visible light absorbed by hemoglobin is different from the surface mucosa.
2. The depth of penetration of light in the tissue layers is directly proportional to the wavelength.

The active site of hemoglobin is heme, and the configuration of the iron atom together with the attached protein ring modifies the wavelength of absorption of light from the visible spectrum, giving rise to its characteristic color. Hemoglobin has an absorption peak at 415 nm. The NBI filter eliminates the red wavelength of light, leaving the blue and green wavelengths. As a result, when the filtered blue and green wavelengths hit the tissue surface being examined, these wavelengths of light are absorbed by hemoglobin contained within the blood vessels while being reflected by the mucosa, enhancing the contrast of these vascular structures with respect to the surrounding mucosa. This allows the endoscopist to observe subtle differences in vascular and patterns which may indicate the presence of dysplasia and early cancer.

In addition, NBI also exploits the differences in penetration of the two different wavelengths of light filtered to enable more details of suspicious lesions to be appreciated. The shorter blue wavelength can only penetrate the superficial layer and hence is absorbed by capillaries on the surface of the mucosa. Green light, with its longer wavelength, is able to penetrate deeper into the mucosa and submucosa, where it is absorbed by deeper vessels. This explains why superficial capillaries have a brown appearance on NBI, while deeper vessels appear cyan in color. By narrowing the spectrum of light which hits the surface mucosa, less scattering occurs compared to when white light is used for endoscopy, result-

ing in sharper and less distorted images of the capillary networks in the mucosa.

13.3 Technical Aspects

To achieve this desired effect, an NBI filter is placed between the xenon lamp and the red–green–blue (RGB) rotatory filter in the light source unit [2]. The NBI filter restricts spectrum of light to two narrow bands of blue at 415 nm and green at 540 nm. In addition, the spectral bandwidth of these filtered wavelengths is also reduced. It can be turned on or off by the endoscopist using a button on the endoscope, which may vary depending on how the buttons have been configured.

However, despite the many advantages of NBI, one of the major drawbacks of the first-generation system is its lack of brightness. This limited its operability, as the viewable distance in NBI mode was severely reduced and the distal tip of the endoscope had to be moved very close to the lesion in question in order to obtain sufficient brightness for viewing. Aware of this limitation, Olympus has performed much research and development to improve the brightness of images in NBI mode. Through the development of a brighter light source, an improved sensitivity of the charge coupled device (CCD), and modifications to the image processor to reduce noise, the newer systems such as the EVIS EXERA III (CV-190 and CLV-190) and EVIS LUCERA ELITE (CV-290 and CLV-290SL) systems have been able to deliver increased brightness, which in turn translates into twice the viewable distance compared to the EVIS EXERA II system described earlier.

13.4 Role of Magnifying Endoscopy Combined with NBI

Magnifying endoscopy is often used in conjunction with NBI to distinguish between neoplastic and non-neoplastic lesions [3, 4]. In some classification systems which will be discussed later in this and other chapters of this book, magnification is essential to differentiate between the types of neoplastic lesions. Two modalities for magnification endoscopy currently exist: digital magnification combined with dual focus and optical zoom.

With dual focus, the endoscopist can toggle between normal focus and near focus using a preconfigured button on the endoscope. The near-field magnification utilizes a two-stage optical lens technology from Olympus, allowing ready use of a 40X magnification capability without the need for use of a cap or hood, as the predetermined magnification setting is fixed and the endoscopist only needs to maneuver the endoscope to achieve the clearest image possible (Fig. 13.2). In contrast, optical zoom requires the use of a cap or hood mounted on the distal tip of the endoscope for the endoscopist to consistently fix the mucosa at a distance of approximately 2 mm. The degree of magnification is controlled by a rocker button is positioned on the endoscope such that it can be operated by the left thumb, with the down configuration allowing the endoscopist to zoom into the lesion and the up configuration for zooming out. An example of an endoscope with optical magnification capabilities is the Olympus CF-H260AZL/I scope, which has an optical magnification of 90X (Fig. 13.3).

Magnification refers to the ability to enlarge an image to several times optical power using a movable lens controlled by the endoscopist,

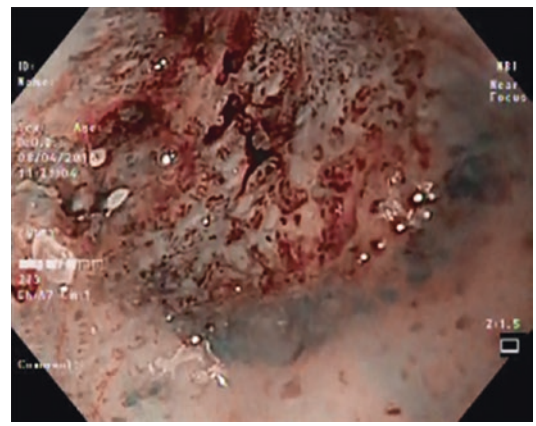

Fig. 13.2 Narrow-band imaging of superficial esophageal squamous cell carcinoma using dual focus magnification

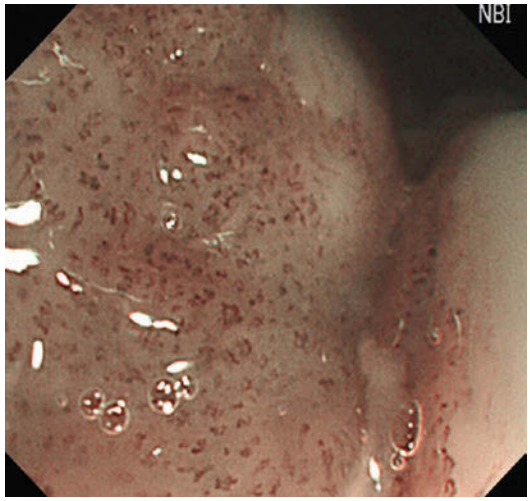

Fig. 13.3 Narrow-band imaging of superficial esophageal squamous cell carcinoma using optical magnification

while resolution is the ability to distinguish between two points that are close together. Pixilation and resultant blur images can occur with conventional endoscopes and when images are viewed in high magnification due to poor resolution. This problem is overcome with a high-definition compatible CCD, which increases the number of pixels in the CCD, with current high-definition endoscopes producing signal images ranging from 850,000 to more than 1,000,000 pixels. Thus, magnifying NBI with optical zoom can produce sharp images even with full magnification when connected to a high-definition system.

13.5 Clinical Application of NBI

NBI has been used extensively in the detection, characterization, and management of neoplastic lesions in the esophagus, stomach, and colon. Several classification systems employing NBI with or without magnification have also been developed to aid in the identification and description of suspicious lesions in various parts of the GI tract. Detection of early cancers and their precursors in the esophagus, stomach, and colon renders the lesions amenable to endoscopic therapy in the form of endoscopic mucosal resection (EMR), endoscopic submucosal dissection (ESD), or endoscopic ablation, with improved prognosis and the avoidance of surgery, which is usually associated with higher morbidity. In particular, magnifying NBI can be used to accurately determine the depth of invasion (i.e., mucosal or submucosal), and to differentiate between high- and low-grade intraepithelial neoplasia. These factors directly impact on the choice of therapy and the consequent efficacy of the treatment modality chosen, as lesions confined to the mucosal layer and histologically well-differentiated tumors in general have low to zero risk of lymph node metastasis.

13.6 Esophagus

The intrapapillary capillary loop (IPCL) or Inoue Classification uses magnifying NBI to describe the vascular patterns of microvessels in the esophageal mucosa, namely the degree of dilatation, tortuous or meandering course, change in caliber, and differences in shapes [5]. In general, increased dilatation of the IPCLs and a tortuous course indicate higher grades of dysplasia. These IPCL features are then used to categorize lesions into non-neoplastic (IPCL-I and IPCL-II), borderline (IPCL-III and IPCL-IV), and cancer (IPCL-V). Squamous cell carcinomas (SCC) are further subclassified to reflect the depth of invasion as intramucosal (IPCL-V1 and IPCL-V2), deep mucosal or superficial submucosal (IPCL-V3) and submucosal cancer (IPCL-VN), based on the IPCL patterns. Using this classification system, Sato et al. [6] demonstrated a sensitivity and specificity for IPCL-VI/V2 of 89.5% and 79.6%, respectively, while that for IPCL-V3 was 58.7% and 83.8%, respectively. With regards to IPCL-VN lesions, there was specificity of 98.6%, although the sensitivity was 55.8%. There was also relatively good inter- and intra-observer agreement in this study.

The effectiveness of NBI in the detection of esophageal SCC was also shown in a multicenter, prospective, randomized controlled trial conducted by Muto et al. [7] Patients with esophageal

SCC were randomly assigned to primary white light endoscopy (WLE) followed by NBI or vice versa in a back-to-back fashion. The sensitivity of primary NBI for detection of superficial esophageal SCC was 97.2% compared to 55.2% with primary WLE. The accuracy of NBI was also 88.9% in this study, compared to 56.5% with primary WLE. However, this came at the expense of a lower specificity (42.1% versus 63.2%, respectively). The diagnostic yield of NBI was especially pronounced with smaller lesions in comparison to WLE, being 94% and 95% for superficial esophageal SCC measuring <10 mm and 11–20 mm, respectively, while that with WLE was 39 and 33%, respectively. An earlier study by Takenaka et al. [8] comparing NBI against the gold standard of Lugol's iodine also produced similar results, with a sensitivity of 90.9% and accuracy of 95.1%.

Detection of dysplasia and esophageal adenocarcinoma (EAC) in the setting of Barrett's esophagus (BE) is another area of interest in the field of IEE using NBI. Earlier classifications using NBI with magnification such as that from Nottingham, Kansas, and Amsterdam, aimed to differentiate normal mucosa from intestinal metaplasia (IM) and dysplasia using mucosal pit patterns and vascular patterns. For instance, villous or ridged patterns with the absent of abnormal vasculature pointed toward IM changes, while distorted, irregular pits with abnormal vessels indicated the presence of dysplasia. Using these features, the sensitivity and specificity of NBI in detecting high-grade intra-epithelial neoplasia (HGIN) ranged 94–100% and 76–98.7%, respectively [9–11].

An international, randomized, crossover trial by Sharma P et al. [12] compared high-definition white light endoscopy (HD-WLE) and NBI in patients referred for BE screening and surveillance. The HD-WLE group had random biopsies by the Seattle protocol together with targeted biopsies of visible lesions, in contrast to the NBI group where targeted biopsies were obtained based on mucosal and vascular patterns noted during endoscopy. Although both modalities of screening and surveillance detected similar rates of IM, fewer biopsies were required per patient to establish this diagnosis with NBI (3.6 versus 7.6; $p < 0.001$). Moreover, NBI detected significantly more areas of dysplasia than HD-WLE (30% versus 21%).

Recently, a simple and internally validated classification system for the detection of HGIN and EAC in BE was developed by the Barrett's International NBI Group (BING). This utilized near-focus technology in combination with NBI to identify absent or irregular mucosal patterns and vessels which did not follow the normal architecture of the mucosa either focally or diffusely. Using the BING criteria, dysplasia was identified with a sensitivity and specificity of 80 and 88%, respectively. The overall accuracy in the identification of dysplasia was 85%, and the inter-observer agreement was substantial with a kappa value of 0.681 [12].

13.7 Stomach

Intestinal metaplasia (IM) is a recognized precursor to gastric cancer in the Correa cascade [13]. The "light blue crest" sign, defined as a fine, blue-white line seen on the gyri of the epithelial surface, has been shown to be highly specific 93%) for gastric IM, although its absence does not exclude this diagnosis. This can be seen on magnifying NBI, and has a high accuracy of 91% [14]. NBI was shown in a multicenter, prospective, randomized study by Ang et al. [15] to increase the detection rate of IM compared to HD-WLE from 7.7 to 17.7% in patients older than 50 years undergoing esophagogastroduodenoscopy. Similarly, NBI in combination with magnifying endoscopy can also be used in the diagnosis of early gastric cancer (EGC).

The vessel plus surface (VS) classification, as its name suggests, leverages on the properties of magnification NBI to clearly visualize the microvascular (MV) and microsurface (MS) patterns [16]. These MV and MS patterns are categorized into regular, irregular, and absent. For instance, a regular MS pattern is defined by a uniform and homogeneous marginal crypt epithelium which appears regular with a symmetrical distribution, whereas an irregular pattern

arises when the marginal crypt epithelium appears as irregular and heterogeneous structures with asymmetrical distribution. Similarly, mucosal capillaries have uniform shapes with regular arrangements and symmetrical distribution in a regular MV pattern, while an irregular pattern displays a more haphazard appearance with tortuous, branched, and bizarrely shaped vessels distributed asymmetrically and in an irregular fashion. In EGC, NBI with magnification also has the ability to identify a demarcation line between cancerous and noncancerous mucosa, which has a high sensitivity of 95% for predicting cancerous lesions [17].

Using the VS classification system, an EGC can be identified by the presence of a clear demarcation line and an irregular MS and/or MV pattern within the demarcation line. In a study by Yao et al. [16], it has been shown that 97% of EGC fall within the mentioned criteria. The importance of a demarcation line has already been emphasized given its high sensitivity for EGC, thus a lesion without a demarcation line is unlikely to be a malignant lesion. However, it needs to be noted that the presence of a demarcation line alone is insufficient for the diagnosis of EGC given its low specificity of 49%. This reinforces the utility of NBI with magnification to identify irregular MS and/or MV patterns as this increases the specificity for the diagnosis of a cancerous lesion to 95%. Moreover, the same investigator also demonstrated in a separate study that magnifying NBI in the context of screening for EGC may decrease the number of biopsies required to establish such a diagnosis [18].

The usefulness of magnifying NBI in EGC has also been demonstrated in several other studies. In a multicenter, prospective, randomized, controlled trial conducted by Ezoe et al. [19], the real-time diagnostic yield of WLE and NBI with magnification for small (>10 mm) depressed gastric lesions were compared. While the accuracy and specificity of magnifying NBI was statistically greater than WLE, the increased sensitivity of magnifying NBI failed to achieve statistical significance. However, when magnifying NBI was combined with WLE, very high rates of accuracy, sensitivity, and specificity were achieved (96.6%, 95%, and 96.8%, respectively), which were statistically greater than either modality alone. It should be noted that the median time taken for this combined approach was longer than that of magnifying NBI alone, which in turn was longer than WLE alone. Li et al. [20] was also able to demonstrate high sensitivity, specificity, and accuracy in using magnifying NBI to differentiate cancerous from noncancerous lesions (97.3%, 84.4%, and 90.2%, respectively) in a prospective study conducted in a single academic center. In this study, magnifying NBI was also able to accurately predict the depth of invasion in 95% of cases. Another study by Maki et al. [21] also demonstrated higher sensitivity (95% versus 64%) and accuracy (92% versus 74%) for magnifying NBI compared to WLE in differentiating EGC and adenoma in superficial elevated lesions of the stomach, although this was at the expense of a lower specificity compared to WLE (88% versus 94%).

In addition, magnifying NBI has also been demonstrated to be effective in determining the horizontal extent of EGC. In a study of 350 consecutive cases of EGC resected en bloc using ESD by Nagahama et al. [22], 66 cases (18.9%) could not be delineated successfully using WLE. Sixty-two of these 66 cases went on to be examined using magnifying NBI, of which 45 (72.6%) were then successfully delineated. This is an important use of magnifying NBI in order to achieve R0 resection for EGC with ESD.

13.8 Colon

A pilot study comparing NBI with WLE and chromoendoscopy conducted by Machida et al. [23] showed that NBI was better in the visualization of the vascular network of colorectal mucosal lesions, although there was no significant difference compared to chromoendoscopy in differentiating neoplastic and non-neoplastic lesions. However, a meta-analysis of earlier studies comparing the adenoma detection rate with

first-generation NBI versus WLE did not show a benefit with the use of NBI, although substantial clinical and statistical heterogeneity between the included studies may have compromised the accuracy of the pooled estimates [24].

In a later study by Leung et al. [25], the newer generation NBI system with twice the brightness of the first-generation NBI system was studied in comparison to HD-WLE. This randomized controlled trial with tandem colonoscopy demonstrated that NBI significantly increased the adenoma and polyp detection rates compared to HD-WLE (48.3% versus 34.4%, $p = 0.01$, respectively, for adenomas; 61.1% versus 48.3%, $p = 0.02$ for polyps), regardless of the experience of the endoscopist in this study. Moreover, NBI was also shown in systematic review by van den Broek et al. [26] to have similar overall accuracy in differentiating neoplastic and non-neoplastic polyps compared to dye-based chromoendoscopy. Several other studies also demonstrated similar findings, with magnifying NBI having better diagnostic accuracy in differentiating neoplastic from non-neoplastic lesions compared to WLE, but being equivalent to that using dye-based chromoendoscopy [3, 27, 28].

Perhaps the most commonly used NBI classification system for colorectal polyps is that of the NBI International Colorectal Endoscopic (NICE) classification system, which was developed by consensus based on the surface pattern, color, and appearance of vessels. This classification system was validated using still images read by NBI-trained Gastroenterology Fellows in a study by Hewett et al. [29]. In this same study, the NICE classification system was also evaluated during real-time colonoscopy, where endoscopists made diagnoses with high confidence for 75% of consecutive small colorectal polyps. In this real-time evaluation, the reported sensitivity and accuracy were 98 and 89%, respectively. In addition to being simplified, the NICE classification system also offers the advantage of not requiring optical magnification, allowing it to be used in centers where this technology is not available.

A well-known example of an NBI classification system for colorectal polyps utilizing magnification endoscopy is the Sano classification [30]. In this classification, NBI in combination with magnification is used to scrutinize the mucosal surface for meshed capillary vessels, irregularity, lack of uniformity, high density of capillary vessels, branching and blind-ending vessels, as well as other features to point out neoplastic lesions and the degree of dysplasia.

Recently, the Japanese NBI Expert Team (JNET) classification was developed [31]. This new classification system incorporates the use of magnification to subdivide NICE type 2 (adenomatous polyps) into NICE type 2A, representing low-grade intraepithelial neoplasia (LGIN), and NICE 2B, representing HGIN and shallow submucosal invasive cancer. The JNET classification system is the first universal magnifying NBI classification system for colorectal polyps, combining the expertise and experience of previous magnifying NBI classifications with their multiple terms and differences in characterization of lesions to predict the histopathology of colorectal polyps.

13.9 Conclusions

IEE with NBI compliments high-quality WLE in the detection and characterization of lesions in the GI tract. This early detection of neoplastic lesions allows for endoscopic therapy such as resection and ablation to be used effectively, avoiding the morbidity associated with surgery. Magnification is a very useful adjunct to NBI, and has been incorporated into many classification systems. Newer classification systems continue to be developed which further refine the endoscopist's ability to predict tumor grade and depth of invasion. Although more validation studies are required for these new classification systems outside their countries of origin, where expertise may differ vastly from the rest of the world, they highlight the ongoing thrust in this exciting field of IEE toward excellence in imaging techniques.

References

1. Gono K, Obi T, Yamaguchi M, et al. Appearance of enhanced tissue features in narrow-band endoscopic imaging. J Biomed Opt. 2004;9:568–77.
2. Gono K. Narrow band imaging: technology basis and research and development history. Clin Endosc. 2015;48:476–80.
3. Chiu HM, Chang CY, Chen CC, et al. A prospective comparative study of narrow-band imaging, chromoendoscopy, and conventional colonoscopy in the diagnosis of colorectal neoplasia. Gut. 2007;56:373–9.
4. Ikematsu H, Matsuda T, Osera S, et al. Usefulness of narrow-band imaging with dual-focus magnification for differential diagnosis of small colorectal polyps. Surg Endosc. 2015;29:844–50.
5. Inoue H, Kaga M, Ikeda H, et al. Magnification endoscopy in esophageal squamous cell carcinoma: a review of the intrapapillary capillary loop classification. Ann Gastroenterol. 2015;28:41–8.
6. Sato H, Inoue H, Ikeda H, et al. Utility of intrapapillary capillary loops seen on magnifying narrow-band imaging in estimating invasive depth of esophageal squamous cell carcinoma. Endoscopy. 2015;47:122–8.
7. Muto M, Minashi K, Yano T, et al. Early detection of superficial squamous cell carcinoma in the head and neck region and esophagus by narrow band imaging: a multicenter randomized controlled trial. J Clin Oncol. 2010;28:1566–72.
8. Takenaka R, Kawahara Y, Okada H, et al. Narrow-band imaging provides reliable screening for esophageal malignancy in patients with head and neck cancers. Am J Gastroenterol. 2009;104:2942–8.
9. Singh R, Anagnostopoulos GK, Yao K, et al. Narrow-band imaging with magnification in Barrett's esophagus: validation of a simplified grading system of mucosal morphology patterns against histology. Endoscopy. 2008;40:457–63.
10. Sharma P, Bansal A, Mathur S, et al. The utility of a novel narrow band imaging endoscopy system in patients with Barrett's esophagus. Gastrointest Endosc. 2006;64:167–75.
11. Kara MA, Ennahachi M, Fockens P, et al. Detection and classification of the mucosal and vascular patterns (mucosal morphology) in Barrett's esophagus by using narrow band imaging. Gastrointest Endosc. 2006;64:155–66.
12. Sharma P, Bergman JJ, Goda K, et al. Development and validation of a classification system to identify high-grade dysplasia and esophageal adenocarcinoma in Barrett's esophagus using narrow-band imaging. Gastroenterology. 2016;150:591–8.
13. Correa P. Human gastric carcinogenesis: a multistep and multifactorial process—First American Cancer Society Award Lecture on cancer epidemiology and prevention. Cancer Res. 1992;52:6735–40.
14. Uedo N, Ishihara R, Iishi H, et al. A new method of diagnosing gastric intestinal metaplasia: narrow-band imaging with magnifying endoscopy. Endoscopy. 2006;38:819–24.
15. Ang TL, Pittayanon R, Lau JY, et al. A multicenter randomized comparison between high-definition white light endoscopy and narrow band imaging for detection of gastric lesions. Eur J Gastroenterol Hepatol. 2015;27:1473–8.
16. Yao K, Anagnostopoulos GK, Ragunath K. Magnifying endoscopy for diagnosing and delineating early gastric cancer. Endoscopy. 2009;41:462–7.
17. Yamada S, Doyama H, Yao K, et al. An efficient diagnostic strategy for small, depressed early gastric cancer with magnifying narrow-band imaging: a post-hoc analysis of a prospective randomized controlled trial. Gastrointest Endosc. 2014;79:55–63.
18. Yao K, Doyama H, Gotoda T, et al. Diagnostic performance and limitations of magnifying narrow-band imaging in screening endoscopy of early gastric cancer: a prospective multicenter feasibility study. Gastric Cancer. 2014;17:669–79.
19. Ezoe Y, Muto M, Uedo N, et al. Magnifying narrowband imaging is more accurate than conventional white-light imaging in diagnosis of gastric mucosal cancer. Gastroenterology. 2011;141:2017–25.
20. Li HY, Dai J, Xue HB, et al. Application of magnifying endoscopy with narrow-band imaging in diagnosing gastric lesions: a prospective study. Gastrointest Endosc. 2012;76:1124–32.
21. Maki S, Yao K, Nagahama T, et al. Magnifying endoscopy with narrow-band imaging is useful in the differential diagnosis between low-grade adenoma and early cancer of superficial elevated gastric lesions. Gastric Cancer. 2013;16:140–6.
22. Nagahama T, Yao K, Maki S, et al. Usefulness of magnifying endoscopy with narrow-band imaging for determining the horizontal extent of early gastric cancer when there is an unclear margin by chromoendoscopy (with video). Gastrointest Endosc. 2011;74:1259–67.
23. Machida H, Sano Y, Hamamoto Y, et al. Narrow-band imaging in the diagnosis of colorectal mucosal lesions: a pilot study. Endoscopy. 2004;36:1094–8.
24. Dinesen L, Chua TJ, Kaffes AJ. Meta-analysis of narrow-band imaging versus conventional colonoscopy for adenoma detection. Gastrointest Endosc. 2012;75:604–11.
25. Leung WK, Lo OS, Liu KS, et al. Detection of colorectal adenoma by narrow band imaging (HQ190) vs. high-definition white light colonoscopy: a randomized controlled trial. Am J Gastroenterol. 2014;109:855–63.
26. van den Broek FJ, Reitsma JB, Curvers WL, et al. Systematic review of narrow-band imaging for the detection and differentiation of neoplastic and nonneoplastic lesions in the colon (with videos). Gastrointest Endosc. 2009;69:124–35.
27. Su MY, Hsu CM, Ho YP, et al. Comparative study of conventional colonoscopy chromoendoscopy, and narrow-band imaging systems in differential diagnosis

of neoplastic and nonneoplastic colonic polyps. Am J Gastroenterol. 2006;101:2711–6.
28. Tischendorf JJ, Wasmuth HE, Koch A, et al. Value of magnifying chromoendoscopy and narrow band imaging (NBI) in classifying colorectal polyps: a prospective controlled study. Endoscopy. 2007;39:1092–6.
29. Hewett DG, Kaltenbach T, Sano Y, et al. Validation of a simple classification system for endoscopic diagnosis of small colorectal polyps using narrow-band imaging. Gastroenterology. 2012;143:599–607.
30. Sano Y, Ikematsu H, Fu KI, et al. Meshed capillary vessels by use of narrow-band imaging for differential diagnosis of small colorectal polyps. Gastrointest Endosc. 2009;69:278–83.
31. Sano Y, Tanaka S, Kudo SE, et al. Narrow-band imaging (NBI) magnifying endoscopic classification of colorectal tumors proposed by the Japan NBI Expert Team. Dig Endosc. 2016;28:526–33.

14 Endocytoscopy for Diagnosis of Early Gastrointestinal Neoplasia

Philip W. Y. Chiu, Hitomi Minami, and Haruhiro Inoue

14.1 Introduction

The diagnosis of the gastrointestinal diseases is usually based on histopathology. The examination of the cytoplasmic morphological changes, irregular enlargement of the nucleus are key features to define neoplastic process [1]. The prerequisite to this diagnostic process is adequate tissue acquisition from the gastrointestinal pathology, followed by histological examination by pathologist. It will be an ideal situation when in vivo imaging can be achieved to cellular levels during diagnostic endoscopy. In vivo cellular imaging will serve as optical real-time biopsy, hence the endoscopist do not need to remove any tissue from the lesion during endoscopy and minimize trauma to the disease. This could have significant advantage especially when endoscopic resection is contemplated so that submucosal fibrosis could be minimized to reduce adhesions.

P. W. Y. Chiu (✉)
Department of Surgery, Faculty of Medicine, The Chinese University of Hong Kong, Hong Kong, Hong Kong
e-mail: philipchiu@surgery.cuhk.edu.hk

H. Minami
Department of Gastroenterology and Hepatology, Nagasaki University Hospital, Nagasaki, Japan

H. Inoue
Digestive Disease Center, Showa University Kita Toyosu Hospital, Tokyo, Japan

Currently, different technologies have been developed to achieve endomicroscopy [2]. These included endocytoscopy and confocal endomicroscopy. The current chapter will focus on review of the technology for endocytoscopy and the current clinical applications and evidence for its efficacy in achieving optical biopsy.

14.2 Endocytoscopy: Technological Development

The proposal of an ultra-high magnifying contact endoscope was reported in 1982 [3]. The magnification power was 500 times at that time. The first reported observation of cellular changes during endoscopy was in 1995 using a rigid-type contact endoscope at vocal cord [4]. Kumagai et al. reported the use of contact endoscope for ex vivo observation of squamous esophageal carcinoma [5]. These reports confirmed the feasibility of observation of cellular neoplastic changes through the concept of endomicroscopy.

Endocytoscopy system was first developed by Olympus Co Ltd. as a contact catheter type that could pass through the working channel of ordinary endoscopy [2]. The two initial prototypes had magnification power of 450 times and 1100 times, respectively, on 14-inch monitor [2, 5]. The outer diameter was 3.4 mm with a length of 250 cm. The catheter type endocytoscope was designed to observe cellular changes by direct contact after

P. W. Y. Chiu et al. (eds.), *Endoscopy in Early Gastrointestinal Cancers, Volume 1*,
https://doi.org/10.1007/978-981-10-6769-3_14

appropriate staining through the working channel of double channel endoscope, with a distal cap attachment to stabilize the endoscope (Fig. 14.1). Both prototypes could allow endoscopists to distinguish between nucleus and cytoplasm after dye staining with methylene blue [6]. However, red blood cells movement within the capillary flow could be observed under 1100 times magnification [2].

In the second phase of development, the endocytoscopy system was integrated into the ordinary diagnostic endoscope [5]. The upper (103 cm) and lower (133 cm) GI endoscopes could achieve a magnification of 580 times in 19-inch monitor, in addition to the optimal magnification and narrow-band imaging capabilities. This integration aimed to enhance the clinical application of endocytoscopy system during diagnostic endoscopy for characterization of disease pathology within the gastrointestinal tract (Fig. 14.2).

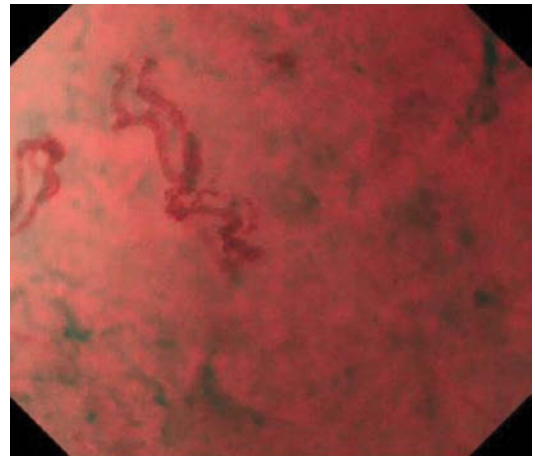

Fig. 14.2 The latest model of endocytoscopy which is incorporated into an ordinary upper gastrointestinal endoscope. The intracapillary papillary loops (IPCL) can be observed during endocytoscopy with narrow-band imaging (NBI)

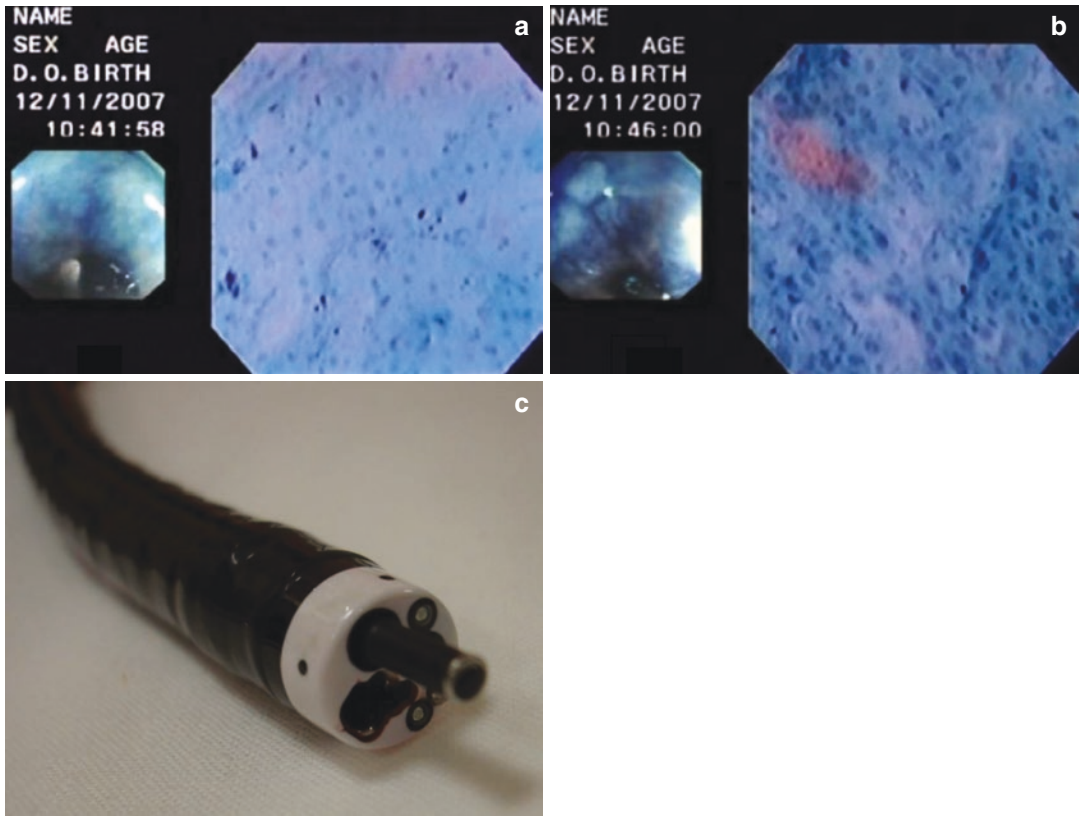

Fig. 14.1 First prototype of Endocytoscopy—comparing normal squamous esophageal mucosa (**a**) to cancerous lesion (**b**); the prototype endocytoscope as a probe based catheter passing through working channel of double channel endoscope (**c**)

14.3 Endocytoscopy: Clinical Application in Upper GI Tract

Kumagai et al. reported in vivo application of rigid contact endocytoscope for examination of superficial esophageal cancers in 12 patients [7]. After dye staining with methylene blue, excellent images were observed to enable differentiation between normal and cancerous lesions through differences in density, heterogenicity as well as variation in nuclei of cells, similar to observation of reverse N/C ratio in cytology. Inoue et al. reported the application of endocytoscopy for examination of gastrointestinal neoplasia in 87 patients, 38 cases in esophagus, 18 cases in stomach and 35 cases in colon [2]. High quality images were obtained in 83 cases (95.4%), while for 4 cases of gastric neoplasia the images were suboptimal due to inadequate staining caused by significant mucous secretion. A classification system based on endocytoscopic findings (Endocytoscopic atypia (ECA)) was applied to differentiate esophageal lesions into five types according to size and uniformity of nuclei, number of cells, and regularity of cellular arrangement (Fig. 14.3). ECA I represents normal; ECA II represents non-neoplastic reactive; ECA III represents borderline; ECA IV strongly suggestive of cancer; and ECA V represents cancer [6]. Minami et al. reported the performance of endocytoscopy for 110 patients from 2003 to 2009. One hundred and forty-six esophageal lesions were classified according to ECA classification. Eighty-one out of 89 ECA-1 to ECA-3 lesions (91.0%) corresponded to Vienna categories 1–3. Seventy-one out of 84 ECA-4 or ECA-5 lesions (91.2%) corresponded to Vienna category 4 or 5 with an accuracy of 91.3% [8, 9].

Endocytoscopy was also applied to diagnose pathology in stomach. Kimura et al. reported the observation of *H. pylori* cultured ex vivo using endocytoscope in stomach [10]. Our group demonstrated the diagnosis of gastric intestinal metaplasia basing on observation of presence of goblet cells upon endocytoscopy achieved a diagnostic accuracy of 86% in 102 suspicious gastric lesions [11] (Fig. 14.4). Kaise et al. applied endocytoscopy for differentiation of benign, gastric adenoma and early gastric cancer in 82 lesions using irregularities within glandular structure and cell nuclei [12]. The sensitivity and specificity using the high-grade ECS atypia as the criterion for diagnosis of gastric cancer were 86 and 100% respectively, and the authors concluded that endocytoscopy is feasible with high accuracy in diagnosis of early gastric cancer in vivo. Sato et al. reported the application of features upon endocytoscopy for differentiation of normal gastric mucosa at body and antrum through observation of pit-dominant type and papilla-dominant type mucosa [13]. These features were indeed similar to those reported upon magnifying

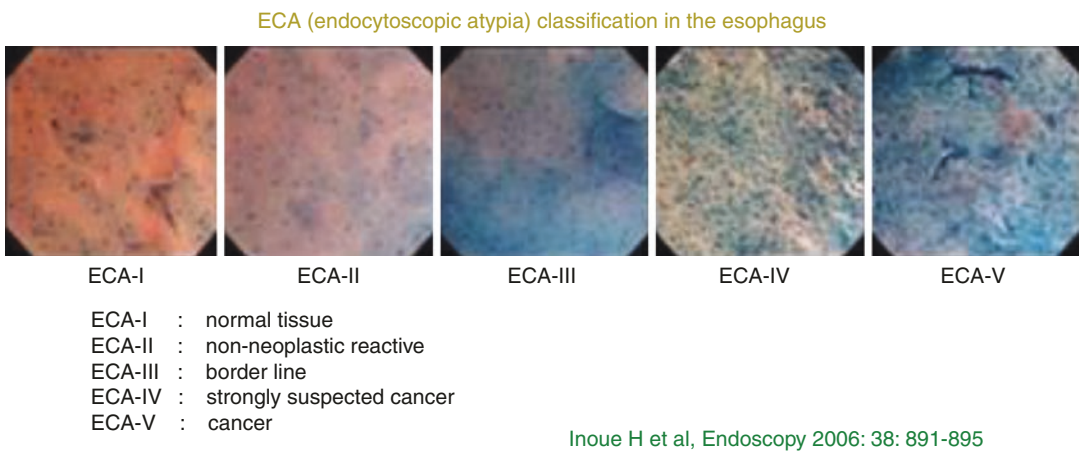

Fig. 14.3 Classification of endocytoscopic findings for squamous esophageal neoplasia

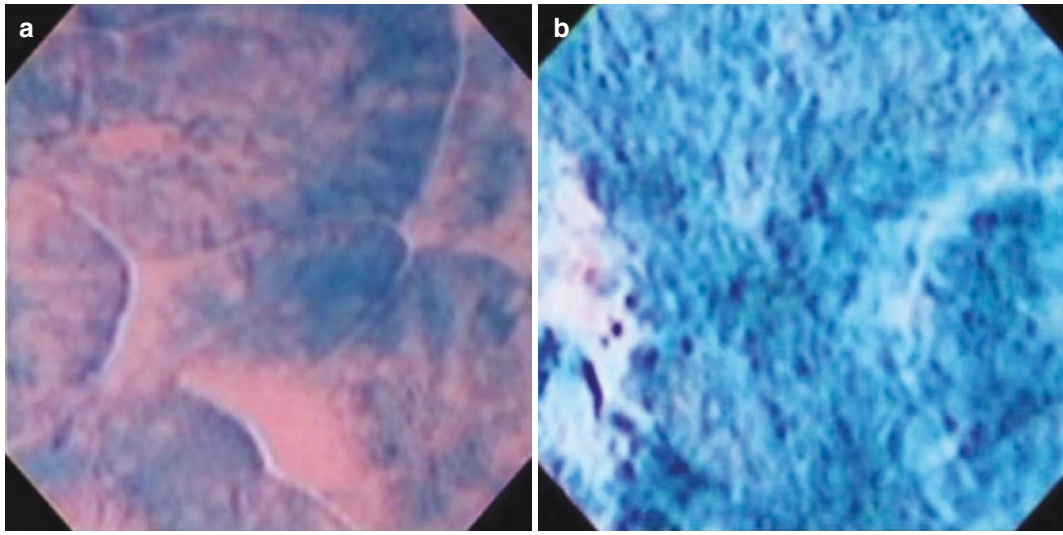

Fig. 14.4 Endocytoscopy for diagnosis of (**a**) gastric intestinal metaplasia with presence of goblet cells and (**b**) early gastric cancer with irregular morphology of the cells and reversed nuclear–cytoplasmic ratio

endoscopy by Yao et al. to differentiate normal gastric body and antrum [14]. In gastric body, mucosa demonstrated regular honeycomb arrangement of subepithelial capillary network (SECN) surrounding each pit. In gastric antrum, since the opening of the glandular pits are arranged in oblique manner, the SECN will appear as coil-shaped. The same features were observed with endocytoscopy attributing to a sensitivity and specificity of 94.4 and 97.1% for gastric corpus, and sensitivity and specificity of 92.0 and 86.7% for gastric antrum, respectively [13]. Tsurudome et al. performed endocytoscopy in 30 patients with early gastric cancer and found that using double staining method of 0.05% crystal violet and 0.1% methylene blue, early gastric cancer demonstrated irregular glandular structures with deeply stained nuclei as well as increased nuclear density and atypia [15].

14.4 Endocytoscopy: Clinical Application in Lower GI Tract

The group from Digestive Disease Center, Showa University Northern Yokohama Hospital first reported the clinical application of endocytoscopy for differentiation of colorectal neoplasia and developed the EC classification [16, 17] (Fig. 14.5). EC 1 are typically benign lesions or hyperplastic lesions, EC2 represents dysplasia while EC3 are further differentiated into EC3a of intramucosal carcinoma and EC3b of submucosal carcinoma. The lesion was usually stained with 1% methylene blue, and the excessive stain would be washed off. The factors for consideration to differentiate neoplasia and non-neoplastic polyps included: (1) Pattern of cellular arrangements; (2) Size, shape, and arrangements of glands; (3) Size and shapes of cells; (4) Size and shape of nuclei; and (5) Nuclear–cytoplasmic ratio. Mori et al. conducted a prospective randomized noninferiority trial comparing endocytoscopy to standard biopsy for diagnosis of colorectal neoplasia [18]. Two hundred and three lesions from 170 patients were randomly assigned to either endocytoscopy group where lesions were interpreted by endocytoscopy, or standard biopsy interpreted by pathologist. The diagnostic accuracy of endocytoscopy to discriminate neoplastic lesions was 94.1% compared to 96.0% for standard biopsy, demonstrating similar accuracy and hence allowing on-site diagnosis possible [18]. One of the important features to recognize the diagnosis of sessile serrated adenoma/polyps (SSAP) is the recognition of dilated crypt

Classification		Endocytoscopic images	Endocytoscopic findings	Histopathology
EC1	a	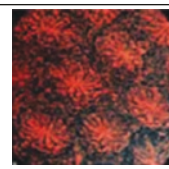	Roundish lumens Fusiform nuclei	Normal mucosa
	b		Narrow serrated lumens Small roundish nuclei	Hyperplastic polyp
EC2			Slit-like smooth lumens Uniform fusiform or roundish nuclei	Dysplasia
EC3	a	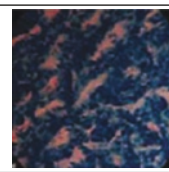	Irregular and rought lumens A large number of roundish nuclei	High grade dysplasias or SMs cancer
	b	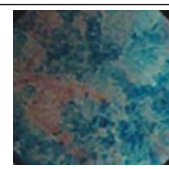	Unclear gland formation Agglomeration of distorted nuclei	SMm cancer or worse

Fig. 14.5 Classification of endocytoscopic findings for colorectal neoplasia

opening. Ogawa et al. applied the observation of a dilated crypt opening under endocytoscopy in 101 lesions to differentiate SSAP from hyperplastic polyps (HP) [19]. The results showed that SSAP had significantly larger luminal area compared to HP, and the use of luminal area to differentiate SSAP showed an accuracy of 78.0% and area under ROC curve of 0.865.

14.5 Endocytoscopy: Future Development

The real-time diagnosis upon recognition of cellular morphological changes, enlargement and irregularities in nuclei as well as reversed N:C ratio required learning and experience of endoscopists. Recently, the development of computer-aided diagnosis (CAD) system recognize endocytoscopic changes to differentiate neoplastic from non-neoplastic lesions [20, 21]. A customized software named EndoBRAIN (Cybernet System Co Ltd., Tokyo, Japan) was developed to analyze images from endocytoscopy. Computer-aided diagnosis (CAD) has potential advantages of improving the accuracy in real-time histological diagnosis, as well as reducing interobserver variation. Mori et al. applied the EndoBRAIN to automatically classify colorectal polyps according to the nuclear characteristics, and compared to the diagnosis by endoscopists from three international institutes [21]. The algorithm for computer-aided diagnosis for endocytoscopy (EC-CAD) is composed of four steps: extraction of nuclei, texture analysis, classifier, and diagnostic output. EC-CAD achieved an accurate for 89% for dimin-

utive polyps and 89% for small polyps, which were significantly higher than those achieved by nonexperts (73%, $P < 0.001$; and 76%, $P < 0.001$, respectively) and comparable with the experts' results (90%, $P = 0.703$, and 91%. $P = 0.106$, respectively). In the future, with the assistance from CAD, endoscopists will be more confident in diagnosis of both diminutive and small colorectal polyps and adopt the strategy of resect and discard, hence renders screening and surveillance endoscopy more cost-effective.

14.6 Summary

Over the past decade, the technology of endocytoscopy has been revolutionized with a better integration and availability for clinical usage. The clinical observation of cellular and morphological changes under endocytoscopy had been investigated with various classifications developed for the diagnosis of superficial esophageal neoplasia and early colorectal neoplasia. The observation of changes in gastric cellular morphology is limited by the difficulties in achieving good staining. Further research will be focus on clinical applications of endocytoscopy to differentiate neoplasia especially in a wide field of premalignant changes so that better target biopsy can be achieved. The clinical application of endocytoscopy will be enhanced by the development of computer-aided diagnosis system.

References

1. Scoazec JY. Tissue and cell imaging in situ: potential for applications in pathology and endoscopy. Gut. 2003;52(Suppl IV):iv1–6.
2. Inoue H, Kazawa T, Sato Y, Satodate H, Sasajima K, Kudo SE, Shiokawa A. In vivo observation of living cancer cells in the esophagus, stomach and colon using catheter type contact endoscope, "Endocytoscopy system". Gastrointest Clin N Am. 2004;14:589–94.
3. Tada M, Watanabe S, Uozumi Y, et al. A new method for the ultramagnifying observation of the colon mucosa. Kyoto Pref Univ Med. 1982;91:349–54.
4. Andrea M, Dias O, Santos A. Contact endoscopy of the vocal cord: normal and pathological patterns. Acta Otolaryngol. 1995;115:314–6.
5. ASGE Technology Committee, Kwon RS, Wong Kee Song LM, Adler DG, Conway JD, Diehl DL, Farraye FA, Kantsevoy SV, Kaul V, Kethu SR, Mamula P, Pedrosa MC, Rodriguez SA, Tierney WM. Endocytoscopy. Gastrointest Endosc. 2009 Oct;70(4):610–3.
6. Inoue H, Sasajima K, Kaga M, Sugaya S, Sato Y, Wada Y, Inui M, Satodate H, Kudo SE, Kimura S, Hamatani S, Shiokawa A. Endoscopic in vivo evaluation of tissue atypia in the esophagus using a newly designed integrated endocytoscope: a pilot trial. Endoscopy. 2006;38(9):891–5.
7. Kumagai Y, Monma K, Kawada K. Magnifying chromoendoscopy of the esophagus: in-vivo pathological diagnosis using an endocytoscopy system. Endoscopy. 2004;36:590–4.
8. Minami H, Inoue H, Yokoyama A, Ikeda H, Satodate H, Hamatani S, Haji A, Kudo S. Recent advancement of observing living cells in the esophagus using CM double staining: endocytoscopic atypia classification. Dis Esophagus. 2012;25(3):235–41.
9. Inoue H, Kudo SE, Shiokawa A. Novel endoscopic imaging techniques toward in vivo observation of living cancer cells in the gastrointestinal tract. Clin Gastroenterol Hepatol. 2005;3(7 Suppl 1):S61–3. Review.
10. Kimura S, Inoue H, Sato Y, Aoyama Y, Shimojima M, Masuyama T, Kudo SE. Ex vivo visualization of Helicobacter pylori using an endocytoscopic probe. Biomed Res. 2006;27(5):255–7.
11. Chiu PW, Ng EK, To KF, Teoh AY, Lam CC, Chan FK, Sung JJ, Lau JY. Recognition of goblet cells upon endocytoscopy indicates the presence of gastric intestinal metaplasia. Dig Endosc. 2014;26(1):52–6.
12. Kaise M, Ohkura Y, Iizuka T, Kimura R, Nomura K, Kuribayashi Y, Yamada A, Yamashita S, Furuhata T, Kikuchi D, Ogawa O, Matsui A, Mitani T, Hoteya S. Endocytoscopy is a promising modality with high diagnostic accuracy for gastric cancer. Endoscopy. 2015;47(1):19–25.
13. Sato H, Inoue H, Hayee B, Ikeda H, Sato C, Phalanusitthepha C, Santi EG, Kobayashi Y, Kudo SE. In vivo histopathology using endocytoscopy for non-neoplastic changes in the gastric mucosa: a prospective pilot study (with video). Gastrointest Endosc. 2015;81(4):875–81.
14. Yao K, Iwashita A, Kikuchi Y, Yao T, Matsui T, Tanabe H, Nagahama T, Sou S. Novel zoom endoscopy technique for visualizing the microvascular architecture in gastric mucosa. Clin Gastroenterol Hepatol. 2005;3(7 Suppl 1):S23–6.
15. Tsurudome I, Miyahara R, Funasaka K, Furukawa K, Matsushita M, Yamamura T, Ishikawa T, Ohno E, Nakamura M, Kawashima H, Watanabe O, Nakaguro M, Satou A, Hirooka Y, Goto H. In vivo histological diagnosis for gastric cancer using endocytoscopy. World J Gastroenterol. 2017;23(37):6894–901.
16. Kudo SE, Wakamura K, Ikehara N, Mori Y, Inoue H, Hamatani S. Diagnosis of colorectal lesions with

a novel endocytoscopic classification—a pilot study. Endoscopy. 2011;43(10):869–75.
17. Sasajima K, Kudo SE, Inoue H, Takeuchi T, Kashida H, Hidaka E, Kawachi H, Sakashita M, Tanaka J, Shiokawa A. Real-time in vivo virtual histology of colorectal lesions when using the endocytoscopy system. Gastrointest Endosc. 2006;63(7):1010–7.
18. Mori Y, Kudo S, Ikehara N, Wakamura K, Wada Y, Kutsukawa M, Misawa M, Kudo T, Kobayashi Y, Miyachi H, Yamamura F, Ohtsuka K, Inoue H, Hamatani S. Comprehensive diagnostic ability of endocytoscopy compared with biopsy for colorectal neoplasms: a prospective randomized noninferiority trial. Endoscopy. 2013;45(2):98–105.
19. Ogawa Y, Kudo SE, Mori Y, Ikehara N, Maeda Y, Wakamura K, Misawa M, Kudo T, Hayashi T, Miyachi H, Katagiri A, Ishida F, Inoue H. Use of endocytoscopy for identification of sessile serrated adenoma/polyps and hyperplastic polyps by quantitative image analysis of the luminal areas. Endosc Int Open. 2017;5(8):E769–74.
20. Misawa M, Kudo SE, Mori Y, Nakamura H, Kataoka S, Maeda Y, Kudo T, Hayashi T, Wakamura K, Miyachi H, Katagiri A, Baba T, Ishida F, Inoue H, Nimura Y, Mori K. Characterization of colorectal lesions using a computer-aided diagnostic system for narrow-band imaging endocytoscopy. Gastroenterology. 2016;150(7):1531–1532.e3.
21. Mori Y, Kudo SE, Chiu PW, Singh R, Misawa M, Wakamura K, Kudo T, Hayashi T, Katagiri A, Miyachi H, Ishida F, Maeda Y, Inoue H, Nimura Y, Oda M, Mori K. Impact of an automated system for endocytoscopic diagnosis of small colorectal lesions: an international web-based study. Endoscopy. 2016;48(12):1110–8.

15 Endoscopic Technologies for Diagnosing and Staging Early GI Cancers: Endoscopic Ultrasonography in GI Diseases

Calvin Jianyi Koh and Khek Yu Ho

15.1 Introduction

Endoscopic ultrasound (EUS) has evolved to be a key tool in the management of gastrointestinal conditions, and is particularly useful in the management of gastrointestinal malignancy, where the stage depends on the depth of invasion, as well as malignant involvement of locoregional lymph nodes, which besides visualization, can be sampled by concurrent fine-needle aspiration or biopsy.

The aim of this section would be to outline the role of EUS in various GI malignancies by anatomic region, and highlight key points that EUS can deliver over other imaging modalities. Like many diagnostic modalities in cancer, EUS is not used in lieu of cross-sectional imaging, but in many cases, can deliver high-resolution locoregional information that complements existing imaging modalities to provide additional information which leads to accurate prognostication for management.

15.2 Endoscopic Ultrasonography Technology and Equipment

In general, echoendoscopes fall into three broad categories [1], radial and linear probes which are incorporated into the endoscope platforms, as well as a third category of specialty probes or "miniprobes" which are modified radial probes that are designed to fit through the channel of a regular endoscope, such as a gastroscope or duodenoscope, and provide high-resolution images at a shallow depth. These also offer additional advantage of being smaller and able to get into tight spaces such as circumferential esophageal tumors for accurate staging.

15.2.1 Radial EUS Scopes

Radial EUS scopes are often used in staging of GI cancers as they offer a 360-degree view perpendicular to the scope that makes it easier to identify the margins as well as the depth of the lesion in relation to surrounding structures. They also have the advantage of being able to "scan" the region quickly for local lymphadenopathy, which sometimes can be harder to appreciate using a linear EUS scope.

C. J. Koh · K. Y. Ho (✉)
Department of Medicine, National University Hospital, Singapore, Singapore
e-mail: khek_yu_ho@nuhs.edu.sg; mdchoky@nus.edu.sg

P. W. Y. Chiu et al. (eds.), *Endoscopy in Early Gastrointestinal Cancers, Volume 1*,
https://doi.org/10.1007/978-981-10-6769-3_15

15.2.2 Linear EUS Scopes

Linear EUS scopes are helpful in situations where both imaging and tissue acquisition are required. The accessory channel in these platforms allow the passage of fine-needle aspiration and biopsy needles for sampling of endosonographically visualized structures not usually accessible in diagnostic endoscopy such as locoregional lymph nodes, as well as solid organ tissue sampling such as pancreas or adrenal gland for primary or secondary tumor involvement.

15.2.3 Specialty Probes

Catheter-based probes typically require a separate unit for image processing and mechanical actuation, but offer the advantage of being able to piggyback on an existing endoscope platform, or even if the situation allows, during the same procedure.

These probes are usually high frequency, typically 20 MHz and above resulting in a very shallow depth of penetration. Consequently, although they are not very good for large tumors where the ultrasound is attenuated rapidly the base, they are excellent for inspecting small mucosal and subepithelial lesions and for intraductal use.

They can also potentially be passed through narrowed malignant strictures such as in esophageal malignancy, although often in such cases, attenuation of ultrasound makes it difficult to visualize the depth of invasion. Such lesions are often advanced and staging information can usually be easily obtained through standard cross-sectional imaging.

A recognized limitation of endoscopic ultrasound for staging particularly in a more confined luminal space such as the esophagus, is that if the malignant stricture is tight enough, the EUS scope is often not able to be pass and oppose the mucosa adequately for accurate image acquisition. Bang JY and colleagues have in a multicenter study evaluated this concern and found that all cases where a standard gastroscope was unable to traverse a stricture were found to be 100% predictive of locally advanced disease (T3 or T4), where EUS is unlikely to make an impact on the clinical management [2].

15.3 Endoscopic Ultrasound in Early Esophageal Neoplasia

Esophageal cancer is the sixth-leading cause of cancer-related mortality and the eight most common cancer worldwide [3]. This comprises two types of cancer that have different risk factors, incidence, and management—esophageal adenocarcinoma and esophageal squamous cell cancer.

Regardless of the subtype, early-stage esophageal cancer can be managed endoscopically [4] as summarized in Table 15.1, either via ablation

Table 15.1 Management of early esophageal cancer (National Comprehensive Cancer Network 2017 [4])

Stage	Description	Esophageal squamous cell carcinoma management	Esophageal adenocarcinoma management
Tis	High-grade dysplasia	Endoscopic ablation, endoscopic resection. Endoscopic resection followed by ablation, or esophagectomy	Endoscopic ablation, endoscopic resection. Endoscopic resection followed by ablation, or esophagectomy
T1a	Tumor invading lamina propria or muscularis mucosa	Endoscopic ablation, endoscopic resection. Endoscopic resection followed by ablation, or esophagectomy	Endoscopic resection. Endoscopic resection followed by ablation or esophagectomy
T1b	Tumor involving submucosa	Esophagectomy	Endoscopic resection or esophagectomy
T2	Tumor invading the submucosa	Neoadjuvant chemoradiation Definitive chemoradiation Or esophagectomy.	Esophagectomy

for very superficial lesions, or endoscopic resection, either using mucosectomy kits or endoscopic submucosal dissection (ESD).

It must be noted that the Japanese further subdivide T1b into SM1, SM2 or SM3, depending on whether the tumor has invaded the upper, middle, or lower third of the submucosal layer, respectively [5], and would generally consider ESD for lesions in the upper part of the submucosa (T1b-SM1), generally up to 200 μm deep. For deeper lesions T1b-SM2, more than half of these lesions are associated with metastasis and should be treated the same as more locally advanced lesions [6]. The principle being that the submucosal space has a rich network of lymphatics and that even with some invasion, the possibility of lymph node involvement increases dramatically.

With such narrow margins for staging, which determines the difference between endoluminal therapy and esophagectomy, endoscopic ultrasound plays a pivotal role in determining the stage, and hence the treatment selection of early esophageal cancer.

15.3.1 Initial Staging

Endoscopic ultrasound has in meta-analysis of 2558 patients shown to be able to distinguish T1 disease with 81.6% sensitivity and 99.4% specificity [7]. A validated algorithm has been developed which combines CT, PET scan as well as EUS to optimize the investigation yield. In this workflow, only patients with CT suggesting no more than locally advanced disease (T1), that the endoscope can pass through, should be evaluated with EUS for suitability for endoscopic therapy [8].

Several limitations of endoscopic ultrasound for staging of esophageal cancer exist. Some data from single-center studies [9, 10], suggest that in the subgroup of T1a and T1b patients were only accurately staged 39 and 51% of the time, respectively. In this study, part of the staging inaccuracy came from lymph node metastases and for anything but lymph nodes immediately adjacent to the GI tract, CT with PET would probably perform better than EUS for the determination of lymph node involvement. This is supported by data from Germany suggesting that in patients with early disease who underwent an upfront PET/CT evaluation, the addition of EUS had an impact on given treatment in 29% of the time [11].

15.3.2 Evaluating Response to Therapy

EUS is also useful to evaluate the response to neoadjuvant chemotherapy. In a meta-analysis of 16 studies encompassing 724 patients, concluded that EUS is relatively sensitive at 81% in T3 disease, while yielding specificity of 95%, 84%, and 96%, respectively, for T1, T2, and T4 disease. In this dataset, EUS did not perform well at N staging, reflecting again the need for multimodal imaging evaluation which is current standard of care.

15.3.3 Summary for EUS in Early Esophageal Neoplasia

In summary, although some studies have raised concerns about its accuracy in early disease, EUS still plays a key role in the staging of early esophageal cancer to determine suitability for endoscopic therapy, and remains the most sensitive test for locoregional evaluation of esophageal cancer. EUS-FNA of suspect lymph nodes further allow confirmation of regional lymph node involvement, although as a scanning tool for regional lymph node staging, EUS expectedly does not perform as well as high-resolution cross-sectional imaging.

15.4 Endoscopic Ultrasound in Early Gastric Neoplasia

15.4.1 Gastric Cancer Incidence and Epidemiology

Nearly a million cases of gastric cancer occur annually, making it the fifth most common malignancy worldwide, and the third leading

cause of cancer death with more than 700,000 deaths annually [12], the majority of cases from Asia, due to overall advanced presentation and poor prognosis of advanced disease. Overall 5-year-survival remains a dismal 24% internationally, but this can rise to as high as 95% if picked up in stage I disease.

Besides addressing the modifiable risk factors, the strongest of which is the presence of Helicobacter pylori, for countries that have high incidence, screening for gastric cancer is an opportunity for secondary prevention. Currently Japan and Korea have well-established screening programs that have shown efficacy in reducing gastric cancer deaths [13, 14].

15.4.2 Early Gastric Neoplasia: The Role of EUS

The availability of screening has driven the development of endoscopic techniques to manage early gastric cancer as with early esophageal cancer discussed above. Endoscopic resection via endoscopic submucosal dissection is the recommended modality in management of early gastric cancer Tis (carcinoma-in-situ) or T1a (tumor invades the lamina propria or muscularis mucosa) [15] in the US National Comprehensive Cancer Network (NCCN).

The Japanese guidelines for ESD for early gastric cancer, in addition to the depth of the lesion (T1a), further take into account the size of the lesion, which by extended criteria should be less than or equal to 3 cm for differentiated tumors and 2 cm for undifferentiated tumors, and should not be ulcerated on the surface which implies deeper invasion.

Hence, given the need for accurate T staging to determine depth of tumor invasion, EUS is currently the only pre-therapeutic modality that assesses this. It provides initial clinical staging of locoregional gastric cancer.

EUS also has a role of assessing perigastric lymph nodes, which have echofeatures that suggest malignant involvement—being hypoechoic, homogenous, and rounded are suggestive of malignant or inflammatory lymph nodes. This can be confirmed with the use of fine-needle aspiration to obtain cytology. Other adjunctive roles EUS may play in gastric cancer would be to identify ascites, and sample the fluid to evaluate for peritoneal involvement which would indicate T4 disease, or sampling of distant lymph nodes, for example, mediastinal lymph nodes that would suggest metastatic disease.

In a large meta-analysis [16] pooling data from 2445 patients who underwent EUS for preoperative staging, considerable heterogeneity in the performance vof EUS for T staging was found, wit the accuracy ranging from 56.9 to 87.7% giving a pooled statistic of 75%. The diagnostic accuracy for N staging was correspondingly lower, with pooled statistic of 64%, ranging from 43 to 84% with considerable heterogeneity amongst studies. This suggests besides the known challenge that EUS is operator dependent, that the populations in which they were evaluated were diverse and that EUS had different performance among the stages, with observed best accuracy for T3 disease followed by T4, T1, and T2.

15.4.3 Factors Influencing EUS Performance

Multiple factors could account for variability in EUS accuracy. Clinicopathologic factors of the tumor such as location of the lesion [17–19], size [17, 19], morphology [18, 19], the presence of ulceration [19, 20], and the histology [17] all have been shown to influence the diagnostic performance of EUS. In terms of inter-operator variability, various factors have been evaluated such as training and volume. It has been also proposed that obtaining good quality images as a surrogate quality marker would help to control for some of these technical differences between endoscopists and improved diagnostic yield [21].

15.4.4 Role of EUS in Excluding Patients from Surgery

The European Society of Gastrointestinal Endoscopy (ESGE) offers another view in the

role of EUS in gastric cancer [22]. They suggest based on evidence from three studies [23–25] that EUS FNA should mainly be offered to avoid unnecessary surgery by proving advanced disease—for example by proving distant lymph nodes—retropancreatic, paraaortic, mesenteric, or mediastinal that would change the course from a curative resection to palliation. In the studies cited, about 15–19% of the patients who had EUS were found to have findings that proved advanced disease and changed their management.

15.4.5 Summary of EUS in Early Gastric Cancer

In summary, EUS, although with its limitations as cited above, is still the best imaging modality and standard of care in the evaluation of early gastric cancer, to evaluate the depth of invasion for consideration of ESD. Although still helpful in sampling lymph nodes, its role in N staging is less accurate when compared to multi-detector CT imaging, and in some situations, it can potentially spare patients needless surgery by proving advanced disease that might not be otherwise apparent.

15.5 Endoscopic Ultrasound in Early Pancreatobiliary Neoplasia

Apart from the ampulla, pancreatobiliary neoplasia has the unique characteristic of not being directly accessible with direct luminal endoscopy, and this is where EUS has the advantage of being able to visualize these lesions sonographically as well as being able to obtain tissue samples for cytopathologic examination with fine-needle aspiration or biopsy.

15.5.1 EUS in Pancreatic Cancer

Pancreatic cancer often presents late, being relatively asymptomatic until it is advanced, where standard treatments are generally ineffective. It affects more than 300,000 people annually [26], and due to dismal prognosis, mortality rate closely mirrors the incidence rate.

While the incidence is not high enough for population screening to be considered, there are studies evaluating the role of screening high-risk populations [27] for pancreatic cancer via MRI and EUS. These include individuals with familial pancreatic cancer, Peutz–Jeghers syndrome, hereditary pancreatitis (PRSS1 mutation), familial atypical multiple mole melanoma syndrome, and hereditary breast ovarian cancer syndrome.

Endoscopic ultrasound has been shown to be more sensitive that CT for detecting pancreatic cancer, particularly for smaller tumors [28] although the two modalities are often complimentary as CT is concurrently done to evaluate metastatic disease and nodal disease not always visualized on EUS. EUS also has the advantage of obtaining a tissue diagnosis with fine-needle aspiration and a meta-analysis by Puli et al. [29] showed that EUS FNA has a polled sensitivity of 86.8% and a specificity of 95.8%. When comparing time periods, there is also an increase in sensitivity over time, suggesting refinements on techniques and equipment.

Depending on the high-risk cohort composition, between 19 and 25% have abnormal EUS findings. The largest multicenter prospective study by Canto et al. [30] (the CAPS 3 study) CT, MRI, and EUS detected pancreatic abnormalities in 11%, 33.3%, and 42.6%, respectively. Eventually 3 out of the cohort of 216 had high-grade dysplasia proved on surgical resection, giving a pick up rate of 1.4%.

Eventually the hope is that systematic targeted screening of high-risk individuals would be able to identify and intervene in early pancreatic cancer.

15.5.2 EUS in Pancreatic Cystic Lesions

Pancreatic cystic lesions are often incidentally diagnosed due to the extensive use of cross-sectional imaging. But although incidental and mostly benign, they have been found in a case–

control study to be associated with an increase in mortality in patients younger than 65 years and an increased risk of pancreatic ductal adenocarcinoma [31].

These cystic lesions are mostly one of four conditions—pancreatic pseudocyst, serous cystadenomas, mucinous cystadenomas, and intraductal papillary mucinous neoplasm (IPMN), and as the latter two have malignant potential, differentiation between these conditions should be attempted as it would affect immediate management and long-term follow-up.

Sampling of the cyst fluid via EUS/FNA plays a key role in evaluation of the pancreatic cystic lesion as it allows access to the cyst fluid for amylase, carcinoembryonic antigen, cytology as well as KRAS mutation analysis. There is also recently available a through-the-needle microforceps which can take biopsies of the cyst wall or intramural nodule, hence allowing direct pathologic examination of the lesion.

15.5.3 EUS in Indeterminate Biliary Stricture

For biliary strictures where brushings have proven indeterminate, endoscopic ultrasound has been shown to be effective, in a meta-analysis by Sadeghi et al. [32] evaluating 20 studies enrolling a total of 957 patients, EUS-FNA had a pooled sensitivity of 80% and specificity of 96% for malignant biliary stricture. While EUS remains an option, newer modalities such as the cholangioscope-directed biopsies are also available and also provide 92–94% accuracy in differentiating benign from malignant strictures in two separate prospective multicenter studies [33, 34].

15.5.4 EUS in Ampullary Lesions

In the evaluation for ampullary cancer for example in surveillance for ampullary adenomas in familial adenomatous polyposis, white light and image-enhanced endoscopic examination with a duodenoscope, and taking targeted mucosal biopsies is still the standard of care. However for instances where the clinical suspicion is high, such as where there is obstructive jaundice and repeated ampullary biopsies are negative, EUS and FNA would be able to sample tissue not otherwise accessible via the standard duodenoscope.

15.6 Endoscopic Ultrasound in Early Rectal Neoplasia

Colorectal cancer, currently the second most common cancer in females and the third most common in males worldwide, is still on a rising trend and it is estimated to increase from an incidence of more than 1.3 million cases per year to 2.2 million cases per year in 2030 [35].

Of these, rectal cancers, defined as within 15 cm from the anal verge lend themselves to ready EUS evaluation due to the relatively straight passage of the rectum. Like other luminal malignances, the depth of invasion influences the management strategy and early rectal cancer (T1-invading submucosa/T2-invading muscularis propria) without nodal involvement can be managed with surgical resection alone without adjuvant chemoradiotherapy if the resection margins are clear [36].

Several meta-analyses comparing EUS, MRI, and CT for the preoperative staging of rectal cancer have been performed, of which one of the earlier pivotal work by Bipat published in 2004 [37] who evaluated 90 articles and showed that although both EUS and MRI were equally sensitive in picking up muscularis propria invasion (94%), EUS had a specificity of 86% versus MRI specificity of 69%. Imaging technologies have since evolved much since then, and a more recent study by Puli et al. in 2009 looking at aggregate data from 5039 patients over 41 studies determined the accuracy of EUS in staging T1 disease at a sensitivity of 87.9% with a specificity of 98.3%.

The inter-operator variability of EUS is further demonstrated by Marusch [38] who evaluated 7096 patients with rectal cancer who underwent EUS and surgery affording an opportunity to compare EUS stage with the pathologic stage of the resected specimen. It was observed

that centers that perform >30 cases per annum tended to have better sensitivity and specificity, suggesting that experience influences the accuracy of EUS.

Due to the possibility of regional lymph nodes beyond the range of the ultrasound probe, such as iliac, retroperitoneal, or mesenteric lymph nodes, cross-sectional imaging—a pelvic MRI is typically obtained for accurate staging. Hence it is unsurprising that EUS does not perform as well as MRI for the evaluation of N stage involvement [39].

A multimodal approach is often considered in many cases, with EUS being complementary rather than replacing MRI. Despite advances in MRI technology, the submucosal layer is not always visualized clearly [40], and hence in early cancers, EUS is still helpful to distinguish T1 from T2 cancers. EUS can also help sample lymph nodes in presumed early cancer (T1 or T2) which if proven positive would lead a change management from surgery alone to neoadjuvant chemoradiotherapy prior to surgical resection.

15.7 Conclusion

EUS allows precise visualization of the layers of the GI tract in higher resolution than any other standard modality and is extremely useful, if not indispensable, in the evaluation of the depth of invasion of early GI malignancies. Accurate staging of early GI malignancies impacts management as endoscopic resection options are available if the cancer has not spread to deeper layers, in particular the submucosa which has a rich lymphocapillary network and portends higher chance of regional lymph node involvement.

EUS also has an additional role in the screening and evaluation of locoregional lymphadenopathy, and can through fine-needle aspiration or biopsy prove nodal involvement and upstage the cancer—directly impacting therapeutic options.

Finally, for pancreatobiliary malignancies, EUS with needle aspiration provides a way to confirm the diagnosis and in some high-risk populations, potentially providing a screening modality that might pick up these cancers early.

References

1. Hawes RH, Fockens P, Varadarajulu S. Endosonography. Philadelphia: Elsevier Saunders; 2011.
2. Ji Young B, Jayapal R, Muhammad H, Udayakumar N, Bronte AH, Robert H, et al. Endoscopic ultrasonography is not required for staging malignant esophageal strictures that preclude the passage of a diagnostic gastroscope. Dig Endosc. 2016;28(6):650–6.
3. Elizabeth CS, Jesper L, Rebecca CF, Florian L, Manish AS, Pernilla L, et al. Oesophageal cancer. Nat Rev Dis Primers. 2017;3:17048.
4. National Comprehensive Cancer Network. 4.2017. Esophageal and Esophagogastric Junction Cancers 2017. Available from: https://www.nccn.org/professionals/physician_gls/pdf/esophageal.pdf.
5. Japan ES. Japanese classification of esophageal cancer, 11th edition: part I. Esophagus. 2016;14(1):1–36.
6. Hiroyuki K, Yasumasa N, Tsuneo O, Hiroyuki K, Yuko K, Motoyasu K, et al. Guidelines for diagnosis and treatment of carcinoma of the esophagus April 2012 edited by the Japan Esophageal Society. Esophagus. 2015;12(1):1–30.
7. Srinivas RP, Jyotsna BKR, Matthew LB, Daphne A, Jamal AI, Mainor RA. Staging accuracy of esophageal cancer by endoscopic ultrasound: a meta-analysis and systematic review. World J Gastroenterol. 2008;14(10):1479.
8. Findlay JM, Bradley KM, Maile EJ, Braden B, Maw J, Phillips-Hughes J, et al. Pragmatic staging of oesophageal cancer using decision theory involving selective endoscopic ultrasonography, PET and laparoscopy. Br J Surg. 2015;102(12):1488–99.
9. Bianco V, Sablowski M, Mehta KS, Hamilton A, Odell D, Gooding WE, et al. Evaluation of the accuracy of endoscopic ultrasound for Stage I esophageal cancer. J Am Coll Surg. 2014;219(3)
10. Edward JB, Jules L, Andrew CC, Mark BO, Rishindra MR. Endoscopic ultrasound is inadequate to determine which T1/T2 esophageal tumors are candidates for endoluminal therapies. J Thorac Cardiovasc Surg. 2014;147(2):765–73.
11. Hulshoff JB, Mul VEM, HEMd B, Noordzij W, Korteweg T, HMv D, et al. Impact of endoscopic ultrasonography on 18F-FDG-PET/CT upfront towards patient specific esophageal cancer treatment. Ann Surg Oncol. 2017;24(7):1828–34.
12. Globocan. Stomach Cancer—Estimated Incidence, Mortality and Prevalence Worldwide in 2012. 2012.
13. Jae Kwan J, Kui Son C, Hoo-Yeon L, Mina S, Boyoung P, Seung Hoon S, et al. Effectiveness of the Korean National Cancer Screening Program in reducing gastric cancer mortality. Gastroenterology. 2017;152(6):1319–395098112.
14. Chisato H, Daisuke S, Hideo Y, Kazuhiko I, Akira F, Hiroshi S, et al. The Japanese guidelines for gastric cancer screening. Jpn J Clin Oncol. 2008;38(4):259–67.

15. NCCN Clinical Practice Guidelines in Oncology—Gastric Cancer Version 5.2017.
16. Roberta C, Natalie C, Rajini S, Rinku S, Laercio Gomes L, Alyson M, et al. A systematic review and meta-analysis of the utility of EUS for preoperative staging for gastric cancer. Gastric Cancer. 2012;15(S1):19–26.
17. Kim J-H, Song KS, Youn YH, Lee YC, Cheon JH, Song SY, et al. Clinicopathologic factors influence accurate endosonographic assessment for early gastric cancer. Gastrointest Endosc. 2007;66(5):901–8.
18. Park JM, Ahn CW, Yi X, Hur H, Lee KM, Cho YK, et al. Efficacy of endoscopic ultrasonography for prediction of tumor depth in gastric cancer. J Gastric Cancer. 2011;11(2):109.
19. Okada K, Fujisaki J, Kasuga A, Omae M, Yoshimoto K, Hirasawa T, et al. Endoscopic ultrasonography is valuable for identifying early gastric cancers meeting expanded-indication criteria for endoscopic submucosal dissection. Surg Endosc. 2010;25(3):841–8.
20. Akashi K, Yanai H, Nishikawa J, Satake M, Fukagawa Y, Okamoto T, et al. Ulcerous change decreases the accuracy of endoscopic ultrasonography diagnosis for the invasive depth of early gastric cancer. Int J Gastrointest Cancer. 2006;37(4):133–8.
21. Shunsuke Y, Tsutomu N, Motohiko K, Takuya I, Yoshito H, Jumpei K, et al. Evaluation of endoscopic ultrasound image quality is necessary in endosonographic assessment of early gastric cancer invasion depth. Gastroenterol Res Pract. 2012;2012:194530.
22. Jean-Marc D, Pierre HD, Christian J, Julio I-G, Alberto L, Geoffroy V, et al. Indications, results, and clinical impact of endoscopic ultrasound (EUS)-guided sampling in gastroenterology: European Society of Gastrointestinal Endoscopy (ESGE) clinical guideline—updated January 2017. Endoscopy. 2017;49(07):695–714.
23. Mortensen MB, Pless T, Durup J, Ainsworth AP, Plagborg GJ, Hovendal C. Clinical impact of endoscopic ultrasound-guided fine needle aspiration biopsy in patients with upper gastrointestinal tract malignancies. A Prospective Study. Endoscopy. 2001;33(6):478–83.
24. Repici A, Hassan C, Pessoa DDP, Pagano N, Arezzo A, Zullo A, et al. Efficacy and safety of endoscopic submucosal dissection for colorectal neoplasia: a systematic review. Endoscopy. 2012;44(02):137–50.
25. Hassan H, Vilmann P, Sharma V. Impact of EUS-guided FNA on management of gastric carcinoma. Gastrointest Endosc. 2010;71(3):500–4.
26. Globocan. Estimated Cancer Incidence, Mortality and Prevalence. 2012.
27. Manoop SB, Pramoda K, Virendra J, Payal S, Rei S, Atsushi I, et al. The role of endoscopic ultrasound in pancreatic cancer screening. Endoscopic Ultrasound. 2016;5(1):8–16.
28. John D, Benedict MD, Glen AL, Stuart S, Thomas FI. Comparison of endoscopic ultrasound and computed tomography for the preoperative evaluation of pancreatic cancer: a systematic review. Clin Gastroenterol Hepatol. 2006;4(6):717–25.
29. Puli SR, Bechtold ML, Buxbaum JL, Eloubeidi MA. How good is endoscopic ultrasound-guided fine-needle aspiration in diagnosing the correct etiology for a solid pancreatic mass?: a meta-analysis and systematic review. Pancreas. 2013;42(1):20–6.
30. Canto MI, Hruban RH, Fishman EK, Kamel IR, Schulick R, Zhang Z, et al. Frequent detection of pancreatic lesions in asymptomatic high-risk individuals. Gastroenterology. 2012;142(4):796–804.
31. Victoria C, Milana F, Linda BH, Alla MR, Eran B. Incidental pancreatic cystic lesions: is there a relationship with the development of pancreatic adenocarcinoma and all-cause mortality? Radiology. 2015;274(1):161–9.
32. Anahita S, Mehdi M, Farhad I, Abbas K, Mohammad B, Reza M, et al. Diagnostic yield of EUS-guided FNA for malignant biliary stricture: a systematic review and meta-analysis. Gastrointest Endosc. 2016;83(2):290–2980.
33. Toshio K. Diagnostic and therapeutic single-operator cholangiopancreatoscopy in biliopancreatic diseases: prospective multicenter study in Japan. World J Gastroenterol. 2016;22(5):1891.
34. Osanai M, Itoi T, Igarashi Y, Tanaka K, Kida M, Maguchi H, et al. Peroral video cholangioscopy to evaluate indeterminate bile duct lesions and preoperative mucosal cancerous extension: a prospective multicenter study. Endoscopy. 2013;45(08):635–42.
35. Melina A, Mónica SS, Mathieu L, Isabelle S, Ahmedin J, Freddie B. Global patterns and trends in colorectal cancer incidence and mortality. Gut. 2016;66(4):683–91.
36. National Comprehensive Cancer Network Clinical Practice Guidelines in Oncology Rectal Cancer Version 3.2017. 2017.
37. Shandra B, Afina SG, Frederik JMS, Aeilko HZ, Patrick MMB, Jaap S. Rectal cancer: local staging and assessment of lymph node involvement with endoluminal US, CT, and MR imaging—a meta-analysis 1. Radiology. 2004;232(3):773–83.
38. Marusch F, Ptok H, Sahm M, Schmidt U, Ridwelski K, Gastinger I, et al. Endorectal ultrasound in rectal carcinoma – do the literature results really correspond to the realities of routine clinical care? Endoscopy. 2011;43(05):425–31.
39. Xiao-Ting L, Xiao-Yan Z, Ying-Shi S, Lei T, Kun C. Evaluating rectal tumor staging with magnetic resonance imaging, computed tomography, and endoluminal ultrasound: a meta-analysis. Medicine. 2016;95(44):e5333.
40. Regina GHBT, Geerard LB. Local staging of rectal cancer: a review of imaging. J Magn Reson Imaging. 2011;33(5):1012–9.

16 Case Atlas and Illustrations: Stomach

Fang Yao, Weixun Zhou, Xi Wu, Yamin Lai, Qingwei Jiang, and Yan You

16.1 Case 1

Multiple well-differentiated adenocarcinoma, 0 IIc, depth of invasion M1, in the lower 1/3 of stomach.

The case well demonstrates the use of ME-NBI to identify the malignant foci among multiple lesions.

This is a 65 –year-old male who has suffered upper abdominal discomfort for about 3 months without any alert symptoms. Physical examination revealed a mild pressing discomfort on the upper abdomen. Lab examination found normal blood routine test with normal CEA and $CA_{19\text{-}9}$. The previous EGD in a local hospital found there were multiple erosions in the gastric antrum, biopsies were taken at several erosive lesions, and the following histologic examination revealed a severe dysplasia lesion on the anterior wall. The abdominal CT scan was normal. The patient was then referred to our hospital for further management.

Magnifying endoscopy with GIF-HZ260 (Olympus Medical System Corporation, Tokyo, Japan) was performed on him. Lots of nodular erosions on the lesser curvature and anterior wall of gastric antrum were found on white light endoscopy. We changed to NBI model and used the low-grade magnification to closely but quickly observe all the lesions. Two of the nodules were discerned with irregular central reddish depression. We put the tip of the scope closer to each target lesion and changed the magnification ratio gradually to maximal level. Observing from the surrounding mucosa to the center,we identified the clear demarcation line (DL), and further examination found the cancerous changing according to VS classification within the DL. One piece of target biopsy was performed for each lesion, and the histologic examination confirmed it to be high-grade intraepithelial neoplasia.

The two lesions were removed completely soon by ESD. The following histologic examination revealed that they were both well-differentiated adenocarcinoma according to Japanese classification or high-grade intraepithelial neoplasia (WHO classification).

16.2 Case 2

Well-differentiated adenocarcinoma, 0 IIa, depth of invasion M1, in the middle 1/3 of stomach.

The case demonstrates the use of ME-NBI to well discern the margin of superficial early gastric cancer and the consistence of ME-NBI with pathology for recognizing the malignancy.

This is a 67-year-old male who has suffered upper abdominal discomfort for about 5 years. Nothing remarkable was found on physical

F. Yao (✉) · X. Wu · Y. Lai · Q. Jiang
Department of Gastroenterology, Peking Union Medical College Hospital, Beijing, China

W. Zhou · Y. You
Department of Pathology, Peking Union Medical College Hospital, Beijing, China

P. W. Y. Chiu et al. (eds.), *Endoscopy in Early Gastrointestinal Cancers, Volume 1*,
https://doi.org/10.1007/978-981-10-6769-3_16

examination. Lab examination revealed normal blood routine test with normal CEA and $CA_{19\text{-}9}$. The diagnosis of EGD 1 year ago in a local hospital was chronic atrophic gastritis.

Magnifying endoscopy with GIF-HZ260 (Olympus Medical System Corporation, Tokyo, Japan) was performed for him. There was a mild elevated lesion on the gastric angulus with irregular shape, the color was mild reddish with heterogeneity. The size of the lesion was about 6.0 cm by 4.0 cm in diameter. Clear circumferential DL was discerned on ME-NBI examination, while the MSP within it was mainly irregular with local absence of MSP, and the MVP is also irregular. The lesion was then assessed as DL(+) + IMSP/AMSP + IMVP, which met the VS diagnosis criteria for gastric adenocarcinoma. However, two pieces of biopsy were taken from the central part of lesion, and the histologic diagnosis was low-grade intraepithelial neoplasia.

Here we had to face the conflict of endoscopic diagnosis to histologic evaluation. Being considered the typical characteristics of malignancy on ME-NBI, ESD was recommended and conducted after full and detailed discussion with the patient. The lesion was en bloc resected successfully, and the further histologic evaluation for the whole specimen identified several small areas of high-grade intraepithelial neoplasia, which corresponded to the results of ME-NBI. The final diagnosis according to Japanese classification was early gastric cancer, Type 0-IIb + IIa, well-differentiated type, 58 × 42 mm in size, M1, ly0, v0, LM(−), VM (−).

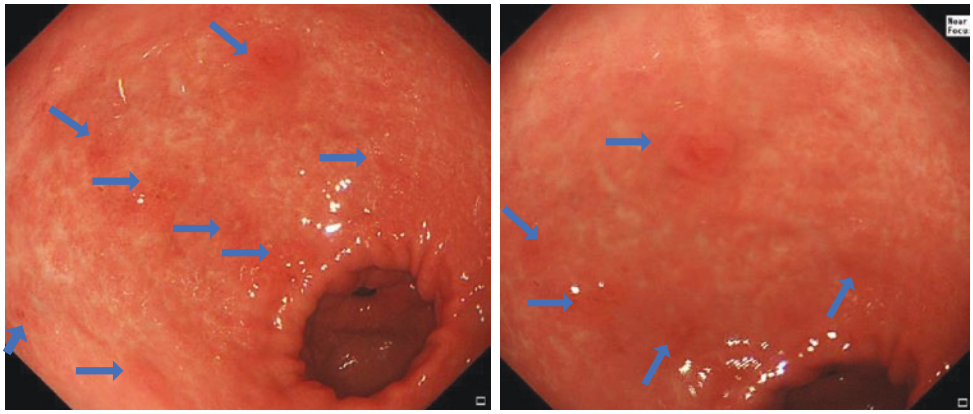

Fig. 16.1 Non-magnified examination on white light endoscopy. We can see multiple nodules with central reddish depression on the lesser curvature and anterior wall of gastric antrum (*arrows*)

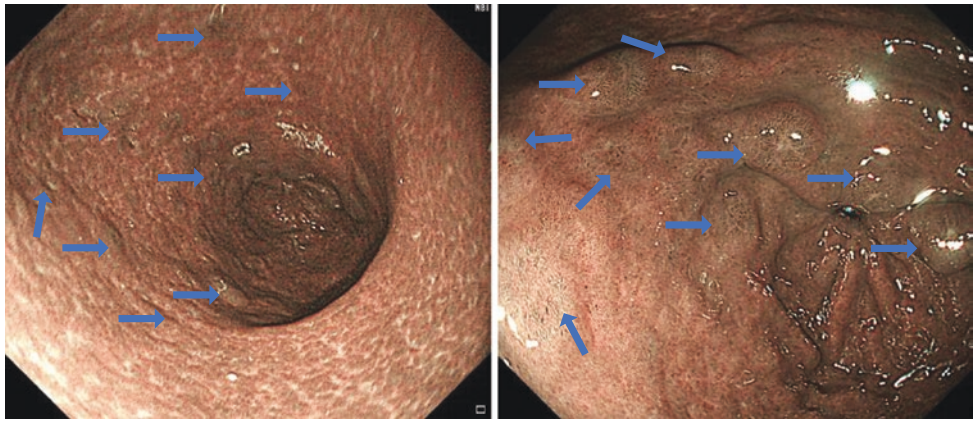

Fig. 16.2 Non-magnified examination on NBI model. The nodules change to brownish with central depression on the lesser curvature and anterior wall of gastric antrum (*arrows*)

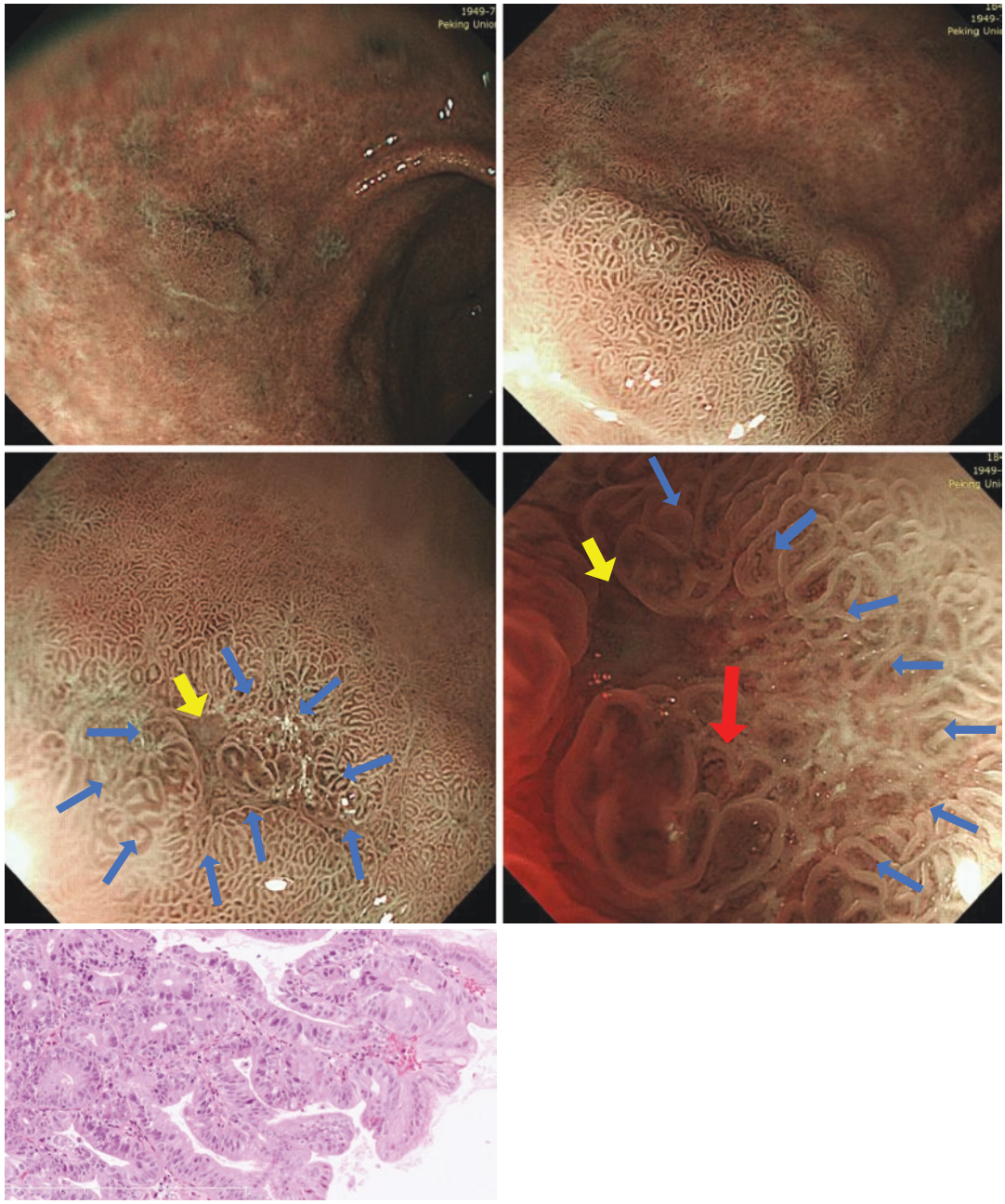

Fig. 16.3 Low-grade magnified NBI reveals a IIa + IIc lesion with size of 1.5 cm by 1.5 cm on the anterior wall of gastric antrum. The margin of central depression is irregular. The previous biopsy scar is identified in the upper part of lesion (yellow *arrows*). Close magnified examination with maximal ratio discerns the demarcation line (DL) between the surrounding mucosa and the lesion (blue arrows). Within the DL, the microsurface pattern (MSP) is obviously irregular with different size and morphology. The distribution is asymmetrical and the arrangement is irregular. The microvascular pattern (MVP) is also irregular comparing to those in the noncancerous mucosa with greater diameter, higher vessel density, and different morphology. The lesion was assessed as DL(+) + IMSP + IMVP. One piece of biopsy was taken from the site as the red arrow shows. The pathologic evaluation confirmed it to be a lesion with high-grade intraepithelial neoplasia

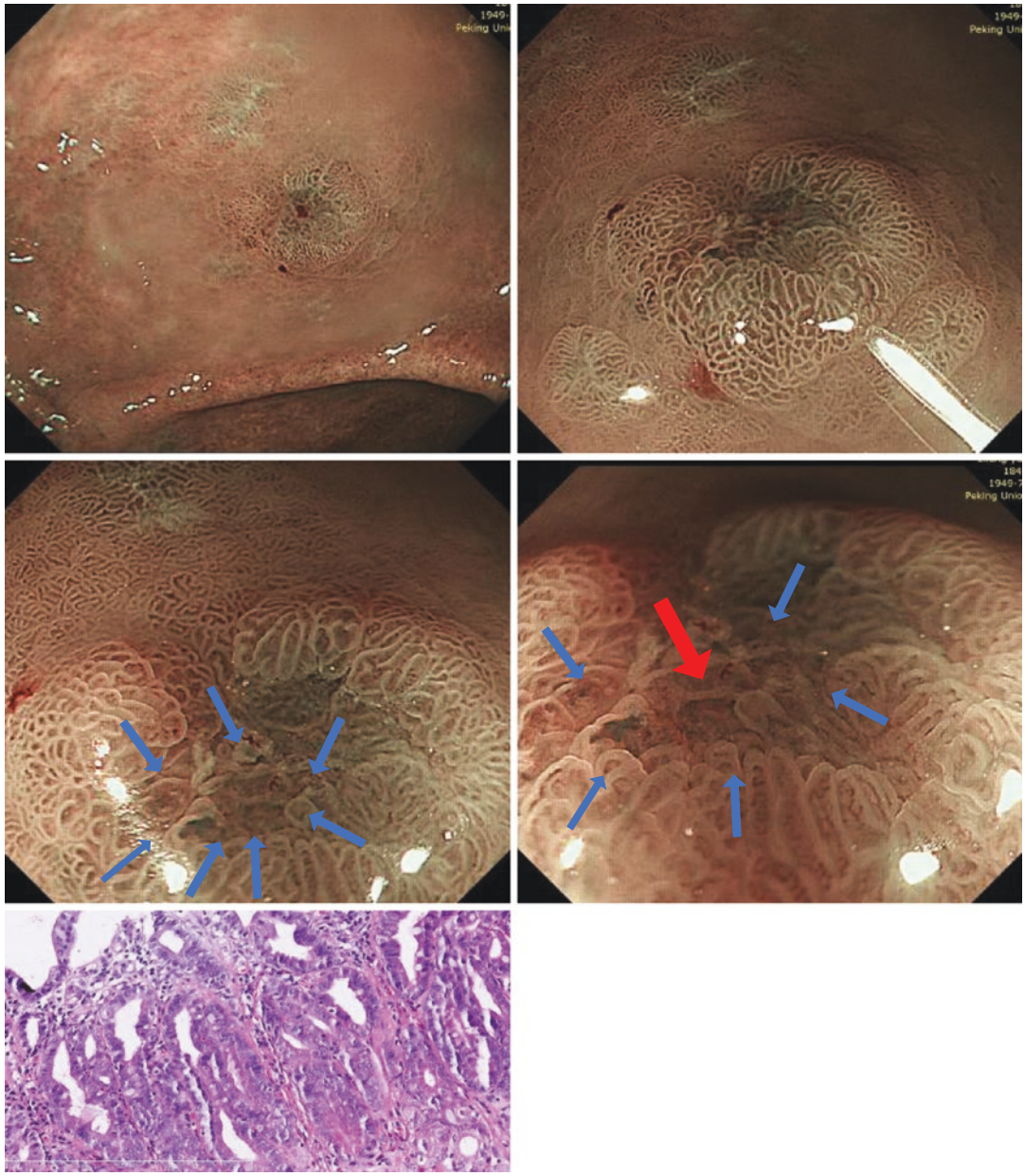

Fig. 16.4 Low-grade magnified NBI finds another IIa + IIc lesion with size of 1.0 cm by 1.0 cm on the lesser curvature of gastric antrum. Close magnified examination also identifies the demarcation line (DL) between the lesion and the surrounding mucosa (blue arrows). In the small area within the DL, the MSP is obviously dilated with different size and morphology. The MVP is also irregular with greater diameter, discordant shape and arrangement. The lesion was assessed as DL(+) + IMSP+ IMVP. One piece of biopsy was taken from the site as red arrow shows. The pathologic examination confirmed it to be a lesion with high-grade intraepithelial neoplasia

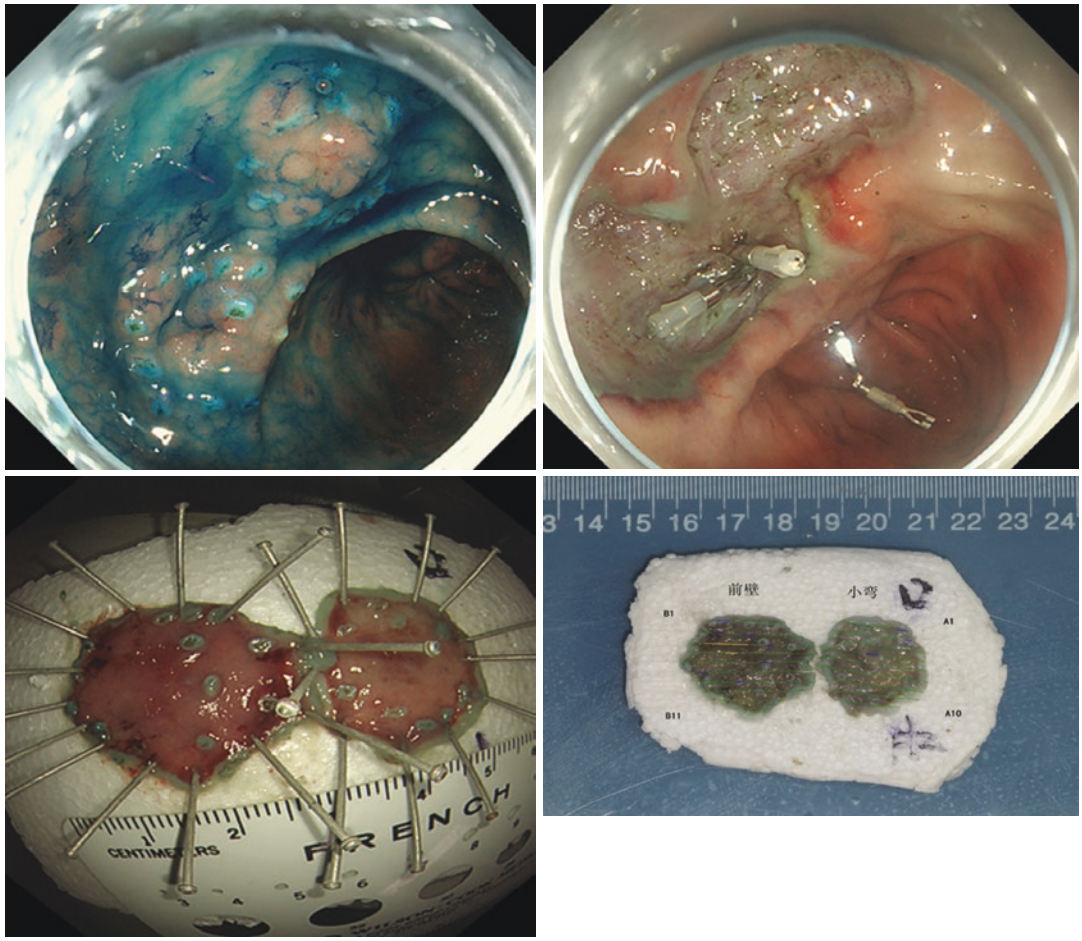

Fig. 16.5 The two lesions were removed by ESD. The pictures demonstrate the lesions with markings, the wound after ESD, the two specimens after ESD and fixed in formalin

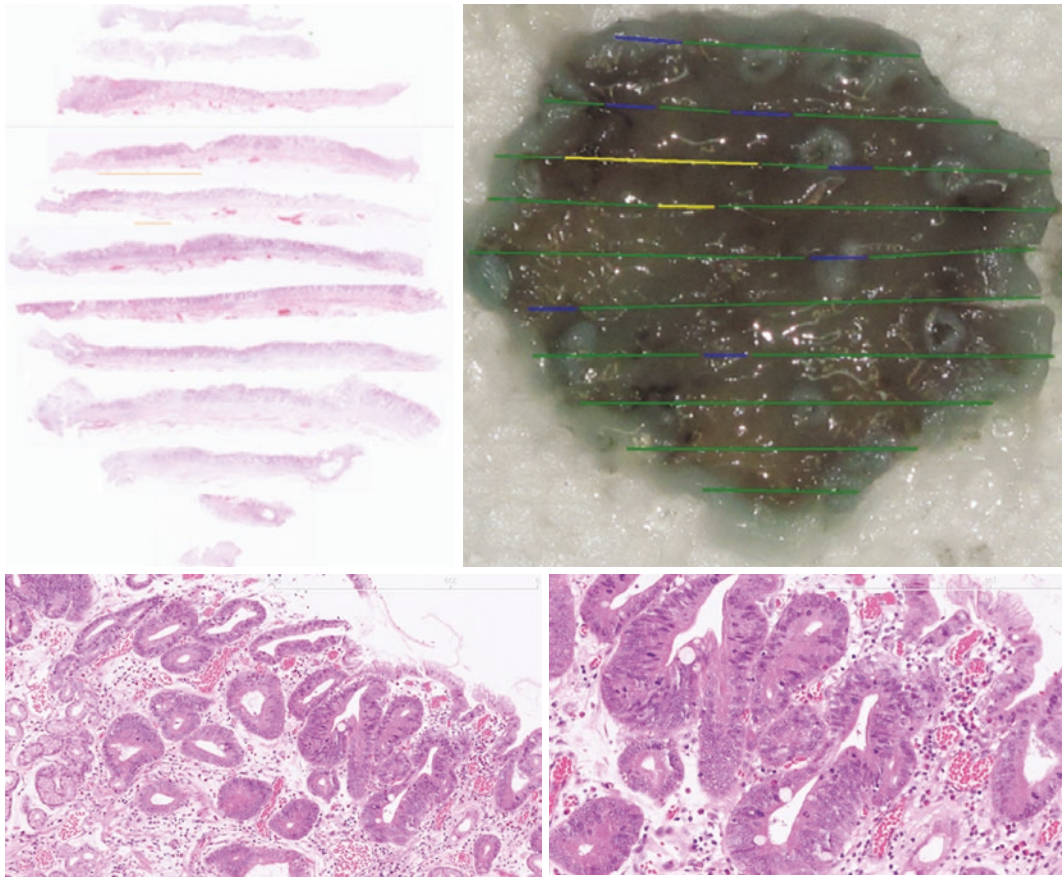

Fig. 16.6 The specimen on the anterior wall was cut every 2 mm and evaluated carefully by pathologist. According to the results of all slides, we reconstructed the cancerous area on the resected specimen and marked it with yellow lines on the photo of the ESD specimen fixed in formalin. The orange lines in slides and yellow lines in specimen indicate the cancerous area, and the histologic findings are demonstrated with higher power field. The final diagnosis according to Japanese classification was early gastric cancer, 0 IIc, well-differentiated type, 7 mm × 4 mm, M1, ly0, v0, LM(−), VM (−)

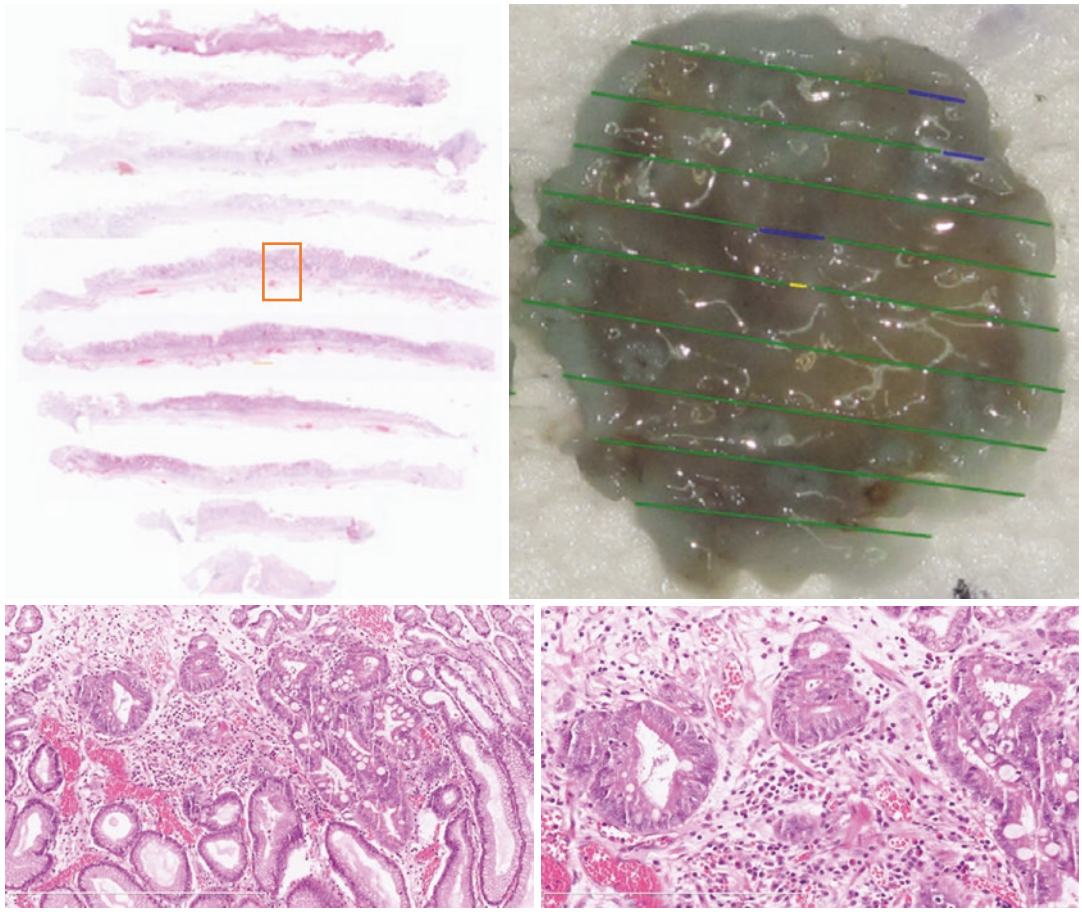

Fig. 16.7 The specimen on the lesser curvature was cut every 2 mm and evaluated carefully by pathologist. According to the results of all slides, we reconstructed the cancerous area on the resected specimen and marked it with yellow lines on the photo of the ESD specimen fixed in formalin. The orange rectangle in slides and yellow lines in specimen indicate the cancerous area, and the histologic findings are demonstrated with higher power field. The final diagnosis according to Japanese classification was early gastric cancer, type 0 IIc, well-differentiated type, 3.0 mm × 1.5 mm, M1, ly0, v0, LM (−), VM (−)

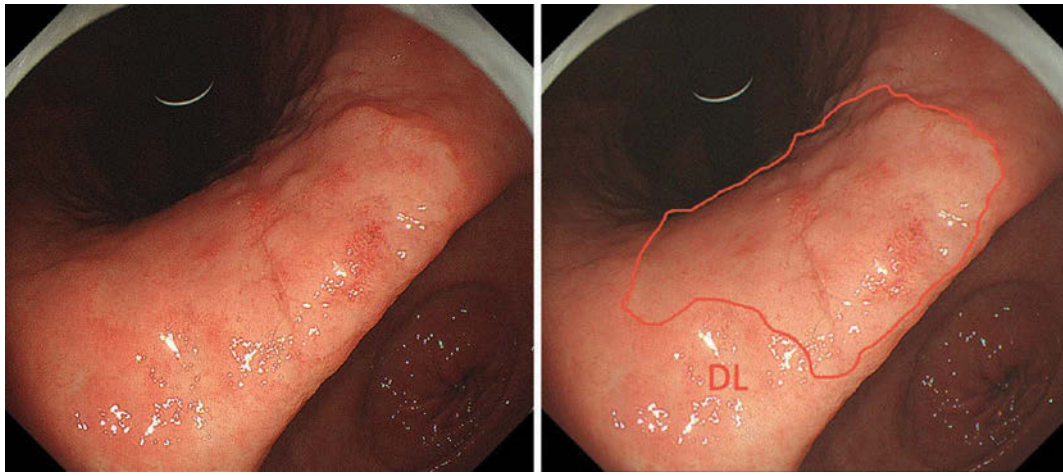

Fig. 16.8 Non-magnified examination on white light endoscopy. We can see a mild elevated lesion on the gastric angulus with irregular margin, the color is mild reddish with heterogeneity. The red line shows the lateral margin between the lesion and the surrounding mucosa (demarcation line, DL). The size of the lesion is about 6.0 cm by 4.0 cm

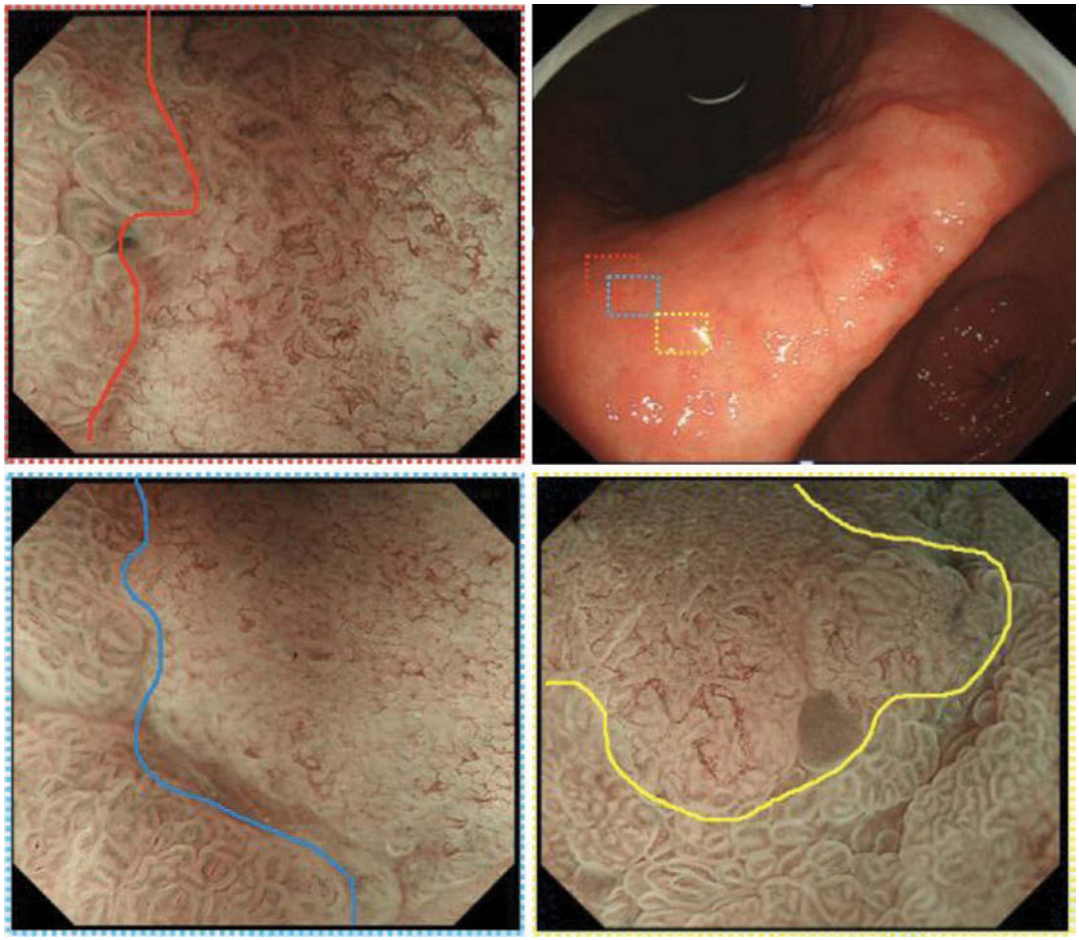

Fig. 16.9 ME-NBI examination was performed for this patient. We started evaluation from the anterior side of the lesion, observing from the surrounding mucosa toward the lesion with maximal magnifying ratio, we could see the abrupt changing of MSP from villous to small, dense round shape, while the morphology and distribution was irregular, which showed a clear DL (colorful curve lines). The MVP within the DL was obviously different comparing with the subepithelial capillary network (SECN) in surrounding mucosa. The lesion was assessed as IMSP + IMVP with DL (+). Applying the tip of black hood against on the background mucosa outside the DL and moving slowly along the circumferential margin of lesion, we could clearly demonstrate the whole DL

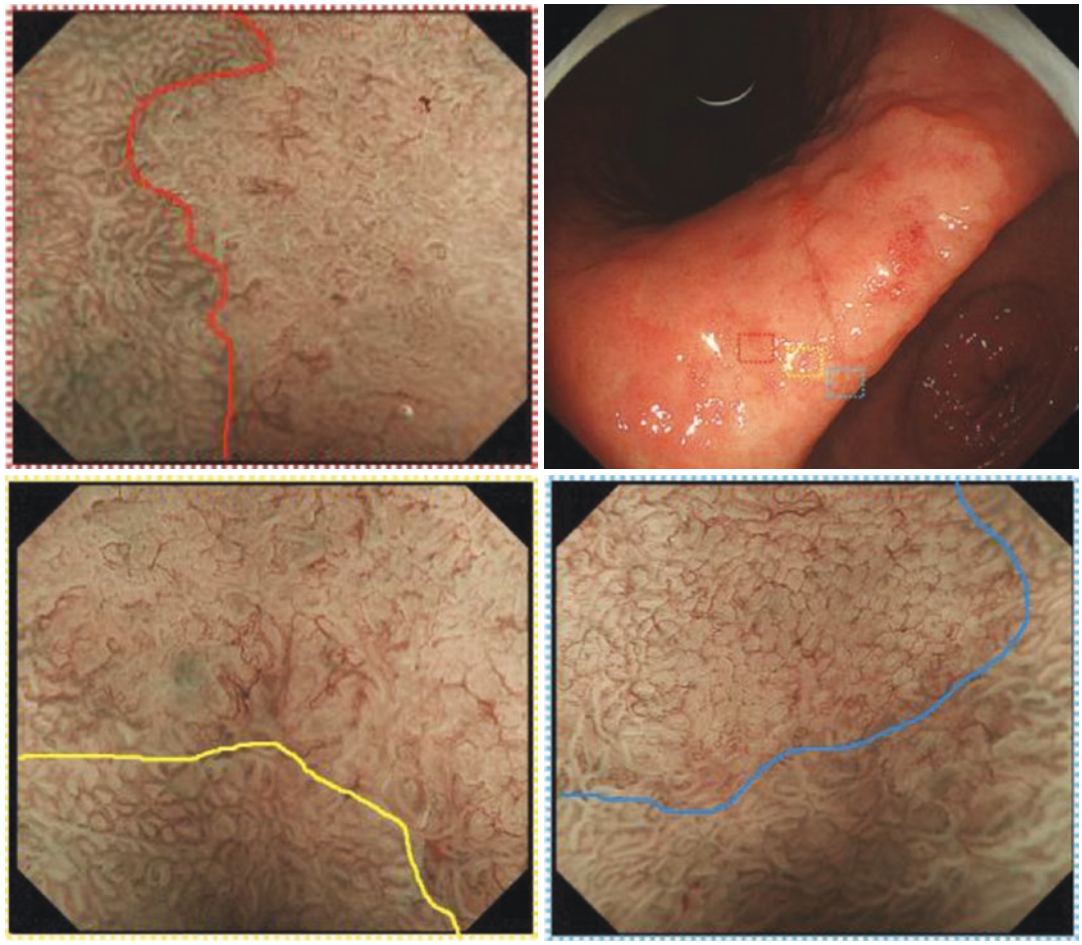

Fig. 16.10 ME-NBI examination of the patient. The scope moved toward anterior anal side of the lesion, the DL was also well indicated. The lesion had typical IMSP + IMVP with DL (+)

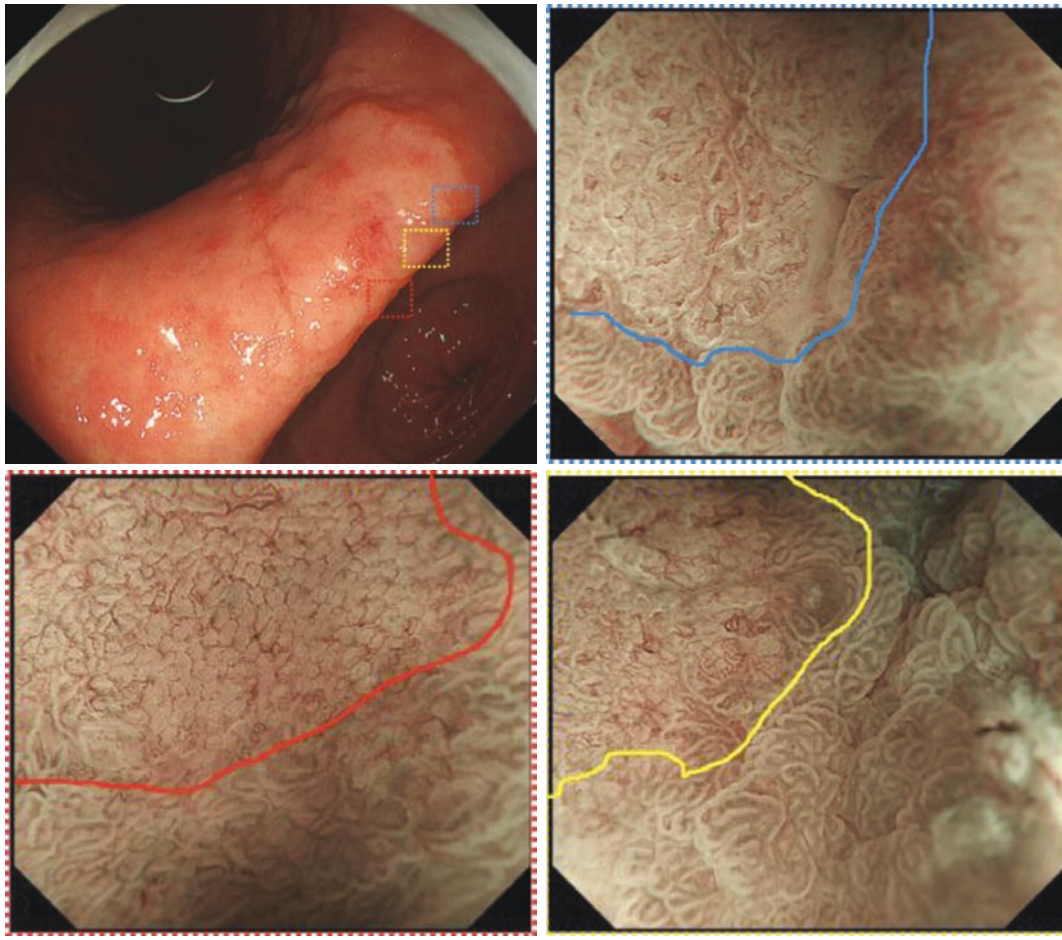

Fig. 16.11 ME-NBI examination of the patient. The scope moved toward anal side of the lesion along the DL. The lesion had typical IMSP + IMVP with DL (+)

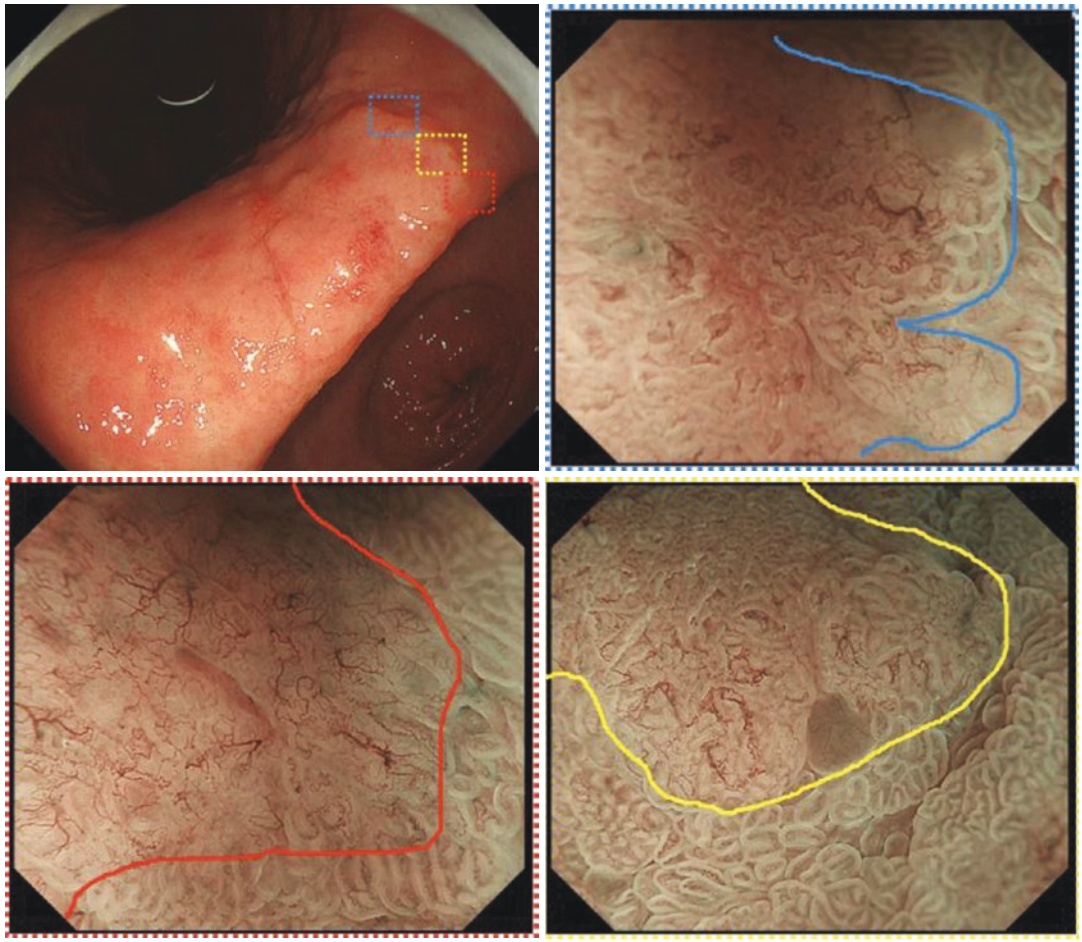

Fig. 16.12 ME-NBI examination of the patient. The scope moved toward posterior side of the lesion along the DL. The lesion had typical IMSP + IMVP with DL (+), and we could see an area of AMSP with IMVP in the left lower picture

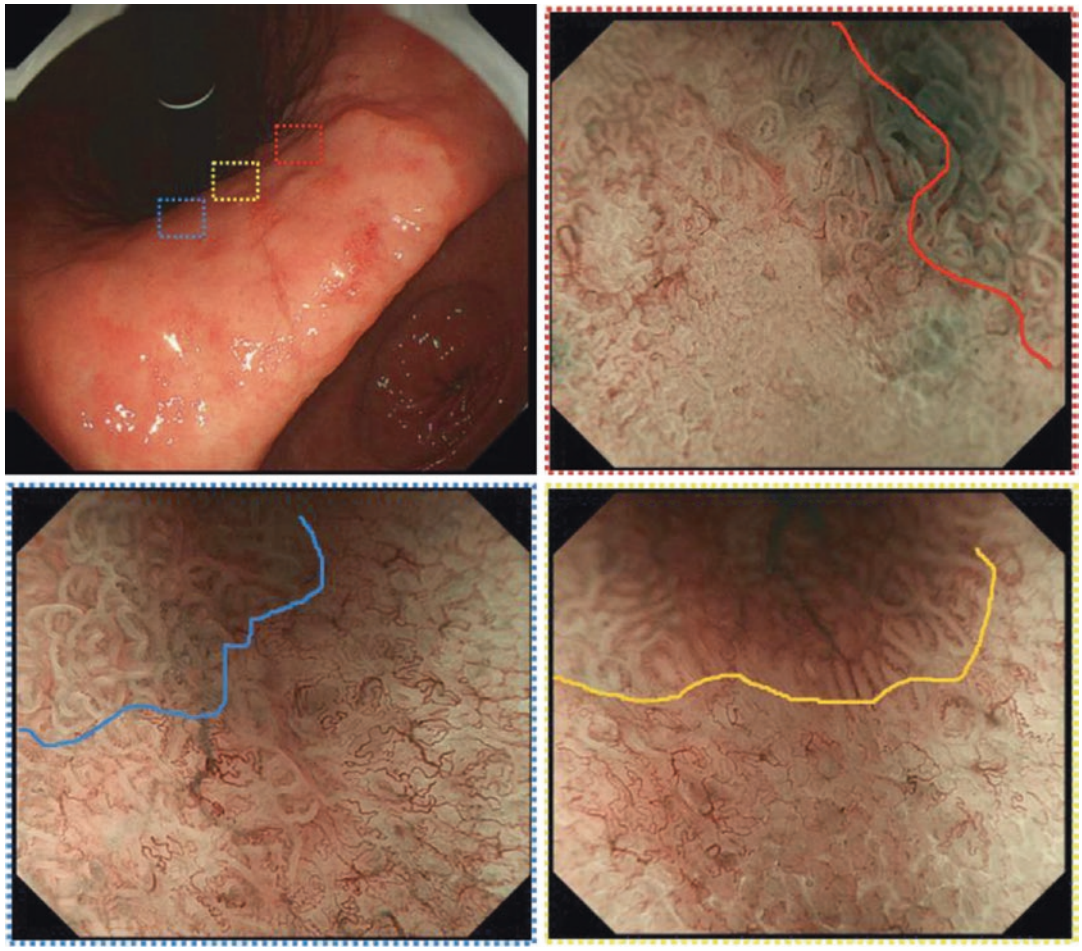

Fig. 16.13 ME-NBI examination of the patient. The scope moved toward oral side of the lesion along the DL. The lesion had typical IMSP and IMVP with DL (+), and we could see areas of AMSP with IMVP in the two lower pictures

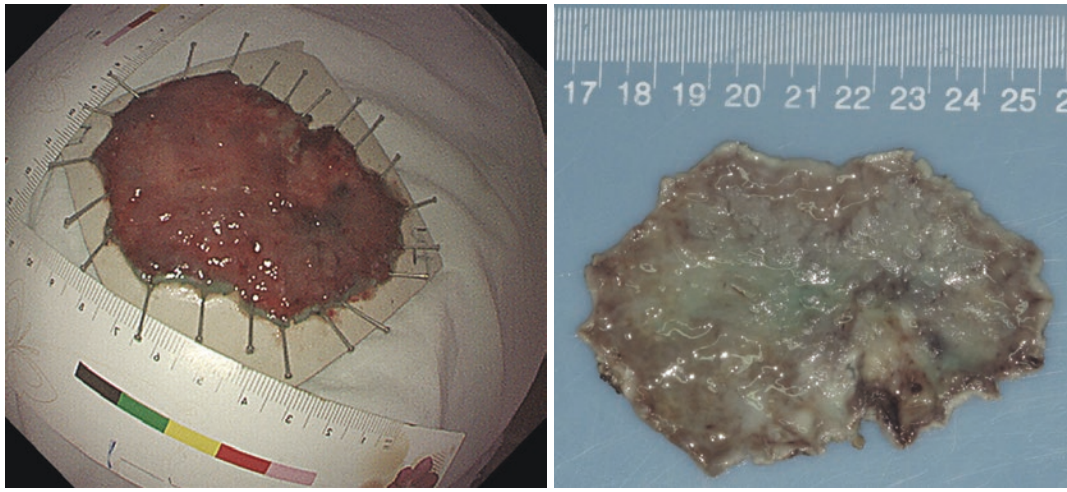

Fig. 16.14 ESD was conducted after full and detailed discussion with the patient, and the lesion was en bloc resected. The specimen after ESD and fixed in formalin are both demonstrated. The size of specimen is 82 × 56 mm

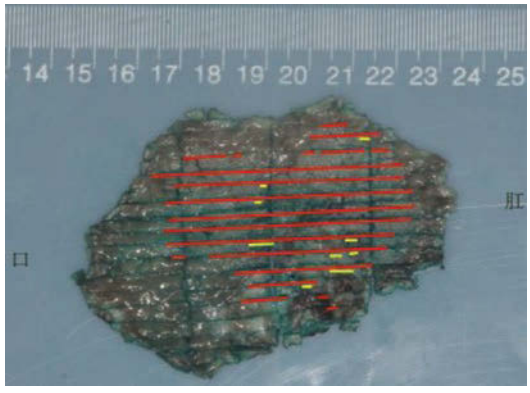

Fig. 16.15 The specimen was cut every 2 mm and evaluated carefully by pathologist. According to the results of all slides, we reconstructed the whole area on the resected specimen and marked it with different color line on the photo. The red lines indicate the areas of low-grade intraepithelial neoplasia, and the yellow lines mean local high-grade intraepithelial neoplasia. The final diagnosis according to Japanese classification was early gastric cancer, Type 0-IIb + IIa, well differentiated, 58 × 42 mm in size, M1, ly0, v0, LM(−), VM (−)

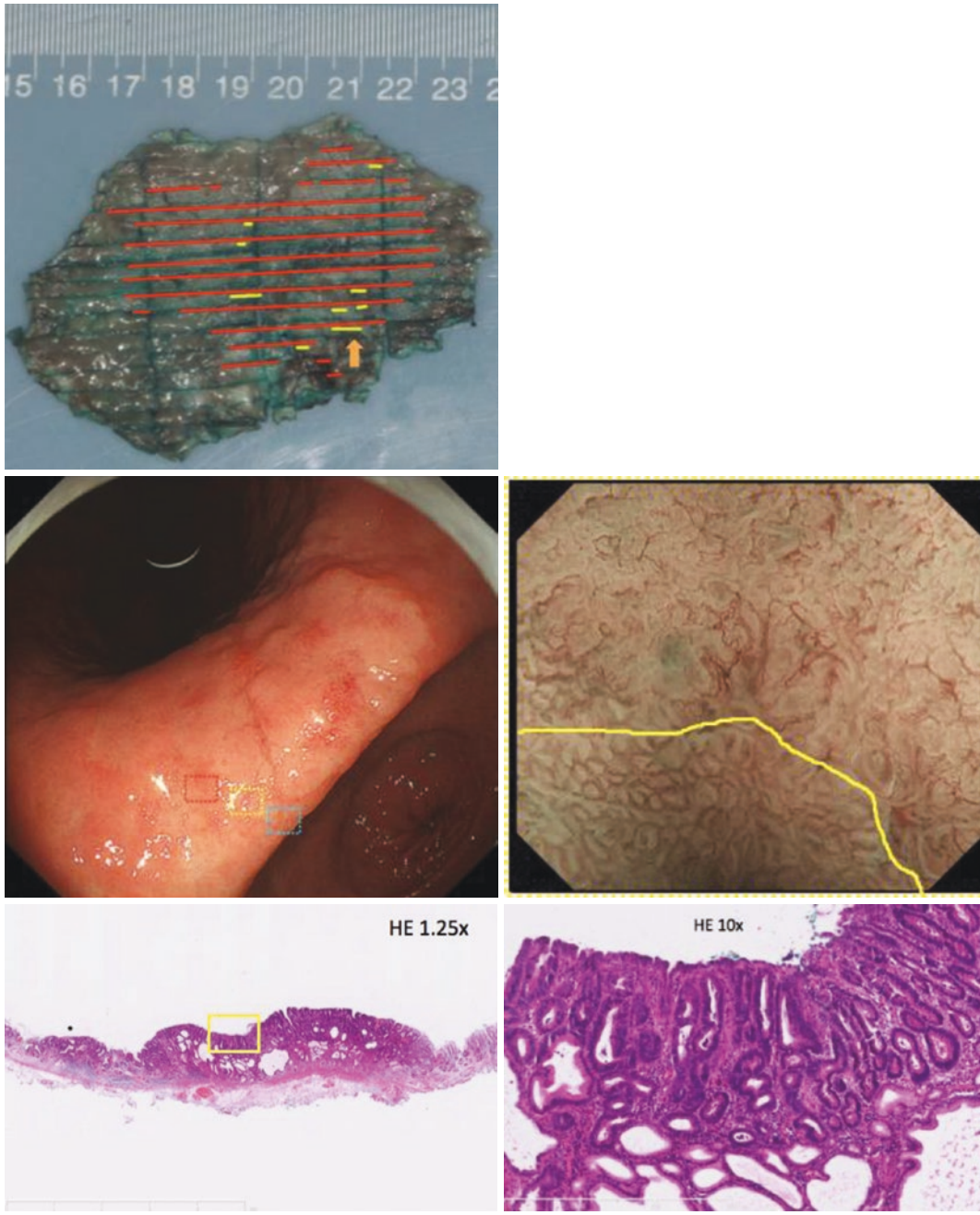

Fig. 16.16 The comparison between endoscopic image and pathologic exam at the site of anterior anal part of lesion (Orange arrow on photo of specimen fixed in formalin). The ME-NBI reveals typical IMSP + IMVP with DL (+). The pathologic images demonstrate the area of local high-grade intraepithelial neoplasia and the margin

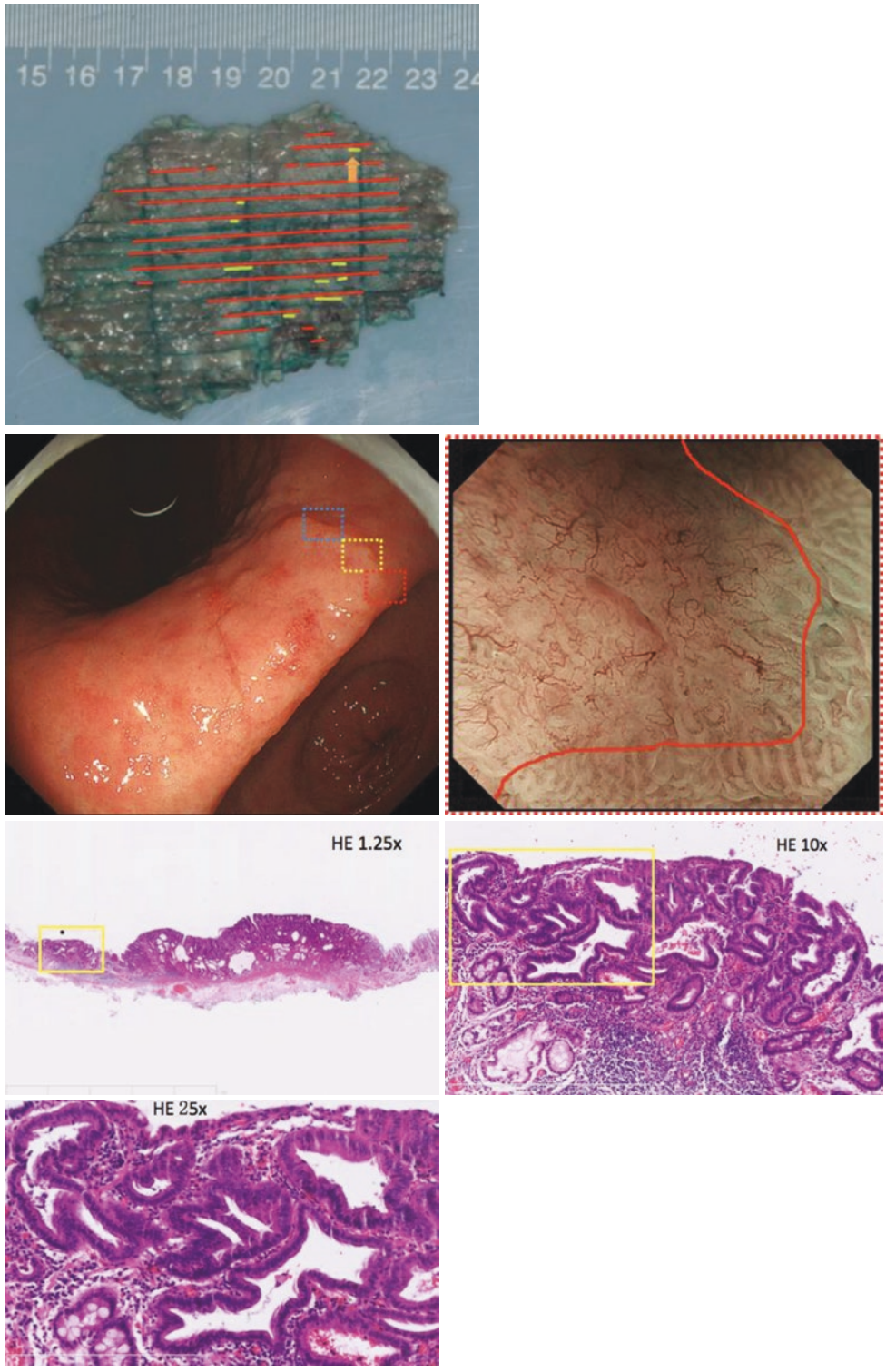

Fig. 16.17 The comparison between endoscopic image and pathologic exam at the site of posterior of lesion (Orange arrow on photo of specimen fixed in formalin). The ME-NBI reveals typical AMSP + IMVP with DL (+). The pathologic images show the area of local high-grade intraepithelial neoplasia

17 Careful Observation Using Magnifying Endoscopy Before Choice of Treatment Strategy for Early Colorectal Lesions

Qing-Wei Zhang and Xiao-Bo Li

Many studies have shown that histology of a colorectal lesion or even whether endoscopic resection is suitable for a suspected colorectal cancer could be accurately diagnosed by careful observation before treatment [1–6]. The morphological parameters observed under white light endoscopy could help in delineating the risk of invasion and the depth of invasion. It has been reported that expansion appearance, deep and irregular depression surface, folds converging toward the tumor, non-lifting sign, submucosal mass-like elevation or large nodule, and depression in laterally spreading tumors (LSTs) are risk factors for deep invasion [1–6].

Magnifying endoscopy, defined as endoscopy used to observe the microstructure of the gastrointestinal mucosa under magnifying view, has been developed with a magnifying power of × 75–125. Magnifying chromoendoscopy (M-CE) has been widely used in differentially diagnosing deep invasive colorectal cancers from superficial submucosal colorectal cancers and intramucosal carcinomas using the pit pattern with high diagnostic efficacy in Japan [7]. Magnifying endoscopy combined with narrow-band imaging (M-NBI) has enabled real-time diagnosis by allowing the surface structures and mucosal microcapillaries to be more carefully observed. In our previous studies, we established superiority of M-CE to M-NBI in diagnosis of deep submucosal cancers, not suitable for endoscopic resection, with higher sensitivity and similar specificity [1, 8–10]. For M-NBI, there were many classifications used for differentiation of deep submucosal cancers and superficial colorectal cancers [11–16]. Among them, the JNET classification is now the mostly used M-NBI classification for diagnosis of colorectal lesions. However, it should be acknowledged that magnifying endoscopy or chromoendoscopy is not widely used in Western countries and classification for non-magnified NBI was established for optical diagnosis of colorectal lesions, named narrow-band imaging international colorectal endoscopic (NICE) classification [17, 18].

Therefore, based on previous published studies for diagnosis of colorectal lesions especially evaluation of whether endoscopic resection is suitable for a suspected colorectal cancer, it is suggested that white light view be firstly performed for assessment and NBI be switched to assess histology of colorectal lesions (hyperplastic polyps or neoplasia). Then, it is recommended that M-NBI be used to evaluate the

Q.-W. Zhang · X.-B. Li (✉)
Division of Gastroenterology and Hepatology, Key Laboratory of Gastroenterology and Hepatology, Ministry of Health, Renji Hospital, School of Medicine, Shanghai Institute of Digestive Disease, Shanghai Jiao Tong University, Shanghai, China

P. W. Y. Chiu et al. (eds.), *Endoscopy in Early Gastrointestinal Cancers, Volume 1*,
https://doi.org/10.1007/978-981-10-6769-3_17

histopathology and further invasiveness of lesions that have been detected by conventional white-light view to make an endoscopic therapeutic decision. It would be better to use M-CE to reevaluate invasion depth of suspected deep invasive colorectal cancers.

In this chapter, we show three cases of colorectal lesions evaluated for histology and invasion depth by application of white light endoscopy, M-NBI, and M-CE for better understanding of optical diagnosis of colorectal lesions.

Case 1

A 2.5 × 3.5 cm LST-G (Is) was detected during the screening colonoscopy (Fig. a, b). Using magnifying endoscopy with narrow-band imaging, JNET 2A was diagnosed with regular vessels and gyrus surface pattern for the LST (Fig. c, d) and the Kudo pit pattern was the type IV under magnifying chromoendoscopy using crystal violet (Fig. e, f). After no suspicion of carcinoma, the LST underwent ESD (Fig. g, h), with final histopathology proved to be tubular adenoma.

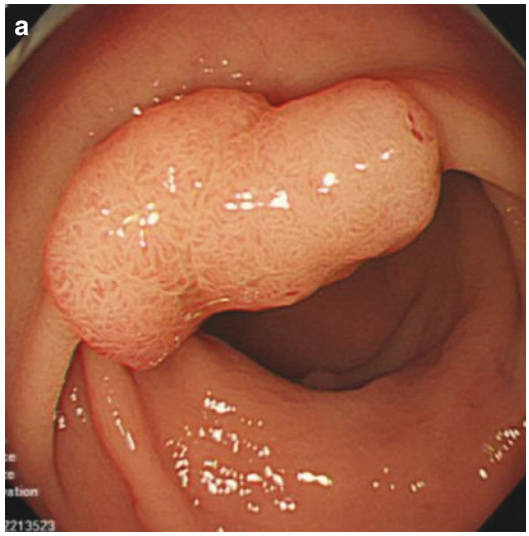

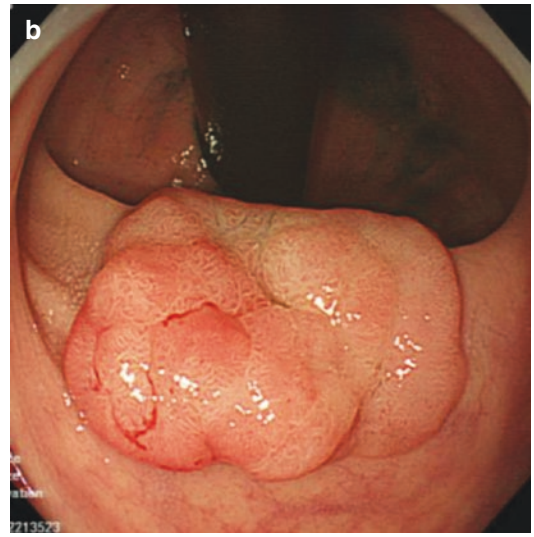

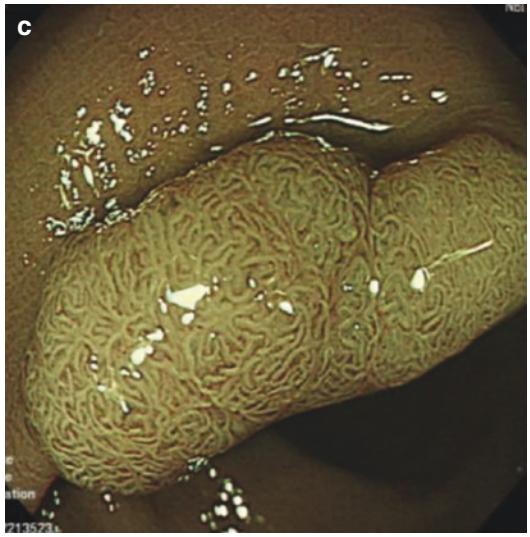

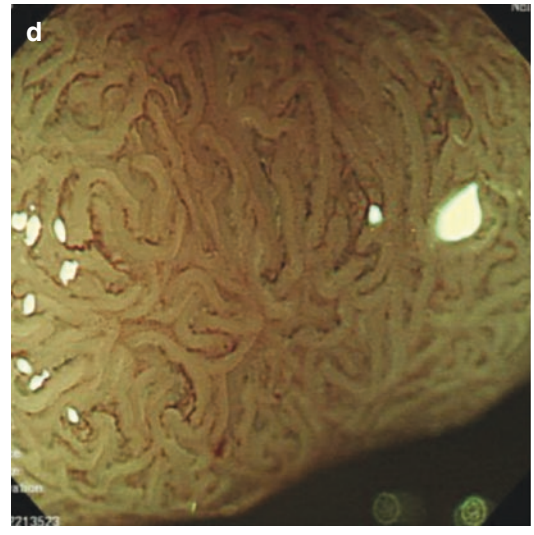

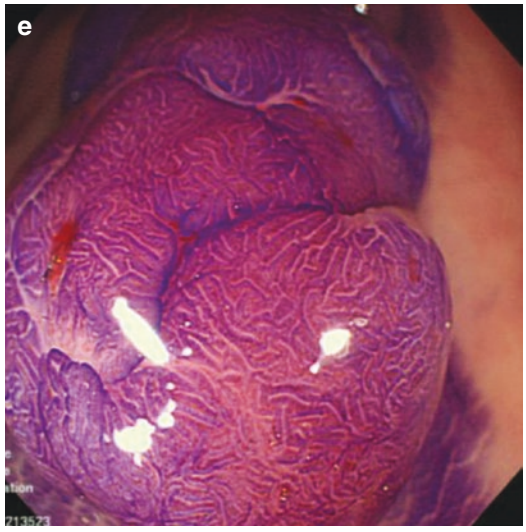
e

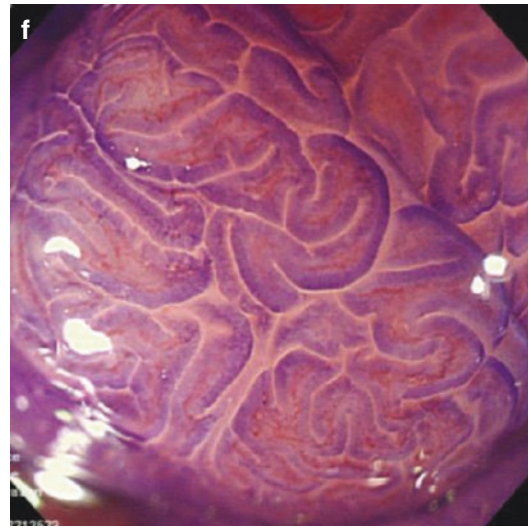
f

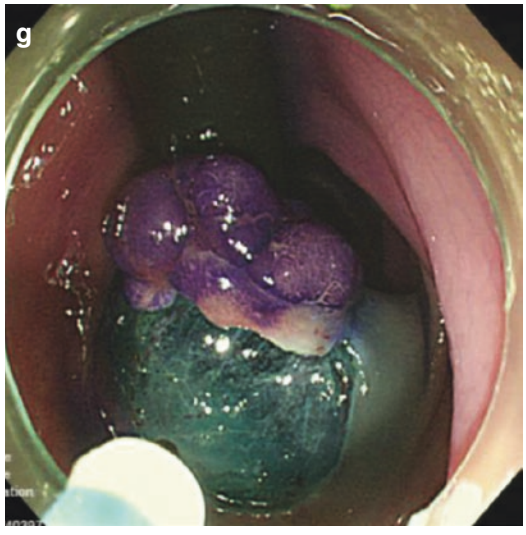
g

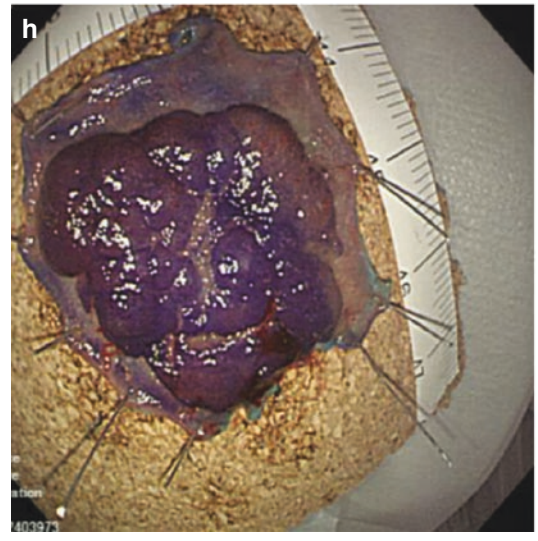
h

Case 2

A 1.5 × 3.5 cm large polypoid lesion (Is) with villous feature was detected in the sigmoid colon (Fig. a). We attached the button from the white light view to the narrow-band imaging view. Villous surface pattern was regular at the base (Fig. b), but it changed to smaller and irregular at the top of the lesion suggesting JNET 2B (Fig. c). After narrow-band imaging observation, the Kudo pit pattern was the type IV with focal VI-low pits under magnifying chromoendoscopy using crystal violet (Fig. d–f). With suspicion of malignancy, the lesion must be resected en bloc with ESD and final histopathology proved to be villous adenoma with focal high-grade dysplasia (Fig. g, h).

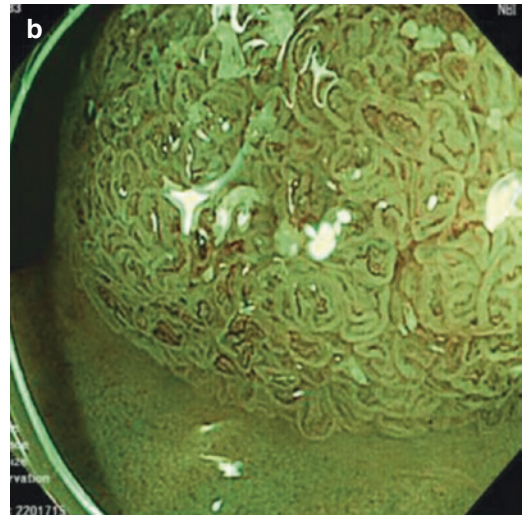

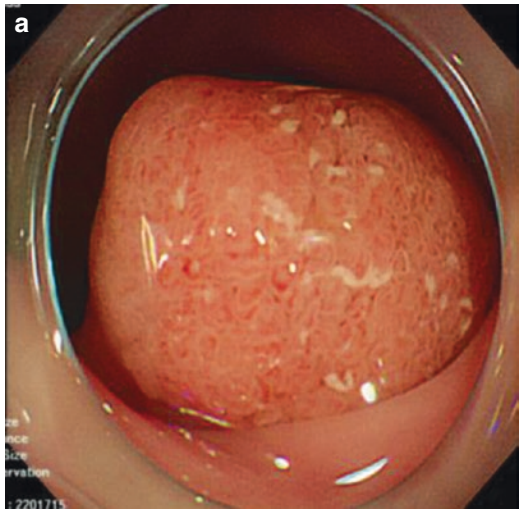

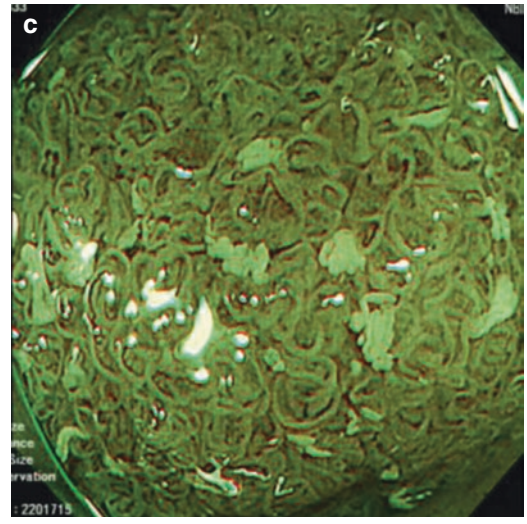

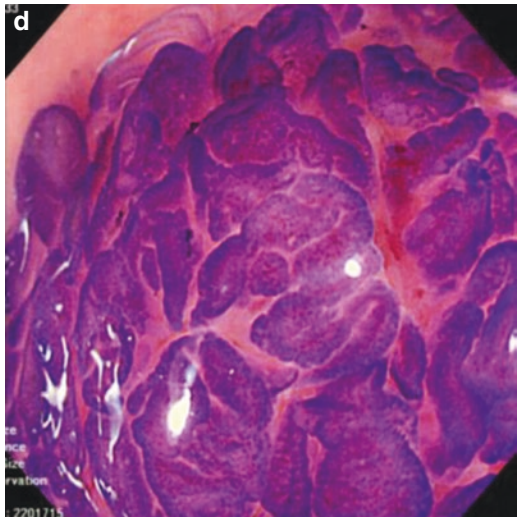
d

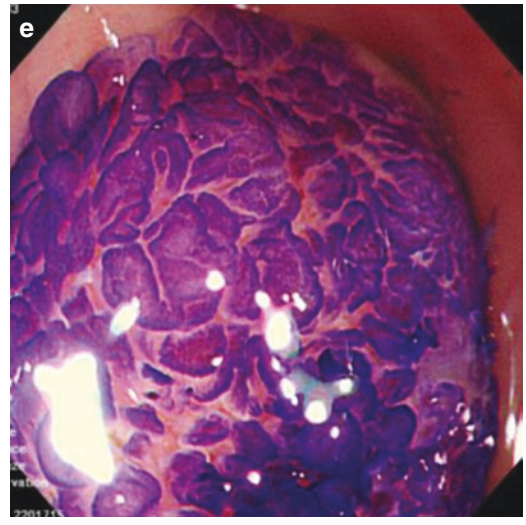
e

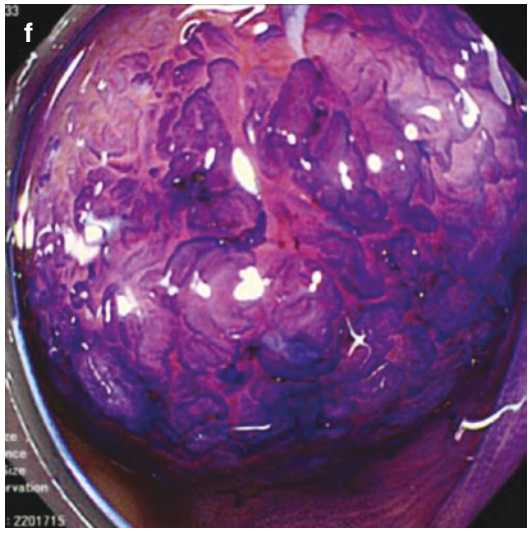
f

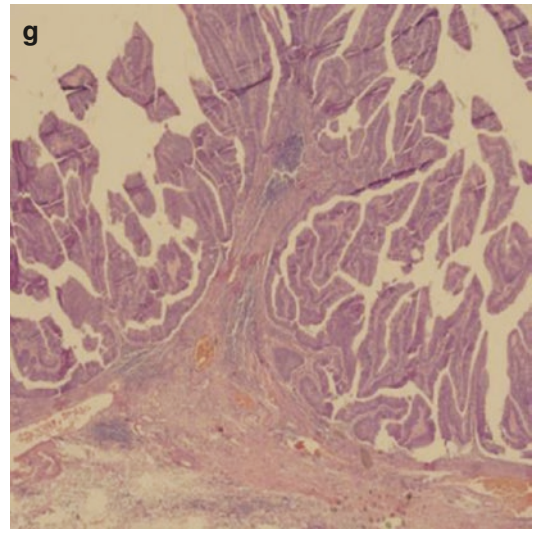
g

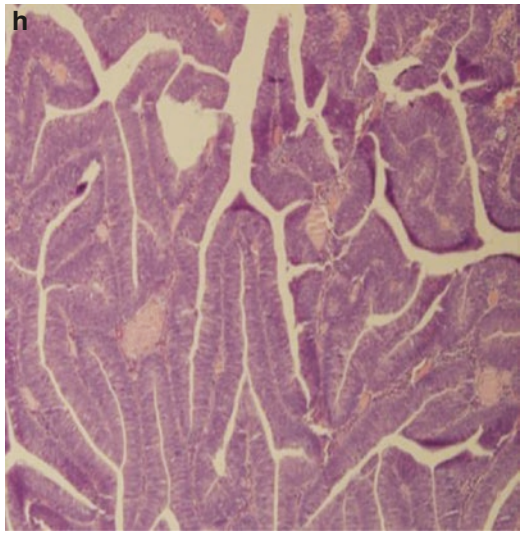

Case 3

A 1.5 × 2.5 cm LST-G was detected in the rectum (Fig. a). Under magnifying endoscopy with narrow-band imaging, JNET 2A was considered for most parts of the lesion (Fig. b) but in little depressed and a larger nodule at the center of the lesion, the JNET 2B was suspected (Fig. c, d). After narrow-band imaging observation, the Kudo pit pattern was the type IV for most parts of the lesion but type Vi-low for some parts of the lesion under magnifying chromoendoscopy using crystal violet (Fig. e, f). It was considered malignancy but could be resected endoscopically with en bloc ESD (Fig. g). Final histopathology proved to be villous adenoma with high-grade dysplasia (Fig. h).

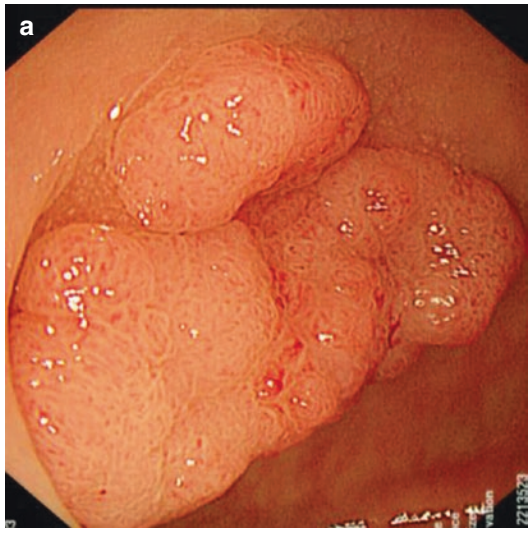

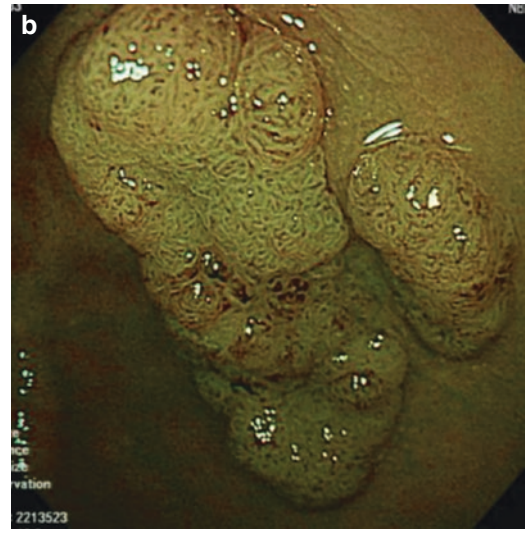

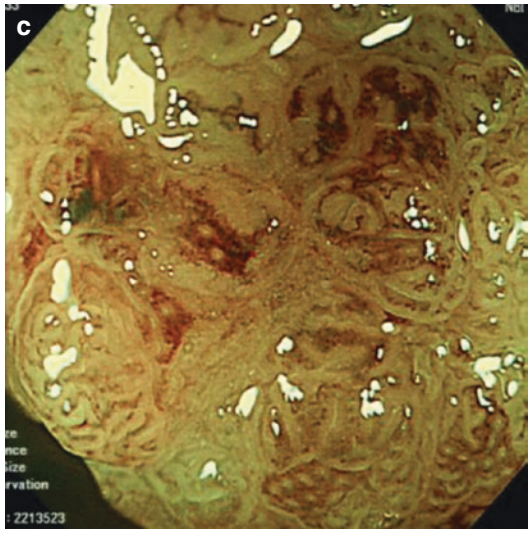
c

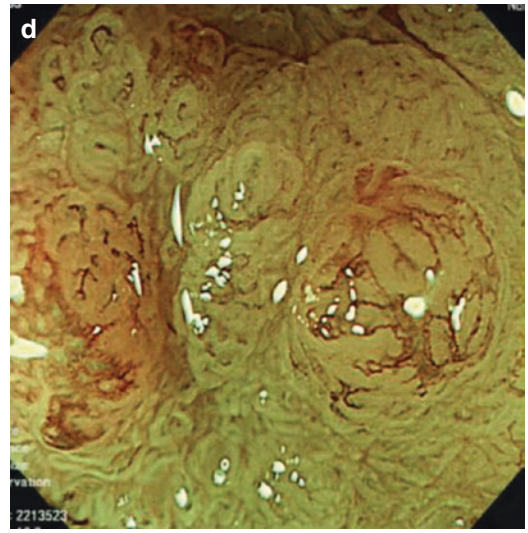
d

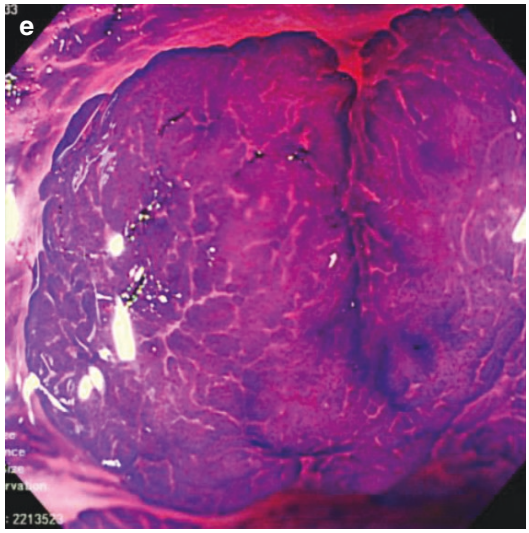
e

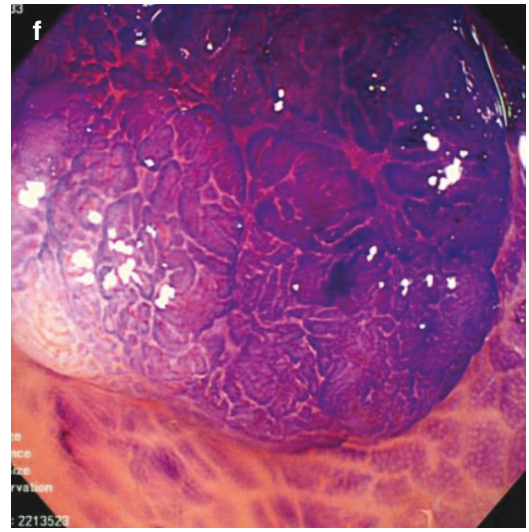
f

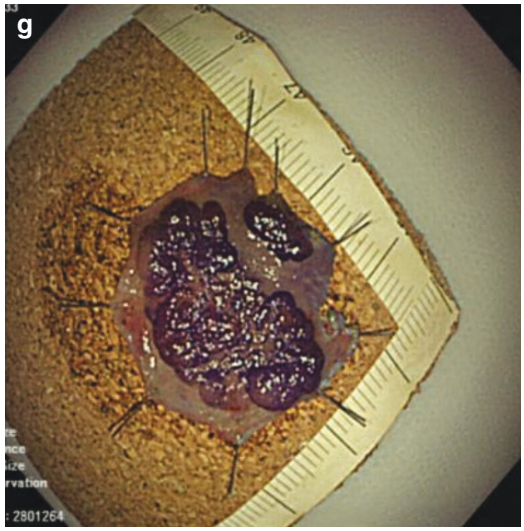

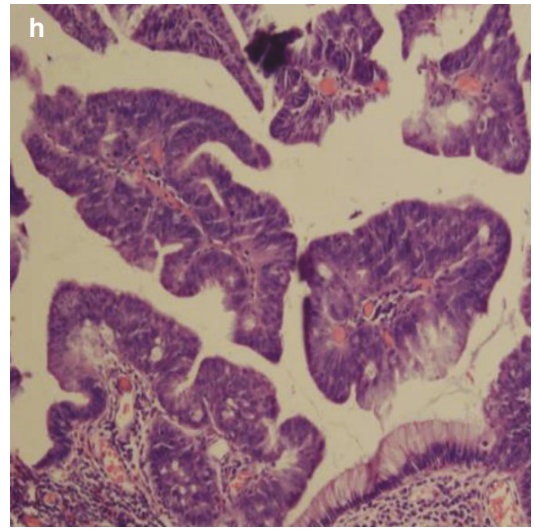

References

1. Zhang QW, Teng LM, Zhang XT, et al. Narrow-band imaging in the diagnosis of deep submucosal colorectal cancers: a systematic review and meta-analysis. Endoscopy. 2017;49:564–80.
2. Uraoka T, Saito Y, Matsuda T, et al. Endoscopic indications for endoscopic mucosal resection of laterally spreading tumours in the colorectum. Gut. 2006;55:1592–7.
3. Yamada M, Saito Y, Sakamoto T, et al. Endoscopic predictors of deep submucosal invasion in colorectal laterally spreading tumors. Endoscopy. 2016;48:456–64.
4. Rotondano G,Bianco MA, Buffoli F, et al. The Cooperative Italian FLIN Study Group: prevalence and clinico-pathological features of colorectal laterally spreading tumors. Endoscopy. 2011;43:856–61.
5. Saitoh Y, Obara T, Watari J, et al. Invasion depth diagnosis of depressed type early colorectal cancers by combined use of videoendoscopy and chromoendoscopy. Gastrointest Endosc. 1998;48:362–70.
6. Kobayashi N, Saito Y, Sano Y, et al. Determining the treatment strategy for colorectal neoplastic lesions: endoscopic assessment or the non-lifting sign for diagnosing invasion depth? Endoscopy. 2007;39:701–5.
7. Matsuda T, Fujii T, Saito Y, et al. Efficacy of the invasive/non-invasive pattern by magnifying chromoendoscopy to estimate the depth of invasion of early colorectal neoplasms. Am J Gastroenterol. 2008;103:2700–6.
8. Zhang QW, Zhang XT, Zhou Y, et al. A trend of preference of magnifying chromoendoscopy to narrow band imaging in diagnosis of T1 colorectal cancer with deep invasion could be observed. Am J Gastroenterol. 2017;112:512–4.
9. Zhang JJ, Gu LY, Chen XY, et al. Endoscopic diagnosis of invasion depth for early colorectal carcinomas: a prospective comparative study of narrow-band imaging, acetic acid, and crystal violet. Medicine (Baltimore). 2015;94:e528.
10. Zhu LY, Ren L, Ge Z, Li XB. Observation of microvessels and invasion in early colorectal neoplasms on narrow band imaging: combination with CD34 and matrix metalloproteinase-7 expression. Eur J Gastroenterol Hepatol. 2014;26:1428–33.
11. Sano Y, Tanaka S, Kudo SE, et al. NBI magnifying endoscopic classification of colorectal tumors proposed by the Japan NBI Expert Team (JNET). Dig Endosc. 2016;28:526–33.
12. Sumimoto K, Tanaka S, Shigita K, et al. Clinical impact and characteristics of the narrow-band imaging magnifying endoscopic classification of colorectal tumors proposed by the Japan NBI Expert Team. Gastrointest Endosc. 2017;85:816–21.
13. Sano Y, Hirata D, Saito Y. The JNET classification. Dig Endosc: NBI magnifying endoscopic classification of colorectal tumors. Dig Endosc. 2018;30:543–45.
14. Sumimoto K, Tanaka S, Shigita K, et al. The diagnostic performance of JNET classification for differentiation among noninvasive, superficially invasive, and deeply invasive colorectal neoplasia. Gastrointest Endosc. 2017;86:700–9.
15. Minoda Y, Ogino H, Chinen T, et al. The objective validity of the JNET classification system for the differential diagnosis of colorectal polyps. Dig Endosc. 2019;31:544–51.
16. Backes Y, Schwartz MP, Ter Borg F, et al. Multicentre prospective evaluation of real-time optical diagnosis of T1 colorectal cancer in large non-pedunculated colorectal polyps using narrow band imaging (the OPTICAL study). Gut. 2019;68:271–9.
17. Hewett DG, Kaltenbach T, Sano Y, et al. Validation of a simple classification system for endoscopic diagnosis of small colorectal polyps using narrow-band imaging. Gastroenterology. 2012;143:599–607 e1.
18. Hayashi N, Tanaka S, Hewett DG, et al. Endoscopic prediction of deep submucosal invasive carcinoma: validation of the narrow-band imaging international colorectal endoscopic (NICE) classification. Gastrointest Endosc. 2013;78:625–32.

18 Case Atlas and Illustrations of Early GI Cancers: Colon

Pises Pisespongsa

The NICE type 1 polyps are most likely nonneoplastic. The color of polyps is similar to or lighter than the background; there is no blood vessels or only isolated lacy vessels on the surface. The surface may show uniform dark spots (Fig. 18.1), white spots (Fig. 18.2), or absence of surface pattern [1] (Fig. 18.3).

The NICE type 2 polyps are most likely intramucosal neoplasia. Their color is darker than the background. There are brown blood vessels surrounding white structures which represent pit pattern. These surface pit pattern may be oval

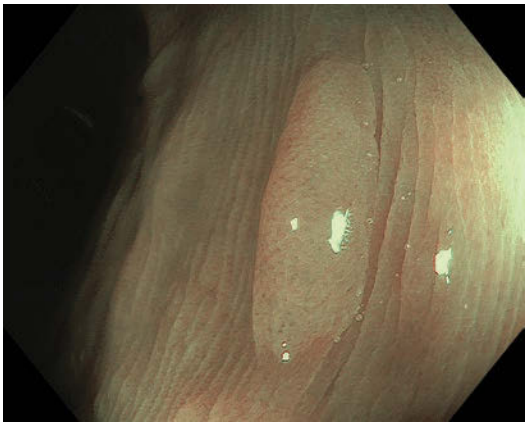

Fig. 18.1 Hyperplastic polyp with uniform dark spots

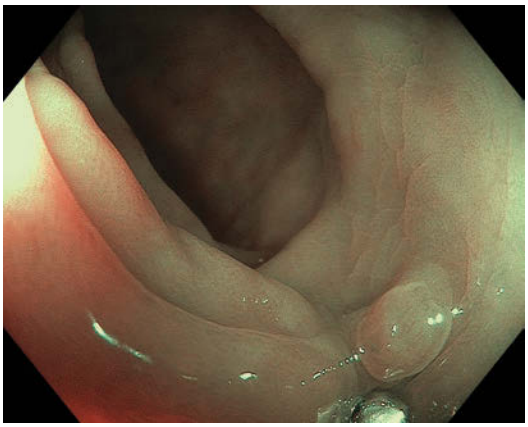

Fig. 18.2 Hyperplastic polyp with uniform white spots

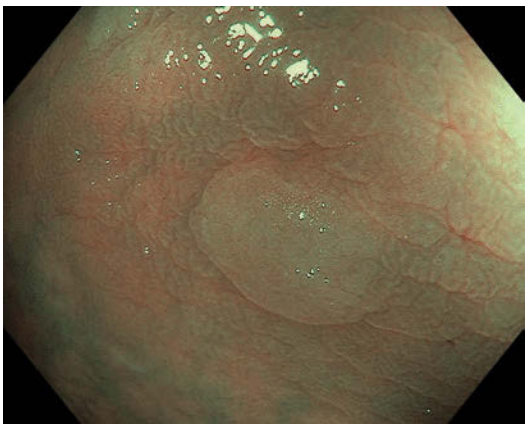

Fig. 18.3 Hyperplastic polyp with absence of surface pattern

P. Pisespongsa (✉)
Bumrungrad International Hospital, Bangkok, Thailand

P. W. Y. Chiu et al. (eds.), *Endoscopy in Early Gastrointestinal Cancers, Volume 1*,
https://doi.org/10.1007/978-981-10-6769-3_18

(Fig. 18.4), tubular (Fig. 18.5), or branched pattern [1] (Fig. 18.6).

The NICE type 3 polyps are most likely invasive cancer. In this group, the color is darker than the background. Moreover, they have area of disrupted blood vessels and the surface pattern are absent [1] (Fig. 18.7).

However, the NICE classification has limitations for differentiation of sessile serrated polyps [2] which are also the precursor lesions of colorectal cancer. The "Workgroup serrAted polypS and Polyposis" (WASP) classification combines four features, namely, cloud-like surface, indistinct border, irregular shape, and dark spots inside the crypts into the NICE classification and the polyps with at least two features should be considered sessile serrated lesions [3] (Figs. 18.8 and 18.9). The mucus cap is a common feature of sessile serrated lesions as well [4] (Fig. 18.10). Some of the sessile serrated lesions may have NICE classification type 1 (Figs. 18.11 and 18.12) while the others may have NICE classification type 2 [3] (Figs. 18.13 and 18.14).

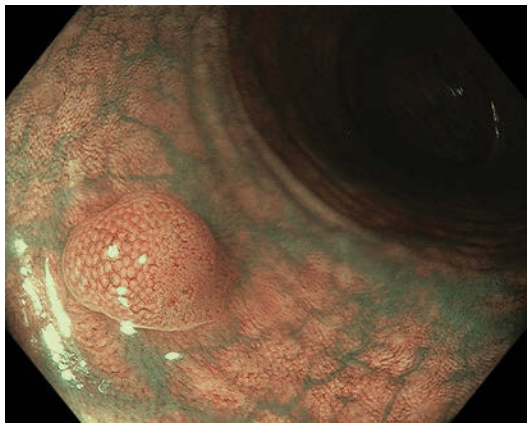

Fig. 18.4 Tubular adenoma with oval surface pattern

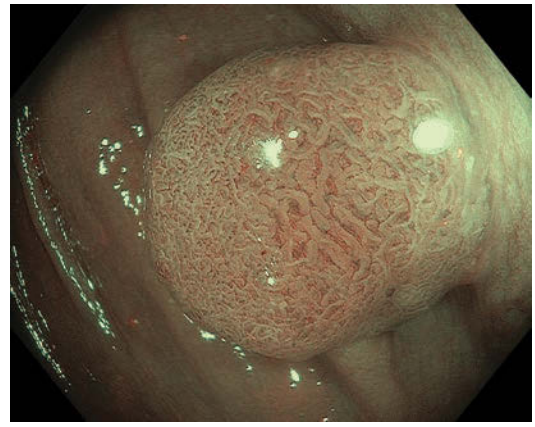

Fig. 18.6 Tubular adenoma with branched surface pattern

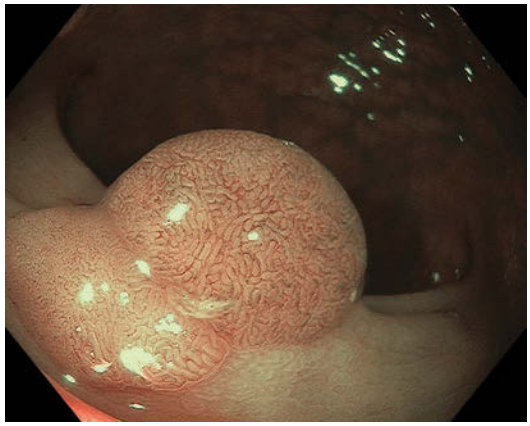

Fig. 18.5 Tubular adenoma with tubular surface pattern

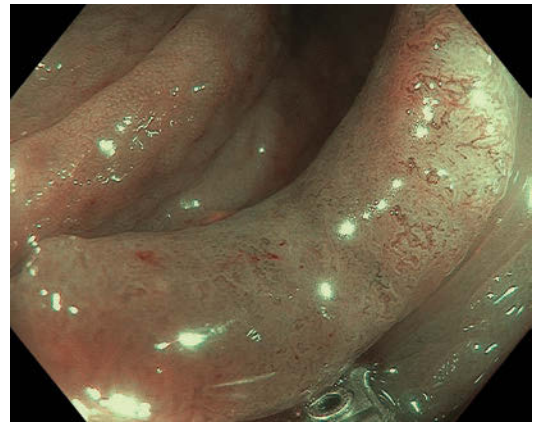

Fig. 18.7 Colonic carcinoma

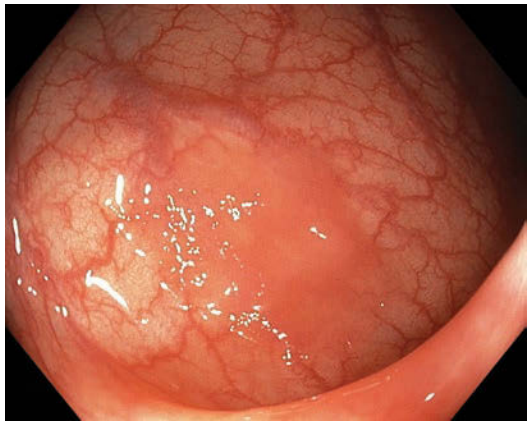

Fig. 18.8 Sessile serrated lesion with white light imaging

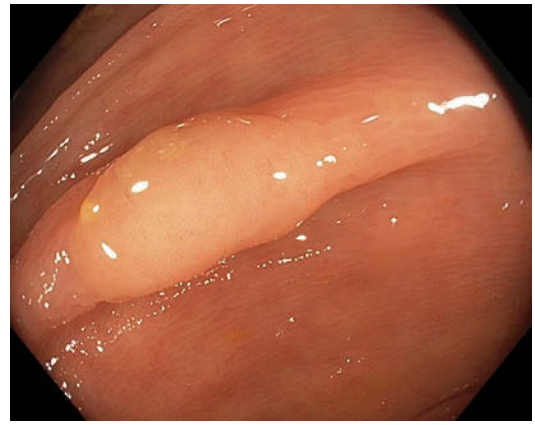

Fig. 18.11 Sessile serrated lesion

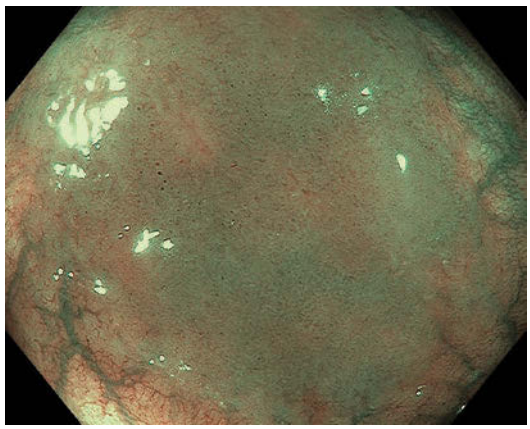

Fig. 18.9 Sessile serrated lesion with cloud-like surface, indistinct border, irregular shape, and dark spots inside the crypts

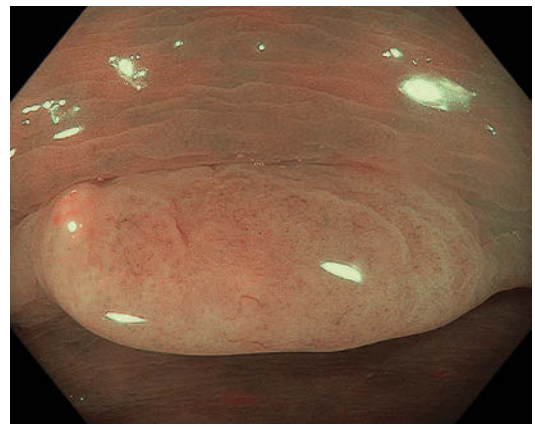

Fig. 18.12 Sessile serrated lesion with NICE 1 pattern

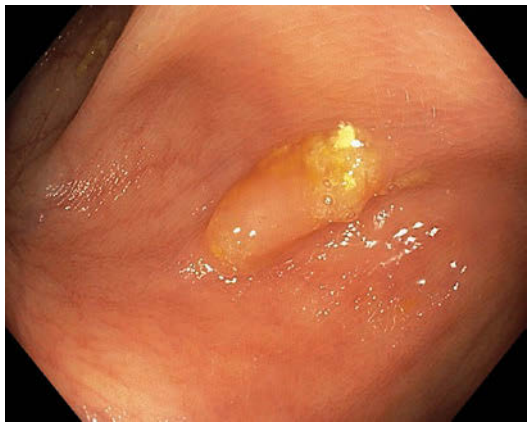

Fig. 18.10 Sessile serrated lesion with mucus cap

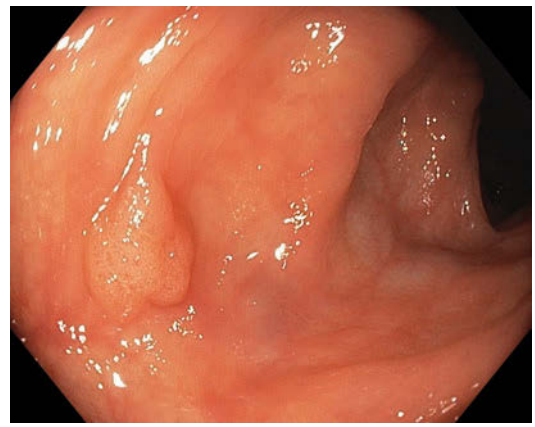

Fig. 18.13 Sessile serrated lesion with white light imaging

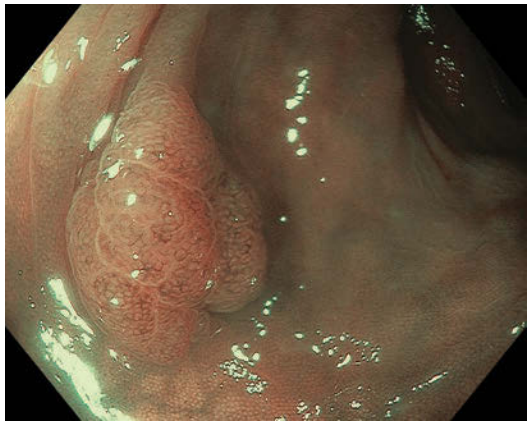

Fig. 18.14 Sessile serrated lesion with NICE 2 pattern

References

1. Sano Y, Tanaka S, Kudo SE, Saito S, et al. Narrow-band imaging (NBI) magnifying endoscopic classification of colorectal tumors proposed by the Japan NBI Expert Team. Dig Endosc. 2016;28:526–33.
2. Kumar S, Fioritto A, Mitani A, et al. Optical biopsy of sessile serrated adenomas: do these lesions resemble hyperplastic polyps under narrow-band imaging? Gastrointest Endosc. 2013;78:902–9.
3. East JE, Vleugels JL, Roelandt P, et al. Advanced endoscopic imaging: European Society of Gastrointestinal Endoscopy (ESGE) Technology Review. Endoscopy. 2016;48:1029–45.
4. Kolb JM, Soetikno RM, Rao AK, et al. Detection, diagnosis, and resection of sessile serrated adenomas and polyps. Gastroenterology. 2017;153:646–8.

Case Atlas and Illustrations: Upper GI

19

Vikneswaran Namasivayam

19.1 Case 1

An 80-year-old male was referred for further management of a gastric lesion diagnosed on evaluation of iron deficiency anemia. Physical examination was unremarkable. OGD showed a 0IIa lesion at the antrum lesser curve extending to the incisura with two focal ulceration seen raising possibility of deeper invasion. ESD was performed and histology showed gastric adenocarcinoma with superficial submucosal invasion that was within the expanded criteria.

Diagnosis: Gastric adenocarcinoma with superficial submucosal invasion within expanded criteria.

Discussion: The presence of early gastric cancer is first suspected on WLE by the presence of an irregular color or surface pattern. The NBI diagnosis of early gastric cancer is made based on the presence of a demarcation line in combination with irregular microsurface or microvascular pattern [1, 2]. This patient has a lesion in the antrum lesser curve that extends to the incisura. It is characterized by a red mucosa with subtle elevation and central depression. This is readily appreciated when compared to the surrounding gastric mucosa. NBI reveals the presence of a demarcation line as well as abnormal microsurface pattern and loss of microvascular pattern which is consistent with early gastric cancer. Surveillance OGD following ESD reveals mucosal healing on WLE and NBI.

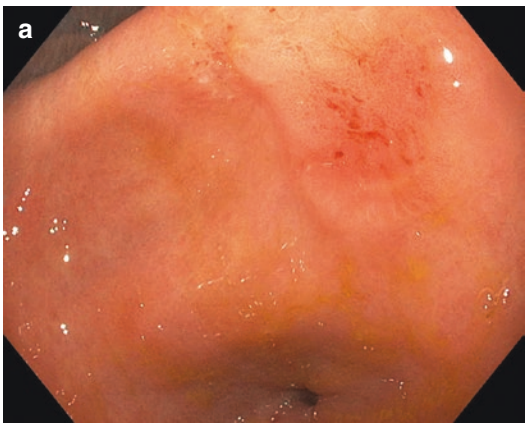

Fig. 19.1a WLE of gastric lesion

V. Namasivayam (✉)
Department of Gastroenterology and Hepatology, Singapore General Hospital, Singapore, Singapore

Duke NUS Medical School, Singapore, Singapore

Yong Loo Lin School of Medicine, Singapore, Singapore
e-mail: vikneswaran.namasivayam@singhealth.com.sg

P. W. Y. Chiu et al. (eds.), *Endoscopy in Early Gastrointestinal Cancers, Volume 1*,
https://doi.org/10.1007/978-981-10-6769-3_19

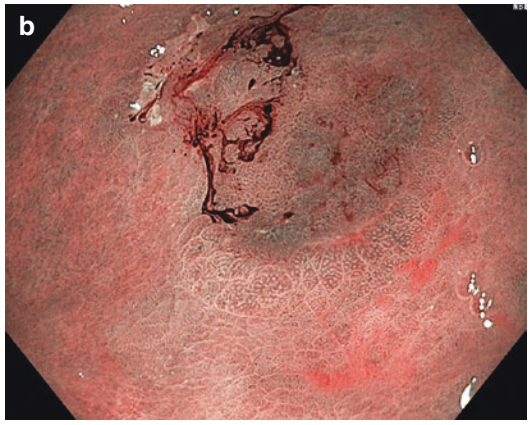

Fig. 19.1b NBI view

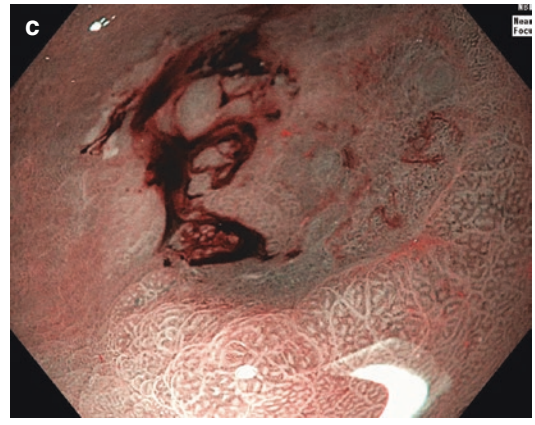

Fig. 19.1c NBI with zoom

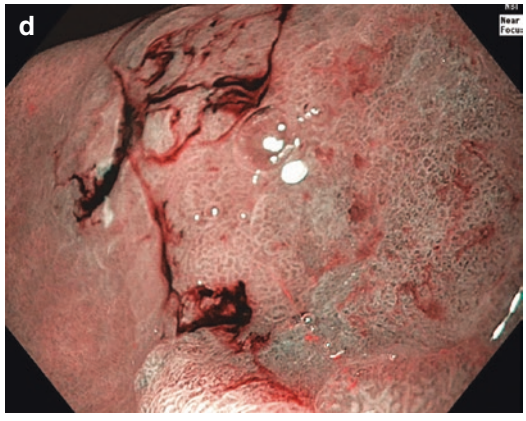

Fig. 19.1d NBI with zoom

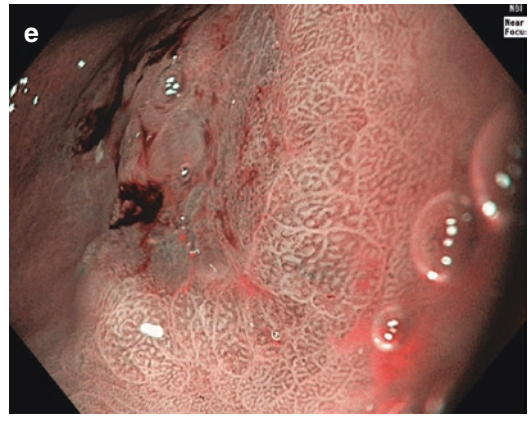

Fig. 19.1e NBI with zoom

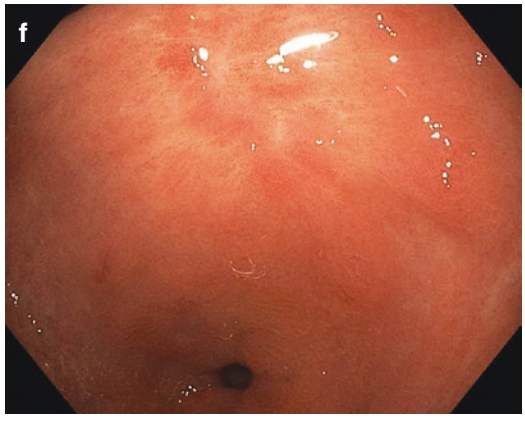

Fig. 19.1f WLE view of surveillance endoscopy after ESD

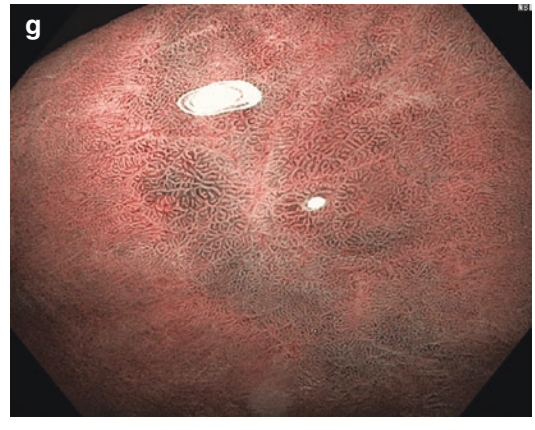

Fig. 19.1g NBI view of surveillance endoscopy after ESD

19.2 Case 2

A 77-year-old female was referred for further management of a gastric lesion diagnosed on evaluation of pernicious anemia. Physical examination was unremarkable. OGD showed a 2 cm prepyloric 0IIa lesion extending to the pyloric ring but not involving the duodenum. NBI imaging revealed white opaque substance (WOS) and relatively regular microsurface pattern in remaining mucosa. Platelet count was 83,000.

ESD was performed. Histology of resected specimen was gastric high-grade dysplasia in background of intestinal metaplasia.

Diagnosis: Gastric prepyloric high-grade dysplasia

Discussion: Pernicious anemia is associated with an increased risk of gastric carcinoma and gastric carcinoid tumors [3]. Magnification endoscopy enables assessment of the microsurface (MS) pattern of the gastric mucosa. NBI with magnification enables assessment of the mucosal microvasculature (MV), which is composed of the subepithelial capillary network (SECN) and collecting venules (CVs). However, in 0IIa gastric lesions the MV pattern may be obscured by WOS [4]. This is evident in this patient who has a WOS deposits with an irregular distribution. WOS correlates with lipid deposits seen on histological specimens after oil red O staining [5]. WOS may be seen in gastric adenoma and carcinoma though more recent studies have described their presence in gastric intestinal metaplasia as well [6]. The presence and distribution of WOS sign may be used as an adjunctive feature in differentiating adenoma (regular, in line with SECN) from carcinoma (irregular) [4].

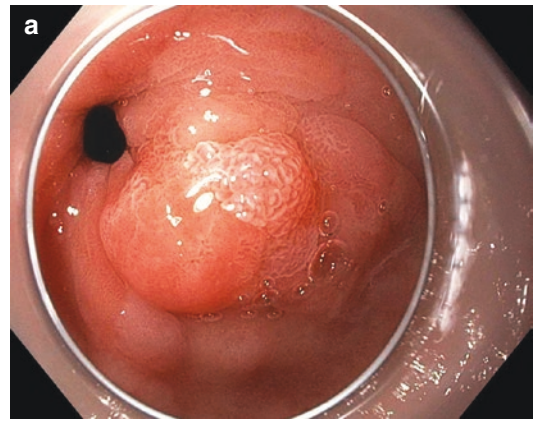

Fig. 19.2a Prepyloric lesion demonstrating WOS pattern on WLE

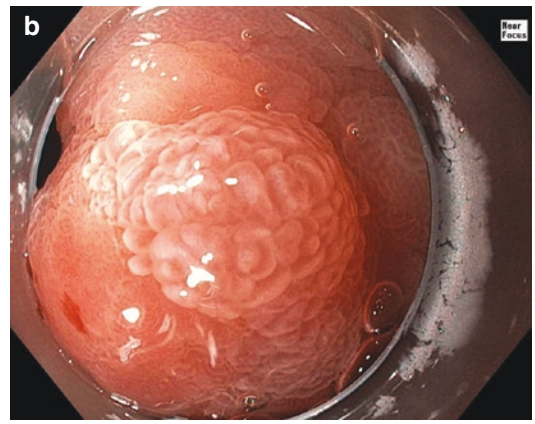

Fig. 19.2b WOS pattern seen on WLE with zoom magnification

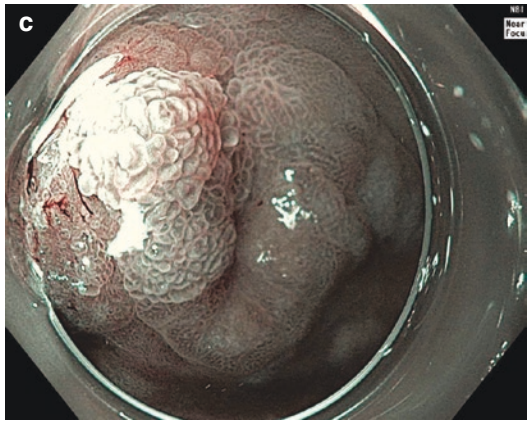

Fig. 19.2c WOS pattern seen on NBI with zoom magnification

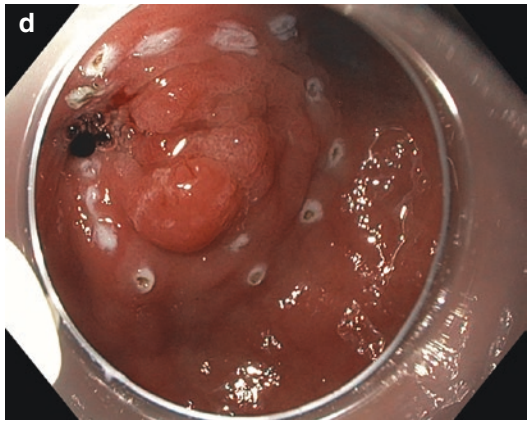

Fig. 19.2d Demarcation of margins for ESD

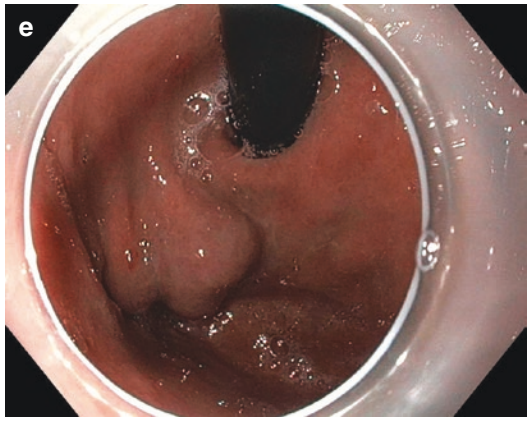

Fig. 19.2e Gastric varix

19.3 Case 3

A 67-year-old male underwent OGD for severe iron and vitamin B12 deficiency anemia (Hb 3.4 g/dL). He had a partial gastrectomy with gastrojejunostomy for peptic ulcer bleeding 40 years ago.

OGD showed two gastric nodules (0Is) in the remnant stomach close to the anastomosis. Endoscopic mucosal resection was performed for both nodules. Histology for both nodules revealed intramucosal adenocarcinoma in a hyperplastic polyp.

Diagnosis: Intramucosal adenocarcinoma in hyperplastic polyps in remnant stomach

Discussion: Gastric carcinoma may develop in the remnant stomach several decades after distal gastrectomy for benign disease [7]. Malignant transformation in gastric hyperplastic polyps is uncommon but is more likely in large polyps more than 2 cm. The presence of malignant transformation may be identified on magnifying NBI by changes in the fine mucosal structures (FMS). A reduction in the FMS (known as micrification) compared to the surrounding reference FMS is indicative of the presence of neoplasia in hyperplastic polyps [8].

ESD in early gastric cancer in the remnant stomach is technically challenging with higher complication rates due to the limited space for manipulation and the presence of staples and severe fibrosis along the anastomosis and suture line. The rate of perforation for ESD is higher in the remnant stomach especially at the anastomotic site [9, 10].

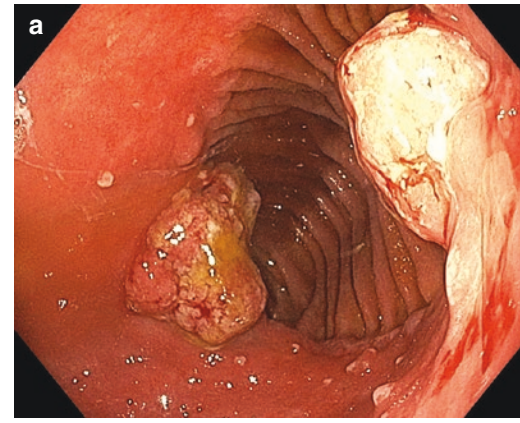

Fig. 19.3a Gastric polyps in remnant stomach

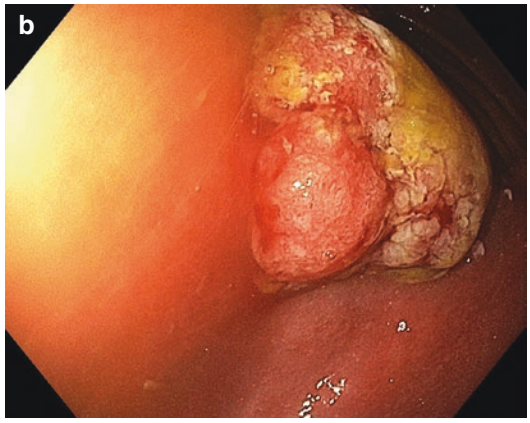

Fig. 19.3b Close up view

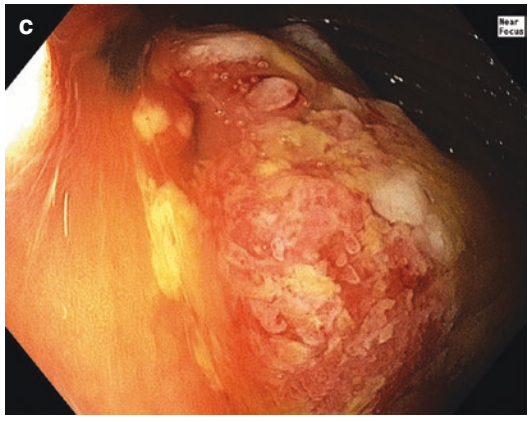

Fig. 19.3c Close up view

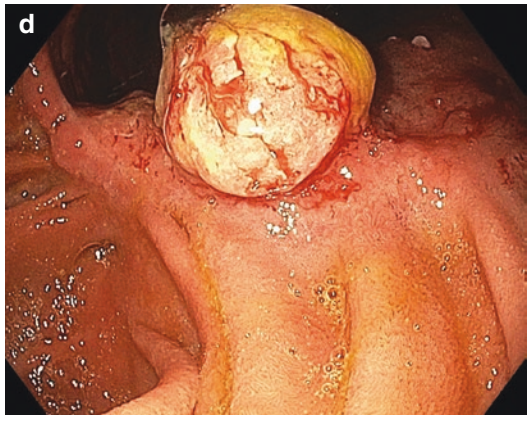

Fig. 19.3d Retroflexed view with WLE

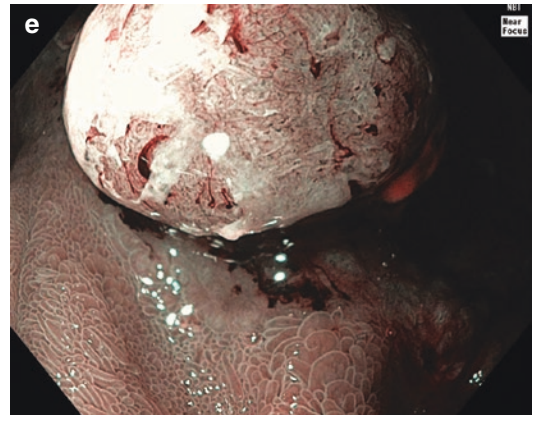

Fig. 19.3e Retroflexed view with NBI zoom

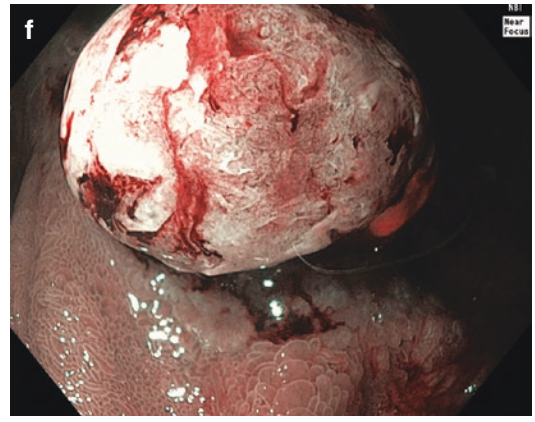

Fig. 19.3f Retroflexed view with NBI zoom

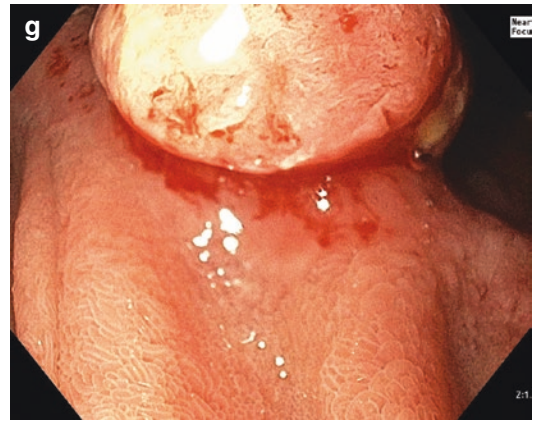

Fig. 19.3g Retroflexed view with WLE zoom

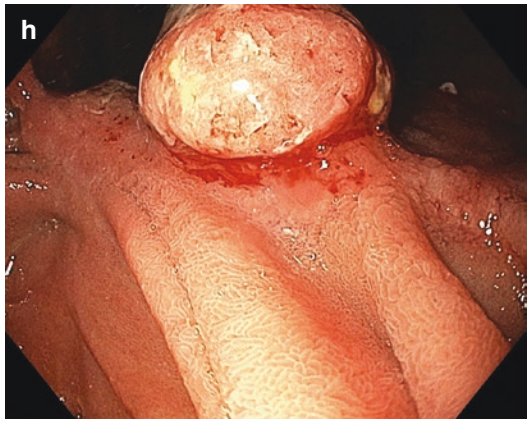

Fig. 19.3h Retroflexed view with WLE

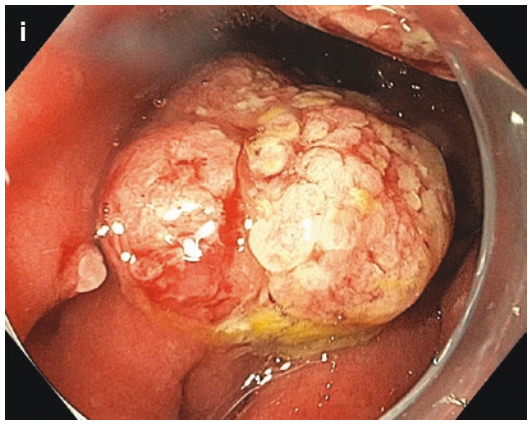

Fig. 19.3i Close up view

19.4 Case 4

A 75-year-old female underwent OGD for unexplained weight loss. It showed a sessile polyp in the gastric body that was resected. Histology was consistent with a gastric hyperplastic polyp.

Diagnosis: Gastric hyperplastic polyp

Discussion: WLE examination reveals a red polypoid lesion with a smooth surface. NBI examination reveals that this polyp has a regular MV and MS (villous) pattern [11]. Malignant transformation is uncommon in gastric hyperplastic polyps. In this patient, there is no evidence of any white opaque substance or micrification within the polyp. This is consistent with the benign histology and absence of malignant transformation [8].

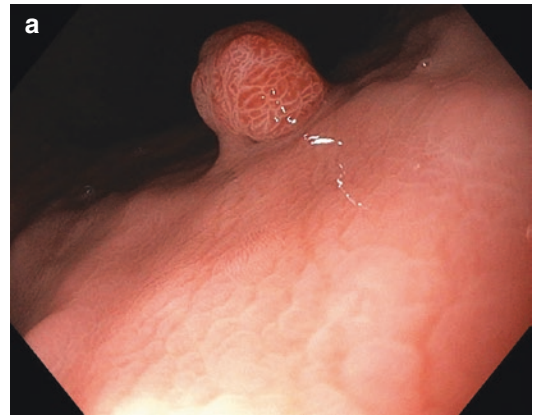

Fig. 19.4a WLE gastric polyp

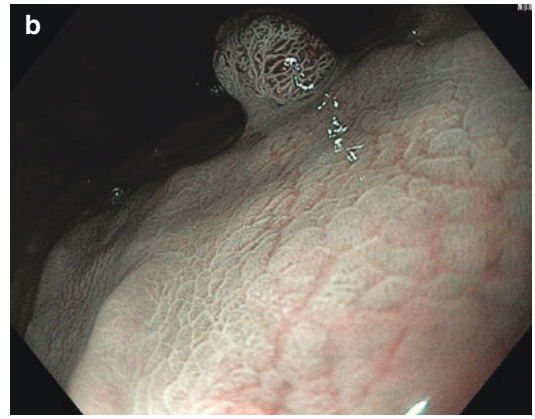

Fig. 19.4b NBI gastric polyp

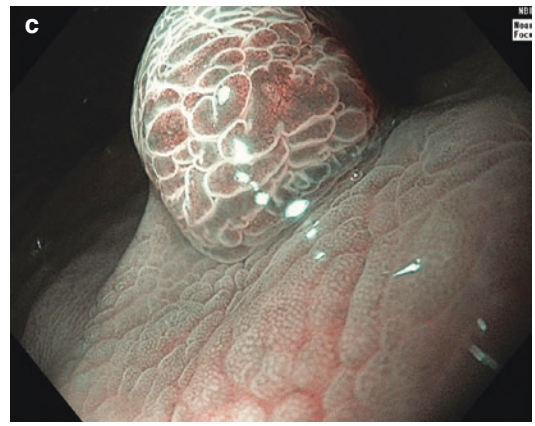

Fig. 19.4c NBI with zoom gastric polyp

19.5 Case 5

A 56-year-old female underwent gastroscopy for iron and vitamin B12 deficiency anemia. Her intrinsic factor antibody was positive. OGD showed gastric atrophy which was clearly evident even on white light endoscopy.

Diagnosis: Pernicious anemia with gastric atrophy

Discussion: Pernicious anemia and gastric atrophy are associated with an increased risk of gastric carcinoma [3, 12]. Careful examination on white light endoscopy is crucial as the recognition of gastric atrophy, would prompt a more careful survey for the possible presence of early gastric cancers.

While gastric atrophy is a histological diagnosis, its presence may be predicted by endoscopic features [13]. These would include mucosal discoloration, prominent submucosal vascular pattern due to mucosal thinning, uneven surfaces, and disappearance of folds.

In this patient, the mucosal thinning exposes the underlying submucosal vascular pattern. NBI with optical zoom further characterizes the marked atrophy in the gastric mucosa. The collecting venules are very prominent but the honeycomb-like subepithelial capillary network pattern can hardly be identified. Neither marginal crypt epithelium nor crypt opening can be identified in the atrophic mucosa. These findings are consistent with gastric atrophy.

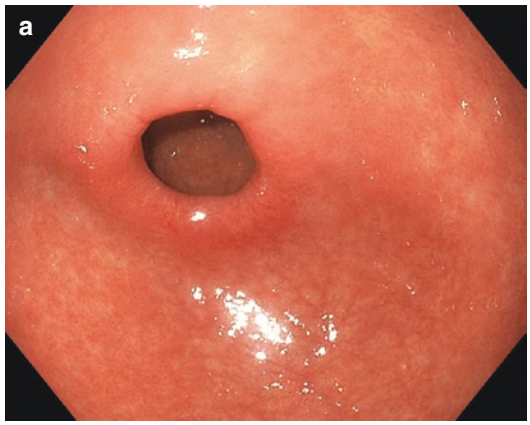

Fig. 19.5a WLE gastric atrophy at antrum

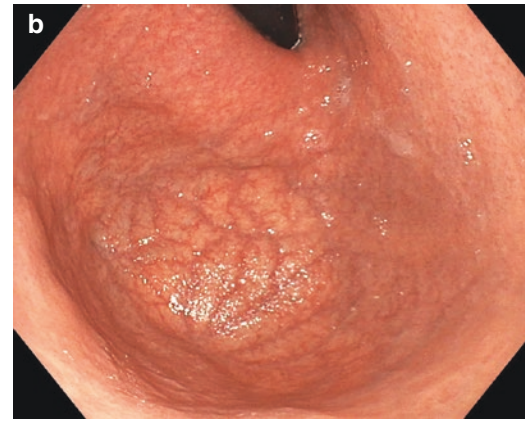

Fig. 19.5b WLE gastric atrophy at fundus

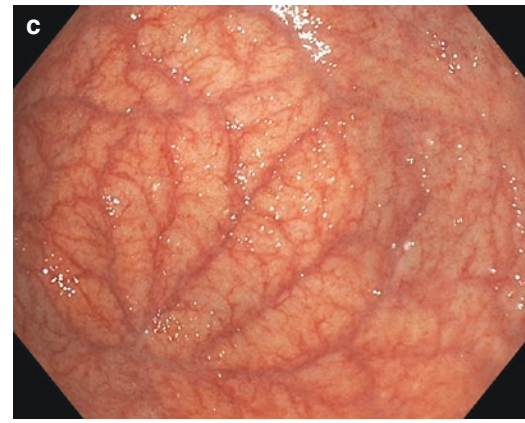

Fig. 19.5c WLE gastric atrophy at fundus close-up view

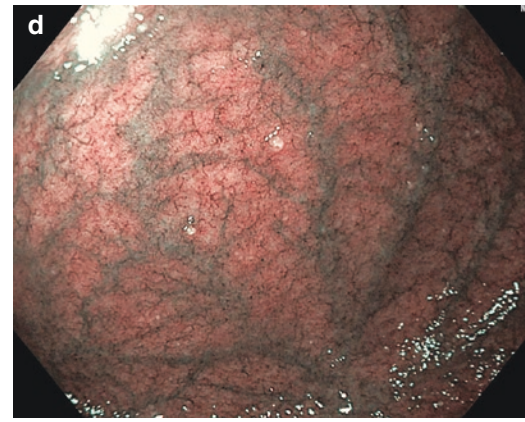

Fig. 19.5d NBI gastric atrophy

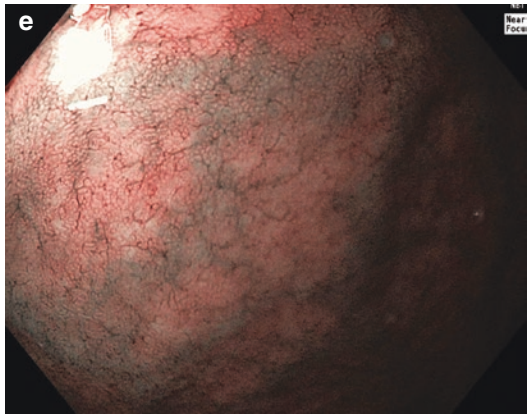

Fig. 19.5e NBI with zoom gastric atrophy

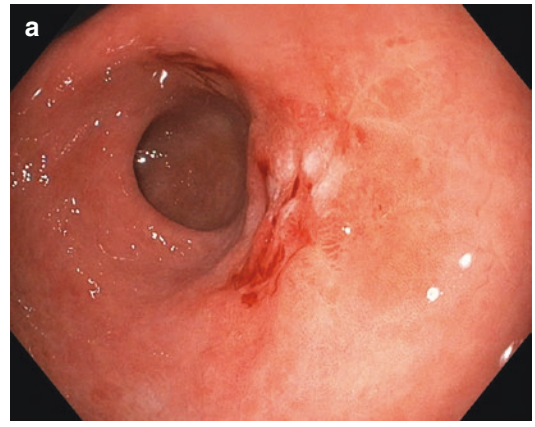

Fig. 19.6a WLE gastric lesion

19.6 Case 6

An 81-year-old female was referred for further evaluation of intermittent epigastric pain. A diagnostic OGD was performed. OGD showed a 0IIa lesion with ulceration extending across the posterior wall of the body to the antrum and incisura.

Diagnosis: Gastric cancer

Discussion: The presence of early gastric cancer may be suspected on WLE by the presence of an irregular color or surface pattern. The diagnosis of early gastric cancer may be made on NBI by the presence of a demarcation line in combination with irregular microsurface and microvascular pattern [1, 2]. This patient has a lesion in the posterior wall of the gastric body which is different in color to the surrounding mucosa and demonstrates superficial elevation. NBI evaluation reveals the presence of a demarcation line and loss of microvascular pattern which, once recognized on NBI, may also be appreciated on WLE as well.

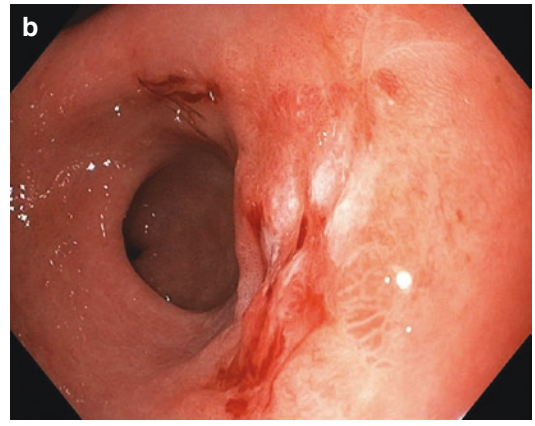

Fig. 19.6b WLE close-up view of gastric lesion

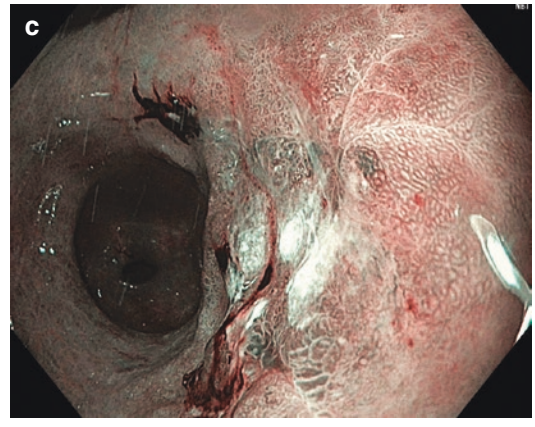

Fig. 19.6c NBI close-up view of gastric lesion

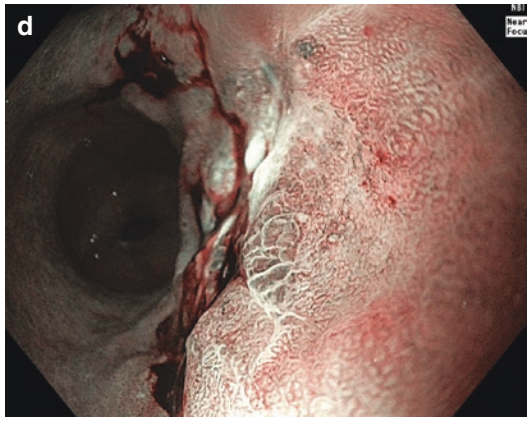

Fig. 19.6d NBI with zoom view of demarcation line and IMVP

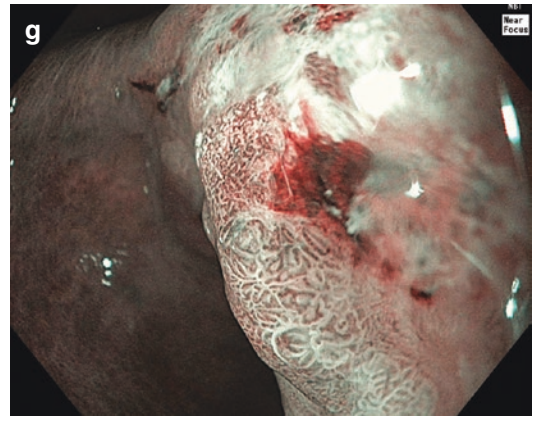

Fig. 19.6g NBI with zoom

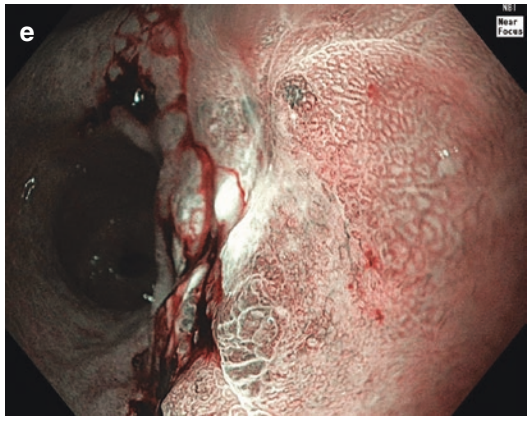

Fig. 19.6e NBI with zoom view of demarcation line and IMVP

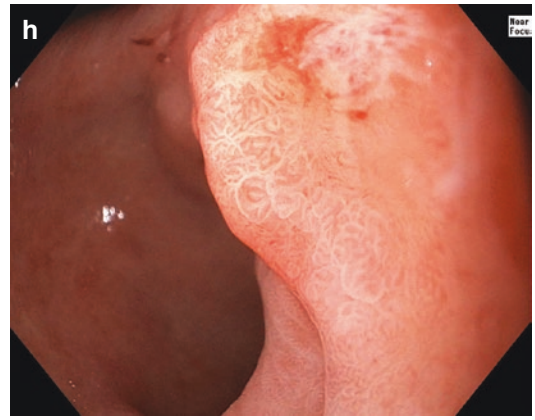

Fig. 19.6h Corresponding area in WLE with zoom

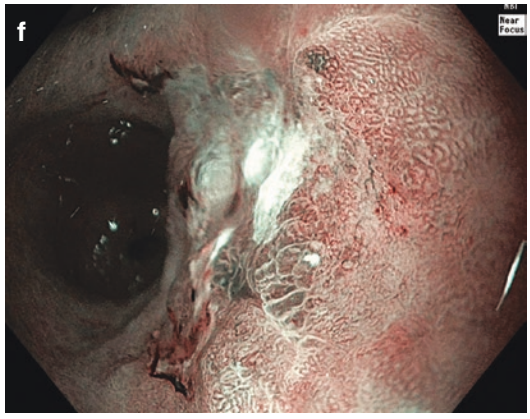

Fig. 19.6f NBI with zoom view of demarcation line and IMVP

19.7 Case 7

A 72-year-old patient underwent OGD for abdominal pain. A previous OGD performed in another country had revealed a H. pylori gastric ulcer which had been treated with eradication therapy.

Diagnosis: Healed gastric ulcer with intestinal metaplasia

Discussion: The identification of a gastric ulcer on OGD raises the possibility of a benign peptic ulcer, malignant ulcer or peptic change within an early gastric cancer. Hence, careful examination is needed to clarify the findings as biopsies may not always be representative. In this

patient, WLE examination reveals abnormal red mucosa in the incisura at the site of the previous gastric ulcer which raises concerns of a sinister diagnosis. However, NBI examination reveals a regular MS, MV pattern and there is no demarcation line. These findings are consistent with gastritis rather than cancer. In addition, light blue crests are seen indicating the presence of intestinal metaplasia.

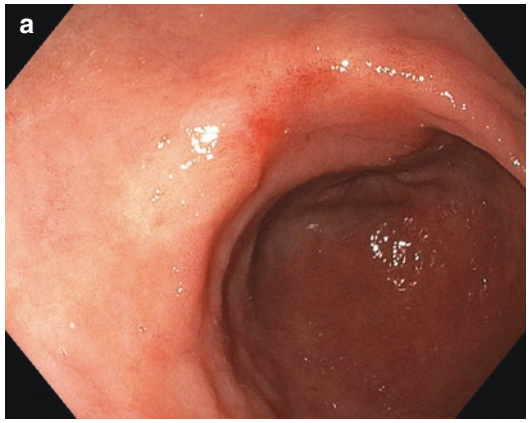

Fig. 19.7a WLE of incisura

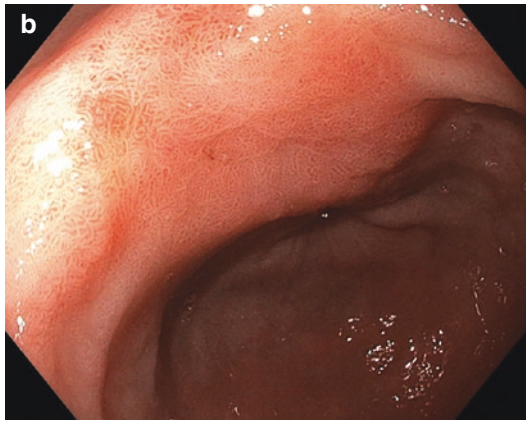

Fig. 19.7b WLE close up view of incisura

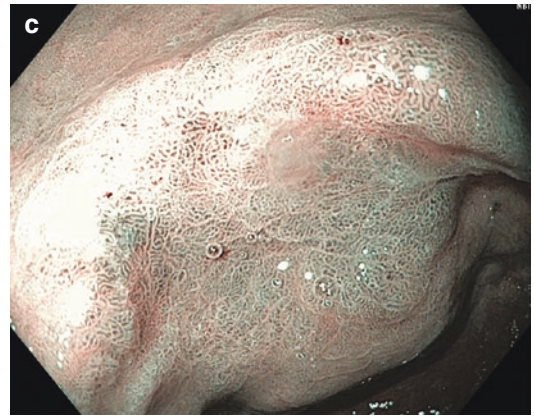

Fig. 19.7c NBI view of incisura

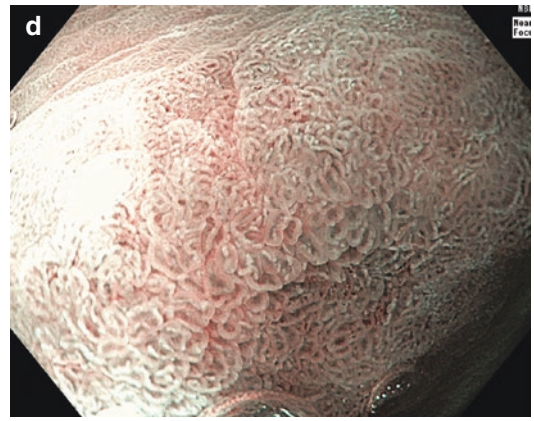

Fig. 19.7d NBI with zoom view of incisura showing light blue crests

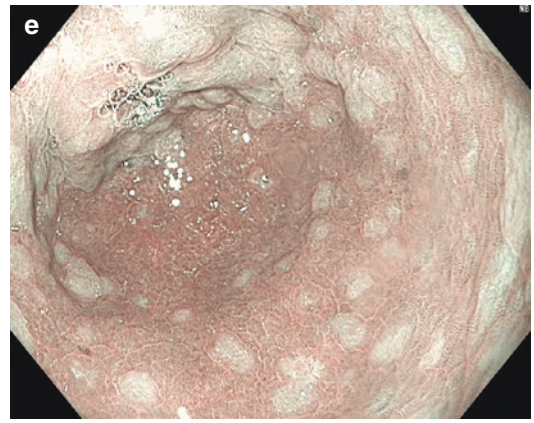

Fig. 19.7e NBI view of antrum

19.8 Case 8

A 77-year-old male was referred for further management of a gastric lesion in the proximal stomach that was diagnosed on endoscopic surveillance for gastric intestinal metaplasia. Biopsies showed gastric low-grade dysplasia. Repeat endoscopy in our unit revealed the presence of a 0IIc lesion in the proximal stomach. Unfortunately the lesion had been tattooed which obscured the borders of the lesion and the MS and MV pattern on NBI. Furthermore, the lesion could not be raised, and hence, endoscopic resection could not be performed.

Diagnosis: Tattoo precludes definitive characterization

Discussion: Extensive biopsies, partial endoscopic removal, and tattooing of lesions that are otherwise amenable to endoscopic resection should be avoided [14]. These maneuvers lead to submucosal fibrosis which makes subsequent ESD technically challenging while increasing the risk of perforation during ESD [15]. The presence of fibrosis is indicated by poor lifting after submucosal injection [16]. The need for tattooing can largely be avoided with adequate photodocumentation of the lesion. Endoscopic tattooing, if needed to guide subsequent surgery, should be placed away from the lesion.

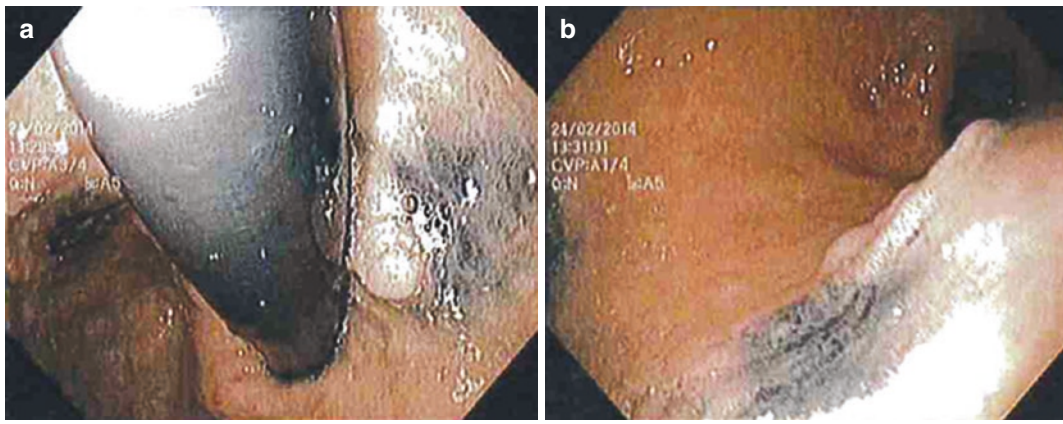

Fig. 19.8 (**a** and **b**) Lesion with tatoo

19.9 Case 9

A 63-year-old female presented with vomiting, weight loss, leg edema, and serum hypoalbuminemia (serum albumin 20 g/L). She was referred for further evaluation of suspected linitis plastica on index endoscopy. OGD showed markedly thickened gastric mucosal folds with adherent mucoid secretion (gastric pH 7) primarily affecting the proximal stomach with relative sparing of the antrum.

Diagnosis: Menetrier's Disease

Discussion: Menetrier's Disease is a rare protein-losing gastropathy characterized by hyperproliferative gastric foveolar epithelium. It is caused by dysregulated epidermal growth factor receptor signaling that leads to expansion of surface mucous cells in the body and fundus of the stomach [17]. The presenting symptoms include epigastric pain, vomiting, generalized edema, and hypoalbuminemia [18]. Endoscopy demonstrates enlargement of gastric folds which is usually confined to the oxyntic mucosa (body and fundus). Sparing of the antrum is typical but not invariable [19]. Diagnosis is confirmed by biopsies showing marked foveolar hyperplasia and glandular atrophy and a paucity of inflammatory infiltrates. The demonstration of glandular atrophy may require full-thickness mucosal biopsies. The differential diagnoses would include polyps and polyposis syndromes. These are differentiated from Menetrier's Disease by family history, extra-gastric manifestations, genetic testing, endoscopic appearance, and histological presentation. Juvenile polyposis syndrome (JPS) patients may have colonic polyps or a family history of JPS. Cronkhite–Canada syndrome may have characteristic hyperpigmentation, hair and nail changes in addition to multiple hamartomatous polyps throughout the gastrointestinal tract [19]. Other differential diagnoses to consider would include lymphoma, gastric carcinoma, gastrointestinal stromal tumors (GIST), tuberculosis, or other infiltrative disease [17]. CMV associated forms of Menetrier's Disease have been described [20, 21]. Cetuximab, a monoclonal antibody to the epidermal growth factor receptor, has been reported to be an effective treatment for Menetrier's Disease [22]. There have also been reports of remission with H. pylori eradication.

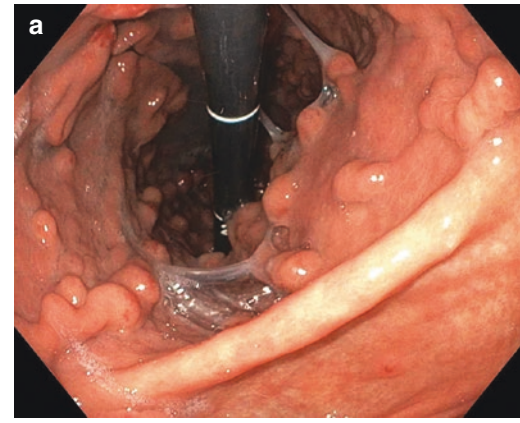

Fig. 19.9a Prominent folds in proximal stomach with mucoid secretions

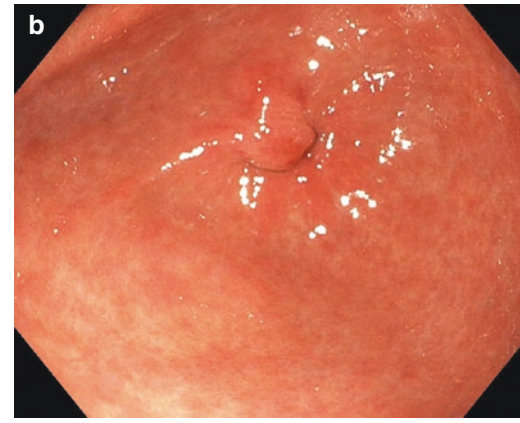

Fig. 19.9b Antrum is relatively normal

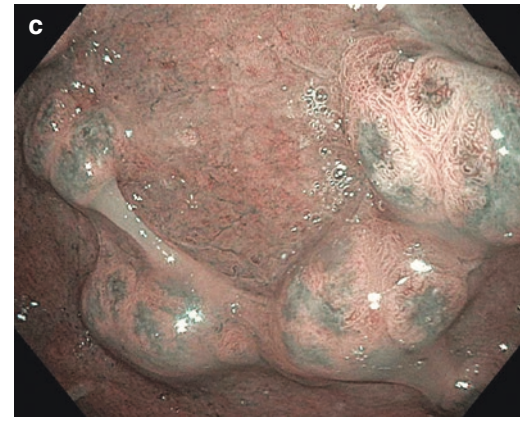

Fig. 19.9c Appearance on NBI

References

1. Yao K. The endoscopic diagnosis of early gastric cancer. Ann Gastroenterol. 2013;26(1):11–22.
2. Ezoe Y, Muto M, Uedo N, Doyama H, Yao K, Oda I, et al. Magnifying narrowband imaging is more accurate than conventional white-light imaging in diagnosis of gastric mucosal cancer. Gastroenterology. 2011;141(6):2017–25. e3
3. Murphy G, Dawsey SM, Engels EA, Ricker W, Parsons R, Etemadi A, et al. Cancer Risk After Pernicious Anemia in the US Elderly Population. Clin Gastroenterol Hepatol. 2015;13(13):2282–9 e1-4.
4. Yao K, Iwashita A, Tanabe H, Nishimata N, Nagahama T, Maki S, et al. White opaque substance within superficial elevated gastric neoplasia as visualized by magnification endoscopy with narrow-band imaging: a new optical sign for differentiating between adenoma and carcinoma. Gastrointest Endosc. 2008 Sep;68(3):574–80.
5. Yao K, Iwashita A, Nambu M, Tanabe H, Nagahama T, Maki S, et al. Nature of white opaque substance in gastric epithelial neoplasia as visualized by magnifying endoscopy with narrow-band imaging. Dig Endosc. 2012 Nov;24(6):419–25.
6. Kanemitsu T, Yao K, Nagahama T, Imamura K, Fujiwara S, Ueki T, et al. Extending magnifying NBI diagnosis of intestinal metaplasia in the stomach: the white opaque substance marker. Endoscopy. 2017 Jun;49(6):529–35.
7. Shimada H, Fukagawa T, Haga Y, Oba K. Does remnant gastric cancer really differ from primary gastric cancer? A systematic review of the literature by the Task Force of Japanese Gastric Cancer Association. Gastric Cancer. 2016;19(2):339–49.
8. Horiuchi H, Kaise M, Inomata H, Yoshida Y, Kato M, Toyoizumi H, et al. Magnifying endoscopy combined with narrow band imaging may help to predict neoplasia coexisting with gastric hyperplastic polyps. Scand J Gastroenterol. 2013;48(5):626–32.
9. Takenaka R, Kawahara Y, Okada H, Tsuzuki T, Yagi S, Kato J, et al. Endoscopic submucosal dissection for cancers of the remnant stomach after distal gastrectomy. Gastrointest Endosc. 2008;67(2):359–63.
10. Tanaka S, Toyonaga T, Morita Y, Fujita T, Yoshizaki T, Kawara F, et al. Endoscopic submucosal dissection for early gastric cancer in anastomosis site after distal gastrectomy. Gastric Cancer. 2014;17(2):371–6.
11. Omori T, Kamiya Y, Tahara T, Shibata T, Nakamura M, Yonemura J, et al. Correlation between magnifying narrow band imaging and histopathology in gastric protruding/or polypoid lesions: a pilot feasibility trial. BMC Gastroenterol. 2012;12:17.
12. Uemura N, Okamoto S, Yamamoto S, Matsumura N, Yamaguchi S, Yamakido M, et al. Helicobacter pylori infection and the development of gastric cancer. N Engl J Med. 2001;345(11):784–9.
13. Kono S, Gotoda T, Yoshida S, Oda I, Kondo H, Gatta L, et al. Can endoscopic atrophy predict histological atrophy? Historical study in United Kingdom and Japan. World J Gastroenterol. 2015;21(46):13113–23.
14. Kim HG, Thosani N, Banerjee S, Chen A, Friedland S. Effect of prior biopsy sampling, tattoo placement, and snare sampling on endoscopic resection of large nonpedunculated colorectal lesions. Gastrointest Endosc. 2015;81(1):204–13.
15. Kim JH, Nam HS, Choi CW, Kang DH, Kim HW, Park SB, et al. Risk factors associated with difficult gastric endoscopic submucosal dissection: predicting difficult ESD. Surg Endosc. 2017;31(4):1617–26.
16. Takeuchi Y, Iishi H, Tanaka S, Saito Y, Ikematsu H, Kudo SE, et al. Factors associated with technical difficulties and adverse events of colorectal endoscopic submucosal dissection: retrospective exploratory factor analysis of a multicenter prospective cohort. Int J Color Dis. 2014;29(10):1275–84.
17. Coffey RJ, Washington MK, Corless CL, Heinrich MC. Menetrier disease and gastrointestinal stromal tumors: hyperproliferative disorders of the stomach. J Clin Invest. 2007;117(1):70–80.
18. Meuwissen SG, Ridwan BU, Hasper HJ, Innemee G. Hypertrophic protein-losing gastropathy. A retrospective analysis of 40 cases in The Netherlands. The Dutch Menetrier Study Group. Scand J Gastroenterol Suppl. 1992;194:1–7.
19. Rich A, Toro TZ, Tanksley J, Fiske WH, Lind CD, Ayers GD, et al. Distinguishing Menetrier's disease from its mimics. Gut. 2010;59(12):1617–24.
20. Setakhr V, Muller G, Hoang P, Lambert AS, Geubel A. Cytomegalovirus-associated protein losing gastropathy in an immunocompetent adult: a case report. Acta Gastro-Enterol Belg. 2007;70(3):296–9.
21. Drut RM, Gomez MA, Lojo MM, Drut R. Cytomegalovirus-associated Menetrier's disease in adults. Demonstration by polymerase chain reaction (PCR). Medicina. 1995;55(6):659–64.
22. Fiske WH, Tanksley J, Nam KT, Goldenring JR, Slebos RJ, Liebler DC, et al. Efficacy of cetuximab in the treatment of Menetrier's disease. Sci Transl Med. 2009;1(8):8ra18.

Case Atlas and Illustrations: Colon

20

Supakij Khomvilai

20.1 Case 1

68 years old male screening colorectal cancer

- Location: Rectum
- Morphology: 0+Is size 3 mm
- NBI: NICE 2 (JNET 2A)
- Treatment: EMR
- Pathology: Tubular adenoma

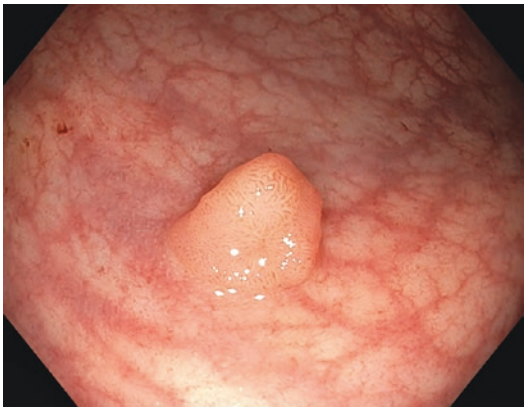

A reddish sessile lesion

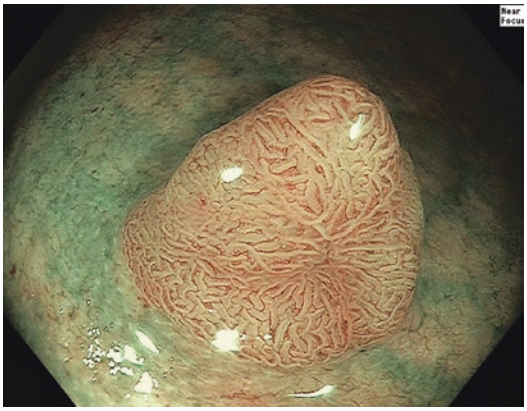

A regular caliber and tubular surface pattern can be seen

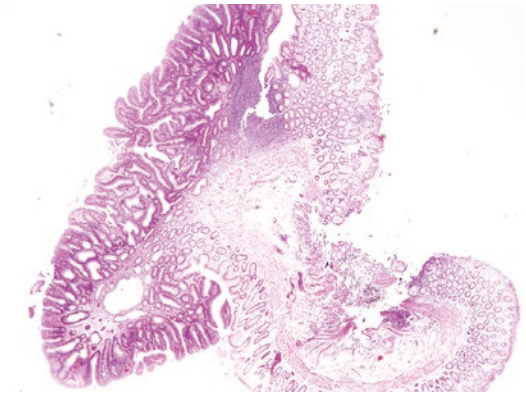

A tubular adenoma with low grade dysplasia

S. Khomvilai (✉)
King chulalongkorn memorial hospital, Bangkok, Thailand
e-mail: supakij.k@chulahospital.org

P. W. Y. Chiu et al. (eds.), *Endoscopy in Early Gastrointestinal Cancers, Volume 1*,
https://doi.org/10.1007/978-981-10-6769-3_20

20.2 Case 2

77 years old male screening colorectal cancer

- Location: Rectosigmoid
- Morphology: 0+IIa+IIc size 2 cm
- NBI: NICE 3 (JNET 3)
- Treatment: Laparoscopic anterior resection
- Pathology: Moderate differentiated adenocarcinoma invade to muscularis propria no LVI no LN pT2N0Mx

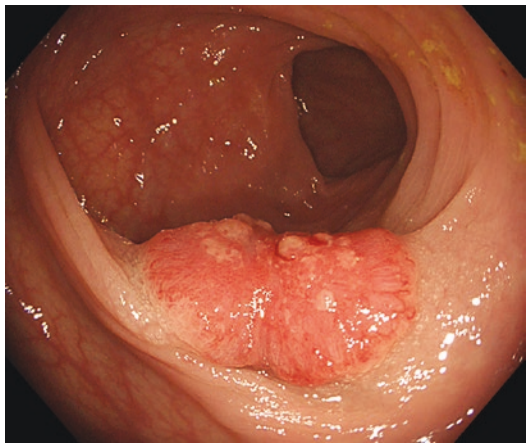

A flat elevated with irregular surface tumor can be seen

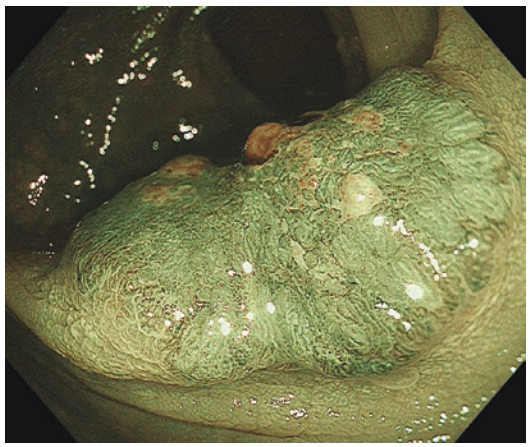

Loose vessel areas can be seen

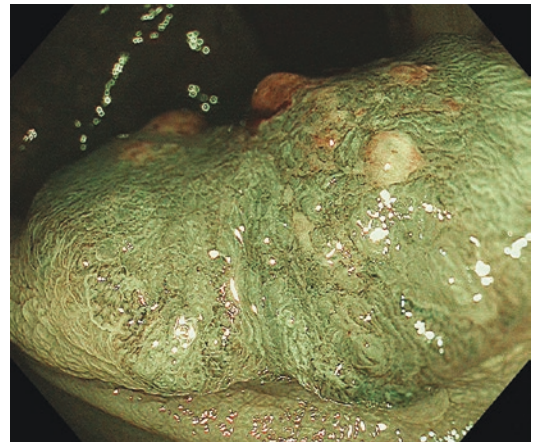

An amorphous area can be seen

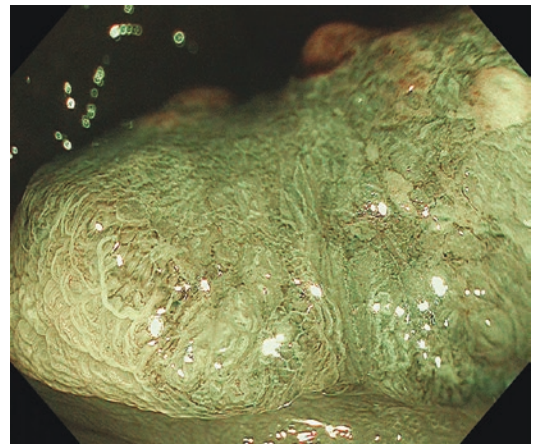

Loose vessel areas can be seen

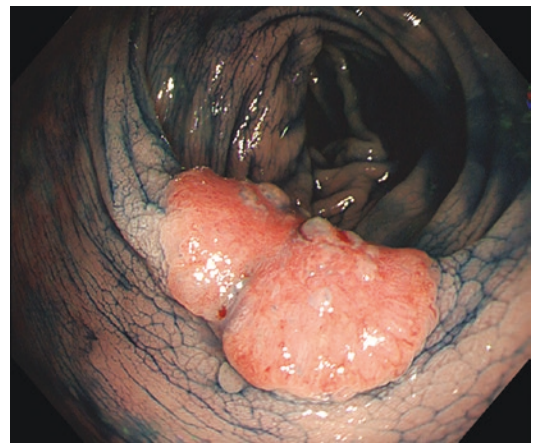

A indigocarmine spraying view. A depressed area with irregular surface can be seen

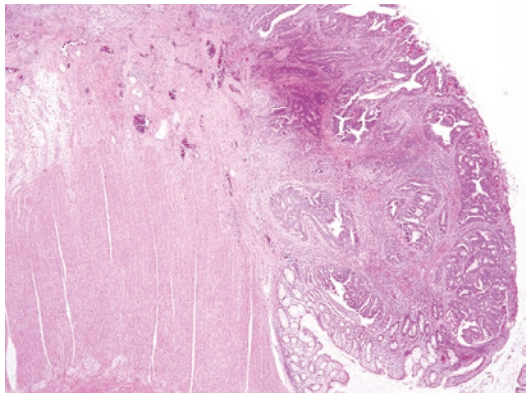

A histology reveales moderate differentiated adeno carcinoma invade to musulavis propria (pMP)

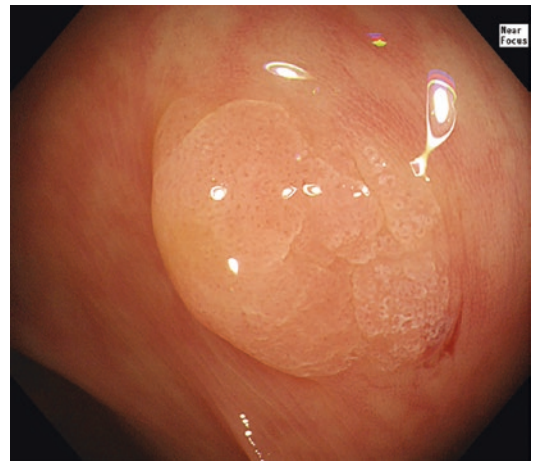

A whity sessile lesion can be seen

20.3 Case 3

62 years old female bowel habit change

- Location: Ascending colon
- Morphology: 0+Is size 5 mm
- NBI: NICE 1 (JNET 1)
- Treatment: EMR
- Pathology: Sessile serrated lesion

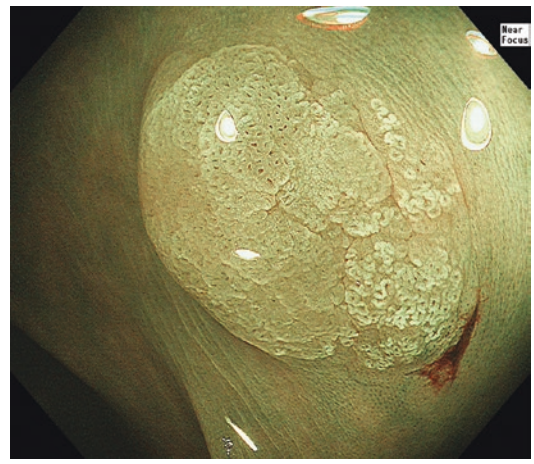

The lesion showed acloud-like surfase. Dilated crypts can be seen in upper part of the lesion

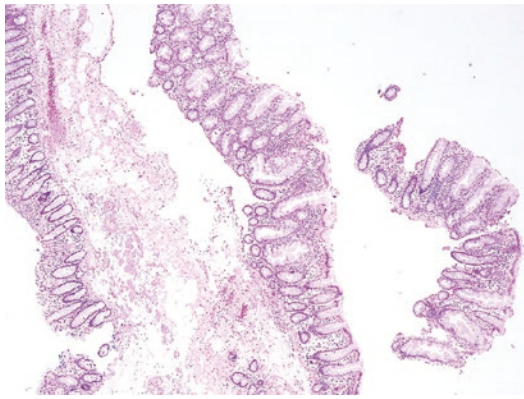

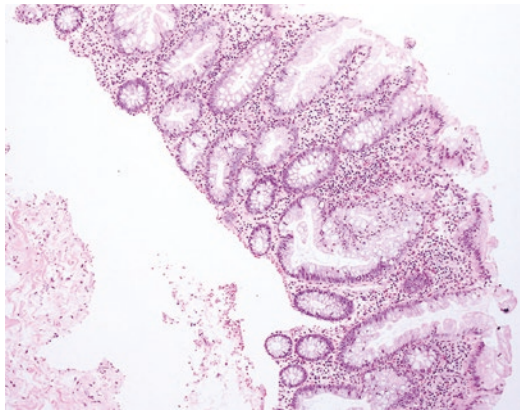

Dilated hyperplastic glands can be seen

20.4 Case 4

62 years old female bowel habit change

- Location: Ascending colon
- Morphology: 0+IIa size 5 mm
- NBI: NICE 2 (JNET 2A)
- Treatment: EMR
- Pathology: Tubular adenoma

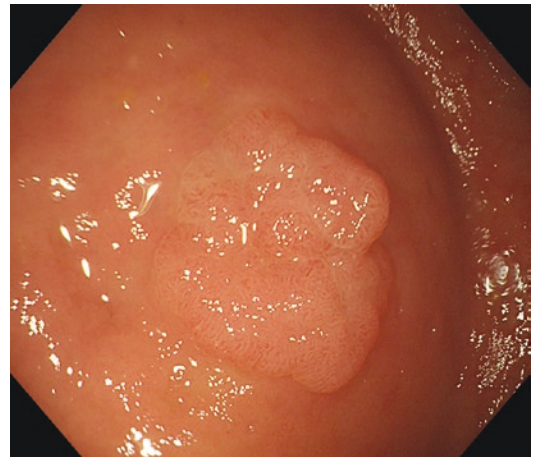

A flat elevated lesion with nodular surface can be seen

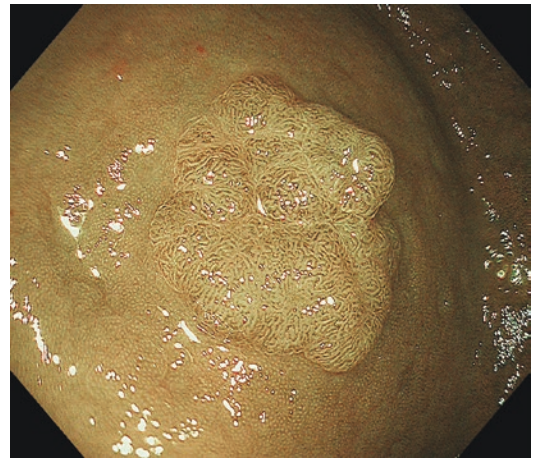

A regular caliver can be seen

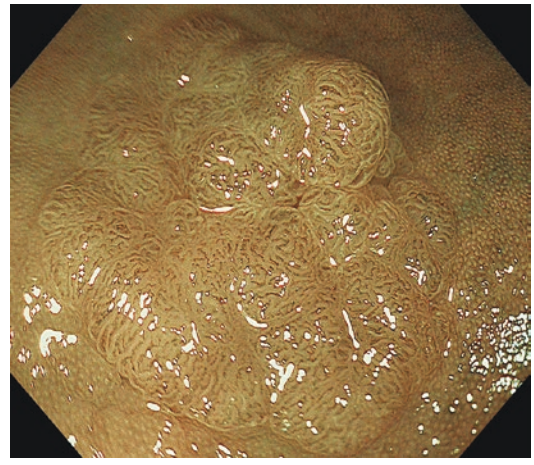

Tubular surface patterns can be seen

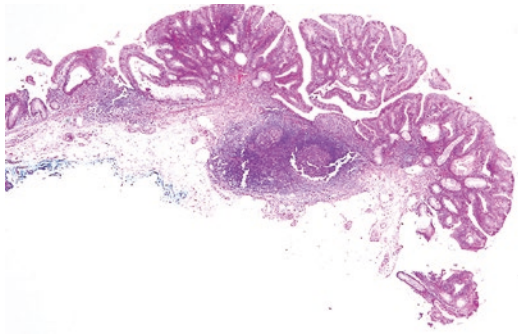

A tubular adenoma with low grade dysplesia

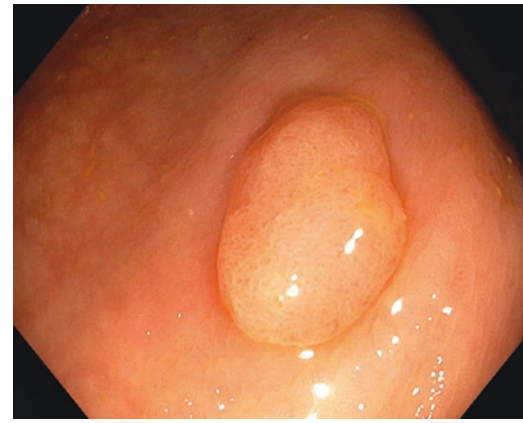

A flat elevated lesion with yellowish mucous can be seen

20.5 Case 5

80 years old male bowel habit change

- Location: Cecum
- Morphology: 0+IIa size 5 mm
- NBI: NICE 1 (JNET 1)
- Treatment: EMR
- Pathology: Sessile serrated lesion

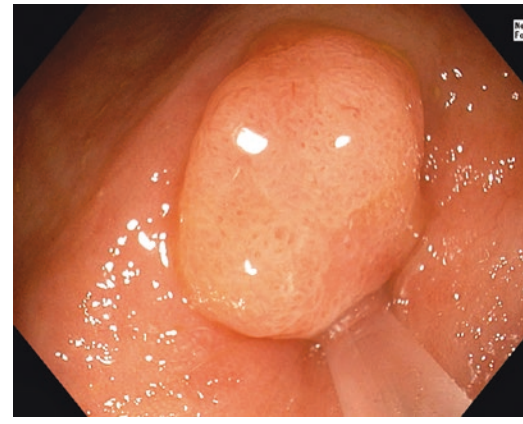

Dilated crypts can be seen

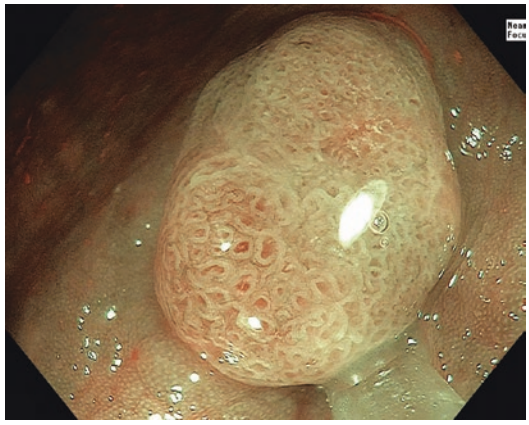

Dilated crypts can be seen in lower part of the lesion

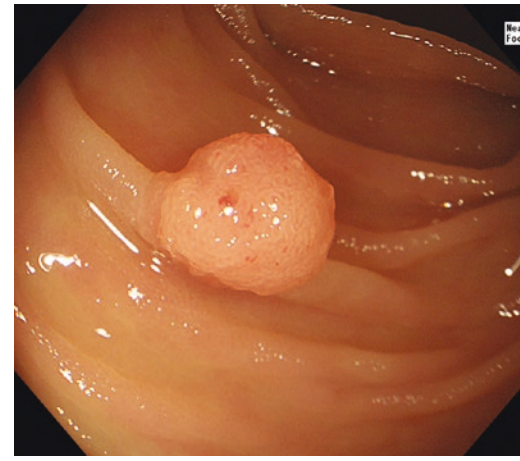

A sessile lesion can be seen

20.6 Case 6

88 years old female with history of bleeding per rectum

- Location: Descending colon
- Morphology: 0+Is size 5 mm
- NBI: NICE 2 (JNET 2A)
- Treatment: EMR
- Pathology: Tubular adenoma

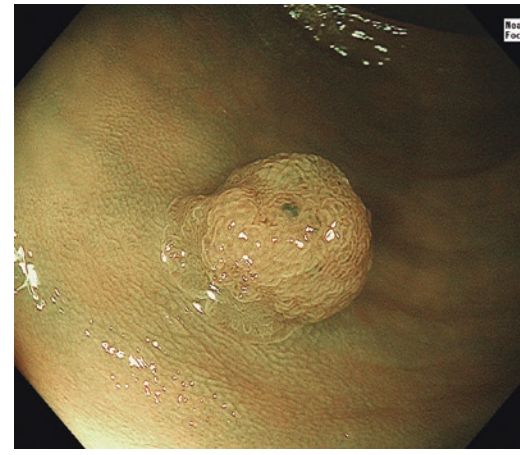

Tubular surface patterns can be seen

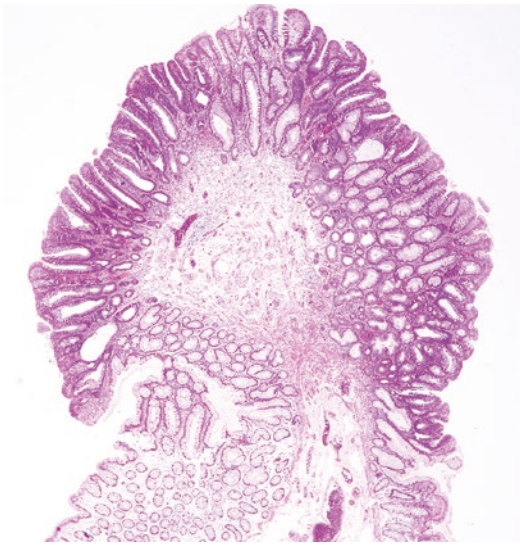

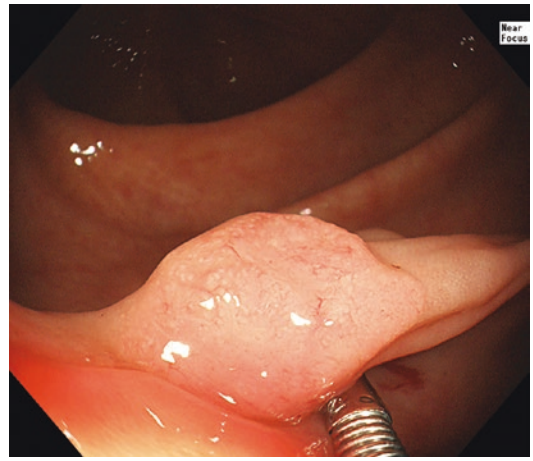

A flat elevated lesion can be seen

20.7 Case 7

79 years old female screening colonoscopy

- Location: Ascending colon
- Morphology: 0+IIa+IIc size 1 cm
- NBI: NICE 3 (JNET 3)
- Treatment: Laparoscopic Right Colectomy
- Pathology: Moderate differentiation adenocarcinoma invade to submucosa with extensive lymphovascular invasion with perineural invasion, LN positive 5/9 apical and 3/20 pericolic pT1N2bMx

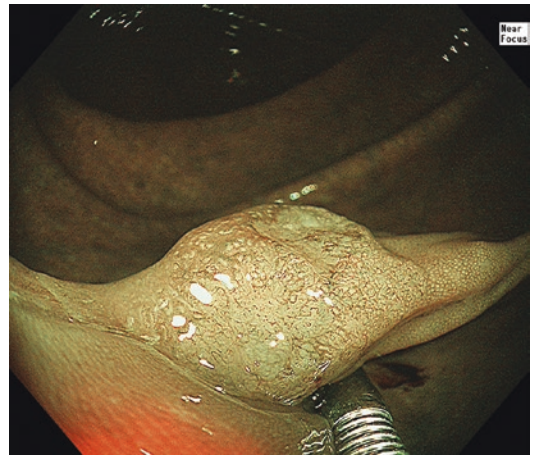

A deprressed area can be seen in the center of the lesion

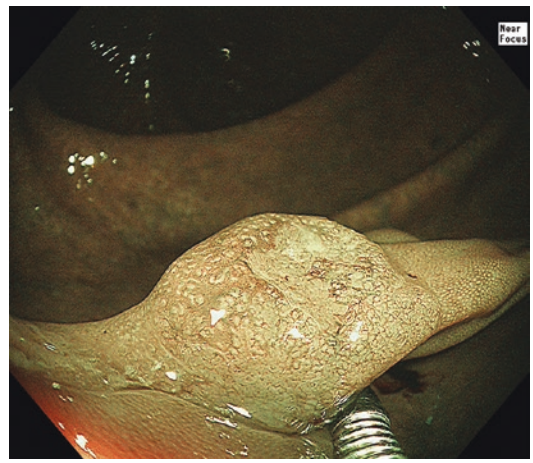

Amorphous areas can be seen in the depressed area